

# STRUCTURAL BEHAVIOUR OF CLOSELY PACKED SEWER LININGS

BY

UDAY KUMAR ROY



A thesis submitted to the Department of Civil Engineering,  
Bangladesh University of Engineering and Technology, Dhaka in  
partial fulfillment of the requirements for the degree

of

MASTER OF SCIENCE IN CIVIL ENGINEERING



#87852#

October, 1994

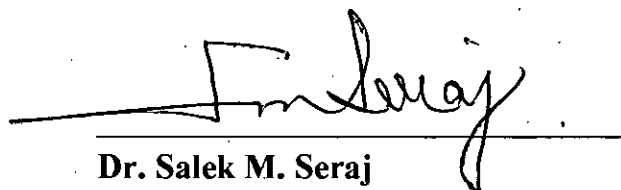
# STRUCTURAL BEHAVIOUR OF CLOSELY PACKED SEWER LININGS

628.2  
1994  
ROY

BY

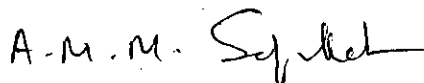
UDAY KUMAR ROY

A thesis approved as to the style and content by:



**Dr. Salek M. Seraj**  
Assistant Professor  
Department of Civil Engineering  
BUET, Dhaka.

: Chairman  
(Supervisor)



**Dr. A. M. M. Safiullah**  
Professor & Head  
Department of Civil Engineering  
BUET, Dhaka

: Member



**Dr. Alamgir Habib**  
Professor  
Department of Civil Engineering  
BUET, Dhaka

: Member



**Dr. J. A. Naser**  
Assistant Professor  
Department of Mech Engineering  
BUET, Dhaka

: Member  
(External)


*To*

*my mother*

## DECLARATION

Declared that except where specific references are made to other investigators, the work embodied in this thesis is the result of the investigation carried out by the author under supervision of Dr. Salek M. Seraj, Assistant Professor of the Department of Civil Engineering, BUET. Neither this thesis nor any part of it has been submitted or is being concurrently submitted elsewhere for any other purpose (except for publications)

October, 1994



Uday Kumar Roy

## ACKNOWLEDGMENT

The author wishes to express his deepest gratitude to his supervisor Dr. Salek M. Seraj, Assistant Professor, Department of Civil Engineering, BUET for his constant guidance, continued encouragement, generous help and unfailing enthusiasm at all stages of this research work. His active interest in this topic and valuable advice were the source of the author's inspiration.

Sincere appreciation and gratitude are also expressed to Dr. A. M. M. Safiullah, Professor and Head, Department of Civil Engineering, BUET for his encouragement and cooperation.

The author would like to extend his special thanks to Dr. M. N. Pavlovic, Reader in Structural Engineering, Imperial College of Science, Technology and Medicine, University of London for kindly making his research findings on sewer linings available to the present project.

The author is greatly indebted to Dr. A. B. M. Badruzzaman, Assistant Professor, Department of Civil Engineering, BUET, for his generous help at the Computer Laboratory at different stages of the research work.

The author is grateful to Dr. Md. Delwar Hossain, Assistant Professor, Department of Civil Engineering, BUET for his kind support during the present study.

Finally, the author also wishes to thank his family and friends who helped him with the necessary advice and information.

## ABSTRACT

Sewer rehabilitation is becoming a subject of major importance to structural designers working in the field of public health engineering. This increasing interest has led to this comprehensive study on the various aspects of sewer lining as a means of sewer renovation.

This research work is devoted to the parametric study of the structural behaviour of various closely packed sewer linings. The literature review has shown that, other than egg-shaped sewers, there is a general lack of information available as to how lining technology can be made available to the renovation of sewers of different shapes and sizes. As the shapes of sewer linings are primarily governed by the shape of the sewer in which the lining is to be inserted, the various shapes of sewers, presently under going construction or constructed in the past, form the core of the investigation. These include egg shaped, inverted egg shaped, horseshoe shaped, semielliptical shaped and the circular shaped - the most widely used sewer shape in Bangladesh and overseas - sewers. The effects of various restraint conditions which simulate different probable temporary support systems during installation of the lining and different loading configurations which may arise at different stages of grouting have also been observed.

Covering the feasible range of geometric, material and loading parameters, comprehensive design curves are presented based on the allowable stress- and deflection-limit criteria specified in the sewerage rehabilitation manual for all the above mentioned lining shapes except for the circular one. Substantial investigations have also been performed on the behavior of circular lining during installation. As expected, the main failure criteria, for circular sewer linings, under grouting load has been found to be buckling. Design recommendations, based on direct stress-limit criteria derived for a hinged arch, have been proposed for circular linings subjected to hydrostatic pressure under different restraint set-ups.

A comparison between various types of restraints has led to enhancement factors for the permissible grouting pressure, or alternatively, to reduction factors in terms of lining thickness which could be used in designing lining systems. Finally, with the help of the proposed design curves and equations, an illustrative design example of each of the lining shapes has been carried out.

# CONTENTS

|                        | <b>Page</b> |
|------------------------|-------------|
| <b>DECLARATION</b>     | i           |
| <b>ACKNOWLEDGMENT</b>  | ii          |
| <b>ABSTRACT</b>        | iii         |
| <b>CONTENTS</b>        | iv          |
| <b>LIST OF FIGURES</b> | ix          |
| <b>LIST OF TABLES</b>  | xv          |
| <b>NOTATIONS</b>       | xvi         |
| <b>ABBREVIATIONS</b>   | xviii       |

## **CHAPTER 1                      GENERAL INFORMATION**

|  |   |
|--|---|
| 1.1 Introduction                               | 1 |
| 1.2 Background of lining technology            | 1 |
| 1.3 Classification of linings                  | 3 |
| 1.4 Properties of different lining materials   | 4 |
| 1.5 Uses of linings                            | 4 |
| 1.6 Present state of art of the research topic | 6 |
| 1.7 Scope of the work                          | 7 |
| 1.8 Limitations of the work                    | 7 |

## **CHAPTER 2                      METHODOLOGY OF ANALYSIS AND DESIGN**

|                                      |    |
|--------------------------------------|----|
| 2.1 Introduction                     | 8  |
| 2.2 Precast and cast-in-place sewers | 8  |
| 2.3 Linings technique                | 9  |
| 2.4 Techniques of grouting           | 9  |
| 2.5 Restraint set-ups                | 11 |
| 2.5.1 Boundary condition 1:          | 11 |
| 2.5.2 Boundary condition 2:          | 13 |
| 2.5.3 Boundary condition 3:          | 13 |
| 2.6 Loading configurations           | 13 |
| 2.7 Calculation of loads             | 15 |
| 2.8 Basis of design                  | 15 |

|   | Page |
|---|------|
| 2.9 Parameters involved in the analysis       | 16   |
| 2.10 Mathematical formulation of the analysis | 16   |
| 2.11 Methodology of the subsequent analyses   | 18   |

### **CHAPTER 3            STRUCTURAL BEHAVIOUR OF EGG-SHAPED SEWER LININGS**

|   |    |
|---|----|
| 3.1 Introduction                                  | 20 |
| 3.2 Two-dimensional finite element discretization | 20 |
| 3.3 Data used in the analysis                     | 23 |
| 3.4 Computation of various constants              | 31 |
| 3.5 Full grouting design curves                   | 31 |
| 3.5.1 Stress-limit criteria                       | 31 |
| 3.5.2 Deflection-limit criteria                   | 36 |
| 3.6 Discussion on parametric analysis             | 39 |
| 3.6.1 Enhancement factor                          | 39 |
| 3.6.2 Reduction factors                           | 42 |
| 3.7 Structural design example                     | 46 |

### **CHAPTER 4            STRUCTURAL BEHAVIOUR OF INVERTED EGG- SHAPED SEWER LININGS**

|   |    |
|---|----|
| 4.1 Introduction                              | 48 |
| 4.2 Two-dimensional finite element (FE) model | 48 |
| 4.2.1 The two-dimensional FE mesh             | 48 |
| 4.2.2 Restraint set-ups                       | 50 |
| 4.2.3 Loading configurations                  | 50 |
| 4.2.4. Parameters included in the analysis    | 54 |
| 4.3 Computation of constants                  | 56 |
| 4.4 Full-grouting design curves               | 56 |
| 4.4.1 Stress-limit criteria                   | 56 |
| 4.4.2 Deflection-limit criteria               | 59 |
| 4.5 Discussion of parametric analysis         | 65 |
| 4.5.1 Enhancement factors                     | 65 |
| 4.5.2 Reduction factors                       | 67 |



## **CHAPTER 5            STRUCTURAL BEHAVIOUR OF HORSESHOE SHAPED LININGS**

|  | Page |
|--|------|
| 5.1 Introduction                                 | 71   |
| 5.2 Two-dimensional finite element mesh          | 71   |
| 5.3 Boundary set-ups                             | 73   |
| 5.4 Loading configurations                       | 73   |
| 5.5 Determination of the dimensionless constants | 73   |
| 5.6 Full grouting design curves                  | 79   |
| 5.6.1 Stress-limit criteria:                     | 79   |
| 5.6.2 Deflection-limit criteria:                 | 82   |
| 5.7 Discussion on the present study              | 85   |
| 5.7.1 Enhancement factor                         | 85   |
| 5.7.2 Reduction factors                          | 87   |

## **CHAPTER 6            STRUCTURAL BEHAVIOUR OF SEMIELLIPTICAL SHAPED LININGS**

|   |     |
|---|-----|
| 6.1 Introduction                                  | 90  |
| 6.2 Two-dimensional finite element (FE) model     | 90  |
| 6.2.1 Two-dimensional FE mesh                     | 90  |
| 6.2.2 Restraint set-ups                           | 93  |
| 6.2.3. Simulation of the restraints               | 93  |
| 6.3 Loading configurations                        | 93  |
| 6.4 Parameters included in the analysis           | 97  |
| 6.5 Determination of the nondimensional constants | 97  |
| 6.6 Full grouting design curves                   | 99  |
| 6.6.1 Stress-limit criteria                       | 99  |
| 6.6.2 Deflection-limit criteria                   | 106 |
| 6.7 Discussion of the present study               | 109 |
| 6.7.1 Enhancement factor                          | 109 |
| 6.7.2 Reduction factors                           | 113 |

**CHAPTER 7                    STRUCTURAL BEHAVIOUR OF CIRCULAR  
SHAPED LININGS**

|  | Page |
|--|------|
| 7.1 Introduction                           | 116  |
| 7.2 Two-dimensional finite element model   | 116  |
| 7.2.1 Two-dimensional finite element mesh  | 116  |
| 7.2.2 Restraint set-ups                    | 118  |
| 7.3 Loading configurations                 | 118  |
| 7.4. Analysis of lining structure          | 118  |
| 7.4.1 Use of non-dimensional equations     | 118  |
| 7.4.2 Effect of restraining on axial force | 122  |
| 7.4.3 Simulation of full-grouting loads    | 122  |

**CHAPTER 8                    CONCLUSIONS AND RECOMMENDATIONS FOR  
FUTURE RESEARCH**

|                      |     |
|----------------------|-----|
| 8.1 Conclusions      | 127 |
| 8.2: Recommendations | 129 |

**REFERENCES** 130

**APPENDIX 1** 132

|   |     |
|---|-----|
| A1.1 Derivation of the design equations for full grouting load<br>(deflection-limit criteria) | 133 |
|---|-----|

**APPENDIX 2** 135

|  |     |
|--|-----|
| A2.1 Graphs used in the determination of dimensionless constants<br>for inverted egg shaped lining | 136 |
| A2.2 Structural design of inverted egg shaped lining   | 142 |

**APPENDIX 3** 143

|  |     |
|--|-----|
| A3.1 Graphs used in the determination of dimensionless constants<br>for horse shoe shaped lining | 144 |
| A3.2 Structural design of horse shoe shaped lining   | 150 |

|  | Page |
|--|------|
| <b>APPENDIX 4</b>  | 152  |
| A4.1 Graphs used in the determination of dimensionless constants<br>for semielliptical shaped lining | 153  |
| A4.2 Structural design of semielliptical shaped lining   | 159  |
| <b>APPENDIX 5</b>  | 161  |
| A5.1 Graphs used in the determination of dimensionless constants<br>for circular shaped lining       | 162  |
| A5.2 Structural design of circular lining  | 166  |

# LIST OF FIGURES

|      |  | Page |
|------|--|------|
| 2.1  | Common shapes of sewer available in different countries  | 10   |
| 2.2  | Support system studied: (a) boundary case 1, (b) boundary case 2 and (c) boundary case 3   | 12   |
| 2.3  | The loading configurations studied: (a) staged grouting, (b) pressure up to crown only (flotation) and (c) uniform pressure  | 14   |
| 3.1  | Shape of sewer lining used in the analysis   | 21   |
| 3.2  | Egg-shaped sewer lining: Two-dimensional finite element mesh adopted in the analysis   | 22   |
| 3.3  | Egg-shaped sewer lining: Half of the mesh used in the analysis   | 22   |
| 3.4  | Egg-shaped sewer lining: Determination of the constant 'A' for staged grouting for (a) boundary case 1, (b) boundary case 2 and (c) boundary case 3  | 25   |
| 3.5  | Egg-shaped sewer lining: Determination of the constant 'C' for flotation load for (a) boundary case 1 (node 11), (b) boundary case 1 (node 1) (c) boundary case 2 and (d) boundary case 3                                      | 26   |
| 3.6  | Egg-shaped sewer lining: Determination of the constant 'E' for uniform pressure for (a) boundary case 1 (node 1), (b) boundary case 1 (node 11) (c) boundary case 2 and (d) boundary case 3                                    | 27   |
| 3.7  | Egg-shaped sewer lining: Determination of the constants 'B <sub>x</sub> ' and 'B <sub>y</sub> ' for staged grouting for (a) boundary case 1, (b) boundary case 2 and (c) boundary case 3                                       | 28   |
| 3.8  | Egg-shaped sewer lining: Determination of the constants 'D <sub>x</sub> ' and 'D <sub>y</sub> ' for flotation load for (a) boundary case 1 (node 5), (b) boundary case 1 (node 6), (c) boundary case 2 and (d) boundary case 3 | 29   |
| 3.9  | Egg-shaped sewer lining: Determination of the constants 'F <sub>x</sub> ' and 'F <sub>y</sub> ' for flotation load for (a) boundary case 1 (node 6), (b) boundary case 1 (node 5), (c) boundary case 2 and (d) boundary case 3 | 30   |
| 3.10 | Egg-shaped sewer lining: Maximum bending stresses at the crown and invert of the lining for flotation (p/Gw=1.5) and additional external pressure for boundary case 1  | 33   |
| 3.11 | Egg-shaped sewer lining: Allowable grouting pressure, based on the stress-limit criteria for various boundary cases  | 35   |
| 3.12 | Maximum deflections at node 5 and node 6 of the lining for full flotation (p/Gw=1.5) and additional external pressure for boundary case 1  | 38   |

|  | Page |
|--|------|
| 3.13 Egg-shaped sewer lining: Allowable grouting pressure based on the deflection-limit criteria for various boundary cases  | 40   |
| 3.14 Egg-shaped sewer lining: Enhancement factor for allowable grouting pressure, based on stress-limit criteria   | 43   |
| 3.15 Egg-shaped sewer lining: Enhancement factor for allowable grouting pressure, based on deflection-limit criteria   | 43   |
| 3.16 Egg-shaped sewer lining: Reduction factor for minimum permissible lining thickness  | 45   |
| 4.1 Inverted egg shaped lining: The shape of the lining used in the analysis   | 49   |
| 4.2 Inverted egg shaped lining: Two-dimensional finite element mesh adopted in the analysis  | 51   |
| 4.3 Inverted egg shaped lining: The support systems studied: (a) boundary case 1, (b) boundary case 2 and (c) boundary case 3  | 52   |
| 4.4 Inverted egg shaped lining: The loading configurations studied: (a) staged grouting, (b) pressure up to crown only and (c) uniform pressure                                | 53   |
| 4.5 Inverted egg-shaped lining: Maximum bending stresses at the crown of the lining for flotation ( $p/Gw=1.5$ ) and additional external pressure (boundary case 1)            | 58   |
| 4.6 Inverted egg-shaped lining: Maximum bending stresses at the crown and invert of the lining for flotation ( $p/Gw=1.5$ ) and additional external pressure (boundary case 2) | 58   |
| 4.7 Inverted egg-shaped lining: Allowable grouting pressure for different boundary conditions, based on stress-limit criteria  | 60   |
| 4.8 Inverted egg-shaped lining: Maximum deflections at nodes 13 and 14 of the lining for full flotation ( $p/Gw=1.5$ ) and additional external pressure (boundary case 1)      | 62   |
| 4.9 Inverted egg-shaped lining: Maximum deflections at nodes 13 and 16 of the lining for full flotation ( $p/Gw=1.5$ ) and additional external pressure (boundary case 2)      | 62   |
| 4.10 Inverted egg-shaped lining: Maximum deflections at nodes 15 and 16 of the lining for full flotation ( $p/Gw=1.5$ ) and additional external pressure (boundary case 3)     | 64   |
| 4.11 Inverted egg-shaped lining: Allowable grouting pressure for various boundary cases, based on deflection-limit criteria  | 66   |
| 4.12 Inverted egg-shaped lining: Enhancement factor for allowable grouting pressure, based on stress-limit criteria  | 68   |

|   | Page |
|---|------|
| 4.13 Inverted egg-shaped lining: Enhancement factor for allowable grouting pressure based on deflection-limit criteria  | 68   |
| 4.14 Inverted egg-shaped lining: Reduction factor for minimum permissible lining thickness based on stress-limit criteria                                     | 70   |
| 5.1 Existing horseshoe sewer  | 72   |
| 5.2 Horseshoe shaped lining: (a) shape of the lining adopted in the analysis and (b) the lining in conjunction with the sewer                                 | 74   |
| 5.3 Horseshoe shaped lining: Two-dimensional finite-element mesh adopted in the analysis  | 75   |
| 5.4 Horseshoe shaped lining: The support systems studied: (a) boundary condition 1, (b) boundary condition 2, and (c) boundary condition 3                    | 76   |
| 5.5 Horseshoe shaped lining: The loading configurations studied: (a) staged grouting, (b) grout up to crown only and (c) uniform pressure                     | 77   |
| 5.6 Horseshoe shaped lining: Maximum bending stresses at the crown and invert for flotation ( $p/Gw=0.8$ ) and additional external pressure (Boundary Case 1) | 81   |
| 5.7 Horseshoe shaped lining: Maximum bending stresses at the crown and invert for flotation ( $p/Gw=0.8$ ) and additional external pressure (Boundary Case 2) | 81   |
| 5.8 Horseshoe shaped lining: Allowable grouting pressure, based on stress limit criteria for various boundary cases   | 83   |
| 5.9 Horseshoe shaped lining: Allowable grouting pressure based on deflection-limit criteria for various boundary conditions                                   | 86   |
| 5.10 Horseshoe shaped lining: Enhancement factors for allowable grouting pressure, based on stress-limit criteria   | 88   |
| 5.11 Horseshoe shaped lining: Reduction factors for minimum permissible lining thickness based on stress-limit criteria                                       | 88   |
| 6.1 Existing semielliptical sewer   | 91   |
| 6.2 Semielliptical shaped lining: (a) Shape of the lining adopted in the analysis and (b) The lining in conjunction with the sewer                            | 93   |
| 6.3 Semielliptical shaped lining: Finite element mesh adopted in the analysis   | 94   |
| 6.4 Semielliptical shaped lining: The support systems studied: (a) boundary condition 1, (b) boundary condition 2 and (c) boundary condition 3                | 95   |
| 6.5 Semielliptical shaped lining: The loading configurations studied: (a) staged grouting, (b) grout up to crown only and (c) uniform pressure                | 96   |

|      | Page  |     |
|------|---|-----|
| 6.6  | Semielliptical shaped lining: Maximum bending stresses at nodes 9 and 26 of the lining for flotation ( $p/Gw=1.25$ ) and additional external pressure (Boundary Case 1)       | 100 |
| 6.7  | Semielliptical shaped lining: Maximum bending stresses at nodes 26 and 9 of the lining for flotation ( $p/Gw=1.25$ ) and additional external pressure (Boundary Case 2)       | 102 |
| 6.8  | Semielliptical shaped lining: Maximum bending stresses at the crown and invert of the lining for flotation ( $p/Gw=1.25$ ) and additional external pressure (Boundary Case 3) | 104 |
| 6.9  | Semielliptical shaped lining: Allowable grouting pressure, based on stress-limit criteria, for various boundary conditions  | 105 |
| 6.10 | Semielliptical shaped lining: Maximum deflections at nodes 1 and 16 of the lining for full flotation ( $p/Gw=1.25$ ) and additional external pressure (Boundary Case 1)       | 107 |
| 6.11 | Semielliptical shaped lining: Maximum deflection at nodes 3 and 17 of the lining for full flotation ( $p/Gw=1.25$ ) and additional external pressure (Boundary Case 3)        | 107 |
| 6.12 | Semielliptical shaped lining: Allowable grouting pressure based on deflection-limit criteria for various boundary cases   | 110 |
| 6.13 | Semielliptical shaped lining: Enhancement factors for allowable grouting pressure, based on stress-limit criteria   | 112 |
| 6.14 | Semielliptical shaped lining: enhancement factors for allowable grouting pressure, based on deflection-limit criteria   | 112 |
| 6.15 | Semielliptical shaped lining: Reduction factors for minimum permissible lining thickness, based on stress-limit criteria  | 114 |
| 7.1: | Circular shaped lining: Geometry of the lining  | 117 |
| 7.2  | Circular shaped lining: Two-dimensional finite element mesh adopted in the analysis   | 117 |
| 7.3  | Circular shaped lining: The support systems studied: (a) boundary condition 1, (b) boundary condition 2 and (c) boundary condition 3  | 119 |
| 7.4  | Circular shaped lining: The loading configurations studied: (a) staged grouting, (b) grout up to crown only and (c) uniform pressure  | 120 |
| 7.5  | Circular shaped lining: A thin ring submerged in a liquid   | 124 |
| 7.6  | Circular shaped lining: Uniformly loaded hinged arch  | 124 |
| 7.7  | Circular shaped lining: Uniformly loaded fixed arch   | 124 |

|  | Page |
|--|------|
| A2.1 Inverted egg shaped lining: Determination of the constant 'A' for staged grouting for (a) boundary case 1, (b) boundary case 2 and (c) boundary case 3  | 136  |
| A2.2 Inverted egg shaped lining: Determination of the constant 'C' for flotation for (a) boundary case 1, (b) boundary case 2 and (c) boundary case 3  | 137  |
| A2.3 Inverted egg shaped lining: Determination of the constant 'E' for uniform pressure for (a) boundary case 1, (b) boundary case 2 (at node 26), (c) boundary case 2 (at node 1) and (d) boundary case 3 | 138  |
| A2.4 Inverted egg shaped lining: Determination of the constants ' $B_X$ ' and ' $B_Y$ ' for staged grouting for (a) boundary case 1, (b) boundary case 2 and (c) boundary case 3                           | 139  |
| A2.5 Inverted egg shaped lining: Determination of the constants ' $D_X$ ' and ' $D_Y$ ' for flotation for (a) boundary case 1, (b) boundary case 2 and (c) boundary case 3                                 | 140  |
| A2.6 Inverted egg shaped lining: Determination of the constants ' $F_X$ ' and ' $F_Y$ ' for flotation for (a) boundary case 1, (b) boundary case 2 and (c) boundary case 3                                 | 141  |
| A3.1 Horse shoe shaped lining: Determination of the constant 'A' for staged grouting for (a) boundary case 1, (b) boundary case 2 and (c) boundary case 3  | 144  |
| A3.2 Horse shoe shaped lining: Determination of the constant 'C' for flotation for (a) boundary case 1, (b) boundary case 2 and (c) boundary case 3  | 145  |
| A3.3 Horse shoe shaped lining: Determination of the constant 'E' for uniform pressure for (a) boundary case 1, (b) boundary case 2 (at node 26), (c) boundary case 2 (at node 1) and (d) boundary case 3   | 146  |
| A3.4 Horse shoe shaped lining: Determination of the constants ' $B_X$ ' and ' $B_Y$ ' for staged grouting for (a) boundary case 1, (b) boundary case 2 and (c) boundary case 3                             | 147  |
| A3.5 Horse shoe shaped lining: Determination of the constants ' $D_X$ ' and ' $D_Y$ ' for flotation for (a) boundary case 1, (b) boundary case 2 and (c) boundary case 3                                   | 148  |
| A3.6 Horse shoe shaped lining: Determination of the constants ' $F_X$ ' and ' $F_Y$ ' for flotation for (a) boundary case 1, (b) boundary case 2 and (c) boundary case 3                                   | 149  |



|  | Page |
|--|------|
| A4.1 Semielliptical shaped lining: Determination of the constant 'A' for staged grouting for (a) boundary case 1, (b) boundary case 2 and (c) boundary case 3  | 153  |
| A4.2 Semielliptical shaped lining: Determination of the constant 'C' for flotation for (a) boundary case 1, (b) boundary case 2 and (c) boundary case 3  | 154  |
| A4.3 Semielliptical shaped lining: Determination of the constant 'E' for uniform pressure for (a) boundary case 1, (b) boundary case 2 (at node 26), (c) boundary case 2 (at node 1) and (d) boundary case 3 | 155  |
| A4.4 Semielliptical shaped lining: Determination of the constants 'B <sub>X</sub> ' and 'B <sub>Y</sub> ' for staged grouting for (a) boundary case 1, (b) boundary case 2 and (c) boundary case 3           | 156  |
| A4.5 Semielliptical shaped lining: Determination of the constants 'D <sub>X</sub> ' and 'D <sub>Y</sub> ' for flotation for (a) boundary case 1, (b) boundary case 2 and (c) boundary case 3                 | 157  |
| A4.6 Semielliptical shaped lining: Determination of the constants 'F <sub>X</sub> ' and 'F <sub>Y</sub> ' for flotation for (a) boundary case 1, (b) boundary case 2 and (c) boundary case 3                 | 158  |
| A5.1 Circular shaped lining: Determination of the constant 'A' for staged grouting for (a) boundary case 1, (b) boundary case 2 and (c) boundary case 3  | 162  |
| A5.2 Circular shaped lining: Determination of the constant 'C' for flotation for (a) boundary case 1, (b) boundary case 2 and (c) boundary case 3  | 163  |
| A5.3 Circular shaped lining: Determination of the constants 'B <sub>X</sub> ' and 'B <sub>Y</sub> ' for staged grouting for (a) boundary case 1, (b) boundary case 2 and (c) boundary case 3                 | 164  |
| A5.4 Circular shaped lining: Determination of the constants 'D <sub>X</sub> ' and 'D <sub>Y</sub> ' for flotation for (a) boundary case 1, (b) boundary case 2 and (c) boundary case 3                       | 165  |

## LIST OF TABLES

|   | Page |
|---|------|
| 1.1 Flexible and rigid linings  | 3    |
| 1.2 Impervious and semiimpervious   | 4    |
| 1.3 Continuos and non-continuos linings   | 4    |
| 1.4 Physical properties of some engineering materials   | 5    |
| 1.5 Permeability of common polymers to air, methane and water vapour  | 6    |
| 3.1 Data used in the analysis, egg-shaped lining  | 23   |
| 3.2 Dimensionless constants for the maximum bending stress in the lining, egg-shaped lining   | 24   |
| 3.3 Dimesionless constants for the maximum inward deflection, egg-shaped lining   | 24   |
| 4.1 Dimensionless constants for the maximum bending stress in the lining, inverted egg-shaped lining                                    | 55   |
| 4.2 Dimesionless constants for the maximum inward deflection, inverted egg shaped lining  | 55   |
| 5.1 Dimensionless constants for the maximum bending stress in the lining, horseshoe shaped lining                                       | 78   |
| 5.2 Dimesionless constants for the maximum inward deflection, horseshoe shaped lining   | 78   |
| 6.1 Dimensionless constants for the maximum bending stress in the lining, semielliptical shaped lining                                  | 98   |
| 6.2 Dimesionless constants for the maximum inward deflection, semielliptical shaped lining  | 98   |
| 7.1 Dimensionless constants for the maximum bending stress in the lining, circular shaped lining  | 121  |
| 7.2 Dimesionless constants for the maximum inward deflection, circular shaped lining  | 121  |
| 7.3 Comparison of axial force developed due to uniform external pressure applied on the circular lining under various restraint set-ups | 123  |

## NOTATIONS

- A      dimensional constants for maximum bending stress (staged grouting)
- $B_x, B_y$     dimensionless constants for maximum deflection (staged grouting)
- C      dimensional constants for maximum bending stress (flotation)
- $D_x, D_y$     dimensional constants for maximum deflection (flotation)
- E      dimensional constants for maximum bending stress (uniform pressure)
- $F_{cr}$     critical axial force in circular lining
- $F_x, F_y$     dimensional constants for maximum deflection (uniform pressure)
- G      unit weight of grout mix
- H      excess head of grout (measured from crown of lining)
- h      height of lining
- K       $\left(\frac{Gw}{E_s}\right)\left(\frac{w}{t}\right)^3$
- $M_x$      $D_x + F_x(H/w)$
- $M_y$      $D_y + F_y(H/w)$
- $N_x$      $D_x + F_x\left(\frac{p}{Gw} - \frac{h}{w}\right)$
- $N_y$      $D_y + F_y\left(\frac{p}{Gw} - \frac{h}{w}\right)$
- p      allowable grouting pressure (measured from the invert of the lining)
- q      uniform pressure intensity
- $q_{cr}$     critical uniform pressure

- R  $\left(\frac{S_s}{Gw}\right)\left(\frac{t}{w}\right)^2$ , radius of circular lining
- S bending stress in lining
- $S_s$  short-term bending stress
- $S_t$  total bending stress due to combined flotation and external pressure
- w width of lining
- $\nu$  Poisson's ratio
- $\gamma$  unit weight of liquid

## ABBREVIATIONS

|      |   |
|------|---|
| EF   | Enhancement factor for allowable grouting pressure        |
| FE   | Finite element  |
| GRC  | Glass reinforced cement                                   |
| GRP  | Glass reinforced plastic                                  |
| HDPE | High density polyethylene                                 |
| LHPE | Low density polyethylene                                  |
| PA   | Polyamide   |
| PP   | Polypropylene   |
| PVC  | Poly vinyl chloride                                       |
| RF   | Reduction factor for minimum permissible lining thickness |
| UP   | Unsaturated polyester or epoxy                            |
| WRC  | Water research centre                                     |

# CHAPTER 1

## GENERAL INFORMATION

### 1.1 INTRODUCTION

Within the last few years a new discipline, expanding quickly into a major consideration for designers of liquid storage and transmission facilities, has developed for those who work in the wastewater treatment field, and for almost all engineers in search of better ways to control pollution. Lining is the name applied to this new technology. Lining, in a general sense, means any material laid down in a holding or conveyance facility to prevent the movement of liquid from one point where its presence is desirable or least objectionable to another point where its presence is undesirable. Although, liquid includes water, oil, brines, sewage, and chemical solutions of all types, the present research concentrates on sewage as liquid. The definition of holding facility can be taken to include such things as concrete, steel, wooden tanks, in addition to cut-and-fill reservoirs. But it is the conveyance system, known as sewers, through which sewage transmits, that has been addressed throughout the present study.

### 1.2 BACKGROUND OF LINING TECHNOLOGY

Modern lining technology came into existence in the 1940s with the introduction of the prefabricated asphalt panels. The first commercial application dates back to 1951 when lining was used in an irrigation canal near Cotulla in Texas, U.S.A. It was a very important industry milestone because it changed the thinking of engineers throughout the world. It was no longer necessary to rely solely on concrete sections as a lining for liquid transmission facilities as in sewers.

A systematic search on the existing literature reveals that very little work has been done to date on the design of linings to be employed within sewers of different shapes and sizes. A through study on the structural performance of egg-shaped sewer linings was conducted by Arnaout (1988). The work involved both computational and experimental investigation on egg-shaped linings and recommended design solutions for such linings.

Arnaout, Pavlovic and Dougill (1988) conducted a parametric study on the structural response of closely packed egg-shaped sewer linings, including the effects of various restraint conditions which simulate different temporary support systems used by contractors during installation. Based on the allowable stress and deflection limit criteria specified by the Water Research Centre sewerage rehabilitation manual (1983), the author presented a comprehensive set of design curves. These design curves covers the practical range of geometric, material and loading parameters. By making a comparison between various types of restraints, the authors have identified enhancement and reduction factors for the permissible grouting pressure, lining thickness etc., which could be used in designing egg-shaped lining systems.

Pavlovic, Arnaout and Hitchings (1993) attempted to model numerically two glass reinforced plastic (GRP) linings (one of them segmental) and one glass reinforced cement (GRC) linings (segmental) by using actual material data and structural test results carried out under uniform pressure. The exercise aimed at the validation of a suitable finite element model as a design tool capable of encompassing a wide range of parameters. The parameters included arbitrary lining geometries, material properties, boundary restraint set-ups, and different load configurations resulting from the way the grouting pressure is applied.

Arnaout and Pavlovic (1988) describes the research work carried out on sewer renovation at the Department of Civil Engineering of Imperial College. The work primarily consists of both material and structural testing as well as numerical modeling of egg-shaped sewer linings where the main emphasis has been placed on aspects relevant to installation conditions, long-term behaviour has also been considered. A brief account of work done on the related topic of circular linings and pipes is also given.

Arnaout, Pavlovic and Dougill (1990) presented a novel method for the experimental determination of the tensile properties of curved members along the direction of their curvature. This consisted of preparing tensile specimens made up of two nominally identified (or at least very similar) curved 'coupon' components of the material in question, which were placed back-to-back so as to minimize bending strain during testing. The proposed technique is of particular relevance to anisotropic composites, and its application to two types of glass reinforced plastic sewer linings has been reported.

Arnaout and Pavlovic (1989) conducted an investigation into the long-term behaviour of egg-shaped sewer linings. Results of a preliminary investigation on the behaviour of egg-shaped sewer linings after renovation have been presented. It focuses mainly on circumstances where the long-term bond of the lining to the grout surrounding can not be confidently relied upon.

### 1.3 CLASSIFICATION OF LININGS

The outline that is followed in the analysis and design of lining systems in this thesis work includes all materials that have actually enjoyed some substantial usage in this field. There are many materials, data on which are limited and any information available is not readily accessible. In a general point of view, linings may be classified in three different ways:

- a) Flexible and rigid linings;
- b) Impervious and semiimpervious linings;
- c) Continuous and non-continuous linings;

Table 1.1, 1.2, and 1.3 (Kays, 1986) show how the common primary linings are categorized in these three classification systems.

The three tables deal with the lining systems that have been more or less accepted by the engineers as proven materials when used in properly designed and operated facilities.

There are various types of plastics; of these glass reinforced plastic (GRP) is highly valued material to be used as a lining in sewer. Steel and concrete linings may also be used.

**Table 1.1.** Flexible and Rigid Linings

| Flexible          | Rigid               |
|-------------------|---------------------|
| 1. Plastics       | 1. Gunite           |
| 2. Elastomers     | 2. Concrete         |
| 3. Compacted Soil | 3. Steel            |
|                   | 4. Asphalt concrete |
|                   | 5. Soil Cement      |



**Table 1.2** Impervious and Semiimpervious Linings

| Impervious    | Semiimpervious      |
|---------------|---------------------|
| 1. Plastics   | 1. Compacted soils  |
| 2. Elastomers | 2. Gunite           |
| 3. Steel      | 3. Concrete         |
|               | 4. Asphalt concrete |
|               | 5. Soil cement      |
|               | 6. Bentonite clays  |

**Table 1.3** Continuos and Non-continuous Linings

| Continuous    | Non-continuous     |
|---------------|--------------------|
| 1. Plastics   | 1. Compacted Soil  |
| 2. Elastomers | 2. Gunite          |
| 3. Steel      | 3. Concrete        |
|               | 4. Asphalt         |
|               | 5. Soil cement     |
|               | 6. Bentonite clays |

## 1.4 PROPERTIES OF DIFFERENT LINING MATERIALS

Different materials may be conveniently used as a sewer lining materials. Properties of some of the materials are given below in Table 1.4 and 1.5 (Jackson, 1983):

## 1.5 USES OF LININGS

- a) The ever increasing need to maintain, repair and eventually renovate existing sewerage system in any country in the world involves very large capital expenditure. The lining technique involves a fraction of the cost of traditional construction methods.
- b) The renovation of sewers prevents the waste water from going to the surrounding soil and thereby reduces the probability of contamination of surrounding soil, ground water etc.

- c) Lining techniques also provide little or no obstruction to the traffic movement, thus avoiding social disruption cost.
- d) The process of strengthening existing sewers leads to the improvement of the structural capacity of the sewer.
- e) Reduced infiltration, improved abrasion and higher chemical resistance are also expected if lining technique can be applied properly.

**Table 1.4:** Physical properties of some engineering materials:

|                   | Density<br>kN/m <sup>3</sup>       | Tensile<br>modulus<br>(kN/mm <sup>2</sup> ) | Tensile<br>strength<br>(N/mm <sup>2</sup> ) | Coefficient<br>of thermal<br>expansion<br>(x 10 <sup>-4</sup> ) | Specific<br>heat<br>capacity<br>(kj/kg/K) |            |
|-------------------|------------------------------------|---|---|---|---|------------|
| PVC               | 13.7                               | 2.4 to 3.0                                  | 40 to 60                                    | 70  | 1.05                                      |            |
| HDPE              | 9.4                                | 0.4 to 1.2                                  | 20 to 30                                    | 120   | 2.3                                       |            |
| LDPE              | 9.0                                | 0.1 to 0.25                                 | 10 to 15                                    | 160   | 1.9                                       |            |
| PP                | 8.8                                | 1.1 to 2.8                                  | 30 to 40                                    | 60  | 1.9                                       |            |
| PA                | 11.1                               | 1.0 to 2.8                                  | 50 to 80                                    | 60  | 1.6                                       |            |
| UP                | 11.8 to 13.7                       | 2.0 to 4.5                                  | 40 to 90                                    | 100   | 2.3                                       |            |
| EP                | 10.8 to 13.7                       | 3.0 to 6.0                                  | 35 to 100                                   | 60  | 1.05                                      |            |
| GRP:<br>Polyester | 50 to 80 % glass<br>unidirectional | 15.7 to 19.6                                | 20 to 50                                    | 400 to 1000   | 10  | 0.95       |
|                   | 45 to 60% glass<br>woven rovings   | 14.7 to 17.6                                | 12 to 14                                    | 200 to 350  | 15  | 1.0 to 1.2 |
|                   | 25 to 45% chopped<br>strand mat    | 13.7 to 15.7                                | 6 to 11                                     | 60 to 180   | 30  | 1.2 to 1.4 |
| GRP:<br>epoxy     | 60 to 80% glass<br>unidirectional  | 15.7 to 19.6                                | 30 to 35                                    | 600 to 1000   | 6   | ---        |
| Mild steel        | 77.5                               | 210   | 370 to 700                                  | 12  | 0.48                                      |            |

**Table 1.5:** Permeability of common polymers to air, methane and water vapour

|                     | Permeability ( $10^{-11}$ cm <sup>3</sup> STP/cm s) |         |              |
|---------------------|---|---------|--------------|
|                     | Air   | Methane | Water vapour |
| HDPE                | 0.19  | 0.39    | 12           |
| LDPE                | 1.36  | 2.9     | 90           |
| Unplasticised PVC   | 0.02  | 0.03    | 275          |
| PP                  | 0.81  | ---     | 51           |
| Natural rubber (NR) | 12.2  | 30.1    | 2300         |

where, PVC = Poly vinyl chloride

HDPE=Highdensity polyethylene

LDPE=Lowdensity polyethylene

PP =Polypropylene

PA =Polyamide

UP =Unsaturated polyester or epoxy

## 1.6 PRESENT STATE OF ART OF THE RESEARCH TOPIC

Although preventive maintenance and renovation in one form or another have taken place from earliest days of sewer construction, it is only relatively recently that sewer rehabilitation has become a subject of increasing interest to structural designers in the public health engineering in the western world. Of particular importance is the use of lining techniques where besides the use of improvement in hydraulic characteristics, reduced infiltration and improved abrasion and chemical resistance may also be expected.

The history of sewerage system of Bangladesh is not very old. The sewerage system that prevails in parts of Dhaka city and some other smaller cities of Bangladesh is not complete and lacks proper maintenance. Up until today, Bangladesh has not used sewer lining techniques in maintenance and renovation of its sewerage system. Adoption of this technique is deemed essential for proper maintenance of the sewerage network.

## **1.7 SCOPE OF THE WORK**

The present study encompasses the analysis and design of various shaped sewer linings, with special reference to installation conditions. The long term performance of sewers having lining during operational conditions has not been included in the study as it is expected that sewers with linings, are on the whole, stronger than their no-lining counterparts. A two-dimensional finite element model of Seraj (1986) has been employed in the analysis. Suitable subroutines have been included in an effort to automate mesh generation, data production etc.

Chapter 2 describes the different types of linings, various types of restraints conditions which simulate different temporary support systems during installation, different types of loading conditions which may arise during grouting. Finally a mathematical basis for analysis and design of sewer lining is discussed. The analysis and design of egg-shaped sewer lining is presented in chapter 3. Chapter 4, 5, 6 and 7 contains similar investigation on inverted egg-shaped, horseshoe shaped, semielliptical shaped, and circular sewer linings. Finally, a comparative study of design and analysis of different types of linings subjected to grouting pressure during installation is carried out in chapter 8. Design examples, using the obtained design curves, are solved and presented in Appendices.

## **1.8 LIMITATIONS OF THE WORK**

From the literature survey it became evident that a very limited research has so far been undertaken on the design implications concerning sewer linings. While the main thrust of the research undertaken on sewer linings has concentrated on the egg shape, a limited amount of work has also been carried out on other lining forms. Most of the work available in the literature deals with not too large size sewers in which buckling of thin linings is not much pronounced. Like the predecessors, the application of the present work is also limited to small to moderate sized sewers. However, in Chapter 8, specific recommendations have been put forward in an effort to accommodate buckling considerations in the design of sewer linings of various shapes.

## CHAPTER 2

### METHODOLOGY OF ANALYSIS AND DESIGN

#### 2.1 INTRODUCTION

To be correct, we should not refer to linings as new. They have been around for many thousands of years. What is new is the rapid growth in their use as a means of controlling seepage from hydraulic facilities. Also new is a developing awareness by users and designers that there is a separate and important technology concerned with the use of linings and that this technology is unlike any other that now exists. When the subject of linings is mentioned, the common reaction is to think of the reservoir, canals, concrete and steel tanks. What is uncommon is to think of sewer linings. It is the subject of this research work to draw attention of all, who work in the structural engineering and/or in the public health engineering, to the most fascinating and challenging subject of the day - the linings of sewers. The huge capital expenditure and indescribable sufferings of traffic during the replacement of existing old sewers has drawn the engineers out of the traditional methods and led to seek for a better and easier solution - the linings of sewers. Since linings are one of the major weapons in the battle to control pollution, the selection of lining materials, as well as the analysis and design of sewer linings have to be done with utmost care.

The types of restraints that may arise during the installation of sewer linings are discussed in this chapter. The different types of loading, different shapes of sewers (which primarily determines the shapes of linings), the mathematical basis for analysis and design of linings are also presented in this chapter.

#### 2.2 PRECAST AND CAST-IN-PLACE SEWERS

Various types of materials are used to transmit sewage. It is more practicable to use less expensive material, since sewers rarely are required to withstand internal pressure. The most commonly used sewer material in different countries is clay pipe, which is made of clay that has been ground, wetted, moulded, dried, and burned in a kiln. Iron and steel pipe are used to convey sewage only under unusual loading conditions or for force mains in which the flow of sewage is pressurized. Concrete pipe is usually a preferred media in case of storm drainage. Generally, all concrete pipes having diameters larger than 610 mm (24 in) is reinforced.

However, reinforced concrete pipe can also be obtained in sizes as small as 310 mm (12 in). The sizes of concrete circular sanitary sewers vary from 12 in to 60 in. It is worth noting that the largest available concrete sewers in Bangladesh is as much as 54 in.

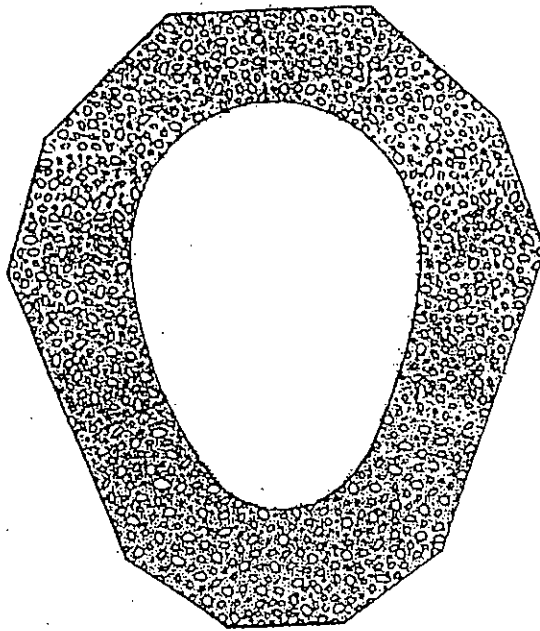
The shape of sewers vary widely from country to country. The majority of sewers presently constructed in Bangladesh and many other countries are of circular cross-sections. However, in the past, a wide variety of non-circular sewer sections are employed. The non-circular sewer shapes includes egg-shaped, inverted egg-shaped, semielliptical, horseshoe, oval, catenary, parabolic and elliptical. The first four of these shapes were the more popular in the past. Typical examples of these popular sections are shown in Fig. 2.1. In Bangladesh, generally, circular shaped sewers are more widely used for sanitary sewage carriage. Recently box-culverts are being constructed extensively in Dhaka city for its storm drainage (Seraj, 1993). In United Kingdom, egg-shaped sewers are more common. In the United States of America, circular and inverted egg-shaped sewers are found in its different states. In addition to these types of sewers, horseshoe and semi-elliptical shaped sewers may be found in many foreign countries including U. S. A (for example, horseshoe shaped sewers are very popular in Dallas, Texas while semielliptical shaped sewers are common in Tulsa, Oklahoma). As the present research concentrates on the linings of existing sewers which needs to be repaired now, only a few sections which were and are in most common use are dealt with. The findings are, however, readily applicable to the above mentioned shaped new sewers as well.

### **2.3 LININGS TECHNIQUE**

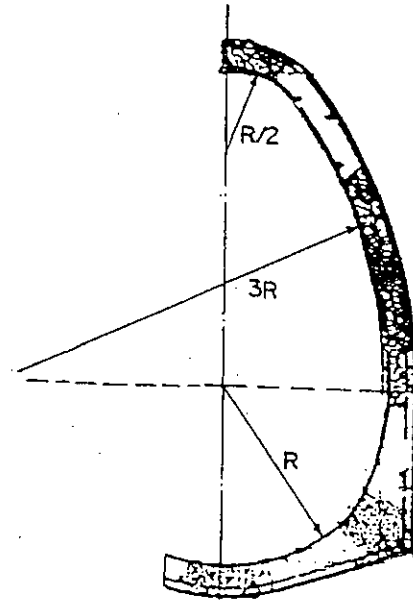
The linings are usually made of glass reinforced plastic (GRP) or glass reinforced cement (GRC). Steel linings are also used. If the sewer is of circular shape, the circular type of linings are to be selected so that it fits within the existing sewer with a roughly uniform gap between the linings and the sewer walls. Similar is the case with other types of sewers. The gap between the lining and the sewer is then filled with a cementitious grout which, when set creates a composite sewer-lining structure.

### **2.4 TECHNIQUES OF GROUTING**

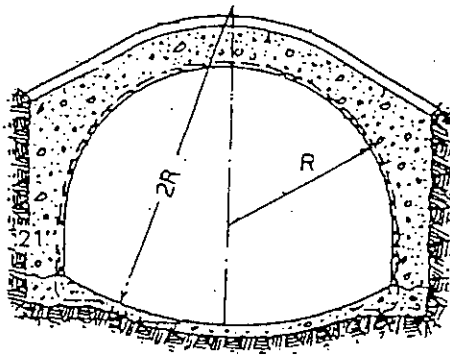
In sewer lining, two techniques of grouting are generally adopted. They are described as follows:



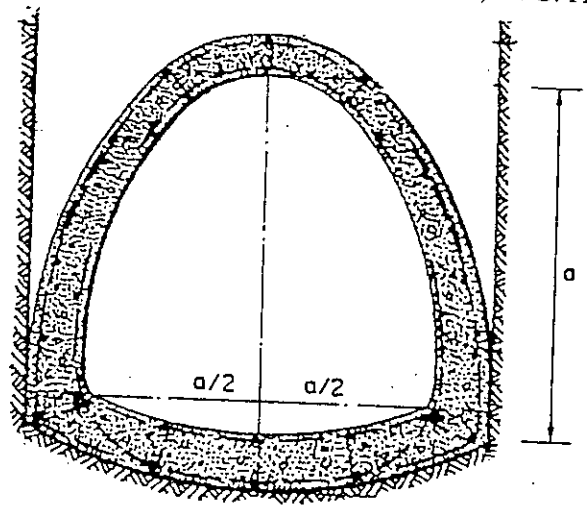
(a) Egg-shaped, London, U. K.



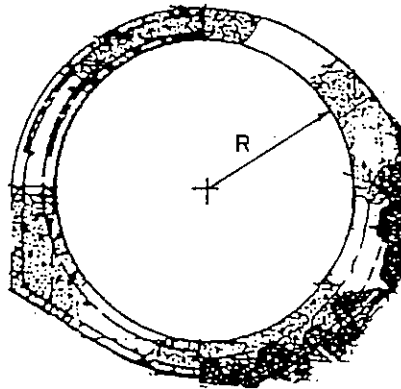
(b) Inverted Egg-shaped, Louisville, U. S. A.



(c) Horseshoe, Dallas, U. S. A.



(d) Semielliptical, Tulsa, U. S. A.



(e) Circular, Dhaka, Bangladesh

Fig. 2.1: Common shapes of sewer available in different countries

### **Staged or partial grouting**

Grouting is performed in two stages in this method. The first stage involves grouting the annulus up to the springing, and this is followed by a second stage which is carried out after the grout of first stage has set. During the second stage of grouting, the rest of the annulus is filled with grout.

### **Full grouting**

In this method, full grouting is performed in a single stage. This technique seems more practical than staged grouting.

## **2.5 RESTRAINT SET-UPS**

Since during installation, the lining is subject to pressures due to grouting, a thicker lining or additional supports may be needed to avoid excessive deformation or overstressing of the lining. With man-entry sewers (height of lining greater than 900 mm), the performance of linings of different shapes such as egg-shaped, inverted egg-shaped, circular etc. is particularly sensitive to the type of support provided during grouting. Keeping this in mind, three support systems that may be used during installation have been considered in this study. The supports consist of hardwood wedges packed at different locations around the cross-section of the lining on the outside together with internal struts positioned at the same locations. *It is assumed that the packing between the sewer and the lining is closely spaced, so that the structure can be conveniently studied by means of a two-dimensional finite element model.* Closely spaced implies that the spacing of restraints installed during grouting along the length of the lining is around 1 to 1.5 meters. The three support systems to be considered in the subsequent analyses are shown in Fig. 2.2 with respect to egg-shaped sewer.

### **2.5.1 Boundary Condition 1:**

This case consists solely of a restraint at the crown (top) of the lining as shown in Fig. 2.2a. It is to be noticed here that normally grout is injected through the invert (bottom) of the lining. As grout moves forward and upward during injection, this may push the lining upward and thereby reduce the annulus gap between the sewer and the lining in the upper part of the sewer. This is why a restraint at the crown is always expected.



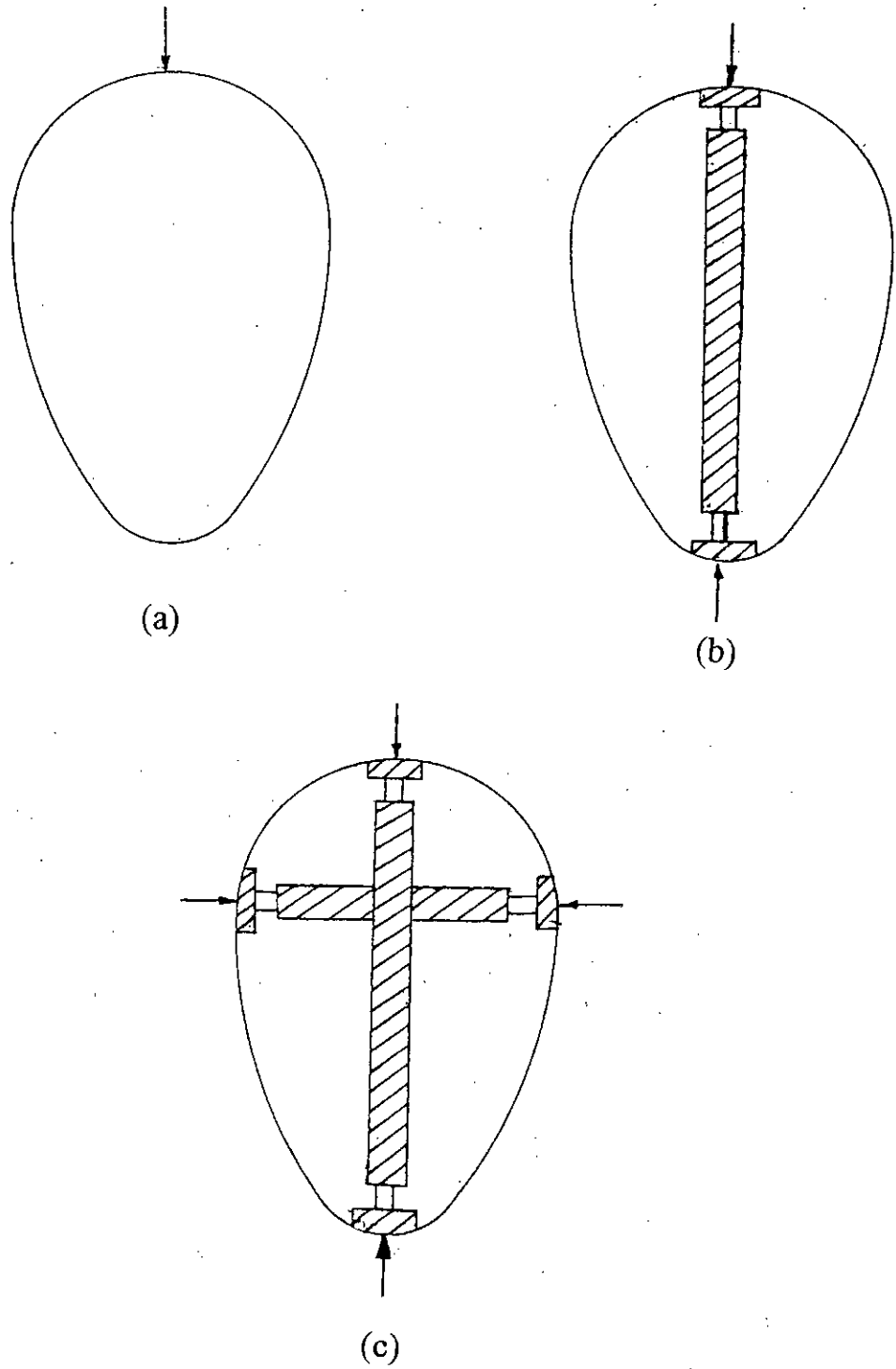


*Fig. 2.2: The support systems studied : (a) boundary case 1, (b) boundary case 2 and (c) boundary case 3*

### **2.5.2 Boundary Condition 2:**

The second support system as shown in Fig. 2.2b comprises restraints at both the crown and the invert of the lining. Like the boundary condition 1, boundary condition 2 imposes restraints on the vertical movement of sewers both at the crown and invert. This boundary condition is vertically stiffer than its former counterpart.

### **2.5.3 Boundary Condition 3:**

This form of support consists of restraints at the crown, invert and springings of the linings (Fig. 2.2c). In addition to vertical restraints, it restricts the horizontal and vertical movement of the lining at some specific points, as for example springings.

All the restraints mentioned under boundary cases 1, 2 and 3 are simulated numerically in the analysis by fixing the horizontal and vertical (not rotation) components of displacements at the nodes at which the struts are attached. *This involves a small approximation in that the deformation in the struts is ignored; the strut being very stiff in comparison to the lining.*

## **2.6 LOADING CONFIGURATIONS**

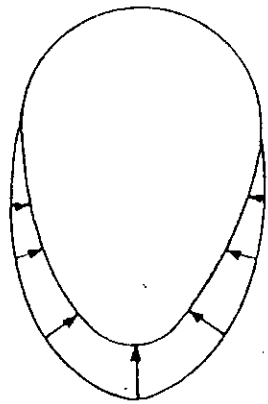
Three loading configurations are included in all the analysis unless otherwise specified. They are as follows:

### **Staged Grouting Pressure:**

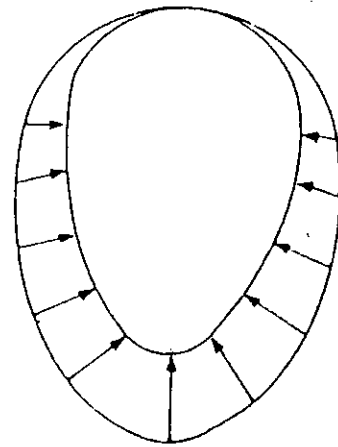
This corresponds to pressure from grout surrounding the lining up to the height of the springings, as shown in Fig 2.3a. This simulates the first phase of staged grouting.

### **Flotation Pressure:**

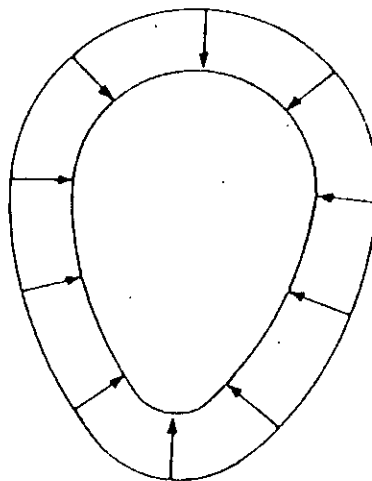
This type of load configuration involves a head of grout up to the crown as in Fig. 2.3b. In this situation, the lining is just covered by grout and hence the buoyancy force acting on the lining is the maximum that can occur. For this reason the loading corresponding to Fig 2.3b is sometimes called the flotation pressure.



(a)



(b)



(c)

*Fig. 2.3: The loading configurations studied: (a) staged grouting, (b) pressure up to crown only (flotation) and (c) uniform pressure*

### **Uniform Pressure:**

The third loading configuration as shown in Fig 2.3c corresponds to the uniform pressure which is being applied on the lining as a consequence of an excess head of grout. Flotation pressure and uniform pressure can be superimposed in order to simulate any grout pressure applied on the lining during full grouting as described earlier in Art. 2.4.

## **2.7 CALCULATION OF LOADS**

For each load configuration and boundary case, the parametric study is carried out by varying one parameter at a time, keeping the others constant. The results are most conveniently given in terms of dimensionless equations linking all the independent parameters together. Such equations are derived on the basis of a curve-fitting exercise. In considering this, it should be noted that, in the case of the loadings corresponding to flotation and the first phase of staged grouting, the applied load is defined by the lining height ( $h$ ) and the specific weight of grout mix ( $G$ ). In these two loading cases, the applied pressure at any point on the lining can be calculated by multiplying the specific weight of the grout mix to the distance from the top of the grouting to the point at which the pressure is calculated. For the uniform load case, on the other hand, the external load is defined by the values of excess head of grout ( $H$ ) and its specific weight but is independent of the height of the lining.

## **2.8 BASIS OF DESIGN**

During installation the lining is subjected to grout pressure. In some cases, this may lead to overstressing of the lining at different sections, which may cause total collapse of the linings. Alternatively, excessive deformation of any part of the lining (e.g. the flat portion of an egg-shaped sewer, the mid-portion of a circular sewer) might occur, affecting the serviceability of the relined sewer. Therefore, a properly designed sewer must satisfy both stress and deflection limit criteria. These criteria are explained below:

- Here the stress-limit criteria is so defined that the maximum bending stress developed during grouting must not exceed the allowable bending stress of the lining material.

- For deflection limit criteria, the limit recommended by Water Research Centre (1983) in its 'Sewerage Rehabilitation Manual' shall be followed. The manual limits the maximum allowable deflection in the lining at 3 percent of the width (w) of the lining.

## 2.9 PARAMETERS INVOLVED IN THE ANALYSIS

The parameters included in the subsequent analyses are divided into geometrical, material, and load parameters, which are as follows:

(a) Geometrical parameters (as shown in Fig. 3.1):

w = width of lining

h = height of lining

t = thickness of lining

(b) Material parameters:

$S_s$  = allowable short-term bending stress of lining material

$E_s$  = short-term modulus of elasticity of material

(c) Load parameters:

G = unit weight of grout mix

H = excess head of grout measured from crown of lining corresponding to uniform pressure load.

## 2.10 MATHEMATICAL FORMULATION OF THE ANALYSIS

As mentioned earlier, it is advantageous and convenient to express the results of the analysis in terms of non-dimensional equations with all the parameters involved in the analysis. Hence the design curves that will be proposed after the extensive parametric analysis on each of the lining of specific shape can be used for any arbitrary material property and lining geometry of that specific shape. The dimensionless equations corresponding to the bending stress (S) and the deflection ( $\delta$ ) at any point on the lining can be written as follows for all the loading cases.

(a) Staged Grouting (Fig. 2.3a)

$$\frac{S}{Gw} = A \left( \frac{w}{t} \right)^2 \quad (2.1)$$

$$\frac{\delta}{w} = (B_x^2 + B_y^2)^{1/2} K \quad (2.2)$$

(b) Flotation (or pressure up to the level of crown) (Fig. 2.3b)

$$\frac{S}{Gw} = C \left( \frac{w}{t} \right)^2 \quad (2.3)$$

$$\frac{\delta}{w} = (D_x^2 + D_y^2)^{1/2} K \quad (2.4)$$

(c) Uniform Pressure (excess head H) (Fig 2.3c)

$$\frac{S}{Gw} = E \left( \frac{H}{w} \right) \left( \frac{w}{t} \right)^2 \quad (2.5)$$

$$\frac{\delta}{w} = (F_x^2 + F_y^2)^{1/2} \left( \frac{H}{w} \right) K \quad (2.6)$$

$$\text{where } K = \left( \frac{Gw}{E_s} \right) \left( \frac{w}{t} \right)^3 \quad (2.7)$$

In these equations,  $\frac{S}{Gw}$  can be regarded as a non-dimensional stress while  $\frac{\delta}{w}$  is the deflection related to the size of the lining, K is a measure of lining flexibility. A, C, E and  $B_x$ ,  $B_y$ ,  $D_x$ ,  $D_y$ ,  $F_x$  and  $F_y$  are all constants which depend on the boundary set-up adopted during the grouting of the annulus and loading configurations used in the analysis. The respective values at any nodal points can be calculated by plotting above mentioned respective equations using a number of sets of data by varying parameters involved.

The total bending stress ( $S_t$ ) and the total deflection ( $\delta_t$ ) at any point in a lining subjected to a head of grout which is greater than the lining height (h) (i.e. full grout) can be divided into values of bending stress and deflection resulting from the two loading cases of pressure to the crown (i.e., flotation) and uniform pressure. This implies that by adding equation 2.3 and 2.5, and 2.4 and 2.6, the following dimensionless equations for the total bending stress and the total deflection can be written as

$$\frac{S_t}{Gw} = \left[ \left( C + E \left( \frac{H}{w} \right) \right) \left( \frac{w}{t} \right)^2 \right] \quad (2.8)$$

$$\frac{\delta_t}{w} = (M_x^2 + M_y^2)^{1/2} K \quad (2.9)$$

where

$$M_x = D_x + F_x \left( \frac{H}{w} \right) \quad (2.10a)$$

$$M_y = D_y + F_y \left( \frac{H}{w} \right) \quad (2.10b)$$

As mentioned earlier that maximum bending stress and the maximum deflection in a lining must not exceed the respective values of  $S_s$  and  $0.03 w$  and so the values of  $S_t$  and  $\delta_t$  in equations 2.8 and 2.9 can be replaced by  $S_s$  and  $0.03w$ , respectively. As the point of injection of the grout is usually located at the invert of the lining, it is convenient to replace the value of  $H$  in equations 2.8 and 2.9 by the equivalent expression  $\frac{P}{G} - h$ , where  $p$  is the allowable grouting pressure measured at the invert of the lining. As a final result equations 2.8 and 2.9 can be rewritten to produce the following design equations

$$R = \left| C + E \left( \frac{P}{Gw} - \frac{h}{w} \right) \right| \quad (2.11)$$

where,

$$R = \frac{S_s}{Gw} \left( \frac{t}{w} \right)^2 \quad (2.12)$$

and

$$\frac{0.03}{K} = \left( N_x^2 + N_y^2 \right)^{1/2} \quad (2.13)$$

where,

$$N_x = D_x + F_x \left( \frac{P}{Gw} - \frac{h}{w} \right) \quad (2.14a)$$

$$N_y = D_y + F_y \left( \frac{P}{Gw} - \frac{h}{w} \right) \quad (2.14b)$$

For any particular lining geometry and material properties, the above equations must be satisfied at the locations of maximum bending stress and deflection in the lining. This, in turn, will determine the maximum allowable grouting pressure ( $p$ ) which can be applied on the lining during installation.

## 2.11 METHODOLOGY OF THE SUBSEQUENT ANALYSES

An existing two-dimensional finite element model will be tailored to meet the requirements of the present research by incorporating new subroutines, especially for automated mesh generation. The performance of the model will be checked against existing numerical experiments.

Different linings (egg-shaped, inverted egg shaped, horseshoe shaped, semielliptical shaped, circular shaped) will be analyzed for different restraint set-ups and loading conditions which may arise during installation. For each combination of restraints and loading conditions, deflections and stresses are to be critically examined.

For each combination of loads and boundary cases as mentioned earlier, an extensive parametric study of the structural behaviour of linings of different shapes is to be carried out by varying one parameter at a time, keeping the others constant. The results can most conveniently be represented in forms of dimensionless equations linking all the parameters together as mentioned earlier. With the help of the above mentioned equations, an extensive design curves for each type of lining will be proposed. Finally, illustrative examples will be solved using the proposed design curves.



# CHAPTER 3

## STRUCTURAL BEHAVIOUR OF EGG-SHAPED SEWER LININGS

### 3.1 INTRODUCTION

This chapter summarizes the results of an analytical study of the two-dimensional structural behaviour of closely packed egg-shaped sewer linings subjected to different hydrostatic pressures during installation and under different point restraint conditions. The basis of analysis, kind of restraints, and configurations of loadings have already been discussed in the Chapter 2. A full parametric study has been carried out and the findings have been thoroughly discussed and summarized by means of equations and design curves. The usage of these plots and/or design curves are illustrated by means of an example at the end of this chapter.

### 3.2 TWO-DIMENSIONAL FINITE ELEMENT DESCRETIZATION

The shape of the lining used in the present study is shown in Fig. 3.1. The height, width and thickness of the lining are  $h$ ,  $w$  and  $t$ , respectively, as are depicted in the figure. This lining section is primarily composed of two circles of radius  $h/3$  and  $h/6$  interconnected by an arc of a circle of radius  $h$ . Hence the lining height ( $h$ ) is equal to 1.5 times the width ( $w$ ) of the lining (i.e.  $h/w = 1.5$ ). This section is divided into as much as twenty two-noded beam elements as shown in Fig. 3.2. On account of symmetry around the vertical axis of both the geometry and the loading configuration, only half of the cross-section is analyzed. This part of the structure consists of ten two-noded beam elements as shown in Fig. 3.3. It is worth mentioning that the number of finite elements (FE) adopted in the analysis follows that of a pioneering work by Arnaout, Pavlovic and Dougill (1988). In fact, in the present chapter the work of Arnaout, et. al. (1988) has been mimicked using the two-dimensional model of Seraj (1986) in an effort to validate the present model prior to using it in studying the behaviour of closely packed sewer linings having (a) inverted egg, (b) horseshoe, (c) semielliptical and (d) circular shaped linings.

The support systems considered in the analysis were shown in Fig. 2.2. The restraints are simulated numerically by fixing the horizontal and vertical components of displacement at the corresponding nodal points at which the struts

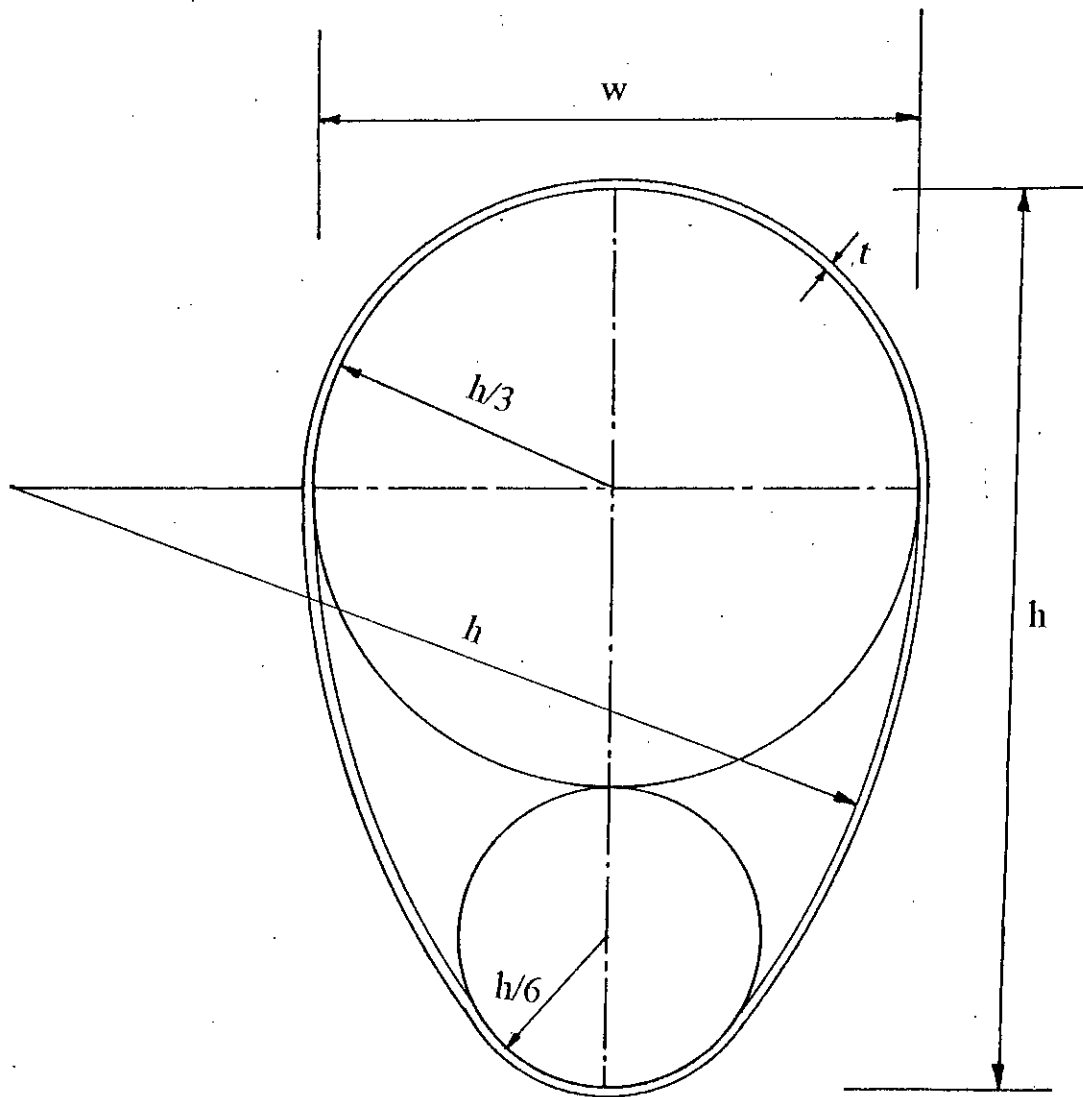


*Fig. 3.1: Shape of sewer lining used in the analysis*

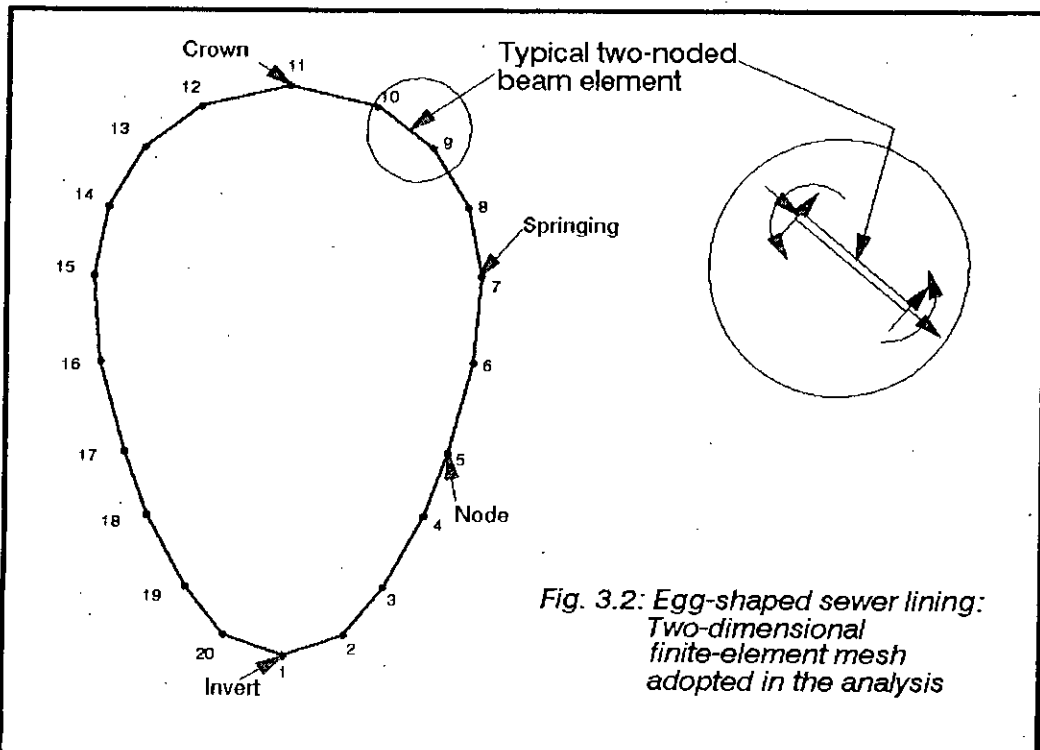


Fig. 3.2: Egg-shaped sewer lining: Two-dimensional finite-element mesh adopted in the analysis

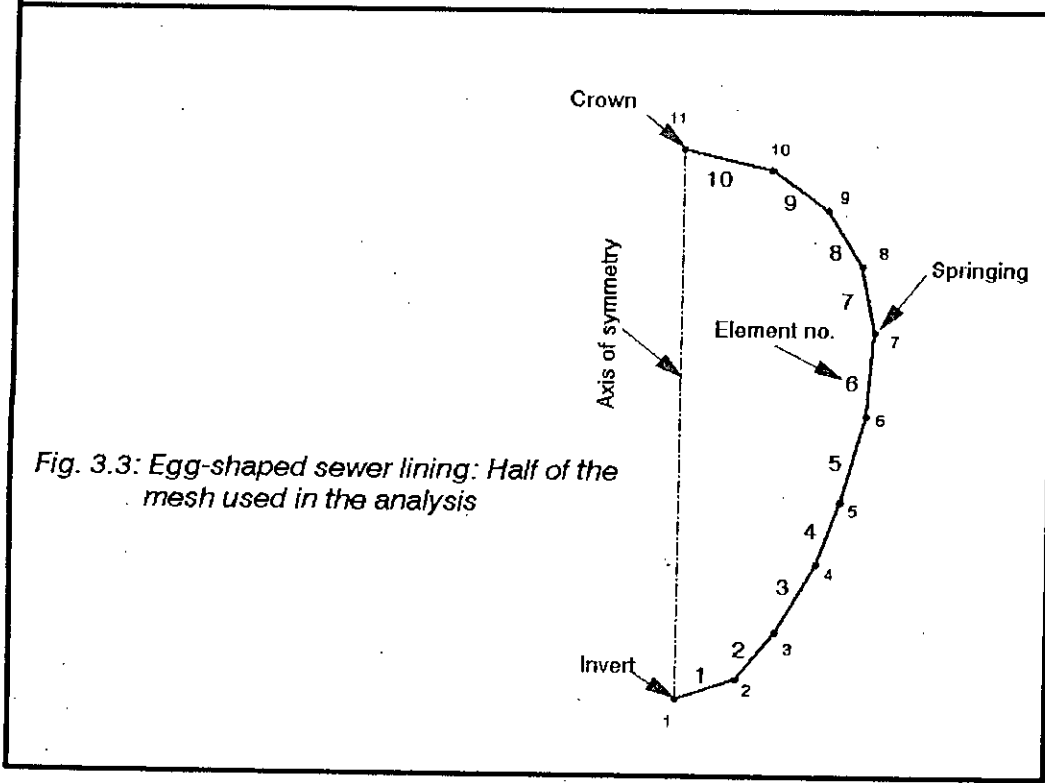


Fig. 3.3: Egg-shaped sewer lining: Half of the mesh used in the analysis

are connected with the lining. This can be explained by taking any one of the three support systems. Here, the third support system (Fig. 2.2c) has been considered for this purpose. The horizontal and vertical components are restrained at node number 7 to which the horizontal strut is joined, and node numbers 1 and 11 (to which the vertical strut is connected). It is to be noted here that the horizontal and rotational components of displacement are restrained at node no 1 and 11 as half of the lining section is taken in the analysis due to symmetry of the structure as mentioned earlier. All the three loading conditions that may arise during grouting (shown in Fig 2.3) have been taken into consideration in the following analysis.

### 3.3 DATA USED IN THE ANALYSIS

The data used in the present parametric analysis are given in Table 3.1. Six sets of data of varying width (w), height (h), and thickness (t) have been employed. Modulus of elasticity of the lining material ( $E_s$ ), Unit weight of grout (G) and the Poisson's ratio ( $\nu$ ) are taken constant throughout the study. One, readily, can vary these values to obtain the same result as given below in Table 3.2 and 3.3. It is to be noticed that for each constant of these two tables, a graph is plotted taking six points which come from six separate computer runs of the program taking six different sets of data.

**Table 3.1: Data used in the analysis**

|                            | 1st Set            | 2nd Set            | 3rd Set            | 4th Set            | 5th set            | 6th set            |
|----------------------------|--------------------|--------------------|--------------------|--------------------|--------------------|--------------------|
| w (mm)                     | 550.0              | 605.0              | 495.0              | 550.0              | 605.0              | 495.0              |
| h (mm)                     | 825.0              | 907.5              | 742.5              | 825                | 907.5              | 742.5              |
| t (mm)                     | 6                  | 6                  | 6                  | 10                 | 10                 | 10                 |
| $E_s$ (kN/m <sup>2</sup> ) | $15.0 \times 10^6$ | $15.0 \times 10^6$ | $15.0 \times 10^6$ | $15.0 \times 10^6$ | $15.0 \times 10^6$ | $15.0 \times 10^6$ |
| G (kN/m <sup>3</sup> )     | 16.5               | 16.5               | 16.5               | 16.5               | 16.5               | 16.5               |
| $\nu$                      | 0.23               | 0.23               | 0.23               | 0.23               | 0.23               | 0.23               |

### 3.4 COMPUTATION OF VARIOUS CONSTANTS

As mentioned earlier, the value of any one of the constants A, C, E,  $B_x$ ,  $B_y$ ,  $D_x$ ,  $D_y$ ,  $F_x$ ,  $F_y$  can be calculated at any nodal point of the FE model by using equations 2.1 to 2.14 in conjunction with the results obtained from the analysis. However, the point or points at which maximum bending stress and maximum deflection occur

are of primary importance. With this view in mind, the respective values of the constants are calculated at the locations of maximum bending stress and maximum deflection; these are shown in Table 3.2 and Table 3.3 respectively. The curves from which these values are determined are shown in Figs. 3.4, 3.5, 3.6, 3.7, 3.8 and 3.9. It may be recalled that the relationships on which Figs. 3.4 to 3.9 have been drawn, were derived on the basis of a curve fitting exercise.

**Table 3.2: Dimensionless constants for the maximum bending stress in the lining. (Note: Positive values of A, C and E imply tensile stresses at the inner surface of the lining)**

| Loading type     | Constants | Boundary Case 1 | Boundary Case 2 | Boundary Case 3 |
|------------------|-----------|-----------------|-----------------|-----------------|
| Staged Grouting  | A         | 0.614 Node 11   | -0.333 Node 1   | 0.085 Node 1    |
|                  |           |                 |                 |                 |
| Flotation        | C         | 0.668 Node 11   | 0.556 Node 11   | 0.213 Node 1    |
|                  |           | -0.355 Node 1   |                 |                 |
| Uniform pressure | E         | -0.363 Node 11  | 0.378 Node 11   | 0.261 Node 1    |
|                  |           | -0.697 Node 1   |                 |                 |

**Table 3.3. Dimensionless constants for the maximum inward deflection in the lining. (Note: Inward deflections are taken as positive )**

| Loading type     | Coefficient | Boundary Case 1 | Boundary Case 2 | Boundary Case 3 |
|------------------|-------------|-----------------|-----------------|-----------------|
| Staged Grouting  | $B_x$       | -0.052 Node-7   | 0.025 Node 5    | 0.00176 Node 4  |
|                  | $B_y$       | -0.061 Node 7   | 0.021 Node 5    | 0.00049 Node 4  |
| Flotation        | $D_x$       | 0.035 Node 5    | 0.048 Node 5    | 0.00545 Node 5  |
|                  |             | 0.012 Node 6    |                 |                 |
|                  | $D_y$       | 0.052 Node 5    | 0.037 Node 5    | 0.001 Node 5    |
|                  |             | 0.046 Node 6    |                 |                 |
| Uniform Pressure | $F_x$       | 0.140 Node 6    | 0.0335 Node 5   | 0.0073 Node 5   |
|                  |             | 0.127 Node 5    |                 |                 |
|                  | $F_y$       | -0.075 Node 6   | 0.0221 Node 5   | 0.0001 Node 5   |
|                  |             | -0.0774 Node 5  |                 |                 |

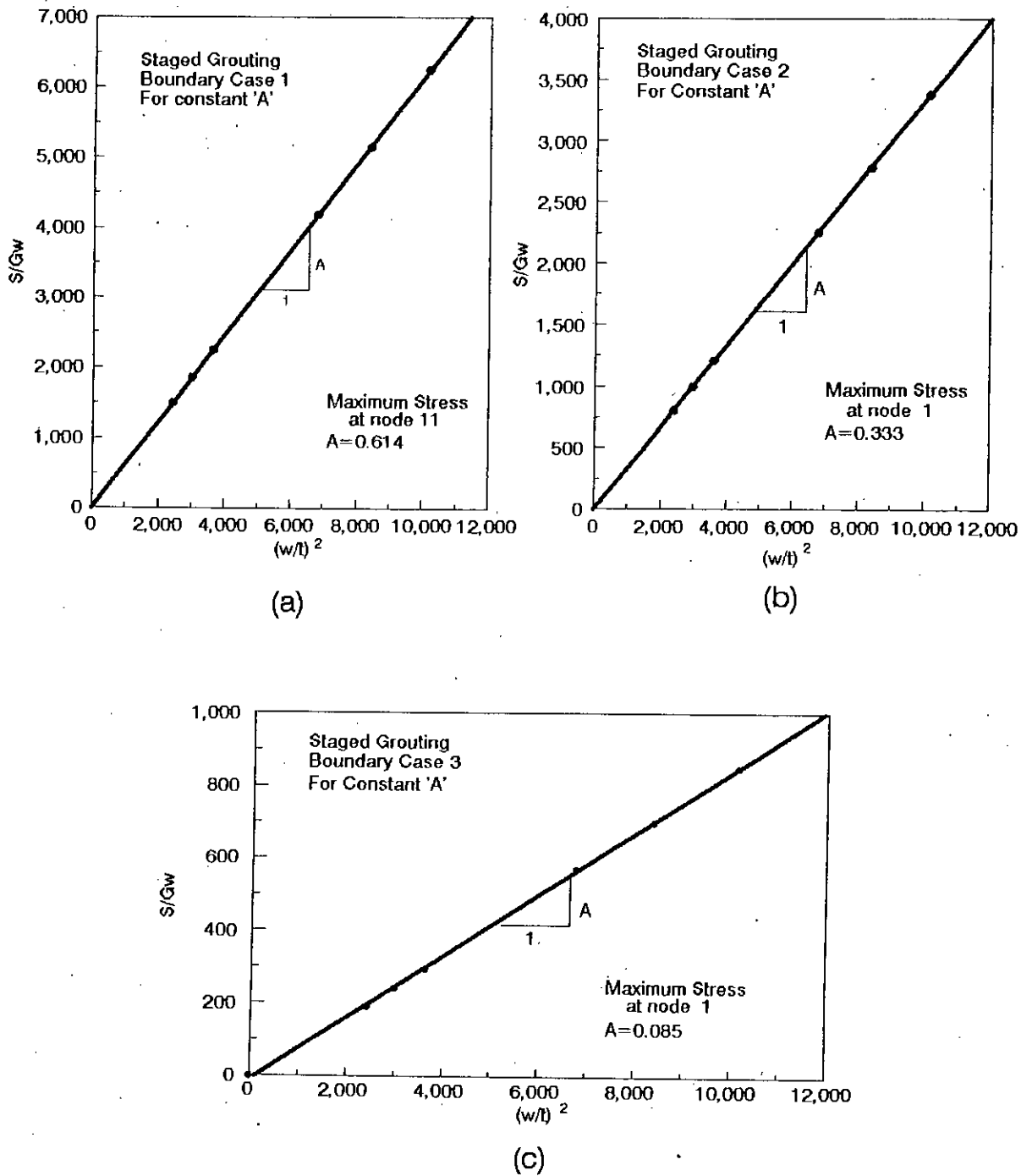
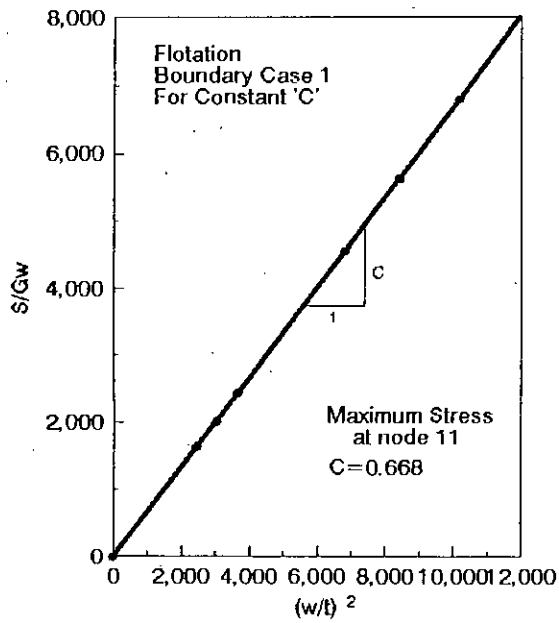
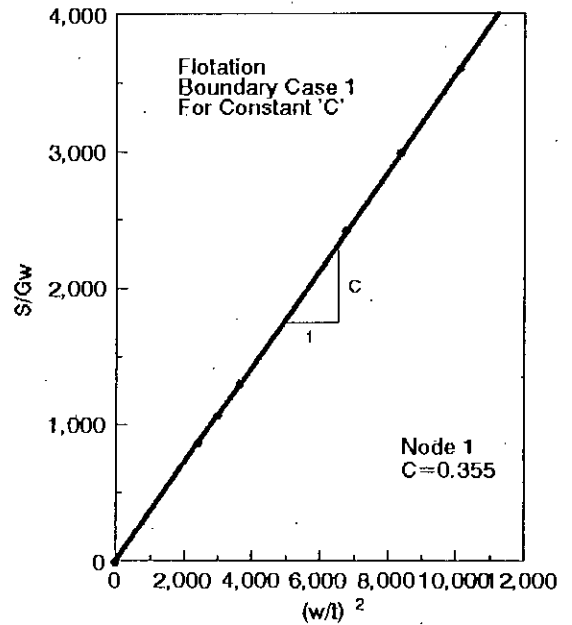


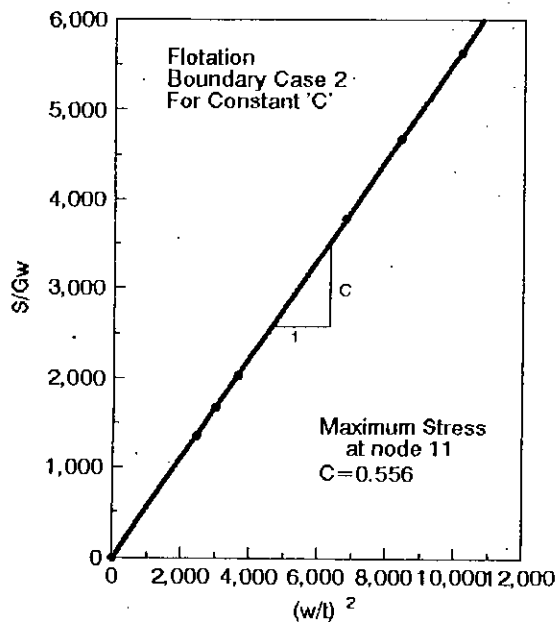
Fig. 3.4: Egg-shaped sewer lining: Determination of the constant 'A' for staged grouting for (a) boundary case 1, (b) boundary case 2 and (c) boundary case 3



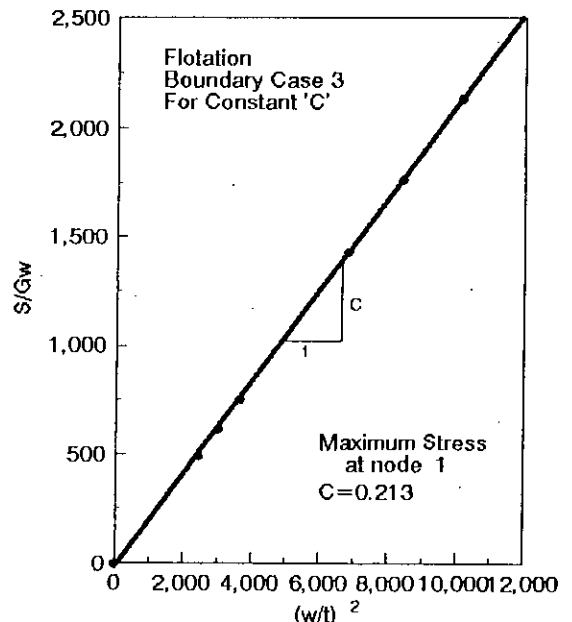
(a)



(b)

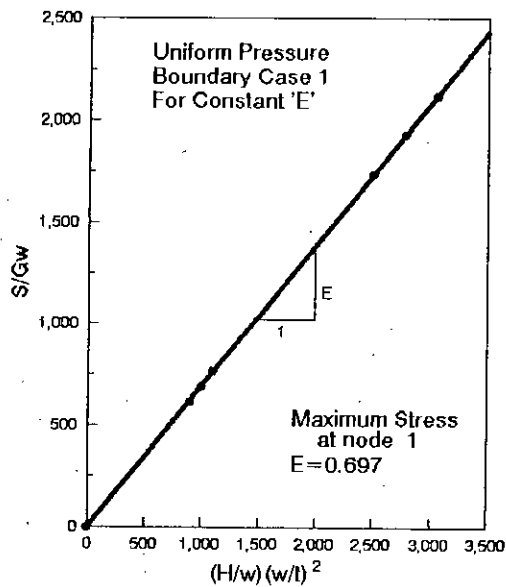


(c)

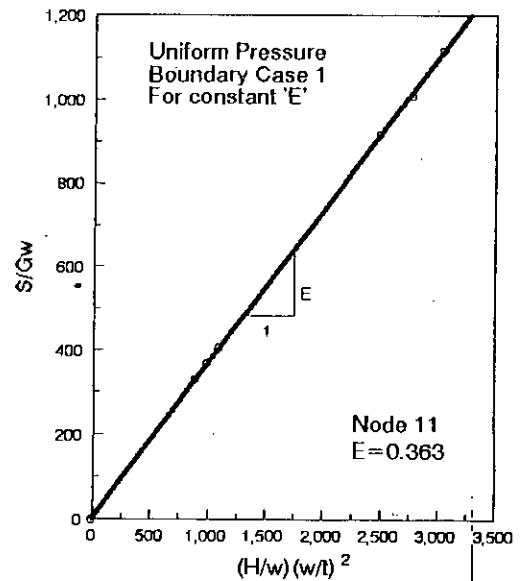


(d)

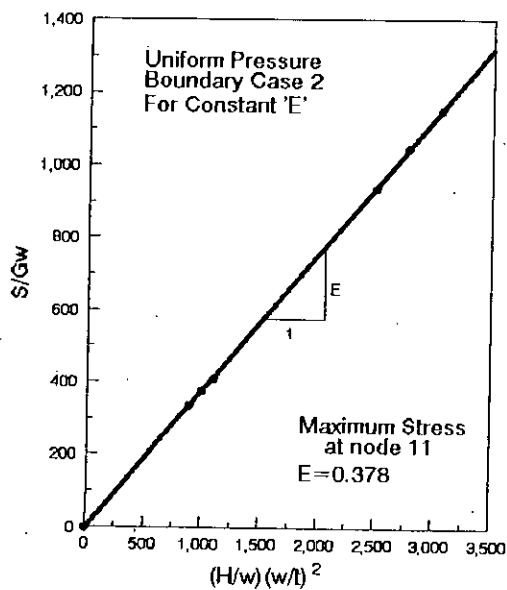
Fig. 3.5: Egg-shaped sewer lining: Determination of the constant 'C' for flotation load for (a) boundary case 1 (node 11), (b) boundary case 1 (node 1), (c) boundary case 2 (node 11), and (d) boundary case 3



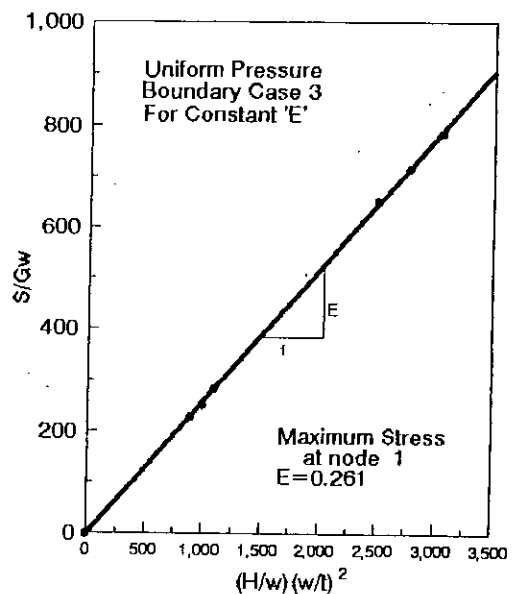
(a)



(b)



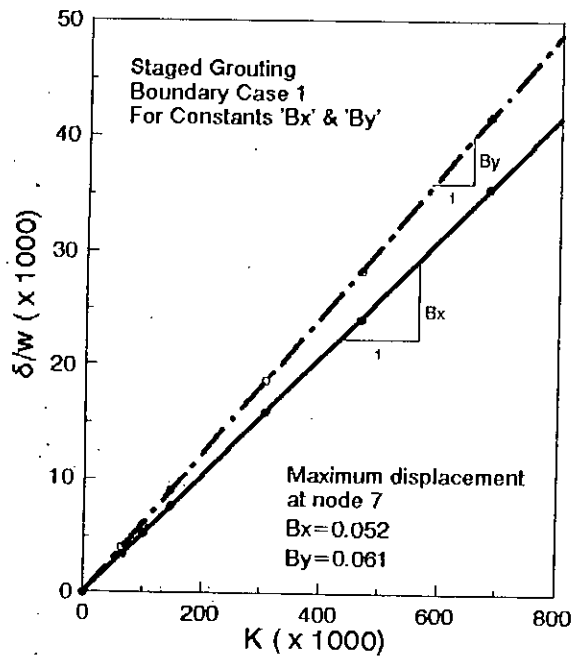
(c)



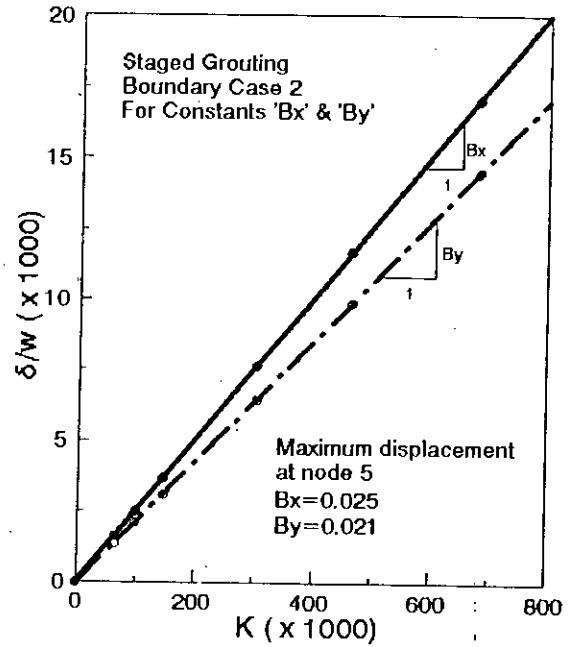
(d)

Fig. 3.6: Egg-shaped sewer lining: Determination of the constant 'E' for uniform pressure for (a) boundary case 1 (node 1), (b) boundary case 1 (node 11), (c) boundary case 2 and (d) boundary case 3

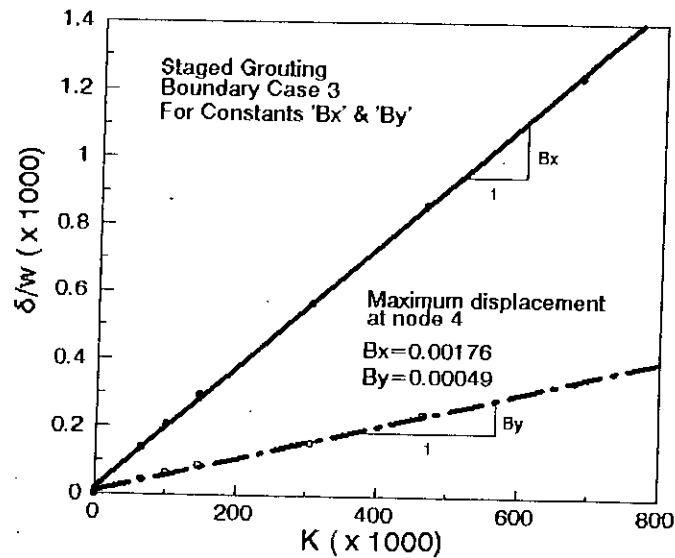




(a)

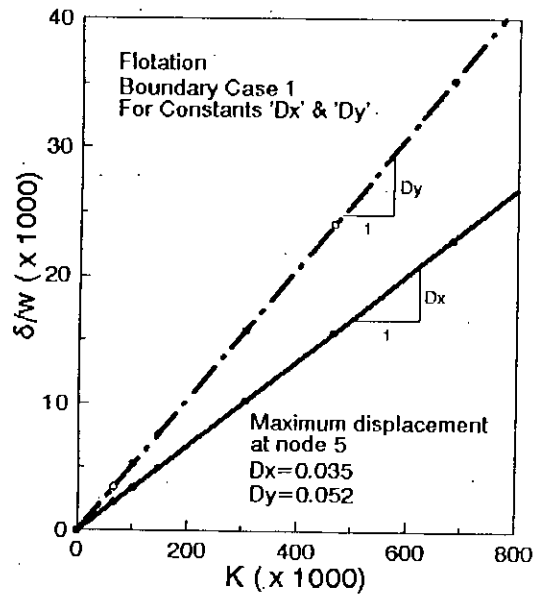


(b)

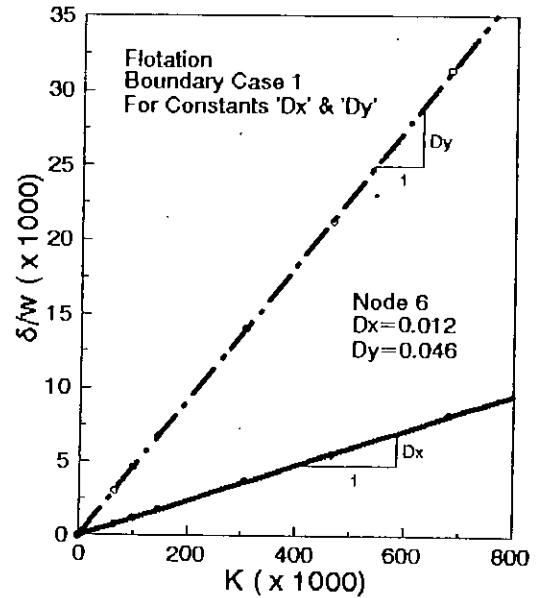


(c)

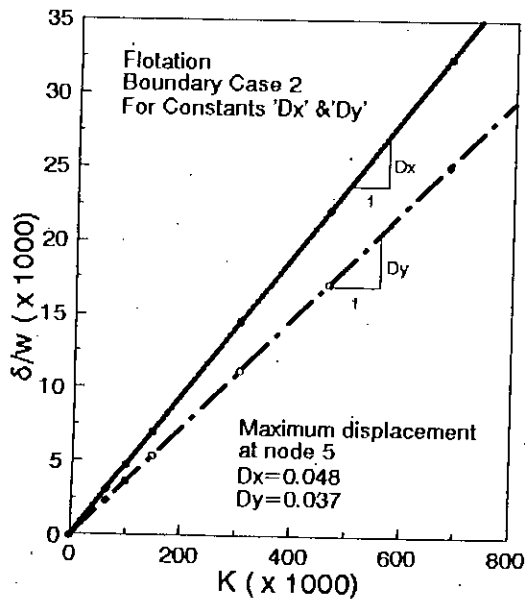
Fig. 3.7: Egg-shaped sewer lining: Determination of the constants 'Bx' and 'By' for staged grouting for (a) boundary case 1, (b) boundary case 2 and (c) boundary case 3



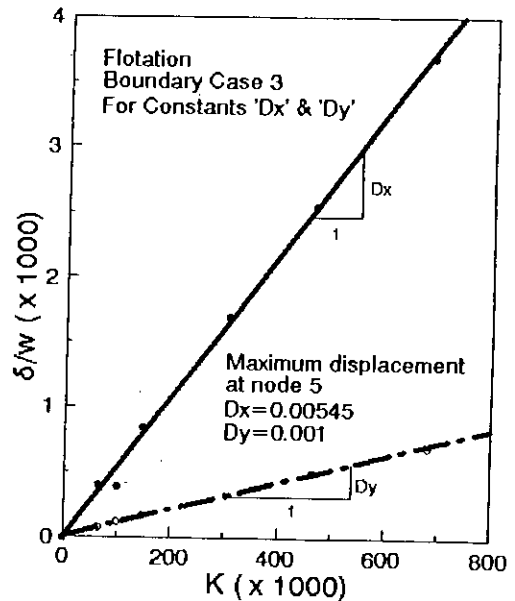
(a)



(b)

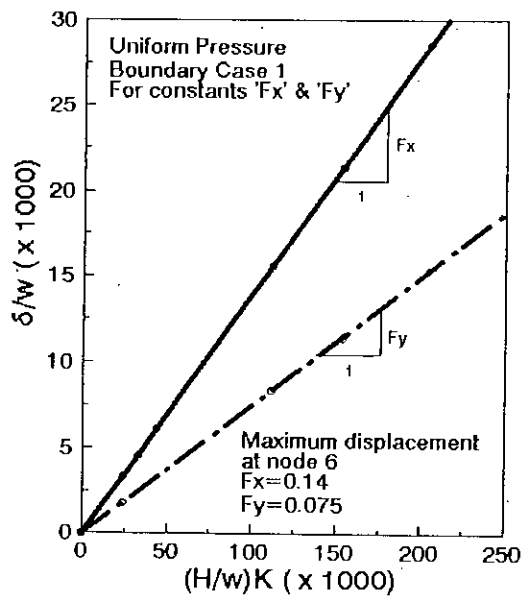


(c)

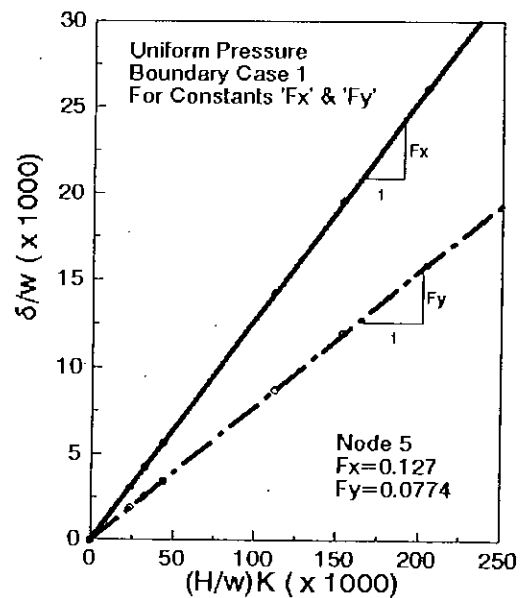


(d)

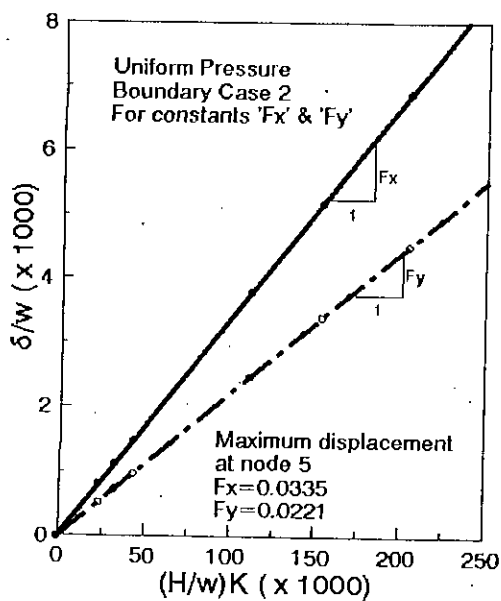
Fig. 3.8: Egg-shaped sewer lining: Determination of the constants 'Dx' and 'Dy' for flotation load for (a) boundary case 1 (node 5), (b) boundary case 1 (node 6), (c) boundary case 2, and (d) boundary case 3



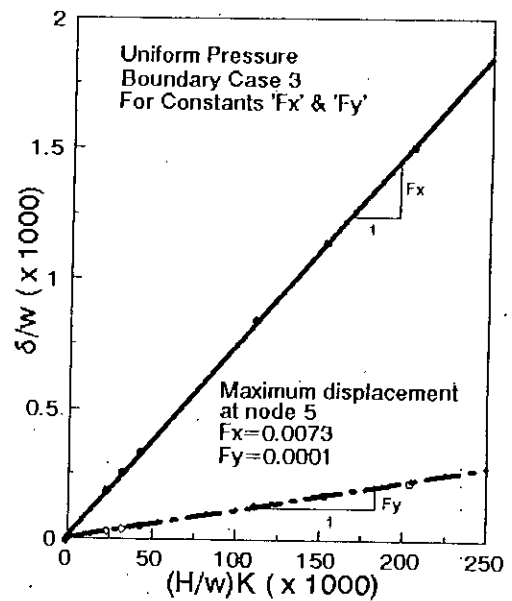
(a)



(b)



(c)



(d)

Fig. 3.9: Egg-shaped sewer lining: Determination of the constants 'Fx' and 'Fy' for uniform pressure for (a) boundary case 1 (node 6), (b) boundary case 1 (node 5), (c) boundary case 2 and (d) boundary case 3

From the aforementioned discussion it is clear that for any particular geometry, material properties and loading conditions, equations 2.1, 2.2, 2.3, 2.4, 2.11, and 2.13 must be satisfied at the location of maximum bending stress and maximum deflection in the lining in order to have satisfactory design solution. This can be restated in another way that these equations will determine the maximum allowable grouting pressure  $p$  that can be applied on the lining during installation if all the other parameters are known.

### 3.5 FULL GROUTING DESIGN CURVES

#### 3.5.1 Stress-Limit Criteria

##### *Boundary Case 1: Restrained at crown against flotation*

In this boundary case, the values of bending stress constants for different loading conditions are shown in the third column of Table 3.2. It can be seen from Table 3.2 that in case of staged grouting the maximum bending stress is located at node 11 and this stress value is less than the maximum bending stress developed in flotation case (grout up to the crown level).

It can further be seen from Table 3.2 that the maximum bending stress in the lining resulting from flotation load is located at the crown of the lining, i.e. at node 11, whereas, in the case of uniform pressure load the maximum bending stress location is at the invert of the lining, i.e. at node 1. This suggests that in the case of full grouting, equation 2.11 must be satisfied at both the nodes 1 and 11 of the lining. Here, it is to be noted that the combined bending stress at other nodes were computed and were found to be less critical than those at nodes 1 and 11. This leads to the following design equations:

At node 11,

$$R = \left| \left\{ 0.668 + (-0.363) \left( \frac{P}{G_w} - 1.5 \right) \right\} \right|$$

$$= \left| -0.363 \frac{P}{G_w} + 1.2125 \right| \quad (3.1)$$

and at node 1,

$$R = \left| -0.355 - (0.697) \left( \frac{P}{G_w} - 1.5 \right) \right|$$

$$= \left| -0.697 \frac{P}{G_w} + 0.6905 \right| \quad (3.2)$$

The design equations 3.1 and 3.2 are graphically shown in Fig. 3.10.

It emerges from Fig. 3.10 and Table 3.2 that a minimum value of R equal to 0.668 is needed in order for the lining to withstand the maximum bending stress at the crown resulting from the flotation load alone.

Furthermore, it is also shown that the allowable grouting pressure resulting from equation 3.2 (at node 1) becomes predominant throughout the full range of R once its value exceeds 0.668, so that, in fact, it is the bending stress at node 1 which is always critical in case of full grouting load.

It is noted that staged grouting becomes never critical in comparison to full grouting. However, if the relevant permissible pressures associated with this type of loading is required, it can readily be obtained by means of equation 2.1 and Table 3.2.

**Boundary Case 2: *Restrained at both the crown and the invert:***

For this case, the values of relevant constants are shown in the fourth column of Table 3.2. It shows that maximum bending stress in the lining resulting from staged grouting occurs at node 1 and the value is less than that resulting from flotation load in which the maximum stress develops at node 11. If the allowable bending stress is needed for staged grouting, it can easily be obtained from equation 2.1 and Table 3.2, as before (Boundary Case 1).

It can also be noticed that the maximum bending stress in the lining resulting from each of the two loading components i.e. flotation and uniform load, is located at the crown of the lining (at node 11). This implies that equation 2.11 must be satisfied at node 11 of the lining, leading to the following design expression

$$R = \left| \left\{ 0.556 + (0.378) \left( \frac{P}{Gw} - 1.5 \right) \right\} \right|$$

$$= \left| -0.378 \frac{P}{Gw} + 0.011 \right| \quad (3.3)$$

where,  $\frac{P}{Gw} \geq 1.5$  i.e.  $\frac{P}{G} \geq h$  holds, because, as for boundary case 1, a full head of grout must be imposed for the critical condition to be realized.

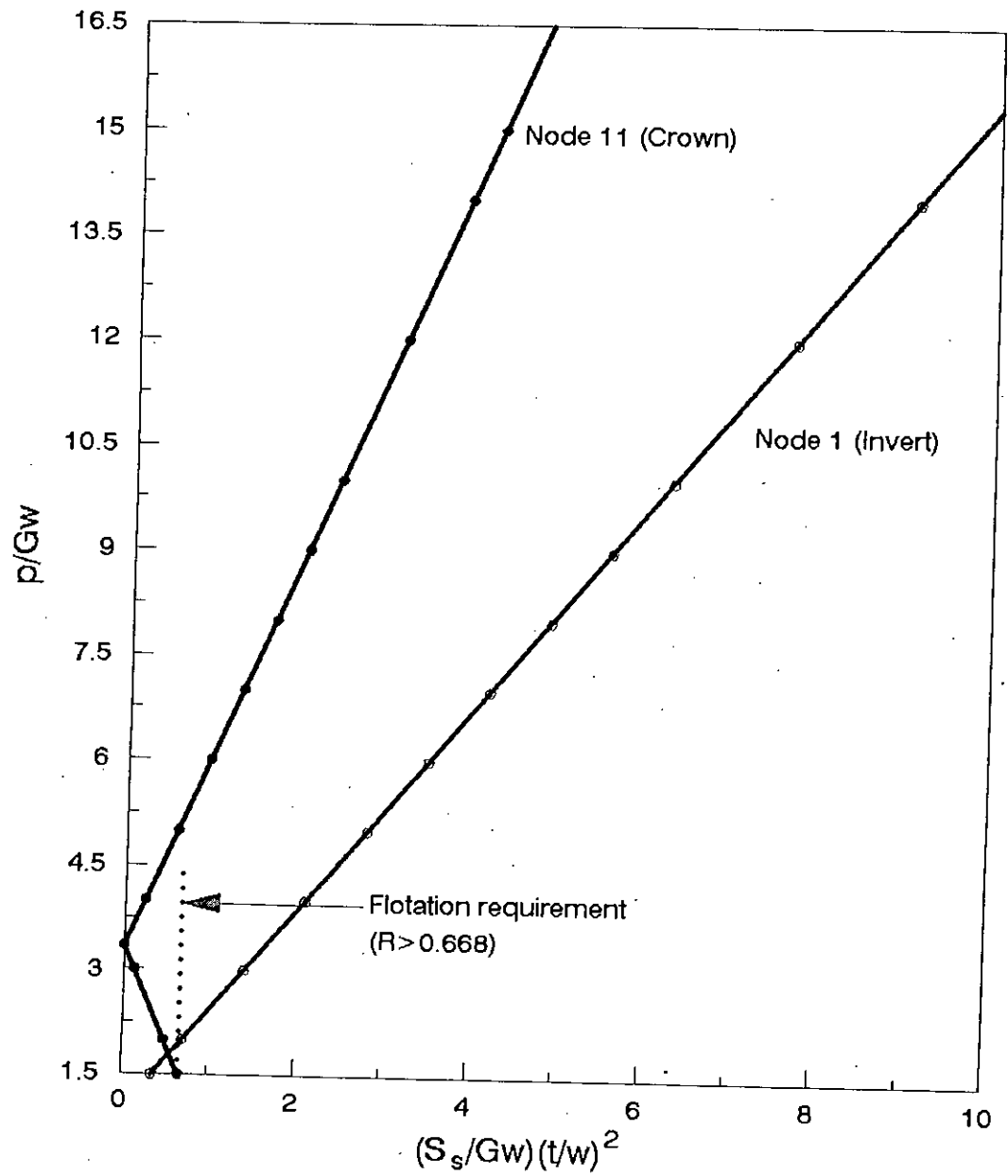


Fig. 3.10: Egg-shaped sewer lining: Maximum bending stress at the crown and invert of lining for flotation ( $p/Gw=1.5$ ) and additional external pressure for boundary case 1

### **Boundary Case 3: Restrained at crown, invert, and springing:**

Once again, similar to the previous two boundary cases, the maximum stress developed in staged grouting has been found to be less critical than the maximum stress developed during flotation load. If any parameter is required (the others must be known) in the former case, this can be readily obtained as before.

For the present boundary case, the maximum bending stress is located at the invert i.e. at node 1 of the lining for both the flotation and uniform pressure cases. Hence, by using Table 3.2 and equation 2.11 at node 1, the following design equation can be written.

$$\begin{aligned} R &= \left| \left\{ 0.213 + (0.261) \left( \frac{P}{Gw} - 1.5 \right) \right\} \right| \\ &= \left| 0.261 \frac{P}{Gw} - 0.1785 \right| \end{aligned} \quad (3.4)$$

where  $\frac{P}{Gw} \geq 1.5$  i.e.  $\frac{P}{G} \geq h$  holds, because it is the full grouting pressure (and not the partial grouting) which causes the critical stress condition in the lining as before for boundary cases 1 and 2.

### **Summary of Stress-Limit Criteria**

Figure 3.11 provides a summary for the above three boundary conditions. It is interesting to note from the figure that, for a small range of  $R$  between 0.668 and 0.794, for a particular grouting pressure the maximum bending stress resulting from boundary condition 2 is slightly greater than the one corresponding to boundary condition 1. This implies that for this range of material and geometrical parameters, boundary condition 2 is more critical than the boundary condition 1, although the fixity in the former condition is higher than that of the latter.

Once the value of  $R$  becomes greater than 0.794, for a particular lining geometry, material characteristics and grouting pressure, the boundary condition 1 becomes more critical than the boundary condition 2. Again, for a particular lining geometry and material properties, boundary condition 3 provides more allowable grouting pressure to be withstood than that of boundary conditions 1 and 2.

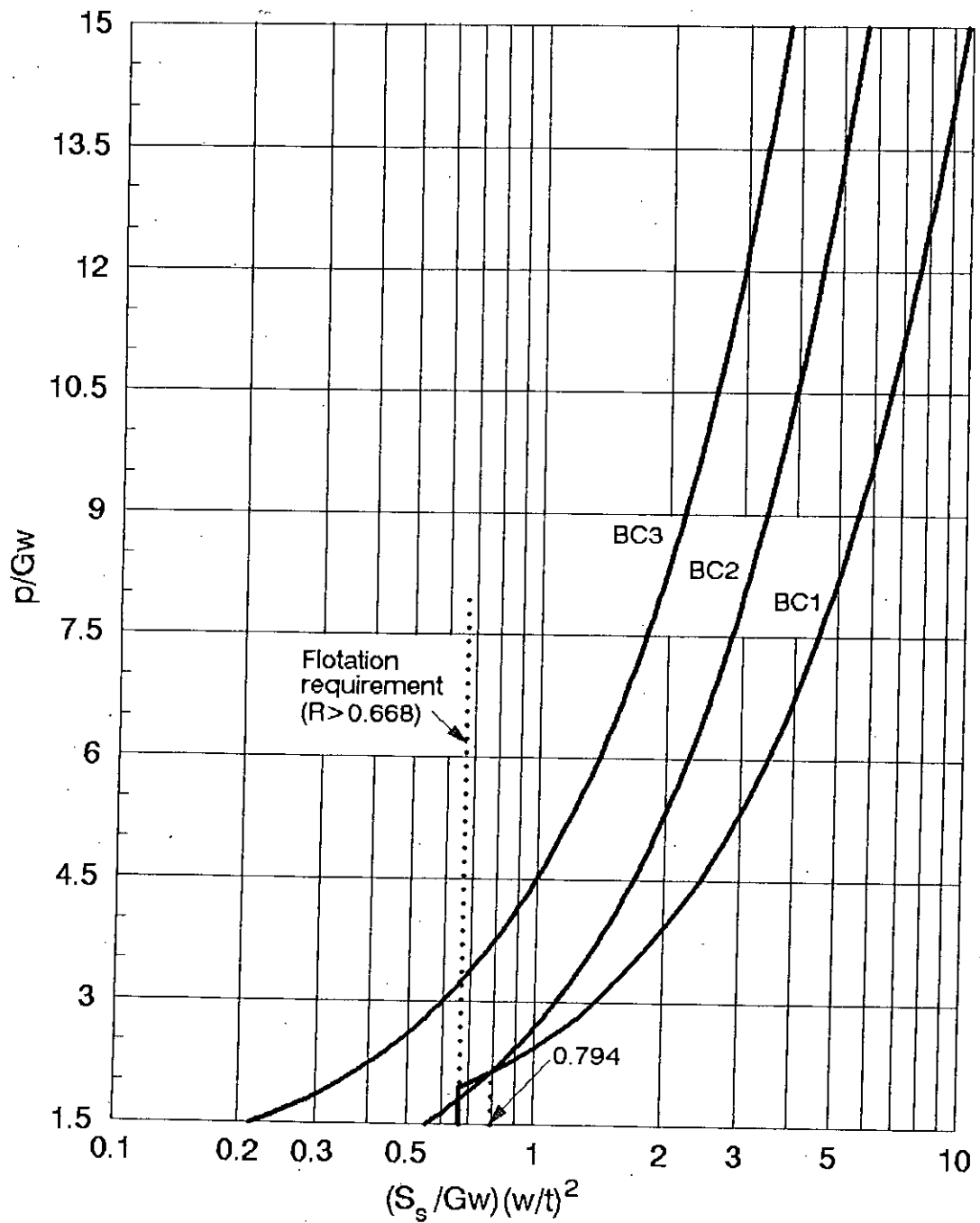


Fig. 3.11: Egg-shaped sewer lining: Allowable grouting pressure, based on the stress limit criteria for various boundary cases



Here another point is to be carefully noticed that unlike the cut-off for boundary case 1 at an abscissa value of 0.668, boundary condition 2 and 3 have characteristics which gradually reach the horizontal axis at the cut-off values of 0.556 and 0.213, respectively.

Once a boundary case is selected, and the geometrical and material parameters are chosen, a value of allowable grouting pressure based on the stress limit criteria can readily be determined using Fig. 3.11. In fact, the allowable grouting pressure is not the only parameter which can be determined from these design curves, any one of the parameters involved can be derived from these curves when the other parameters are chosen within a practically feasible range. Thus, if a designer needs the thickness of the lining, the designer must decide earlier how much pressure is going to be applied on the lining, the width of the egg-shaped lining, and the allowable bending stress of the lining material.

### 3.5.2 Deflection-Limit Criteria

#### **Boundary Case 1: *Restrained against flotation only:***

In this case the values of relevant constants are tabulated in the third column of Table 3.3. It is interesting to note from Table 3.3 that the maximum deflection in the lining resulting from staged grouting is greater than the one resulting from flotation load alone because the magnitude of the square root of  $B_x$  and  $B_y$  (0.08) is higher than that of the  $D_x$  and  $D_y$  (0.063). This leads to the requirement in both the cases of flotation and full grouting load that a minimum value of abscissa equal to 0.08 is needed in order for the lining to withstand the maximum allowable deflection of 3 percent of  $w$ .

Hence it is apparent that full flotation and uniform pressure cases become critical beyond the value of  $0.03/K$  equal to 0.08. From the analysis it is seen that, in case of full flotation, maximum displacement occurs at node 5, whereas that for the uniform pressure case occurs at node 6. This implies that from design point of view equation 2.13 must be satisfied at both nodes 5 and 6 for full-grouting. This leads to the following design equations:

At node 5,

$$\begin{aligned} N_x &= D_x - 1.5F_x + F_x \left( \frac{P}{Gw} \right) \\ &= 0.035 - 1.5 \times 0.127 + 0.127 \left( \frac{P}{Gw} \right) \end{aligned}$$

$$\begin{aligned}
&= -0.1555 + 0.127 \frac{P}{G_w} \\
N_y &= D_y - 1.5F_y + F_y \left( \frac{P}{G_w} \right) \\
&= 0.052 - 1.5(-0.0774) - 0.0774 \left( \frac{P}{G_w} \right) \\
&= 0.1681 - 0.0774 \frac{P}{G_w}
\end{aligned}$$

Thus from equation 2.13, after detailed calculation as given in Appendix 1, the following relationship can be found:

$$\frac{0.03}{K} = 0.148 \frac{P}{G_w} - 0.161 \tag{3.5}$$

Similarly, at node 6, the following relationship holds

$$\frac{0.03}{K} = 0.159 \frac{P}{G_w} - 0.19 \tag{3.6}$$

Equation 3.5 and 3.6 are pictorially shown in the Fig. 3.12. It is realized from Fig. 3.12 that for values of  $\frac{0.03}{K}$  between 0.08 and 0.2858 ( $0.08 \leq \frac{0.03}{K} \leq 0.2858$ ), the maximum deflection occurs at node 5, but for values of  $\frac{0.03}{K}$  greater than 0.2858 the deflection at node 6 becomes predominant. This can be restated in other words that equation 3.5 is valid for  $1.5 < \frac{P}{G_w} < 3.0$  and equation 3.6 is valid for  $\frac{P}{G_w} > 3.0$ . At the same time these two equations corresponding to partial grouting must always be satisfied for  $\frac{0.03}{K} \geq 0.08$  as explained before.

### **Boundary Case 2: Restrained both at crown and invert**

In this boundary condition, for the case of partial grouting, the maximum deflection which occurs at node 5, is less than that of flotation load and uniform pressure case; hence this proves to be less critical. If because of installation technique, the allowable pressure or other parameters are required, it can be found easily by means of equation 2.2 and Table 3.3.

The maximum deflection in the lining resulting from the combined effect of flotation and uniform pressure loads, is located at node 5 of the lining, because for both the individual cases, the maximum displacement occurs at node 5 and they are of the same sense. This suggests that for values of  $\frac{P}{G_w}$  which is equal to or

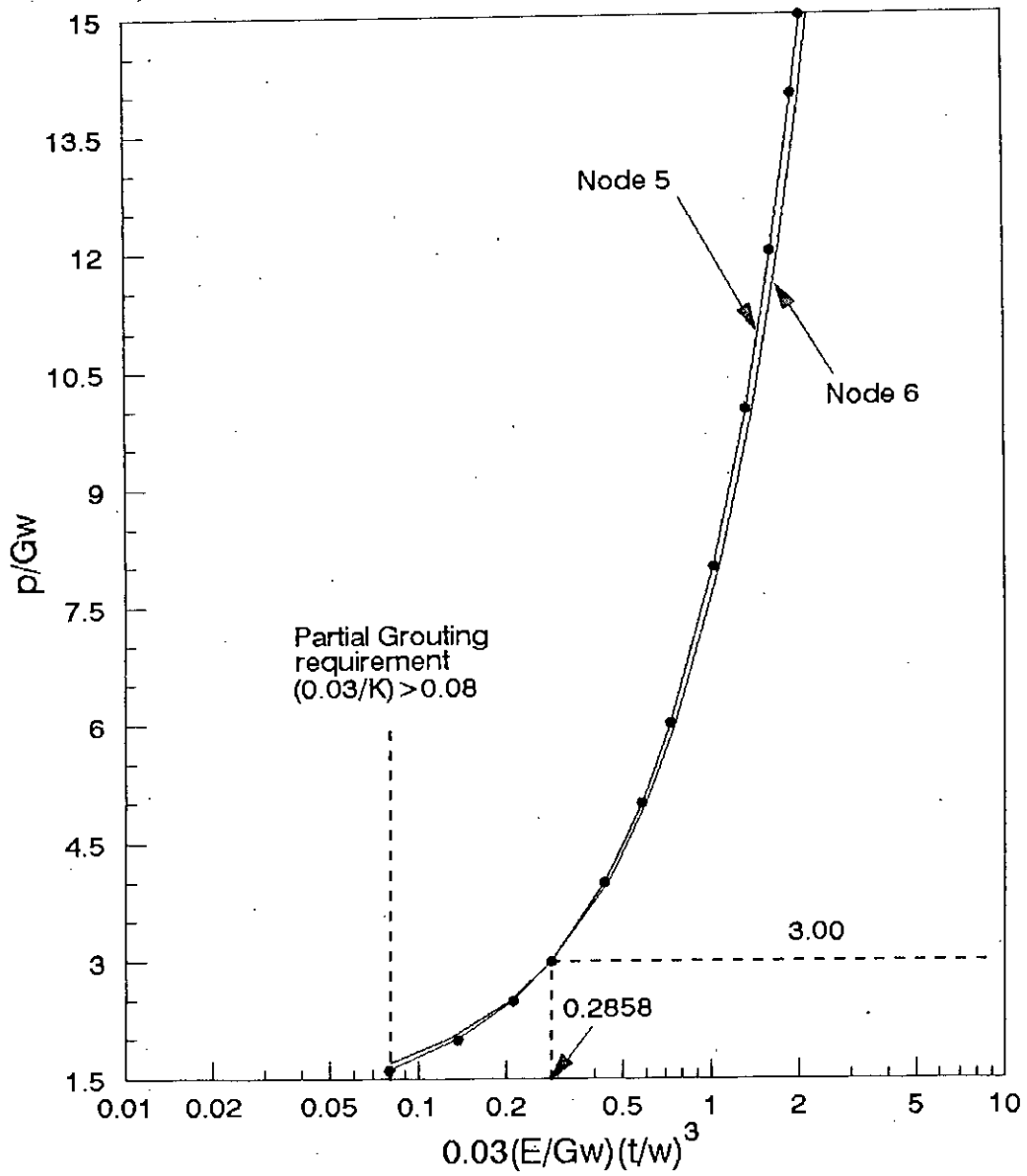


Fig.: 3.12: Egg-shaped sewer lining: Maximum deflection at node 5 and 6 of the lining for full flotation ( $p/Gw=1.5$ ) and additional external pressure for boundary case 1

greater than 1.5 equation 2.13 must be satisfied at node 5. As a result the following design equation can be written:

$$\frac{0.03}{K} = 0.04 \frac{P}{Gw} + 0.0002 \quad (3.7)$$

### **Boundary Case 3: *Restrained at crown, invert and springing***

In case of partial grouting, similar findings to those corresponding to boundary condition 2 apply.

For full grouting, maximum deflection occurs at node 5 for the same reason as described in case of boundary condition 2. This leads to the following design expression

$$\frac{0.03}{K} = 0.0073 \frac{P}{Gw} - 0.0054 \quad (3.8)$$

### **Summary of Deflection-Limit Criteria**

Figure 3.13 summarizes the results of the above three boundary conditions, and hence can be used to determine the allowable grouting pressure on any particular lining based on the deflection-limit criteria. It is seen from the figure that for a particular lining geometry and material properties, the lining under boundary condition 2 can sustain higher pressure than that of boundary condition 1. Again, boundary condition 3 provides more allowable pressure than that of both the boundary conditions 1 and 2. Unlike the cut-off for boundary condition 1 at an abscissa value of 0.08, boundary condition 2 reaches the abscissa at a value of 0.062.

## **3.6 DISCUSSION ON PARAMETRIC ANALYSIS**

### **3.6.1 Enhancement Factor**

The present two-dimensional parametric analysis of egg-shaped sewer linings has revealed that both the maximum bending stress and the maximum deflection in a lining resulting from the grouting pressure load can be reduced considerably when additional restraints are introduced during installation. This implies that an *enhancement* in the value of the grouting pressure can be achieved, thus providing adequate grouting of the annulus in addition to filling the voids in the neighbouring

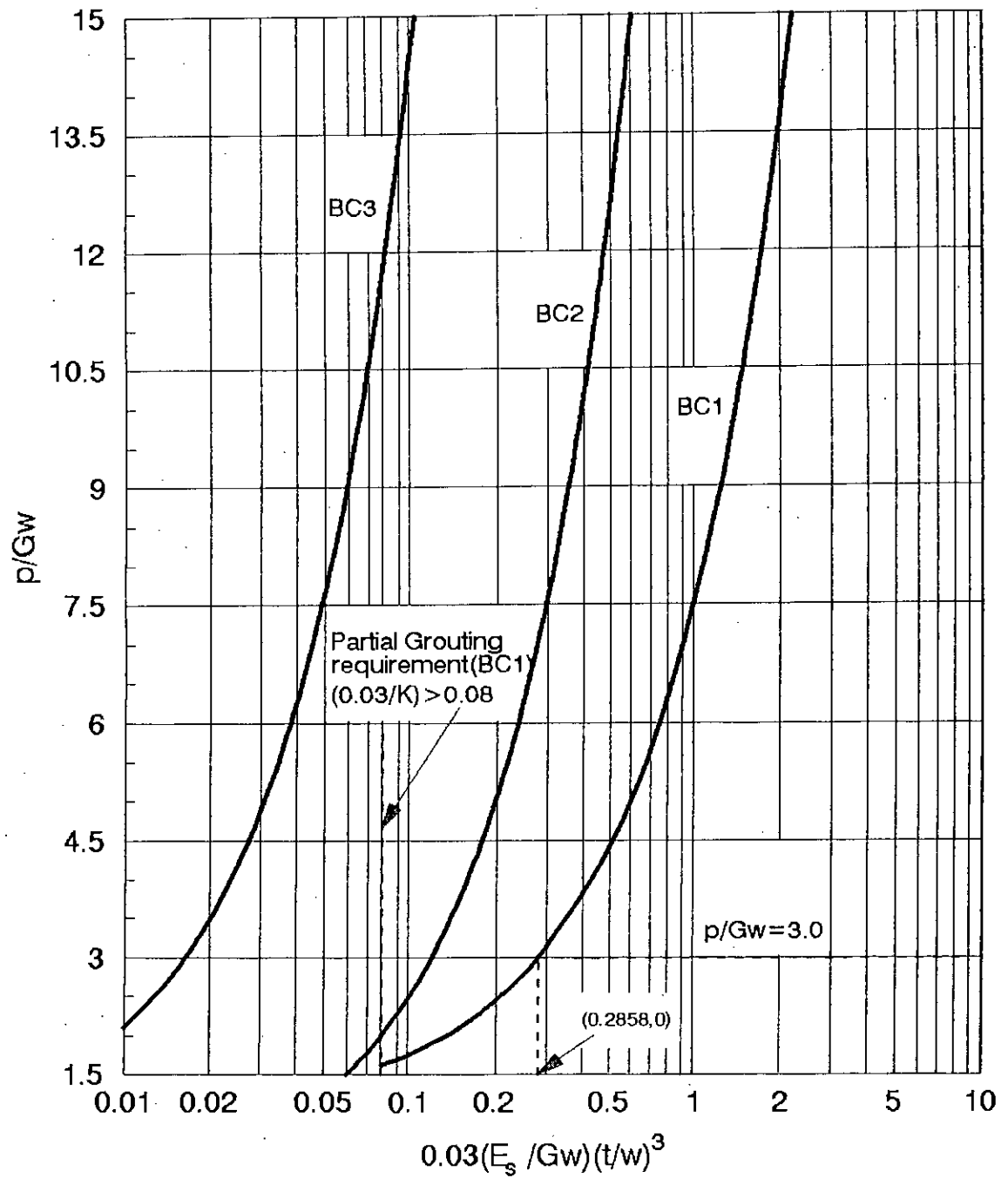


Fig. 3.13: Egg-shaped sewer lining: Allowable grouting pressure based on the deflection-limit criteria for various boundary cases

soil surround. This gives rise to the introduction of a factor called enhancement factor (EF) which can be defined as follows:

*Enhancement factor can be defined as the ratio of the allowable grouting pressure which could be applied on any particular lining for boundary case 2 or 3 to the one corresponding to boundary case 1 i.e.*

$$EF_i = \frac{P_i}{P_1} \quad (3.9)$$

Here  $i$  corresponds to 2 or 3 i.e. boundary case 2 or 3 while the other constants are defined earlier.

### Enhancement Factor for Stress-Limit Criteria:

The expression used to calculate the values of enhancement factor for stress-limit criteria can be obtained from equations 3.2, 3.3, and 3.4; and these are as follows:

$$P_i = \frac{Gw}{E_i} (R - C_i + 1.5E_i) \quad (3.10a)$$

$$\text{and } P_1 = \frac{Gw}{E_1} (R - C_1 + 1.5E_1) \quad (3.10b)$$

$$\text{Hence } (EF)_i \text{ stands for } EF_i = \frac{E_1}{E_i} \frac{R - C_i + 1.5E_i}{R - C_1 + 1.5E_1} \quad (3.11)$$

where,  $R$  must be greater than or equal to 0.668 (flotation requirement)

### Enhancement Factor for Deflection-Limit Criteria:

The expressions used for the calculation of enhancement factor for deflection limit criteria are derived from equations 3.5, 3.6, 3.7 and 3.8 and the expressions are as follows:

$$P_2 = \left( \frac{0.03}{K} - 0.0002 \right) \times 25Gw \quad (3.12)$$

$$P_3 = \left( \frac{0.03}{K} + 0.0054 \right) \times 137Gw \quad (3.13)$$

and

$$P_1 = \left( \frac{0.03}{K} + 0.16 \right) \times 6.75Gw \quad (3.14a)$$

$$\text{for } (0.08 \leq \frac{0.03}{K} \leq 0.2858)$$

$$= \left( \frac{0.03}{K} + 0.19 \right) \times 6.33Gw \quad (3.14b)$$

$$\text{for } \frac{0.03}{K} \geq 0.2858$$

Two values of EF are determined for each of the boundary cases 2 and 3. These are based on the stress and deflection limit criteria outlined earlier, and the lower of these two values are adopted in design. These are shown graphically in the Figs. 3.14 and 3.15. *It is found that stress limitations of the material are the most critical factor and that they actually always govern the design calculations of the enhancement factor.*

It is seen from Figs. 3.14 and 3.15 that the value of enhancement factor decreases with the increase in the lining width and the specific gravity of the grout mix. On the other hand, enhancement factor increases when the thickness and allowable short-term bending stress of the lining increase.

It emerges from the figures that boundary case 3 provides a value of near about two to three times the one corresponding to boundary case 2.

Finally, it emerges from Fig. 3.14 that, in the case of boundary condition 2, a minimum value of R greater than 0.794 is needed in order to get the values of enhancement factors higher than one; this implies that no beneficial effect can result from the use of boundary condition 2 for values of R less than 0.794, as the restraints give rise to higher bending stresses than those arising from boundary conditions.

### **3.6.2 Reduction Factors**

Once a value of allowable grouting pressure ( $p_1$ ) is determined for any particular lining geometry and material properties using boundary case 1 as a restraint set-up, it is noted that a considerable reduction in the allowable thickness of the lining can be achieved if the boundary case 2 or 3 is used instead, thus leading to a more economical design. This gives rise to the introduction of another factor called the reduction factor (RF). *The reduction factor is defined as the ratio of the lining thickness resulting from the use of boundary case 2 or 3 to the one corresponding to boundary case 1.* As for the previous section, two values of RF are determined for each boundary cases 2 and 3 based on the stress and deflection limit criteria. Here again, stress limitations prove to be more critical, and the equation used to calculate the values of RF is as follows:

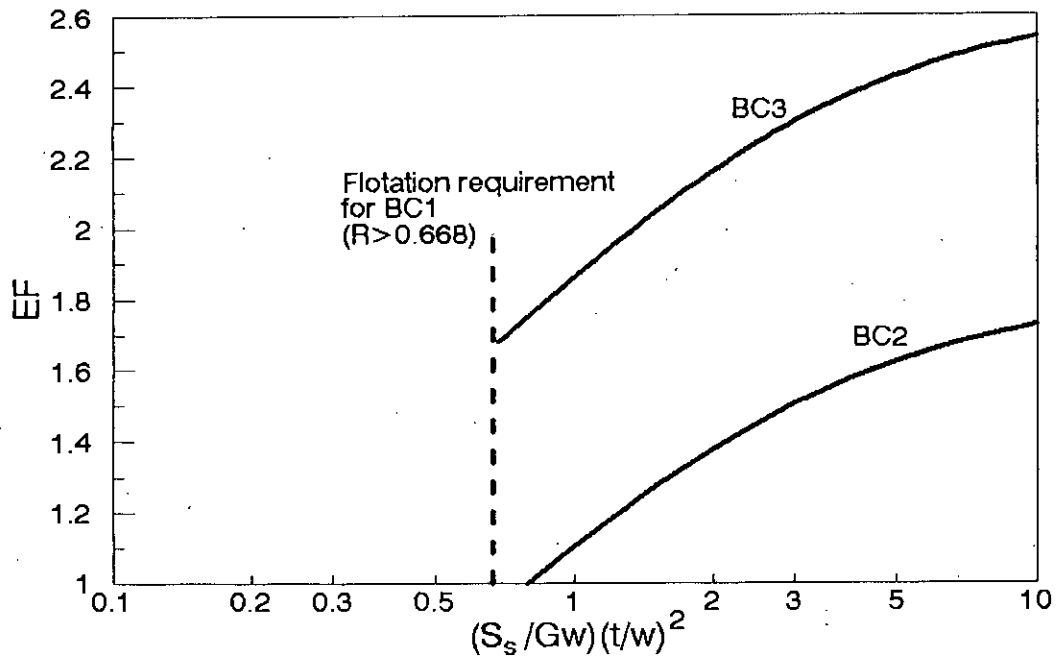


Fig. 3.14: Egg-shaped sewer lining: Enhancement factor for allowable grouting pressure, based on stress-limit criteria

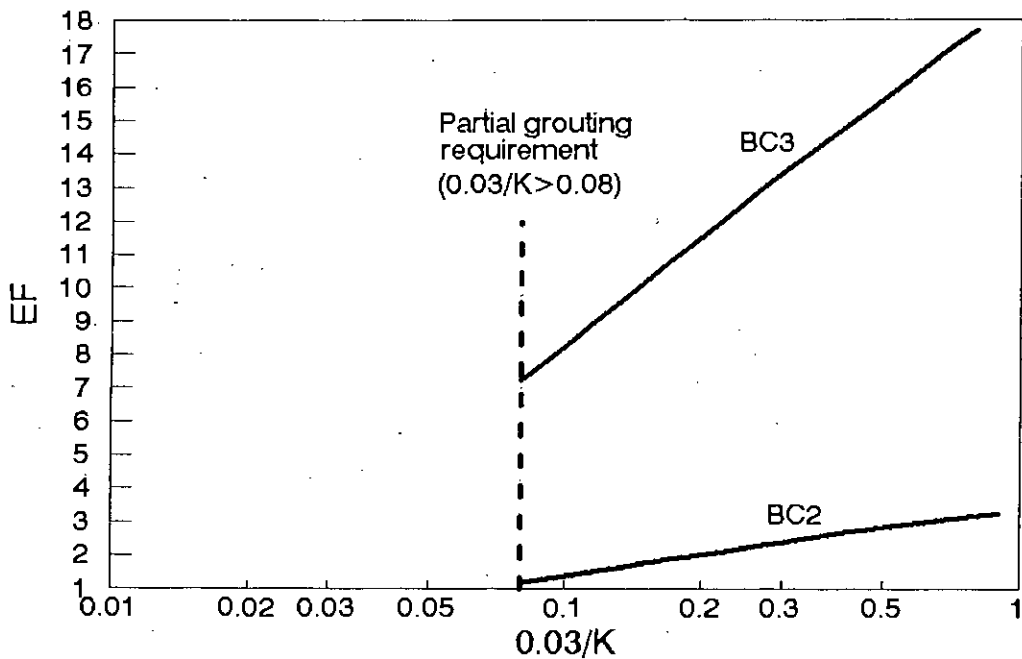


Fig. 3.15: Egg-shaped sewer lining: Enhancement factor for allowable grouting pressure, based on deflection-limit criteria



$$RF_i = \frac{t_i}{t_1} \quad (3.15)$$

$$\text{where } t_i = [C_i + (\frac{P}{Gw} - 1.5)E_i]^{1/2}$$

$$\text{and } t_1 = [C_1 + (\frac{P}{Gw} - 1.5)E_1]^{1/2}$$

with  $i$  corresponding to boundary cases 2 or 3, and other variables being defined by equations 3.2, 3.3, 3.4 and Table 3.2.

It is shown from Fig. 3.16 that the reduction factor increases as the width of the lining and the specific gravity of grout increase.

It is also noted that for high values of  $\frac{P_1}{Gw}$ , the reduction factor virtually tends towards a constant value.

Furthermore, it is clear from the figure that larger reduction factor can be achieved by using boundary case 3 in comparison to the boundary case 2 (about 1.22 to 1.42 times).

Figure 3.16 shows that, for boundary case 2, reduction factor less than one can not be achieved unless the values of  $\frac{P_1}{Gw}$  becomes greater than 2.13. This, again, implies that no beneficial effect can result from the use of boundary case 2 if the value of  $p_1$  which is defined earlier is less than  $2.13Gw$

Another point to be noticed here is that in case of boundary case 3, the reduction factor remains constant for an initial small range of  $\frac{P_1}{Gw}$  (1.5 to 1.949); this is only because of flotation requirement for boundary case 1 which states that the value of  $R$  must be equal to or greater than 0.668 in order to withstand the maximum bending stress at the crown.

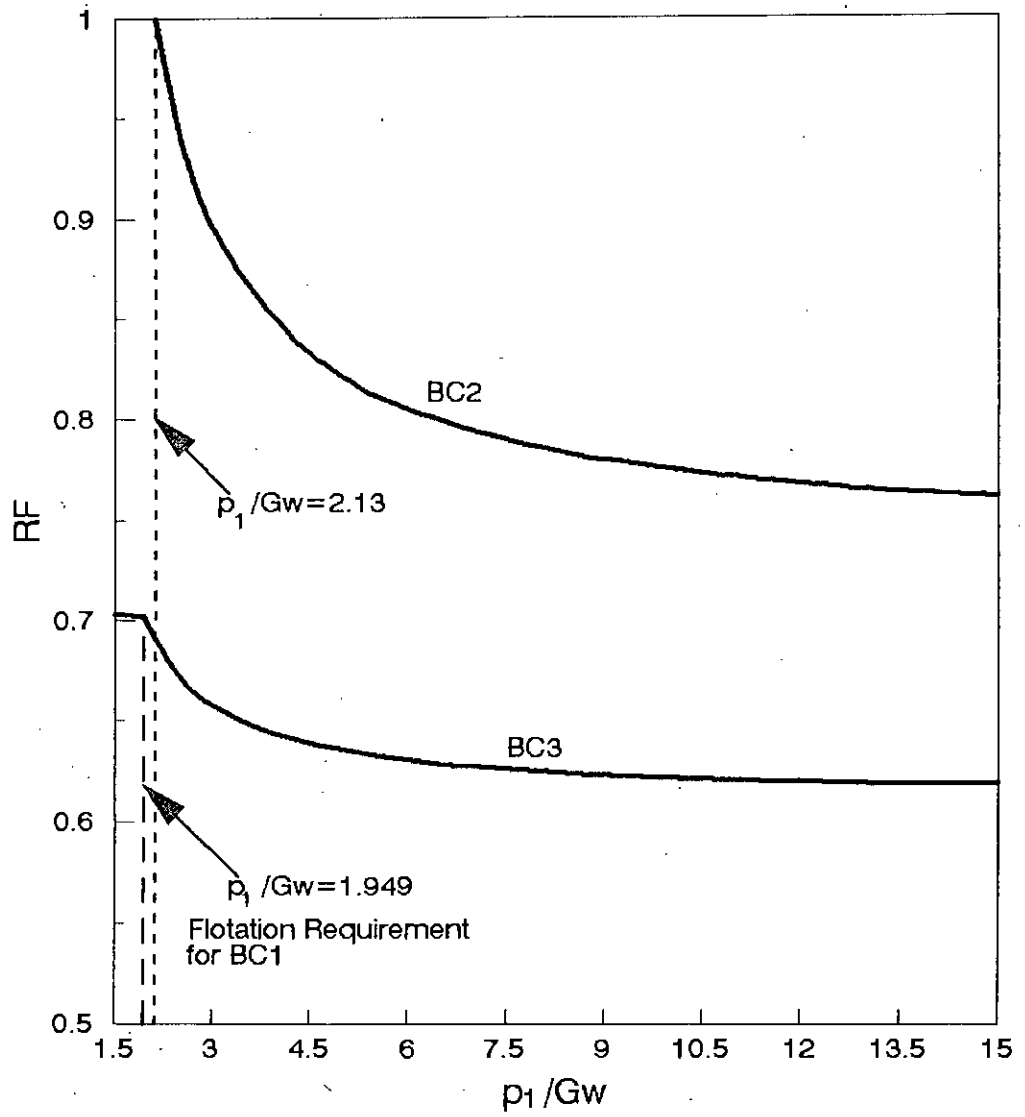


Fig. 3:16: Egg-shaped sewer lining: Reduction factors for minimum permissible lining thickness

### 3.7 STRUCTURAL DESIGN EXAMPLE

The following design example demonstrates the use of the structural design method outlined in this chapter. It is important to note that, in addition to the present short-term installation design checks, long-term design checks which is not performed in this research work must also be carried out. Finally, the use of a particular lining material in this example is merely illustrative.

An existing brick-sewer is egg-shaped. Its different parameters are as follows:-

a) Geometrical parameters:

Overall height of the sewer = 900 mm.

Overall width of the sewer = 600 mm

Let the minimum annular grouting thickness = 25 mm

Let the lining thickness  $t = 10$  mm

b) Material properties:

Let the value of the short-term Young's modulus of the GRP lining material be equal to  $20 \times 10^6$  kN/m<sup>2</sup>.

Let the value of the allowable short-term bending modulus  $S_s$  of the GRP lining material be equal to  $60 \times 10^3$  kN/m<sup>2</sup>.

Let the unit weight of the grout mix be equal to 16.5 kN/m<sup>3</sup>.

The most cheapest and convenient support system is boundary case 1. Hence adopting this boundary case, the allowable grouting pressure during installation is to be determined.

#### **Solution:**

Step 1:

Using the values of the geometrical parameters, the internal dimensions of the lining are to be found out. These are

$$h = 900 - (25 \times 2 + 10 \times 2)$$

$$= 830 \text{ mm}$$

$$w = 600 - (25 \times 2 + 10 \times 2)$$

$$= 530 \text{ mm.}$$

Step 2:

Using the values of the material parameters, the non-dimensional strength of the lining  $R$  and permissible deflection parameter  $0.03/K$  are to be calculated and these are as follows:

$$R = (S_s / Gw)(t/w)^2$$

$$= \left( \frac{60 \times 10^3}{16.5 \times 0.53} \right) \left( \frac{0.01}{0.53} \right)^2$$

$$= 2.443$$

and

$$\frac{0.03}{K} = 0.03 \frac{E_s}{Gw} \left( \frac{t}{w} \right)^3$$

$$= 0.03 \frac{20 \times 10^6}{16.5 \times 0.53} \left( \frac{0.01}{0.53} \right)^3$$

$$= 0.461$$

Step 3:

Using Fig. 3.11 for stress-limit criteria and boundary case 1 as the temporary support system the following is obtained

$$p/Gw = 4.51$$

or,  $p = 52 \times 16.5 \times 0.53$   
 $= 39.44 \text{ kN/m}^2$  which is equivalent to a head of grout equal to  
 $(39.44/16.5) = 2.39 \text{ m}$  from the invert of the lining.

Step 4:

Using Fig. 3.13 for deflection-limit criteria and boundary case 1, the following is obtained.

$$p/Gw = 4.0$$

or,  $p = 4.0 \times 16.5 \times 0.53$   
 $= 34.98 \text{ kN/m}^2$  which is equivalent to a head of grout equal to  
 $(34.98/16.5) = 2.12 \text{ m}$  from the invert of the lining.

Hence the minimum of these two values i.e. 2.12 m head of grout from the invert of the lining can be applied on the lining during installation.

# **CHAPTER 4**

## **STRUCTURAL BEHAVIOUR OF INVERTED EGG-SHAPED SEWER LININGS**

### **4.1 INTRODUCTION**

In Chapter 3, the design procedure of egg-shaped sewer linings has been described in details and the usage of the proposed design curves have been clarified by an illustrative example. In this chapter, an attempt has been made to analyze and design inverted egg-shaped sewer linings. For a particular lining geometry and similar grouting load, the structural response of an inverted egg-shaped lining differs from that of egg-shaped lining. It is needless to mention that inverted egg-shaped lining is to be inserted into the same shaped sewer after allowing for an annulus gap. Although inverted egg-shaped sewer is not available in our country, this type of sewer was constructed in many foreign countries in the past. The renovation of these sewers has made an acute challenge before the engineers as replacement of existing sewers with a new one involves huge capital expenditure and possible traffic disruption. Lining technique, as a means of renovating inverted egg-shaped sewers, demands extensive research because of its unusual shape, and varied and peculiar type of load the lining is subjected to during installation and during service conditions. After an extensive numerical investigation on inverted egg-shaped sewer linings, the findings have been discussed in detail and design curves have been proposed. Their uses is illustrated with a design example in Appendix 2.

### **4.2 TWO-DIMENSIONAL FINITE ELEMENT (FE) MODEL**

A linear two-dimensional finite element program of Seraj (1986) is used in order to simulate the behaviour of inverted egg-shaped linings under various probable load during installation.

#### **4.2.1 The Two-Dimensional FE Mesh**

The shape of the lining used in the analysis is shown in Fig. 4.1. The thickness of the lining is assumed to be constant all around the cross-section. Due to symmetry of the lining geometry, loading and boundary conditions about the vertical axis (i.e.

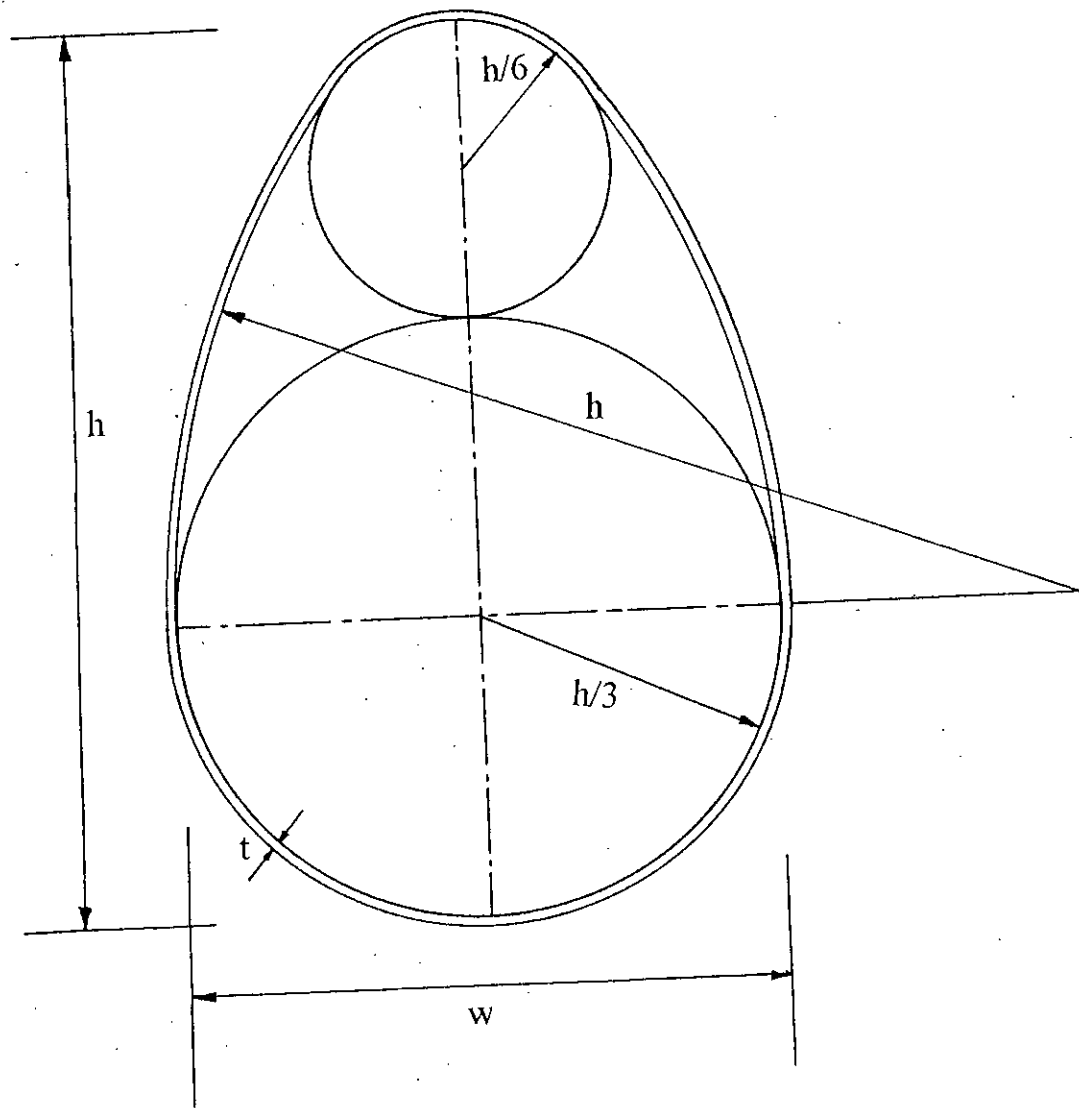


*Fig. 4.1: Inverted egg shaped lining: The shape of the lining used in the analysis*

Y-axis), only half of the cross-section, shown in Fig. 4.2, is analyzed. The cross-section which is under study is situated at the X-Y plane of symmetry.

The elements used in the analysis are two-noded beam elements each having three degrees of freedom (horizontal and vertical displacement, and rotation) at each node. The mesh adopted consists of 25 elements, the node numbers corresponding to crown, springing and invert being 26, 11 and 1.

#### **4.2.2 Restraint Set-Ups**

The three support systems considered in the analysis are shown in Fig. 4.3. The first support system (Fig. 4.3a) consists solely of a restraint at the crown of the lining, while the second (Fig. 4.3b) comprises restraints at the crown and invert of the lining. The third form of support system (Fig. 4.3c) consists of restraints at both the crown, invert and springing of the lining.

These restraints are simulated numerically in the analysis by fixing the horizontal and vertical components of displacement at the corresponding nodal points. As half of the cross-section is analyzed, the horizontal and rotational components of displacements at nodes 1 and 26 of the lining are restrained. In addition, in Fig. 4.3a, the vertical displacement at node 26 is set to zero for boundary case 1; in Fig. 4.3b, for boundary case 2, the vertical displacements are made equal to zero at nodes 1 and 26. Similarly, in Fig. 4.3c, restraints have been imposed on the vertical displacement at node 1 and 26, and on vertical and horizontal displacements at node 11 (springing) in order to simulate boundary case 3.

#### **4.2.3 Loading Configurations**

Three loading configurations which are used in the present study are shown in Fig 4.4. Figure 4.4a corresponds to pressure from grout surrounding the lining up to height of the springing (staged grouting). The second load configuration, called flotation, involves a head of grout up to the crown (node 26) as shown in Fig. 4.4b. The third form of loading (shown in Fig. 4.4c) corresponds to the uniform pressure which is being applied on the lining as a consequences of an excess head of grout.

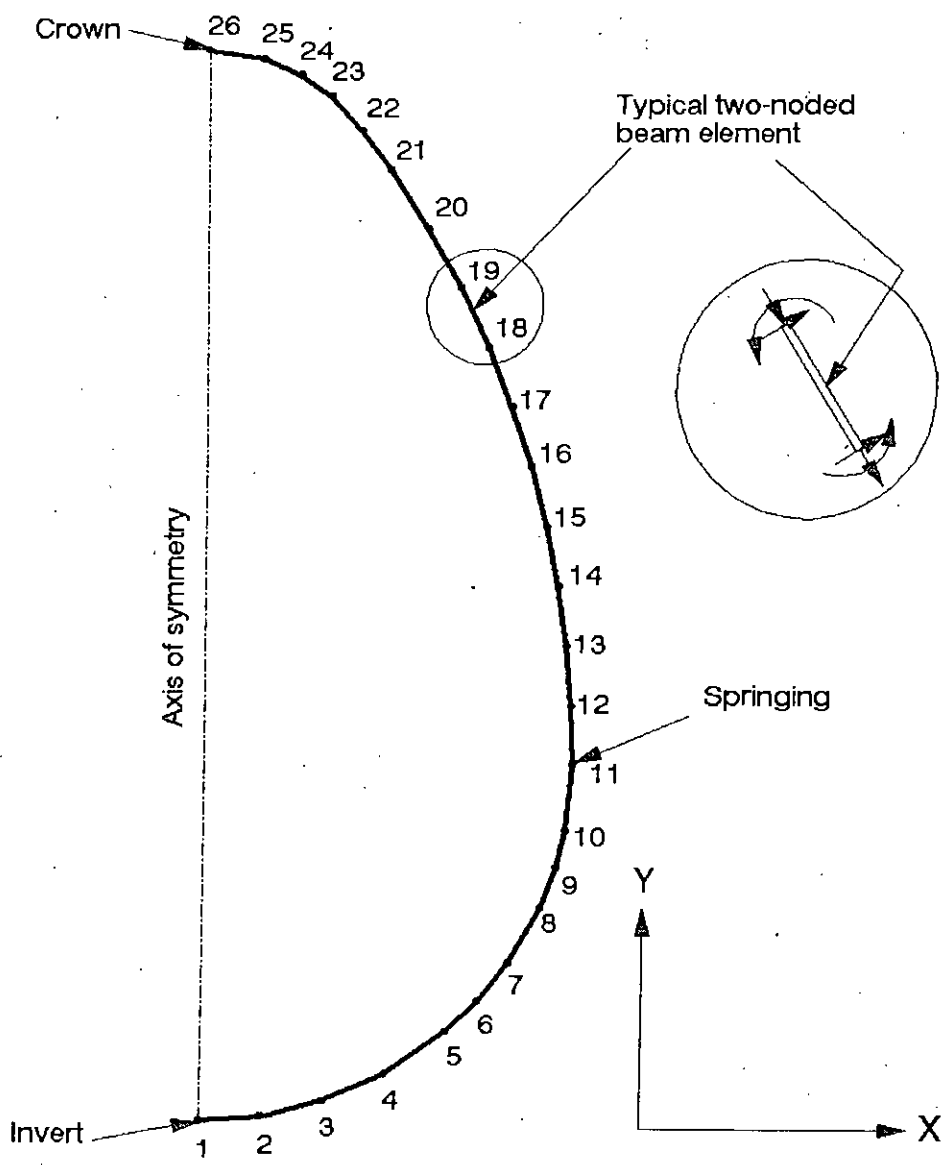
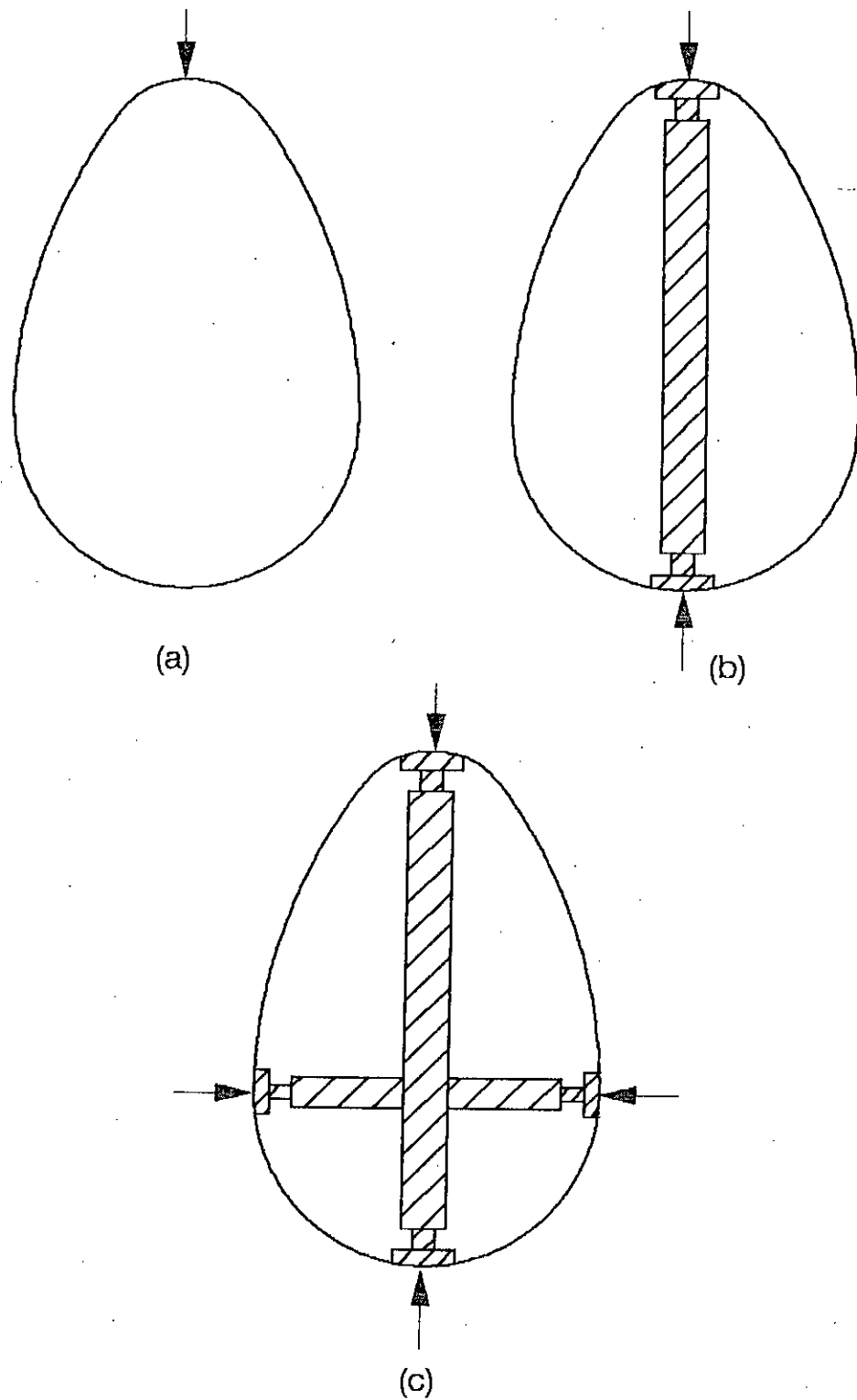
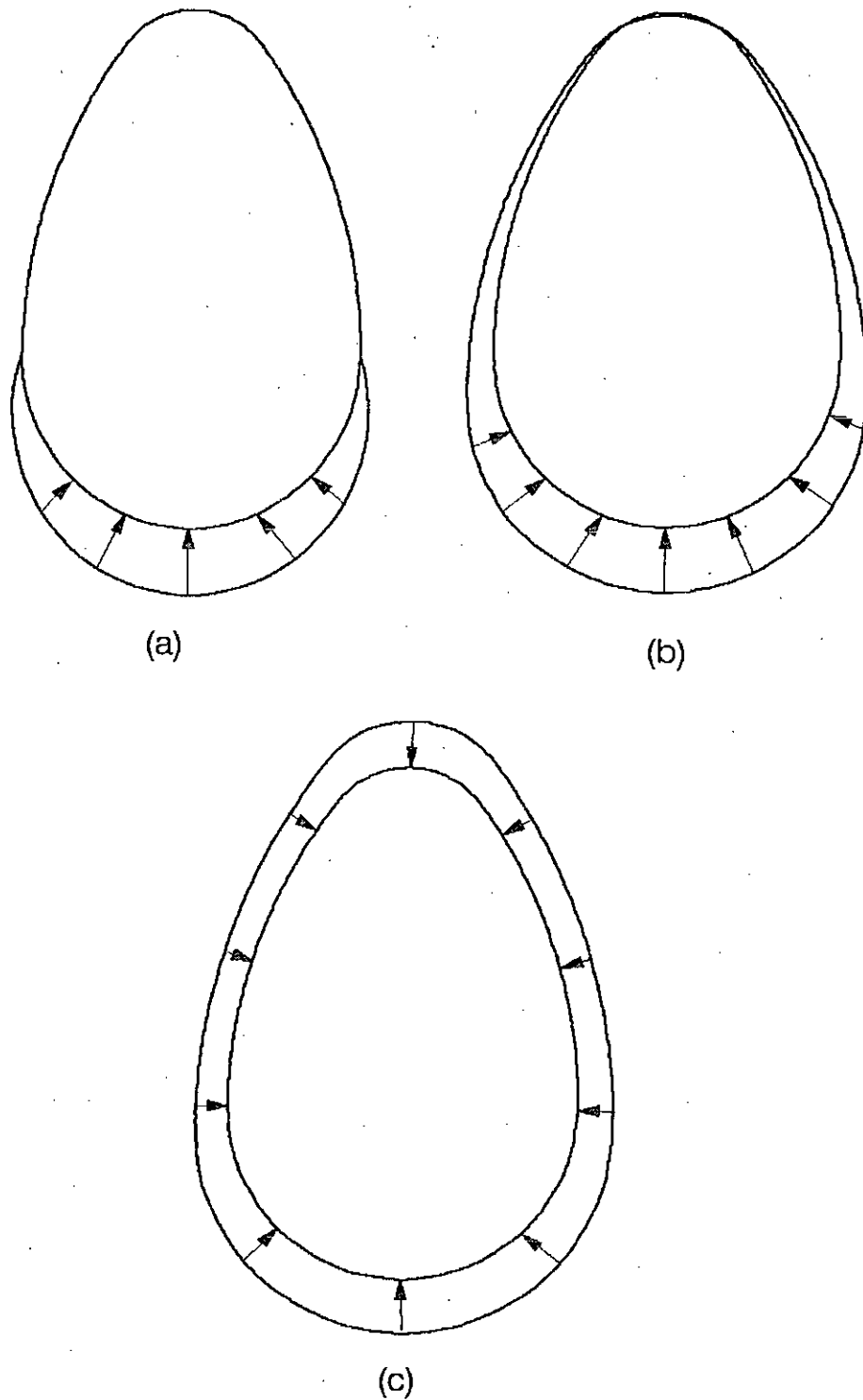


Fig. 4.2: Inverted egg shaped lining: Two-dimensional finite-element mesh adopted in the analysis





*Fig. 4.3: Inverted egg shaped lining: The support systems studied: (a) boundary case 1, (b) boundary case 2 and (c) boundary case 3*



*Fig. 4.4: Inverted egg shaped lining: The loading configurations studied:  
(a) staged grouting, (b) pressure up to crown only and  
(c) uniform pressure*

#### 4.2.4. Parameters Included in the Analysis

The parameters included in this study are as follows:

(a) Geometrical parameters:

$w$  = width of lining

$h$  = height of lining

$t$  = thickness of lining

(b) Material parameters:

$S_s$  = allowable short-term bending stress of lining material

$E_s$  = short-term modulus of elasticity of material

(c) Load parameters:

$G$  = unit weight of grout mix

$H$  = excess head of grout measured from crown of lining corresponding to uniform pressure load.

### 4.3 COMPUTATION OF CONSTANTS

For each load and boundary case, the parametric analysis is carried out by varying one parameter at a time, keeping the others constants. The results (bending stresses and deflections) are given in terms of dimensionless equations linking all the independent parameters together as described in chapter 2. In these equations, the bending stress is made non-dimensional by dividing it by the product of unit weight of grout mix and the width of the lining. The deflection is made dimensionless by expressing it in terms of the width of the lining. The non-dimensional bending stress ( $S/Gw$ ) and deflection ( $\delta/w$ ) are plotted against  $(w/t)^2$  and lining flexibility  $K$  respectively for staged grouting and flotation load, and against  $(H/w)(w/t)^2$  and  $(H/w)K$  for uniform pressure. These plots are given in Appendix 2. From these plots, bending stress constants and deflection constants are computed for different boundary cases and different loading configurations. These are shown in Table 4.1 and 4.2 respectively.

**Table 4.1: Dimensionless constants for the maximum bending stress in the lining. (Note: positive values of A, C and E imply tensile stresses in the inner surfaces of the lining)**

|                  | Constant | Boundary Case 1 | Boundary Case 2                    | Boundary Case 3 |
|------------------|----------|-----------------|------------------------------------|-----------------|
| Staged grouting  | A        | 0.3081 Node 26  | -0.1118 Node 1                     | -0.0192 Node 1  |
| Flotation        | C        | 0.34012 Node 26 | 0.3437 Node 26<br>0.0030446 Node 1 | 0.2033 Node 26  |
| Uniform pressure | E        | -0.7048 Node 26 | -0.3938 Node 1<br>0.0608 Node 26   | 0.294 Node 26   |

**Table 4.2: Dimensionless constants for the maximum deflections in the lining (Note: Inward deflections are taken as positive)**

|                  | Constants      | Boundary Case 1   | Boundary Case 2   | Boundary Case 3   |
|------------------|----------------|-------------------|-------------------|-------------------|
| Staged Grouting  | B <sub>x</sub> | 0.00 Node 1       | -0.00568 Node 16  | 0.0000678 Node 4  |
|                  | B <sub>y</sub> | 0.0628 Node 1     | -0.00447 Node 16  | 0.0002633 Node 4  |
| Flotation        | D <sub>x</sub> | 0.008658 Node 13  | 0.008085 Node 13  | 0.005891 Node 15  |
|                  |                | 0.0081325 Node 14 | 0.0039 Node 16    | 0.0057213 Node 16 |
|                  | D <sub>y</sub> | -0.00216 Node 13  | -0.0025 Node 13   | 0.0005876 Node 15 |
|                  |                | -0.002226 Node 14 | -0.003403 Node 16 | 0.00055 Node 16   |
| Uniform Pressure | F <sub>x</sub> | 0.1477 Node 14    | 0.03354 Node 16   | 0.006393 Node 16  |
|                  |                | 0.14188 Node 13   | 0.01959 Node 13   | 0.005944 Node 15  |
|                  | F <sub>y</sub> | 0.0919 Node 14    | 0.02245 Node 16   | 0.0008141 Node 16 |
|                  |                | 0.0911 Node 13    | 0.01981 Node 13   | 0.0006874 Node 15 |

## 4.4 FULL-GROUTING DESIGN CURVES

### 4.4.1 Stress-Limit Criteria

#### **Boundary Case 1: *Restrained at crown only***

For this case, Table 4.1 shows that the maximum bending stress in the lining resulting from each of the two loading types (i.e. flotation and uniform pressure) is located at the crown (i.e. at node 26) of the lining. Thus, using equation 2.11 and appropriate constants from Table 4.1, the following design equation follows (using equation 2.11):

$$R = \left| 0.34012 - 0.7048 \left( \frac{P}{Gw} - 1.5 \right) \right| \\ = \left| \left( 1.39732 - 0.7048 \frac{P}{Gw} \right) \right| \quad (4.1)$$

It is further noticed that the maximum stresses developed at the crown, for above mentioned loading configurations, are of opposite sense. (in case of flotation compressive stress developed at the outside of the lining whereas in case of uniform pressure loading the same developed at the inside of the lining). Hence their effect on the lining will be less than the one if the load were applied separately. From similar considerations, the combined bending stresses are critically examined at all other points and have been found to be less than that at the crown.

Table 4.1 also shows that staged grouting is less critical than the flotation load alone. If staged grouting is employed for lining technique, then design information can readily be obtained from equation 2.1 and Table 4.1

Still another aspect of this analysis is yet to be analyzed which is whether the staged grouting remains less critical than the combined effect of flotation and uniform pressure load or not. Fig. 4.5 answers the question. It is clear from the figure that up to the value of  $\frac{P}{Gw}$  equal to 2.42, staged grouting is critical; once its value exceeds 2.42, the latter case becomes dominant.

#### **Boundary Case 2: *Restrained at the crown and the invert***

It appears from table 4.1 that the maximum bending stress resulting from flotation load is located at the crown of the lining (i.e. at node 26), whereas in case of uniform pressure load, the maximum bending stress is located at the invert of the

lining (i.e. at node 1). This suggests that equation 2.11 must be satisfied at both the nodes 1 and 26 of the lining. The combined stresses at other nodes have been calculated and proved to be less critical than those at nodes 1 and 26.

The above discussion leads to the following design expression, which are graphically shown in Fig 4.6.

At node 26,

$$R = \left| 0.3437 + 0.0608 \left( \frac{P}{G_w} - 1.5 \right) \right| \quad (4.2)$$

$$= \left| 0.2525 + 0.0608 \frac{P}{G_w} \right|$$

and at node 1,

$$R = \left| + 0.0030446 - 0.3938 \left( \frac{P}{G_w} - 1.5 \right) \right| \quad (4.3)$$

$$= \left| 0.5937 - 0.3938 \frac{P}{G_w} \right|$$

It emerges from Fig. 4.6 and Table 4.1 that a minimum value of R equal to 0.3437 is needed in order for the lining to withstand the maximum bending stress at the crown resulting from flotation load alone.

It can also be shown from the figure that the allowable grouting pressure resulting from equation 4.3 at node 1 becomes predominant throughout the full range of R once its value exceeds the abscissa value equal to 0.407, and before this i.e. within the abscissa range of 0.3437 to 0.407, equation 4.2 at node 26 determines the allowable grouting pressure.

Staged grouting, in comparison to full grouting, is less critical. The relevant permissible pressures associated with this technique, for staged grouting, can readily be obtained by means of Table 4.1 and equation 2.1

### **Boundary Case 3: Restrained at crown, invert and springings**

It can be seen from Table 4.1, that the maximum bending stress in the lining resulting from flotation load alone occurs at the crown at node 26 of the mesh taken for analysis. Similar is the case with the uniform pressure load. This simply means that equation 2.11 is to be satisfied at node 26 (crown) of the lining, leading to the following design equation:

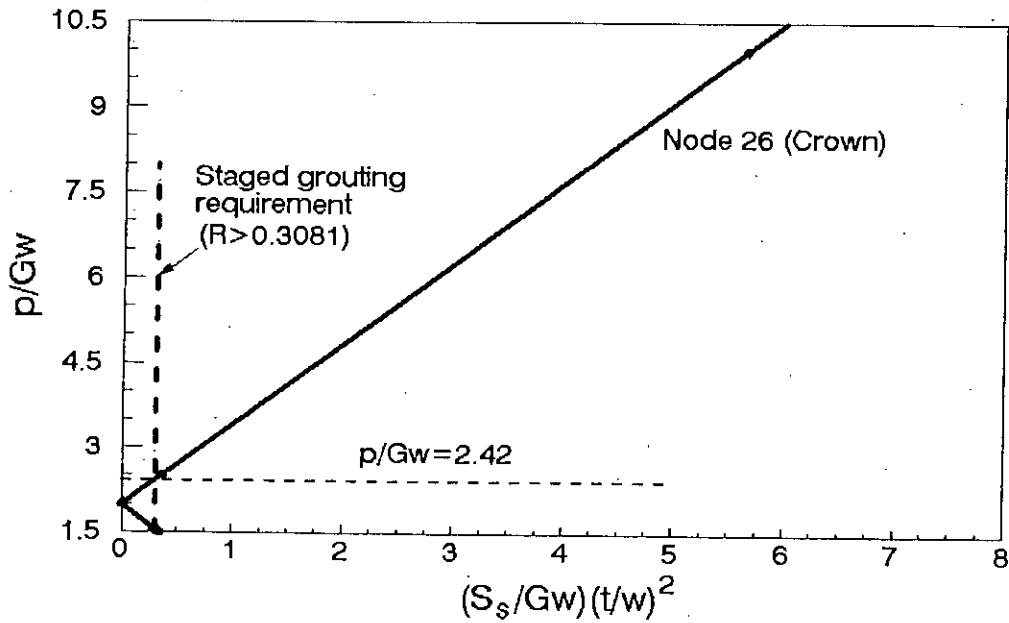


Fig.: 4.5: Inverted egg shaped lining: Maximum bending stress at the crown of the lining for flotation ( $p/Gw=1.5$ ) and additional external pressure (Boundary Case 1)

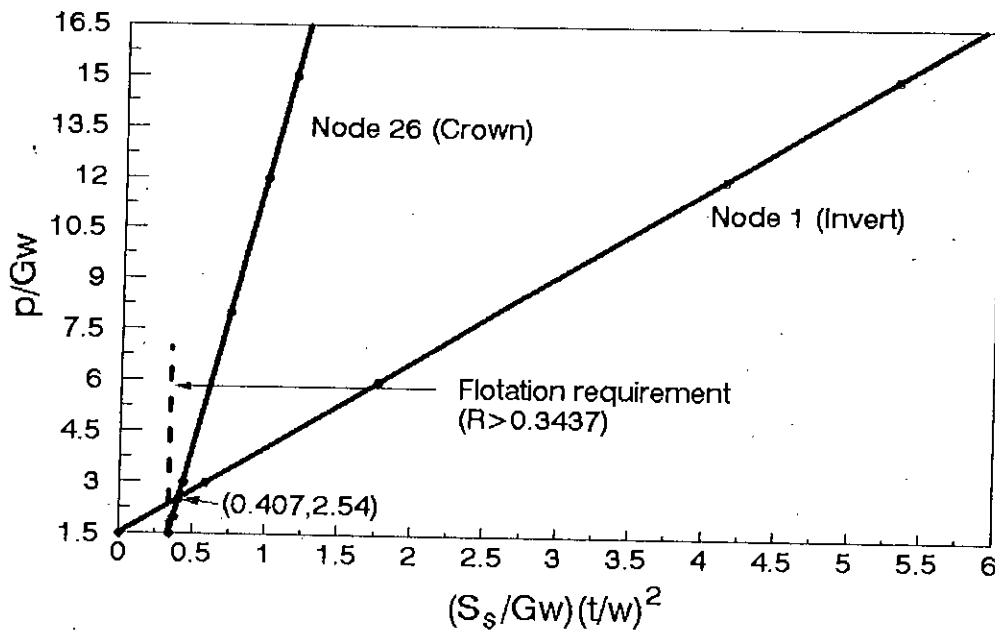


Fig. 4.6: Inverted egg shaped lining: Maximum bending stress at the crown and invert of the lining for flotation ( $p/Gw=1.5$ ) and additional external pressure (Boundary Case 2)

$$\begin{aligned}
R &= 0.2033 + 0.294 \left( \frac{P}{G_w} - 1.5 \right) \\
&= 0.294 \frac{P}{G_w} - 0.2377 \qquad (4.4)
\end{aligned}$$

where  $\frac{P}{G_w} > 1.5$

In this boundary case, a full head of grout must be imposed for the critical condition to be realized.

If partial grouting conditions is adopted for lining the sewer in this boundary case, it can be readily obtained by means of equation 2.1 and Table 4.1.

### Discussion on Stress-Limit Criteria

Figure 4.7 provides a summary of the above three boundary conditions as applied to inverted egg-shaped sewer linings. Therefore, once a boundary case is selected and the geometrical and material parameters are chosen, a value of allowable grouting pressure based on the stress-limit criteria can be determined using Fig. 4.7. Alternatively, any of the quantities engaged in Fig. 4.7 may be ascertained, provided all other variables are known.

It can easily be concluded from Fig 4.7 that there is a finite range of abscissa values (0.3437 to 0.4223) for which boundary condition 2 is slightly more critical than boundary condition 1.

It is also inferred from the Figure that unlike the cut-off for boundary condition 1 at an abscissa value of 0.3081, design curves for boundary conditions 2 and 3 have characteristics which reach the horizontal axis at values of 0.3437 and 0.2033 respectively. Boundary condition 3 is more critical than boundary case 1 within the abscissa range of 0.3081 to 0.592. Again, within the abscissa range of 0.34 to 0.81, than boundary condition 3 is more critical in comparison to boundary condition 2.

### 4.4.2 Deflection-Limit Criteria

#### Boundary Case 1: *Restrained against flotation only*

It is interesting to note from Table 4.2 that maximum deflection in the lining resulting from staged grouting is greater than the one resulting from flotation load alone. This leads to the requirement that a minimum value of abscissa equal to



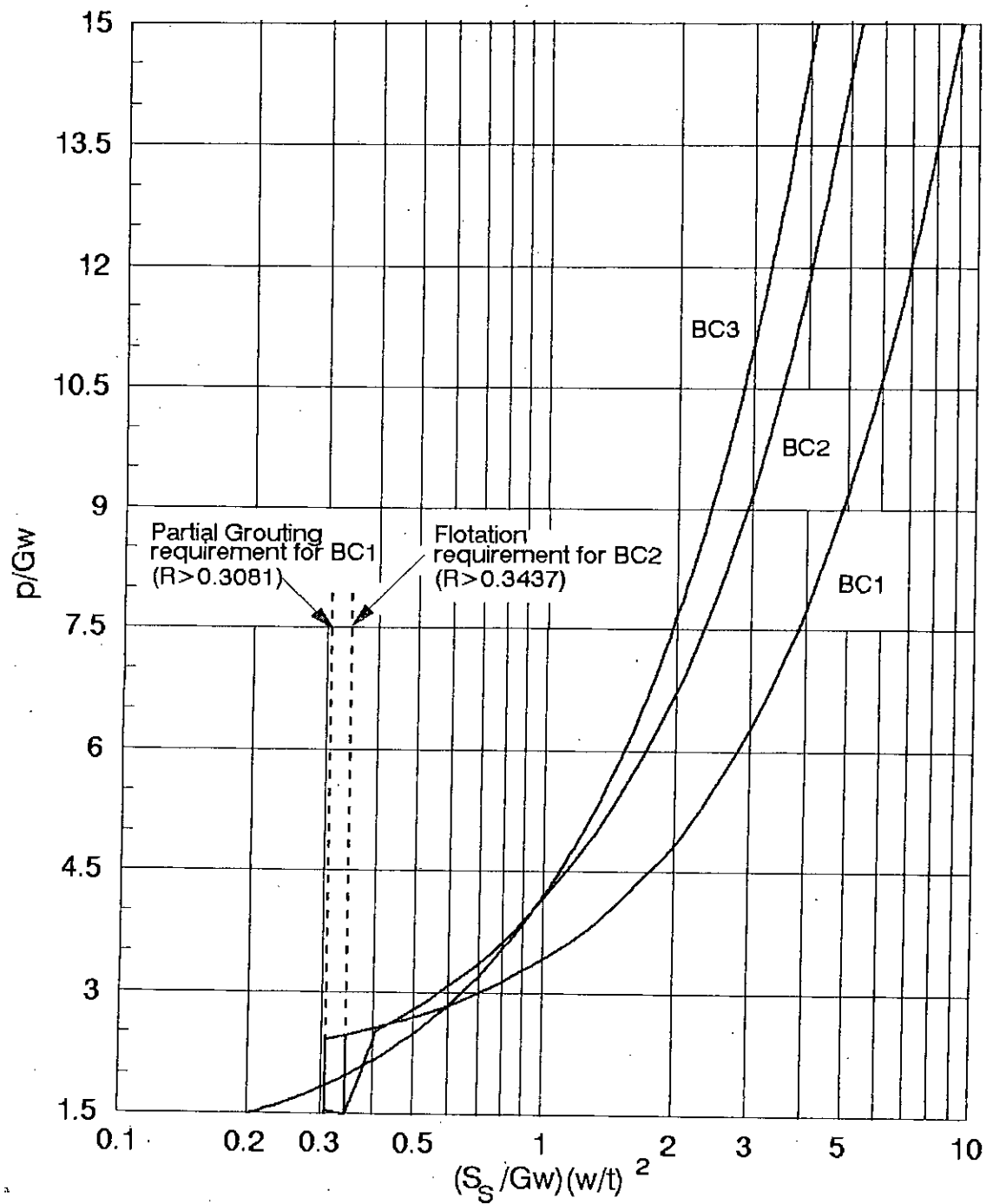


Fig. 4.7: Inverted egg shaped lining: Allowable grouting pressure for different boundary conditions, based on stress-limit criteria

0.0628 is needed in order for the lining to withstand the maximum allowable deflection of 3% of  $w$ . Beyond this value, the full flotation and uniform pressure cases become critical.

In case of flotation, maximum deflection occurs at node 13, whereas the same occurs at node 14 for uniform pressure. This is why equation 2.13 must be satisfied at both the nodes, which gives rise to the following design expressions:

At node 13,

$$\frac{0.03}{K} = \left| 0.169 \frac{P}{Gw} - 0.224 \right| \quad (4.5)$$

At node 14,

$$\frac{0.03}{K} = \left| 0.174 \frac{P}{Gw} - 0.25 \right| \quad (4.6)$$

By comparing these two equations, one may find that equation 4.6 at node 14 is always critical, as combined displacement due to flotation and uniform pressure becomes always maximum at this node. This has been shown in Fig. 4.8.

### **Boundary Case 2: Restrained at crown and invert**

Table 4.2 shows that unlike the boundary condition 1, in the present case the maximum deflection in the lining resulting from staged grouting is less than that resulting from flotation load alone. This imposes a requirement that a minimum value of  $\frac{0.03}{K}$  equal to 0.00846 is needed in order to withstand the maximum deflection of 3% of  $w$ . Once the value of  $\frac{0.03}{K}$  exceeds 0.00846, the combined effect of flotation and uniform pressure becomes critical.

Because of the same reasons as described under boundary condition 1, two design equations at nodes 13 and 16 are derived and these are as follows:

At node 13,

$$\frac{0.03}{K} = \left| 0.0279 \frac{P}{Gw} - 0.0333 \right| \quad (4.7)$$

At node 16,

$$\frac{0.03}{K} = \left| 0.04036 \frac{P}{Gw} - 0.0554 \right| \quad (4.8)$$

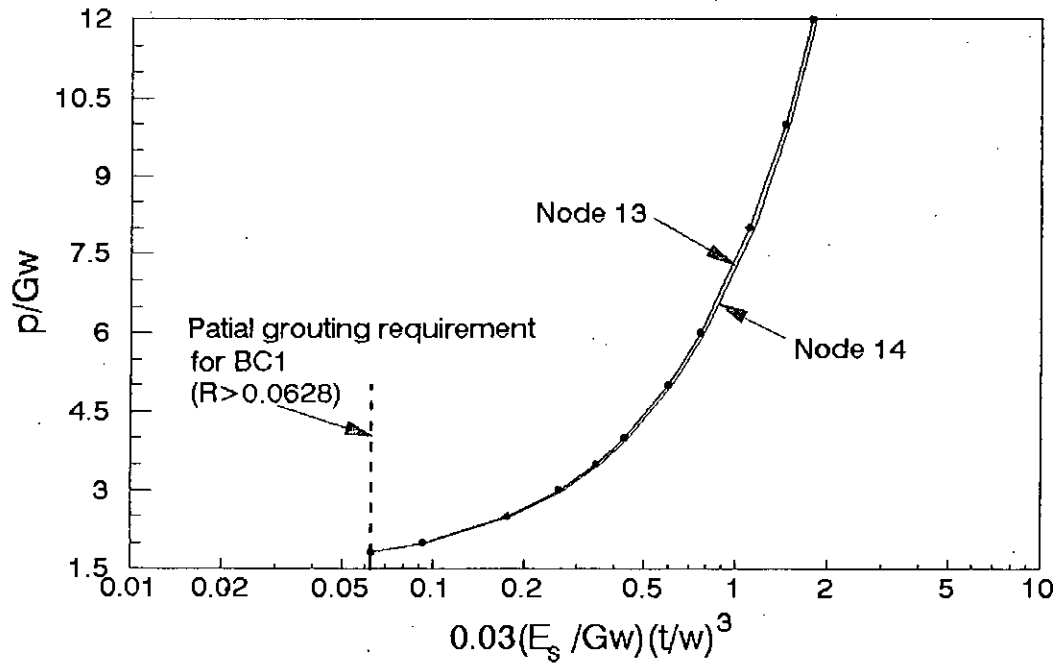


Fig. 4.8: Inverted egg shaped lining: Maximum deflections at nodes 13 and 14 of the lining for full flotation ( $p/Gw=1.5$ ) and additional external pressure (Boundary Case 1)

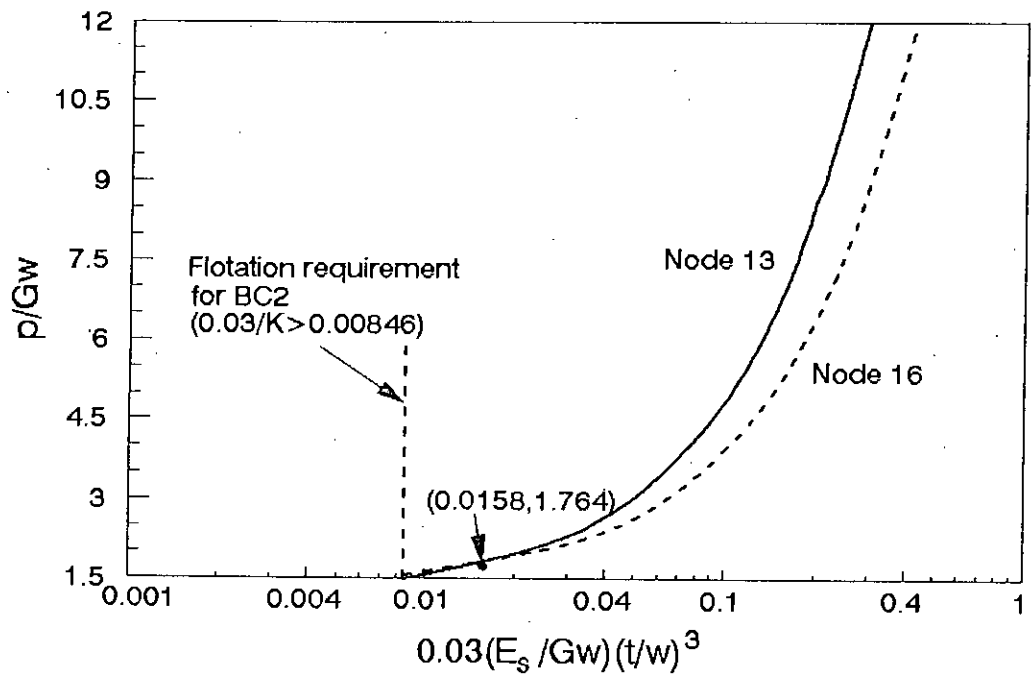


Fig. 4.9: Inverted egg shaped lining: Maximum deflections at nodes 13 and 16 of the lining for full flotation ( $p/Gw=1.5$ ) and additional external pressure (Boundary Case 2)

Equations 4.7 and 4.8 are graphically shown in Fig. 4.9. This clearly depicts that for values of  $\frac{0.03}{K}$  between 0.00846 and 0.0158, the deflection at node 13 is dominant. But after this, the maximum deflection occurs at node 16. This limits the use of the above two equations as follows:

$$\text{Equation 4.7 is valid for } 1.5 \leq \frac{P}{G_w} \leq 1.764 \quad \text{and}$$

$$\text{Equation 4.8 is valid for } \frac{P}{G_w} \geq 1.764$$

Once again, as mentioned earlier, the above equations must always be satisfied corresponding to flotation loading which implied  $\frac{0.03}{K} \geq 0.00846$

For this boundary case, the partial grouting have not been found to be critical. But, if required because of installation technique, relevant information can be found using pertinent data of Table 4.2 and equation 2.2

### **Boundary Case 3: Restrained at crown, invert and springings of lining**

It is clear from Table 4.2 that during staged grouting, maximum deflection occurred at node 4 and its magnitude is much less than the flotation load as well as the combined load corresponds to flotation and uniform pressure

The maximum deflection in this boundary case due to flotation load occurs at node 15 whereas the same is located at node 16 due to uniform pressure. Hence, equation 2.13 must be satisfied at both nodes 15 and 16 for combined load of flotation and uniform pressure. This gives rise to the following two design equations:

At node 15,

$$\frac{0.03}{K} = \left| 0.005984 \frac{P}{G_w} - 0.00296 \right| \quad (4.9)$$

At node 16,

$$\frac{0.03}{K} = \left| 0.00644 \frac{P}{G_w} - 0.00392 \right| \quad (4.10)$$

These two equations are plotted in Fig. 4.10. It emerges from Fig. 4.10 that 0.00592 is the minimum value of  $\frac{0.03}{K}$  to withstand the maximum deflection at node 15 resulting from the flotation load. It is also shown that allowable grouting pressure resulting from equation 4.10 at node 16 becomes predominant once the

87852

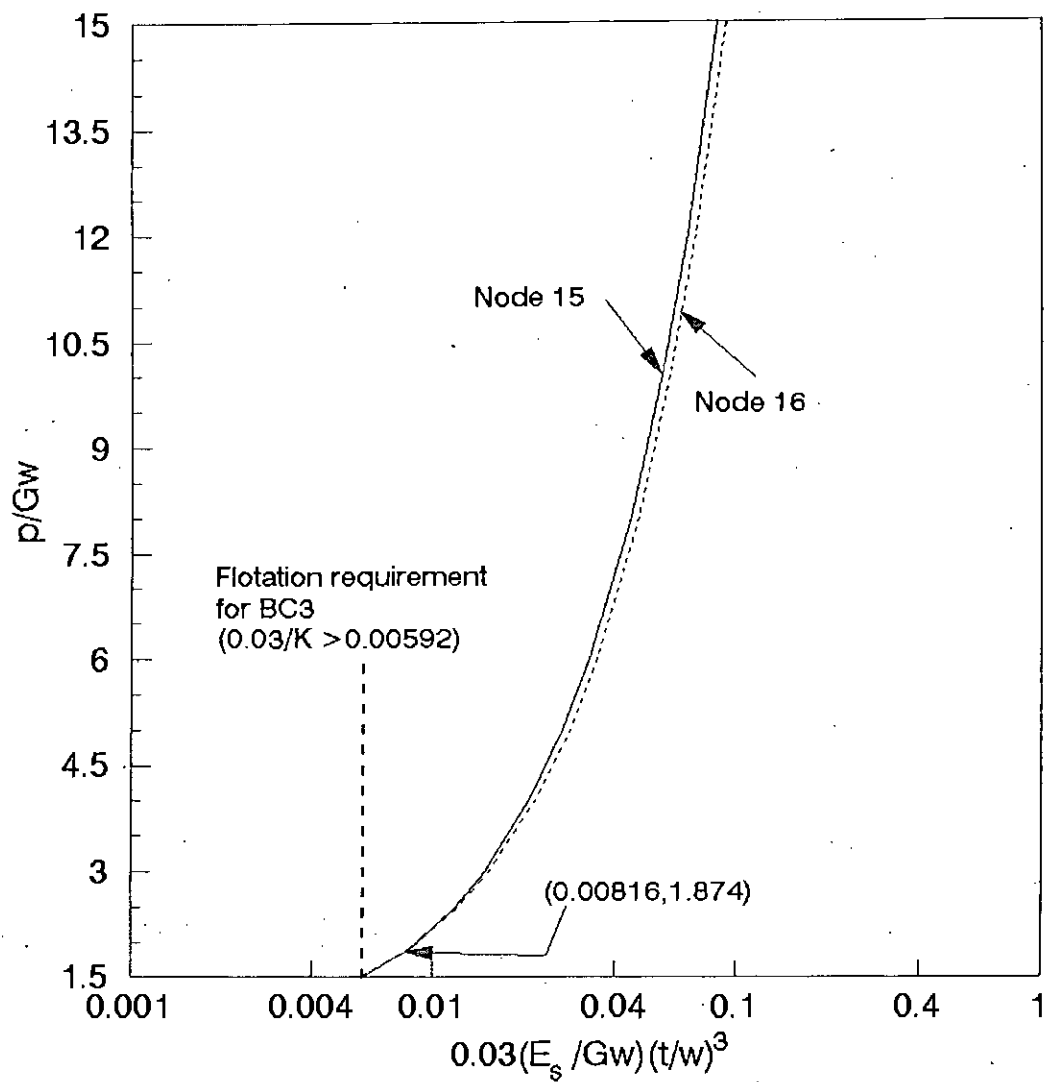


Fig.:4.10: Inverted egg shaped lining: Maximum deflections at nodes 15 and 16 of the lining for full flotation ( $p/Gw=1.5$ ) and additional external pressure (Boundary Case 3)

value of  $\frac{0.03}{K}$  exceeds 0.00816. Within the abscissa range of 0.00592 to 0.00816 the deflection at node 15 determines the design criteria.

### Summary of Deflection-Limit Criteria

Figure 4.11 summarizes the results of the above three boundary cases based on deflection limit criteria and hence can be used to determine the allowable grouting pressure in any particular lining. It is found from the figure that unlike the cut-off for boundary condition 1 at an abscissa value of 0.0602, boundary condition 2 and 3 gradually reaches the horizontal axis. It is also found from the figure that for a particular lining geometry and material property, boundary condition 3 gives the higher allowable pressure than boundary condition 2 and 3. Also boundary condition 2 allows greater pressure to be withstood than boundary condition 1 during installation.

## 4.5 DISCUSSION OF PARAMETRIC ANALYSIS

### 4.5.1 Enhancement Factors

The study of inverted egg-shaped lining has revealed that both the maximum bending stress and the maximum deflection in a lining resulting from grouting pressure can be reduced by introducing additional restraints during installation. The restraints give rise to the enhancement factor (EF) which has been described in detail in chapter 3. In the present study, similar computations can be made to determine the enhancement factors for both the stress-limit and deflection-limit criteria. For stress-limit criteria, EF can be calculated by using equations 4.1, 4.2, 4.3 and 4.4. The mathematical definition of enhancement factor, as before, is

$$(EF_i) = \frac{P_i}{P_1} \quad (4.11)$$

where i corresponds to boundary cases 2 or 3, and

$$P_1 = 1.42Gw(R + 1.39732) \quad (4.12a)$$

for  $R > 0.3081$

$$P_2 = 16.45Gw(R - 0.2525) \quad (4.12b)$$

for  $0.3437 < R < 0.407$

$$P_2 = 2.54Gw(R + 0.5937) \quad (4.12c)$$

for  $R > 0.407$  and

$$P_3 = 3.4Gw(R + 0.2377) \quad (4.12d)$$

for  $R > 1.5$

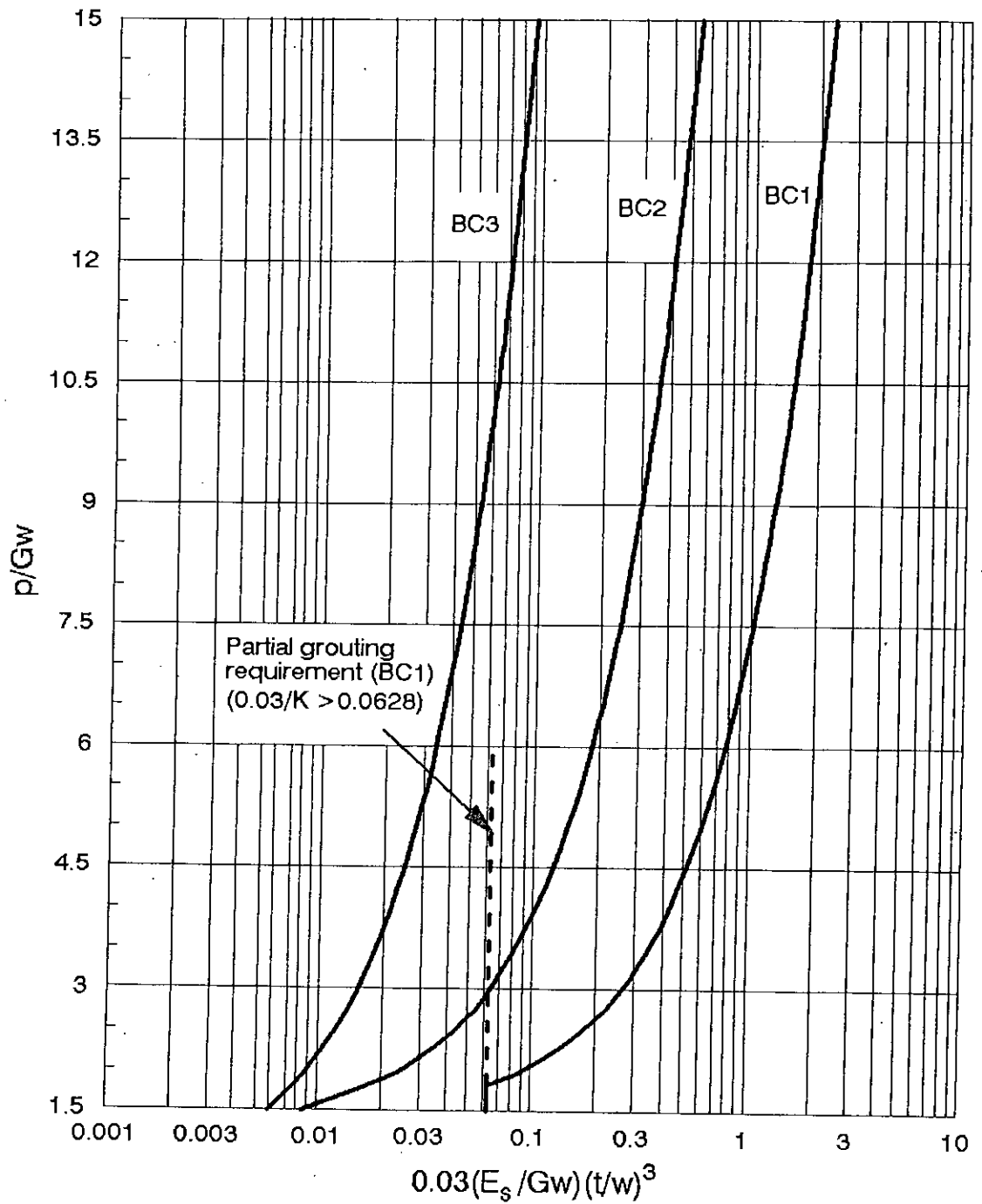


Fig. 4.11: Inverted egg shaped lining: Allowable grouting pressure for various boundary cases, based on deflection limit-criteria

With the help of the equations 4.11 and 4.12, enhancement factor, based on stress limit criteria, is calculated for boundary case 2 and 3 and potted in Fig. 4.12.

Taking the help of equations 4.6, 4.7, 4.8, 4.9, and 4.10, enhancement factors, based on deflection-limit criteria, are computed for boundary cases 2 and 3. This is shown pictorially in Fig 4.13.

For a particular lining geometry and material properties, after calculating two enhancement factors for both the stress and deflection limit criteria (from Figs. 4.12 and 4.13), the lower value is to be taken in design. It is found from these figures that stress-limitation of the material are the most critical factor and they actually always govern the design calculations of the enhancement factor because this criteria gives a value much lower than what may be found from deflection limit criteria.

It is found from the figures that EF increases as the short-term bending stress of the material ( $S_s$ ) and the lining thickness ( $t$ ) increase and EF decreases with the increase of the width of the lining ( $w$ ).

It follows from Fig. 4.12 that at a value of  $R$  equal to 0.81, boundary conditions 2 and 3 provide the same enhancement factor. When value of  $R$  exceeds 0.81, boundary condition 3 gives a higher value of enhancement factor than that of boundary condition 2.

Curves for boundary conditions 2 and 3 reaches the abscissa at the values of 0.424 and 0.592, respectively. This means that for boundary case 2, a minimum value of  $R$  greater than 0.424 is needed in order to get a value of EF higher than one. This implies that no beneficial effect can result from the use of boundary case 2 for a value of  $R$  less than 0.424. Similar reasoning also applies to boundary condition 3 and in this case the value of  $R$  must be greater than 0.592 to have an enhancement factor greater than unity.

#### **4.5.2 Reduction Factors**

Once a value of allowable grouting pressure ( $p_1$ ) is determined for any particular lining using boundary case 1 as a restraint set-up, a considerable reduction in allowable lining thickness can be achieved if boundary case 2 or 3 is used instead.



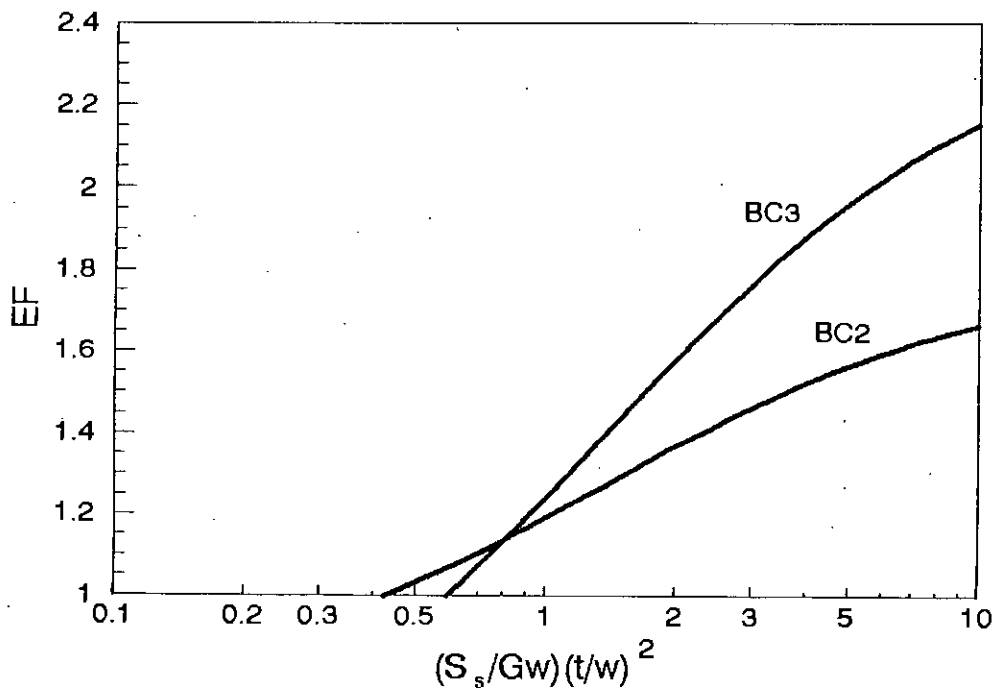


Fig. 4.12: Inverted egg shaped lining: Enhancement factor for allowable grouting pressure based on stress-limit criteria

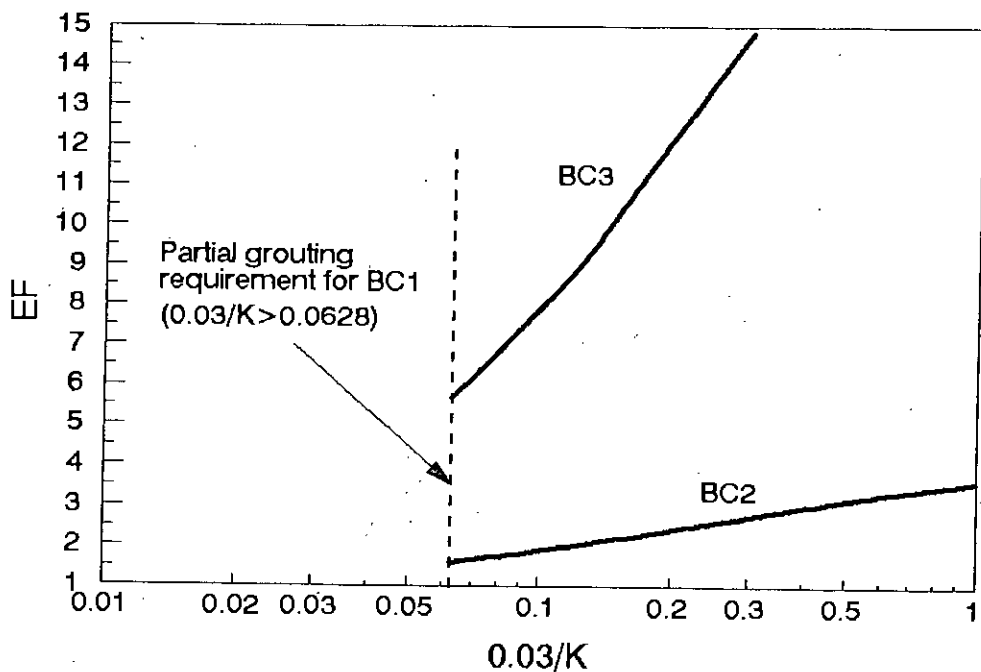


Fig. 4.13: Inverted egg shaped lining: Enhancement factor for allowable grouting pressure based on deflection-limit criteria

This gives rise to the reduction factor (RF) as defined in chapter 3. Symbolically,

$$(RF)_i = \left( \frac{t_i}{t_1} \right) \quad (4.13)$$

Two values of RF are determined for each of boundary case 2 or 3 based on stress and deflection -limit criteria. Here, again stress limitations proved to be more critical and, hence, aspects regarding this criteria will be discussed here. The equations used to calculate the RF for the stress-limit criteria can be determined from equations 4.1, 4.2, 4.3 and 4.4. The final equations after some rearrangements of these equations to achieve a reduction factor less than one are given below

$$(RF)_2 = \frac{t_2}{t_1} = \sqrt{\frac{0.5937 - 0.3938 \frac{P}{Gw}}{1.39732 - 0.7048 \frac{P}{Gw}}} \quad (4.14a)$$

$$(RF)_3 = \frac{t_3}{t_1} = \sqrt{\frac{0.2377 - 0.294 \frac{P}{Gw}}{1.39732 - 0.7048 \frac{P}{Gw}}} \quad (4.14b)$$

The above mentioned equations are pictorially shown in Fig 4.14. It is shown from Fig. 4.14 that reduction factor increases with the width and the specific gravity of the grout.

Figure 4.14 shows that for boundary condition 2 and 3, values of  $\frac{P}{Gw}$  greater than 2.58 and 2.823 are needed, respectively, to have reduction factors less than one. This again means that no beneficial effect can result from the use of boundary condition 2 and 3 if the values of  $\frac{P}{Gw}$  is less than 2.58 and 2.823, respectively.

Fig 4.14 depicts that at a value of  $\frac{P_1}{Gw}$  equal to 3.56, the reduction factor for both the boundary cases are same (= 0.85). For  $\frac{P_1}{Gw}$  greater than 3.56, boundary condition 3 provides higher reduction factor than that of boundary condition 2 and the factor becomes lower for the former boundary case than the latter when the value of  $\frac{P_1}{Gw}$  becomes less than 3.56.

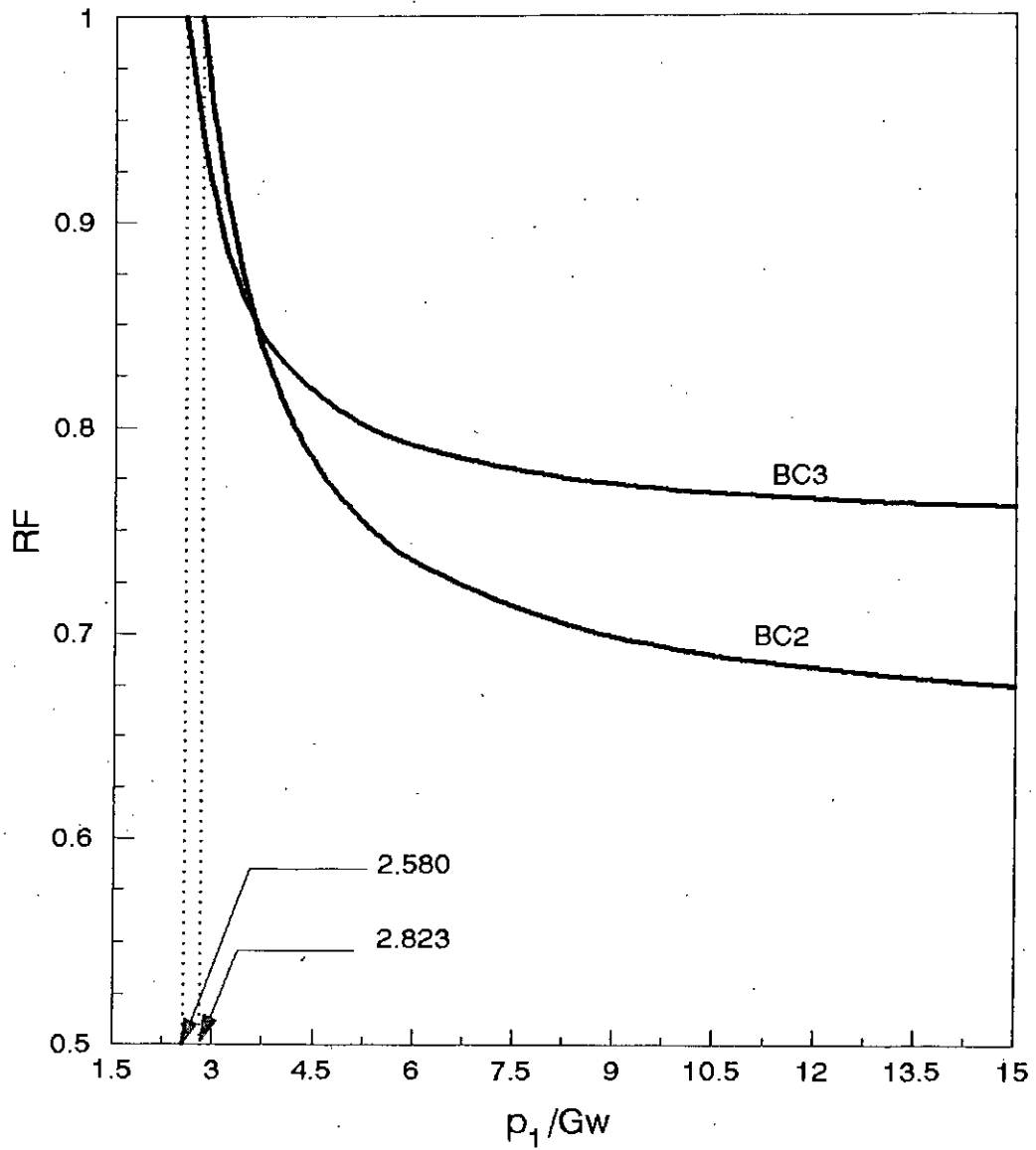


Fig.: 4.14: Inverted egg shaped lining: Reduction factors for minimum permissible lining thickness based on stress-limit criteria

## CHAPTER 5

# STRUCTURAL BEHAVIOUR OF HORSESHOE SHAPED LININGS

### 5.1 INTRODUCTION

The present chapter gives a detail description of the analysis and design procedure of a lining which can be safely inserted into a sewer having horse-shoe shape. The analysis and design are exclusively based on the stress and deflection criteria. The design of sewer linings of any shape is, of course, a complicated task, because the structural response of the lining during installation differs from that of in-service condition (when grout has been set). From this point of view, a properly designed lining must be so designed that it is structurally sound in both the situations. In this chapter, the design of horseshoe shaped lining includes only installation conditions. The analysis carried out here, comprises exclusively of probable loadings that may arise during installation. The horseshoe shaped sewer is not available in our country. But this shape of sewer was popular in many western counties. The question of renovation of these sewers arises now. The daring guarantee offered by lining in renovating the sewers, leads to many engineers to seek for a rational design of this structure. In this chapter, an attempt has been made to put forward specific design recommendations for horseshoe shaped sewer linings. This shape of lining differs from the previously described two linings where axial force developed during loading was not so much as to be included in the design. In the present case, because of the geometry of the structure, the lower part of the structure is subjected to appreciable amount of axial force. Although, the presently prescribed design is based on allowable bending stress and allowable deflection of the lining, the effect of axial force developed in certain portion of the structure should also be checked against possible buckling failures.

### 5.2 TWO-DIMENSIONAL FINITE ELEMENT MESH

The shape of the sewer shown in Fig. 5.1 is available in many states of America. It is seen that there is a sharp kink at the bottom to corners of the sewer. Since higher concentrated stresses are expected at or close to the sharp bends, these higher stresses may be catered for by using thicker liner at the corners or by smoothing the corners by employing circular arcs. In the present study, the corners of the

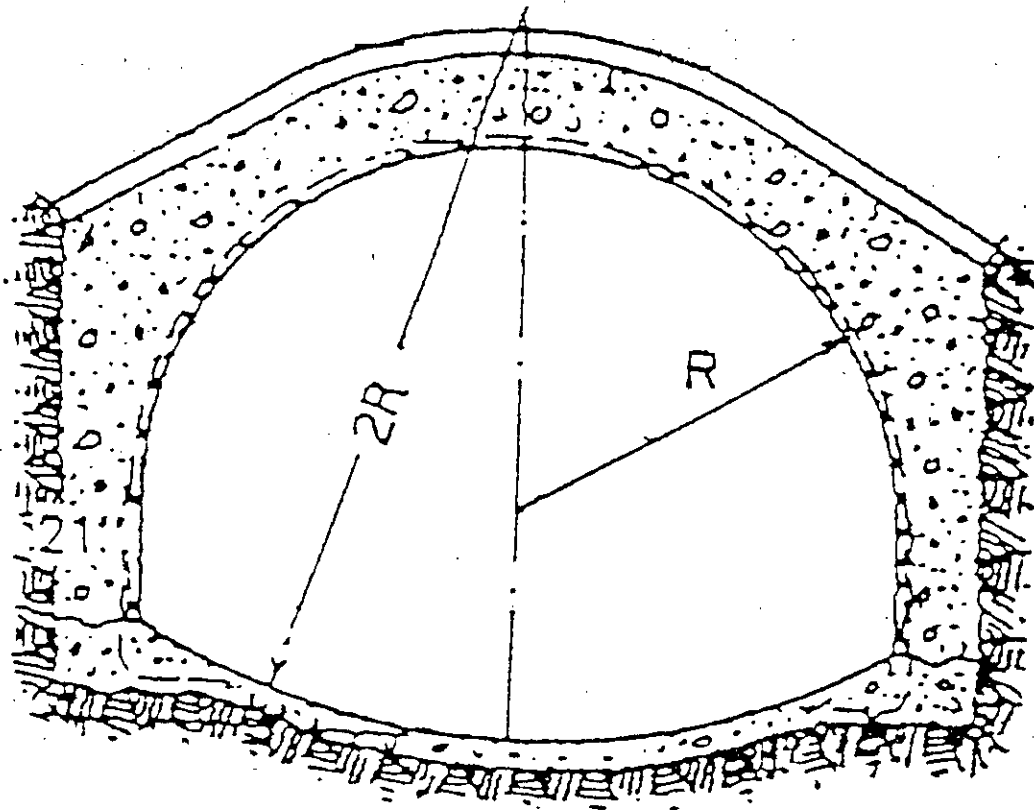


Fig. 5.1: Existing horseshoe sewer, Dallas, U. S. A.

sewer lining have been given slightly different geometry than the actual sewer. While the smoothing approach adopted here has been shown in Fig. 5.2a, the liner geometry in conjunction of the horseshoe sewer is given in 5.2b. It is clear from the figure that the height of the lining ( $h$ ) is 0.8 times of its width (i.e.  $h/w=0.8$ ). Again, the annulus gap between the sewer and the lining remains no longer uniform like the previous cases as introduction of mid-circular arcs causes the gap to increase at or close to the sharp-bending points than the gap that exists at the upper and lower portion of the lining.

Both the geometry of the lining and the loading is symmetrical about the Y-axis, and hence, only half of the lining can be analysed. The half portion of the lining which is to be analysed is shown in Fig. 5.3. This portion of the structure consists certainly of three circular arcs, one of radius  $2R$ , another of  $0.52R$  and the other is of  $R$ . The first, second and third circular arcs are divided into 9, 5, and 16 numbers of beam elements giving 30 elements in total.

### **5.3 BOUNDARY SET-UPS**

Three types of boundary conditions are included in the analysis. These are shown in Fig. 5.4. The simulation of the restraint of all the three types of boundary set-ups are exactly the same as those of previously described egg-shaped and inverted egg shaped linings.

### **5.4 LOADING CONFIGURATIONS**

The three loading configurations included in the analysis are shown in Fig. 5.5. The first comprises of loading up to springing of the lining, the second consists of loading up to the crown and the third is all-around uniform load case. Figure 5.5a simulates the first stage of partial grouting described in Chapter 2, and the summation of the loadings shown in Fig. 5.5b and 5.5c represents the full grouting loading which is also described earlier in chapter 2.

### **5.5 DETERMINATION OF THE DIMENSIONLESS CONSTANTS**

For each of the boundary cases the lining is analysed for all the three loadings just described. For all the boundary cases and loading configurations, the lining is analysed by varying the geometrical parameters a number of times. The results obtained from the analysis are the bending stresses, deflections, axial forces and the

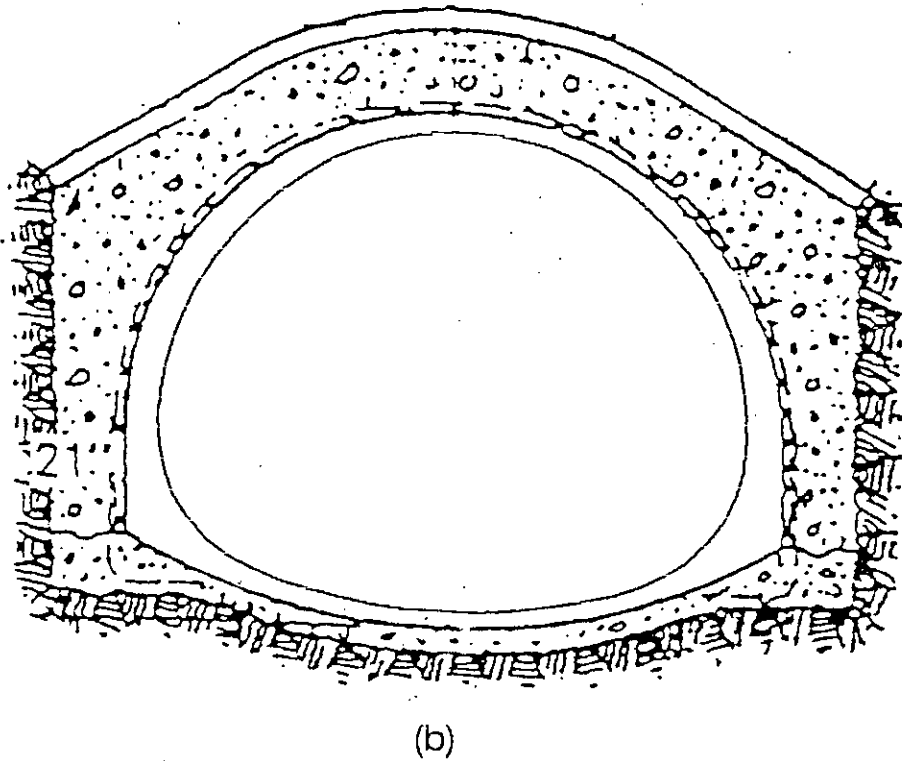
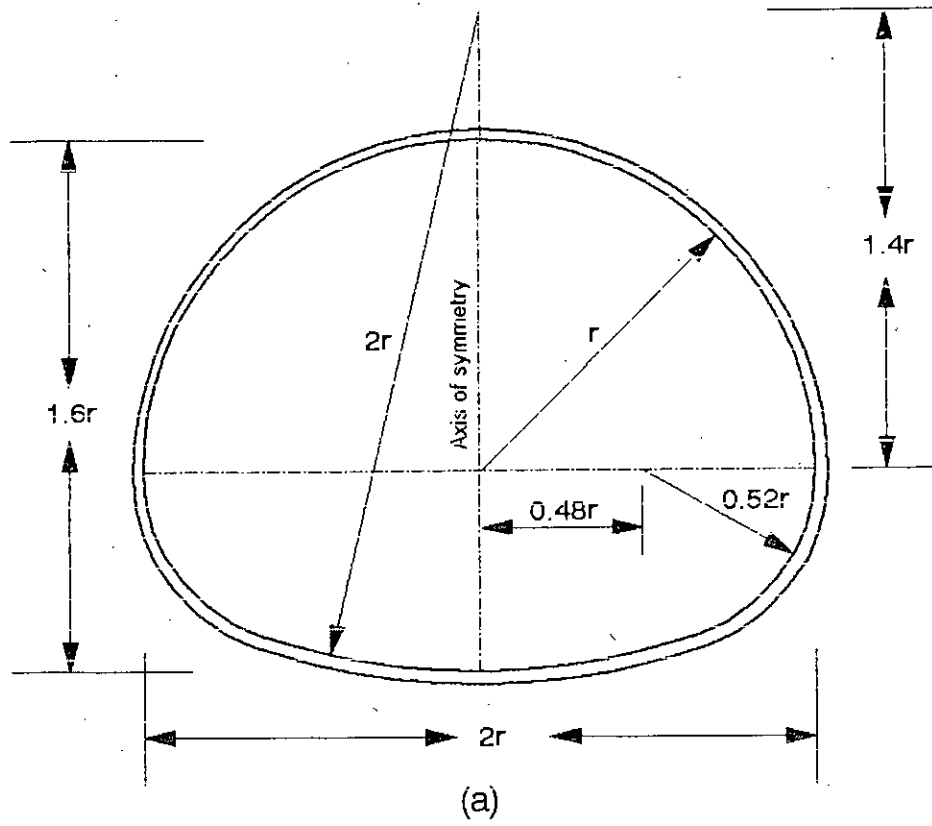


Fig.: 5.2: Horseshoe shaped lining: (a) shape of the lining adopted in the analysis and (b) the lining in conjunction with the sewer

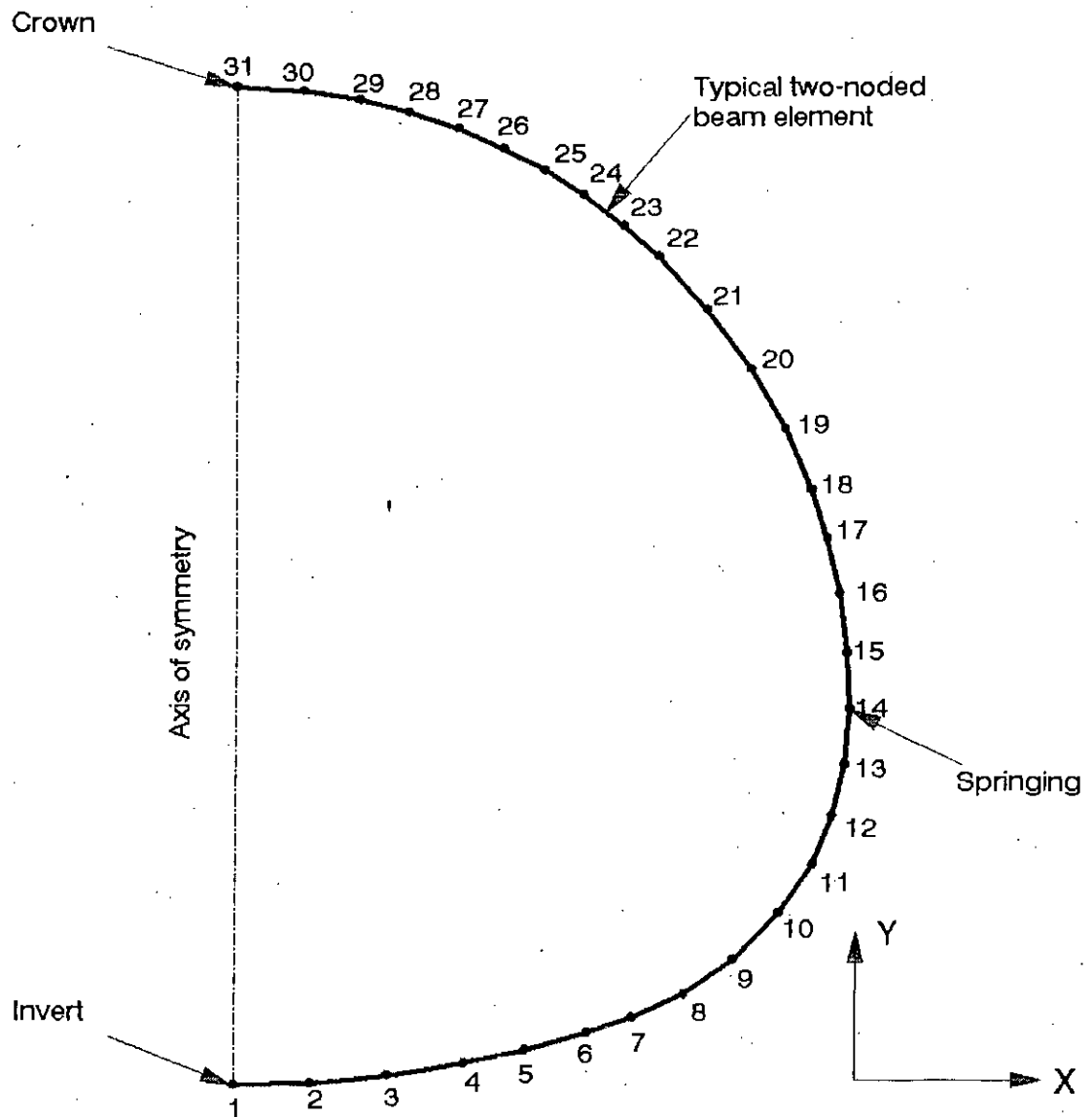
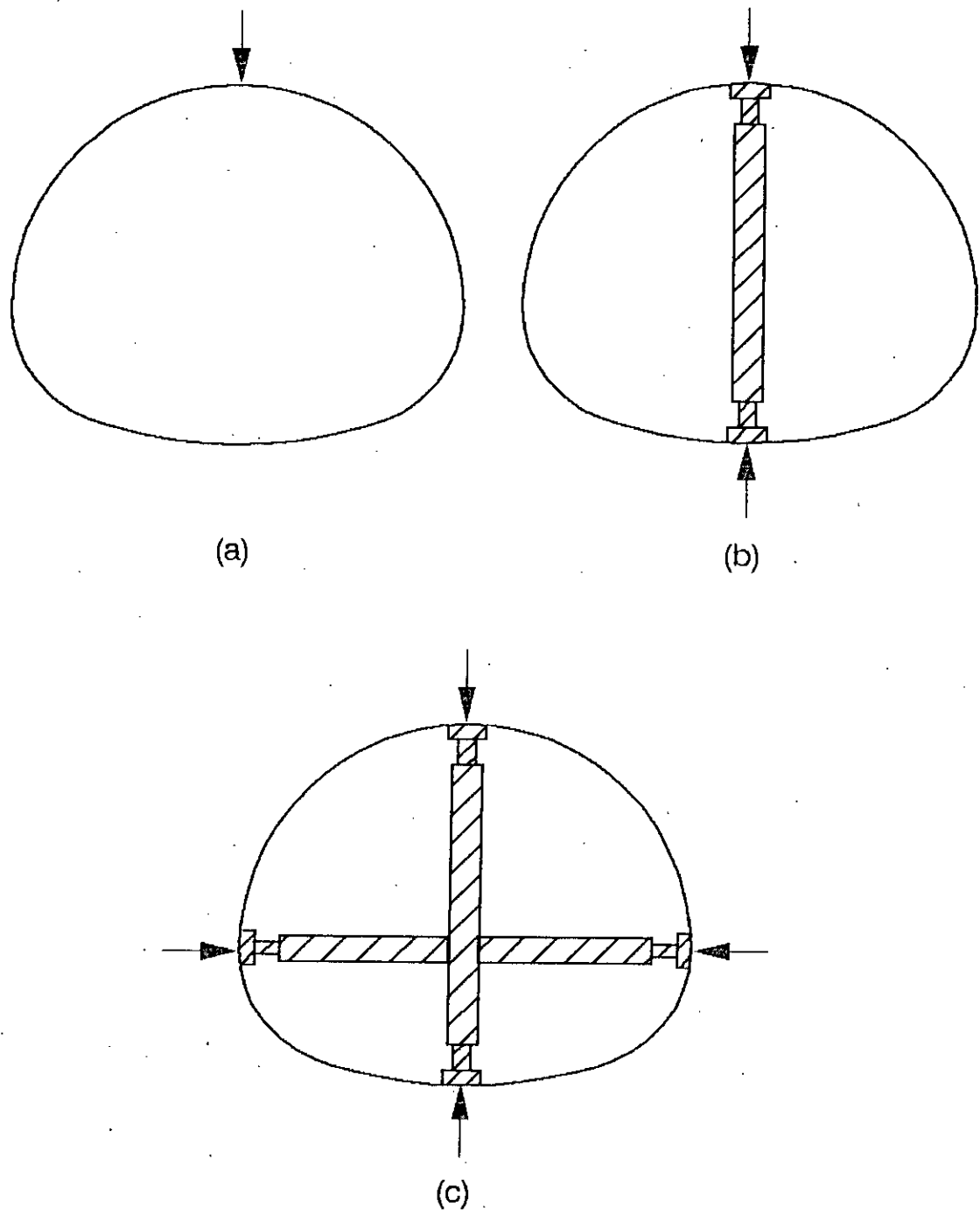
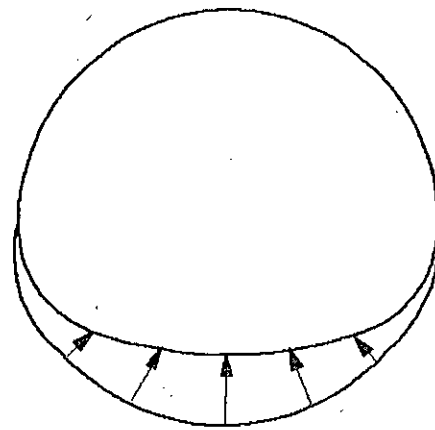


Fig. 5.3: Horseshoe shaped lining: Two-dimensional finite element (FE) mesh adopted in the analysis

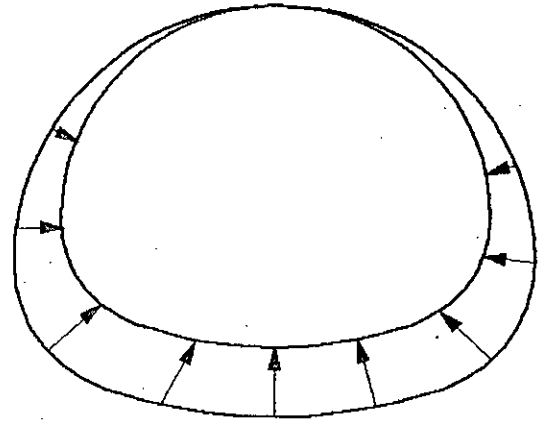




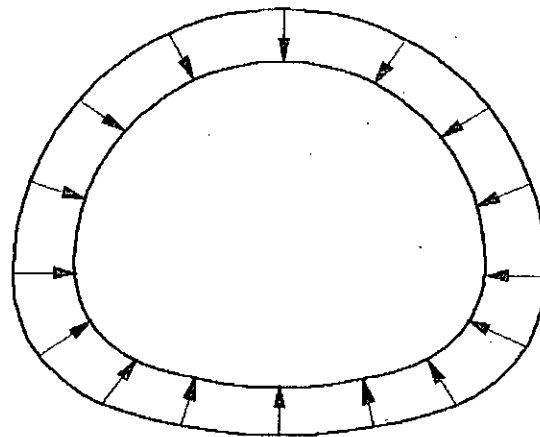
*Fig: 5.4: Horseshoe shaped lining: The support systems studied:  
 (a) boundary condition 1, (b) boundary condition 2 and  
 (c) boundary condition 3*



(a)



(b)



(c)

*Fig. 5.5: Horseshoe shaped lining: The loading configurations studied: (a) staged grouting, (b) grout up to crown only and (c) uniform pressure*

shear forces. Of the bending stresses and deflections at all nodes, the greatest is pointed out and plotted as per equation 2.1 and 2.2, 2.3 and 2.4 or 2.5 and 2.6. These curves are shown in Appendix 3. From these curves, the coefficients A, C and E for maximum bending stresses, and  $B_x$ ,  $B_y$ ,  $D_x$ ,  $D_y$ ,  $F_x$ ,  $F_y$  for maximum deflections for each of the three loading cases are determined. The coefficients are shown in Table 5.1 and 5.2.

**Table 5.1: Dimensionless constants for the maximum bending stress in the lining. (Note: Positive values of A, C and E imply tensile stresses at the inner surface of the lining)**

|                  | Coefficient | Boundary Case 1 | Boundary Case 2 | Boundary Case 3 |
|------------------|-------------|-----------------|-----------------|-----------------|
| Staged Grouting  | A           | 0.1956 Node 31  | -0.0674 Node 1  | -0.0204 Node 1  |
| Flotation        | C           | 0.4482 Node 31  | -0.1381 Node 1  | -0.05347 Node 1 |
|                  |             | 0.2477 Node 1   | 0.1063 Node 31  |                 |
| Uniform pressure | E           | 0.1961 Node 1   | -0.1027 Node 31 | -0.0611 Node 1  |
|                  |             | 0.0783 Node 31  | -0.00711 Node 1 |                 |

**Table 5.2: Dimensionless constants for the maximum deflection in the lining (Note: Inward deflections are taken as positive)**

|                  | Coefficient | Boundary case 1 | Boundary case 2  | Boundary case 3  |
|------------------|-------------|-----------------|------------------|------------------|
| Staged Grouting  | $B_x$       | 0.00 Node 1     | -0.0012 Node 19  | 0.0000271 Node 5 |
|                  | $B_y$       | 0.0361 Node 1   | -0.00213 Node 19 | 0.00242 Node 5   |
| Flotation        | $D_x$       | 0.00 Node 1     | 0.002187 Node 20 | 0.0000759 Node 5 |
|                  | $D_y$       | 0.07722 Node 1  | 0.004662 Node 20 | 0.000654 Node 5  |
| Uniform pressure | $F_x$       | 0.00 Node 1     | 0.0023 Node 20   | 0.000083 Node 5  |
|                  | $F_y$       | 0.04071 Node 1  | 0.00485 Node 20  | 0.0007164 Node 5 |

## 5.6 FULL GROUTING DESIGN CURVES

### 5.6.1 Stress-Limit Criteria:

#### Boundary Case 1: *Restrained at crown against flotation*

The values of bending stress constants A, C, and E for this boundary case for different loading conditions are shown in the third column of Table 5.1. It is seen from these values that the absolute magnitude of C (flotation load case) at node 31 (at the crown) is the greatest of all the five values tabulated in the column. This means that a minimum value of R equal to 0.4482 is needed in order for the lining to withstand the maximum bending stress at the crown resulting from flotation load alone.

It can be seen from the table that in case of flotation load maximum bending stress occurred at node 31 or the crown, whereas that for uniform pressure is located at node 1. This suggests that, in case of full grouting (flotation plus uniform pressure) equation 2.11 must be satisfied at both the nodes 31 and 1 of the lining. This is why the values of C and E are computed at nodes 1 and 31, respectively, to visualise the effect of full grouting load. In this connection, the combined bending stresses at all other nodes were computed and found to be less critical than those at nodes 1 and 31. The above discussion leads to the following design equations which are shown graphically in Fig. 5.6.

At node 31,

$$\begin{aligned} R &= \left| 0.4482 + 0.0783 \left( \frac{P}{Gw} - 0.8 \right) \right| \\ &= \left| 0.38556 + 0.0783 \frac{P}{Gw} \right| \end{aligned} \quad (5.1)$$

At node 1,

$$\begin{aligned} R &= \left| 0.2477 + 0.1961 \left( \frac{P}{Gw} - 0.8 \right) \right| \\ &= \left| 0.09082 + 0.1961 \frac{P}{Gw} \right| \end{aligned} \quad (5.2)$$

It emerges from Fig. 5.6 that the allowable grouting pressure resulting from equation 5.1 remained critical with the range of R-value between 0.4482 and 0.582; once its value exceeds 0.582, equation 5.2 becomes dominant i.e. bending stress at node 1 becomes critical.

Staged grouting is not critical in comparison to full grouting; the relevant permissible grouting pressures associated with this technique can be obtained by means of Table 5.1 and equation 2.1.

### **Boundary Case 2: Restrained at crown and invert of the lining**

In this boundary case, the relevant bending stress constants for different loading configurations are given in Table 5.1. It is seen from the table that the maximum bending stress resulting from flotation load is located at the invert of the lining (i.e. at node 1), whereas in the case of uniform pressure load, the maximum bending stress location is at the crown (i.e. at node 31) of the lining. This implies that equation 2.11 is to be satisfied at both the nodal points. The combined bending stresses at other nodes were calculated and proved to be less critical than those at nodes 1 and 31. This leads to the following two design expressions

At node 1,

$$\begin{aligned} R &= \left| -0.1381 - 0.00711 \left( \frac{p}{G_w} - 0.8 \right) \right| \\ &= \left| -0.132412 - 0.00711 \frac{p}{G_w} \right| \end{aligned} \quad (5.3)$$

At node 31,

$$\begin{aligned} R &= \left| 0.1063 - 0.1027 \left( \frac{p}{G_w} - 0.8 \right) \right| \\ &= \left| 0.18846 - 0.1027 \frac{p}{G_w} \right| \end{aligned} \quad (5.4)$$

These two equations are pictorially shown in Fig. 5.7. It emerges from Fig. 5.7 and Table 5.1 that a minimum value of R equal to 0.1381 is required to take care of the maximum bending stress developed in horseshoe lining during flotation loading.

It is seen from the figure that within the range of R-value 0.1381 and 0.1563, the stress at node 1 i.e. the invert is critical; and beyond the value of R equal to 0.1563, the maximum bending stress occurs at node 31 i.e. at the crown of the lining.

As for the boundary condition 1, partial grouting is less critical than the other two types of loadings in the present case. If staged grouting is employed during the installation of the sewer lining; the allowable grouting pressure can readily be determined in a manner similar to boundary condition 1.

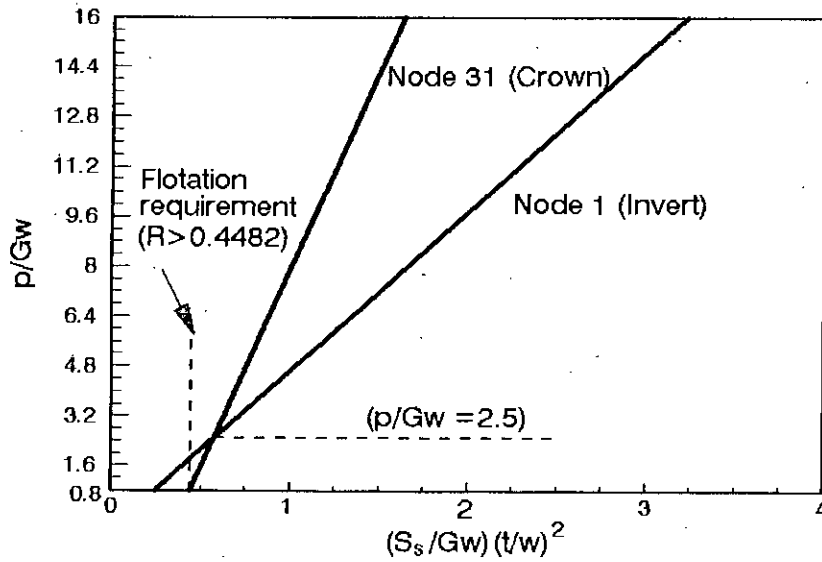


Fig. 5.6: Horseshoe shaped lining: Maximum bending stresses at the crown and invert for flotation ( $p/Gw=0.8$ ) and additional external pressure (Boundary Case 1)

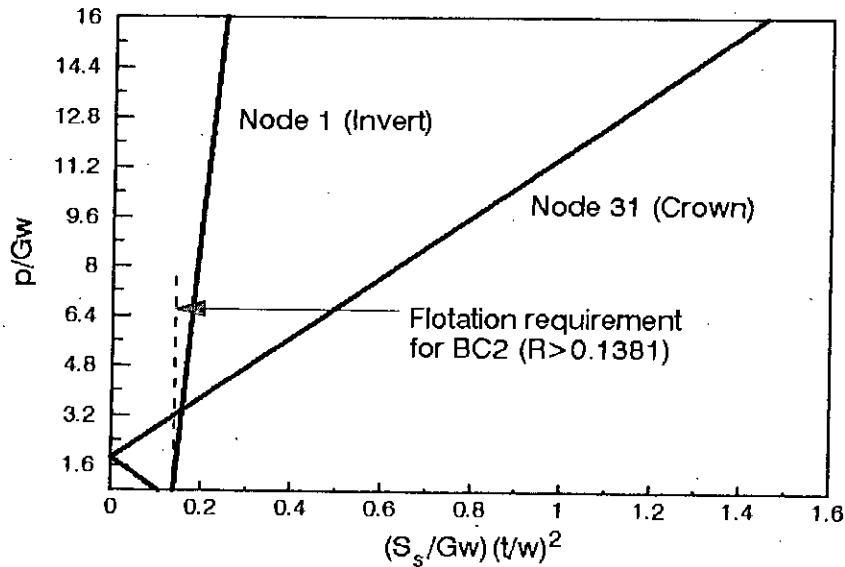


Fig. 5.7: Horseshoe shaped lining: Maximum bending stresses at the crown and invert for flotation ( $p/Gw=0.8$ ) and additional external pressure (Boundary Case 2)

### **Boundary Case 3: Restrained at Crown, invert and springing of the lining**

In this boundary case, the maximum bending stress is located at the invert of the lining for both the loading cases. Hence, at node 1, by using equation 2.11 the following design expression can be written

$$\begin{aligned} R &= \left| -0.05347 - 0.0611 \left( \frac{P}{Gw} - 0.8 \right) \right| \\ &= \left| -0.00459 - 0.0611 \frac{P}{Gw} \right| \end{aligned} \quad (5.5)$$

with  $\frac{P}{Gw} > 0.8$  ( $\frac{P}{G} > h$ ), because as for the boundary cases 1 and 2, a full head of grout must be imposed on the lining for the critical condition to be realised. Once again, if partial grouting conditions are required, they can be found by means of equation 2.1 and Table 5.1.

### **Summary of Stress-Limit Criteria**

All the findings and conclusions, described earlier for the three boundary cases under study for full grouting, are summarised in Fig. 5.8. From this figure, the allowable grouting pressure on a particular lining for any boundary case, based on the stress-limit criteria, can be obtained, if the geometrical and material parameters of the lining are chosen earlier.

It is seen from Fig. 5.8 that for a given value of  $R$ , boundary condition 2 gives allowable grouting pressure higher than that of boundary condition 1. Similar is the case with boundary case 3. Hence it can be said that restraining action causes the lining to withstand more pressure. Lining under boundary condition 3 provides higher allowable pressure except for a small range of  $R$  in which boundary condition 2 gives the greater value of allowable grouting pressure.

### **5.6.2 Deflection-Limit Criteria:**

#### **Boundary condition 1: Restrained at crown only**

For this boundary case, Table 5.2 shows that the maximum deflection in the lining, resulting from each of the flotation and uniform pressure loading cases, is located

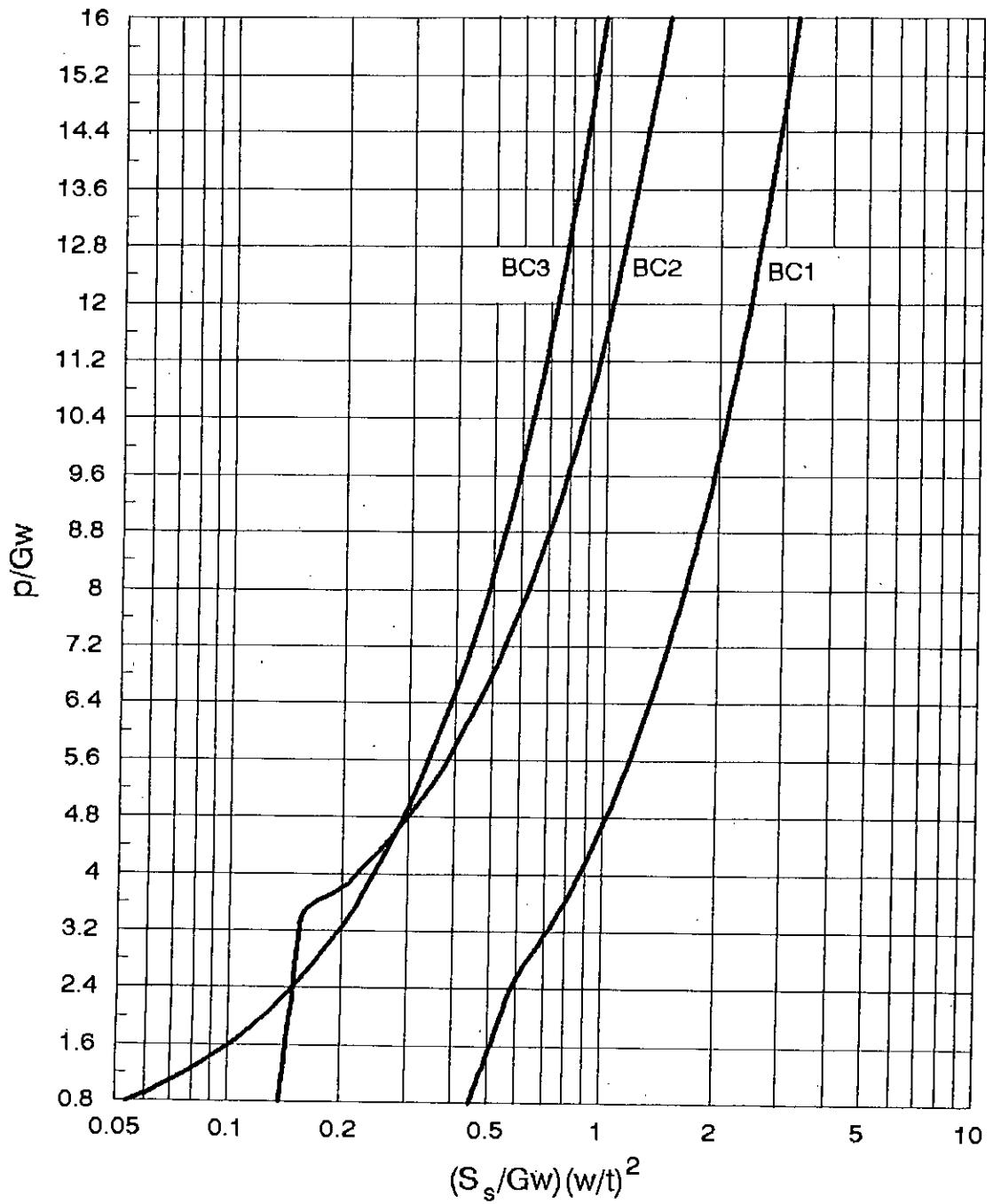


Fig.5.8: Horseshoe shaped lining: Allowable grouting pressure based on stress-limit criteria for various boundary cases



at the invert of the lining (at node 1). This means that equation 2.13 must be satisfied at node 1 of the lining, leading to the following design equation

$$\frac{0.03}{K} = \left| 0.04071 \frac{P}{Gw} + 0.044652 \right| \quad (5.6)$$

where  $\frac{P}{Gw} > 0.8$  i.e.  $\frac{P}{G} > h$  holds, because in this boundary case flotation rather than partial grouting is critical. If needed, the latter case can be calculated using Table 5.2 and equation 2.2.

### **Boundary Case 2: Restrained at crown and invert**

From Table 5.2, it is seen that the maximum deflection for staged grouting, flotation and uniform pressure loading occurs at nodes 19, 20 and 20, respectively. Hence for full grouting (flotation plus uniform pressure), the maximum deflection will occur at node 20. By using equation 2.13, the following design equation can be deduced at this node of maximum displacement

$$\frac{0.03}{K} = \left| 0.0053677 \frac{P}{Gw} - 0.0094436 \right| \quad (5.7)$$

for  $\frac{P}{G} \geq h$ . Partial grouting is not critical in comparison with flotation or full grouting.

### **Boundary Case 3: Restrained at crown, invert and springing of the lining**

In this boundary case, it is interesting to note from Table 5.2 that the maximum deflection in the lining resulting from staged grouting greater than the one resulting from the flotation load alone this leads to the requirement that a minimum value of  $\frac{0.03}{K}$  equal to  $0.00242 \left( = \sqrt{0.0000273^2 + 0.00242^2} \right)$  is needed in order for the lining to withstand the maximum deflection of 3% of  $w$ . Beyond this value, the full flotation and uniform pressure case becomes critical.

The maximum deflection in the lining resulting from the combined effect of flotation and uniform pressure loads is located at node 5 of the lining, leading to the following design equation for  $\frac{P}{G} \geq h$ :

$$\frac{0.03}{K} = \left| 7.212 \times 10^{-4} \frac{P}{Gw} + 8.144 \times 10^{-5} \right| \quad (5.8)$$

## Summary of the Deflection-Limit Criteria

Figure 5.9 summarises the results of the above three boundary conditions. This can now be used to determine the allowable grouting pressure for a particular lining subjected to any of the boundary conditions described in Art. 5.3 and when subjected to full grouting load. It is noted from the figure that unlike the cut-off for the curve of boundary condition 3 at an abscissa value of 0.00242, curves for boundary conditions 1 and 2 reaches the horizontal axis.

## 5.7 DISCUSSION ON THE PRESENT STUDY

### 5.7.1 Enhancement Factor

Enhancement factor (EF) has already been in Chapter 3. In the present case, two values of enhancement factors are determined for each of boundary cases 2 and 3. These are based on the stress and deflection limit criteria outlined earlier and lower value is adopted in design. However, it is found that stress-limitations of the material involved gives the lower value and that they actually govern the design calculations for enhancement factors. As a result, the expression used to calculate the enhancement factor can be derived from equations 5.1, 5.2, 5.3 and 5.5. The EFs in the present study is given below

$$EF_i = \frac{P_i}{P_1} \quad (5.9)$$

where  $i$  corresponds to boundary case 2 or 3.

Here,

$$P_1 = \frac{R - 0.38556}{0.0783} G_w \quad (5.10a)$$

for  $0.4482 < R < 0.582$ ,

$$= \frac{R - 0.09082}{0.1961} G_w \quad (5.10b)$$

for  $R > 0.582$ ,

$$P_2 = \frac{R - 0.132412}{0.00711} G_w \quad (5.11a)$$

for  $0.1381 < R < 0.1563$ ,

$$= \frac{R + 0.18846}{0.1027} G_w \quad (5.11b)$$

for  $R > 0.1563$ , and

$$P_3 = \frac{R - 0.00459}{0.0611} G_w \quad (5.12)$$

for  $R > 0.8$

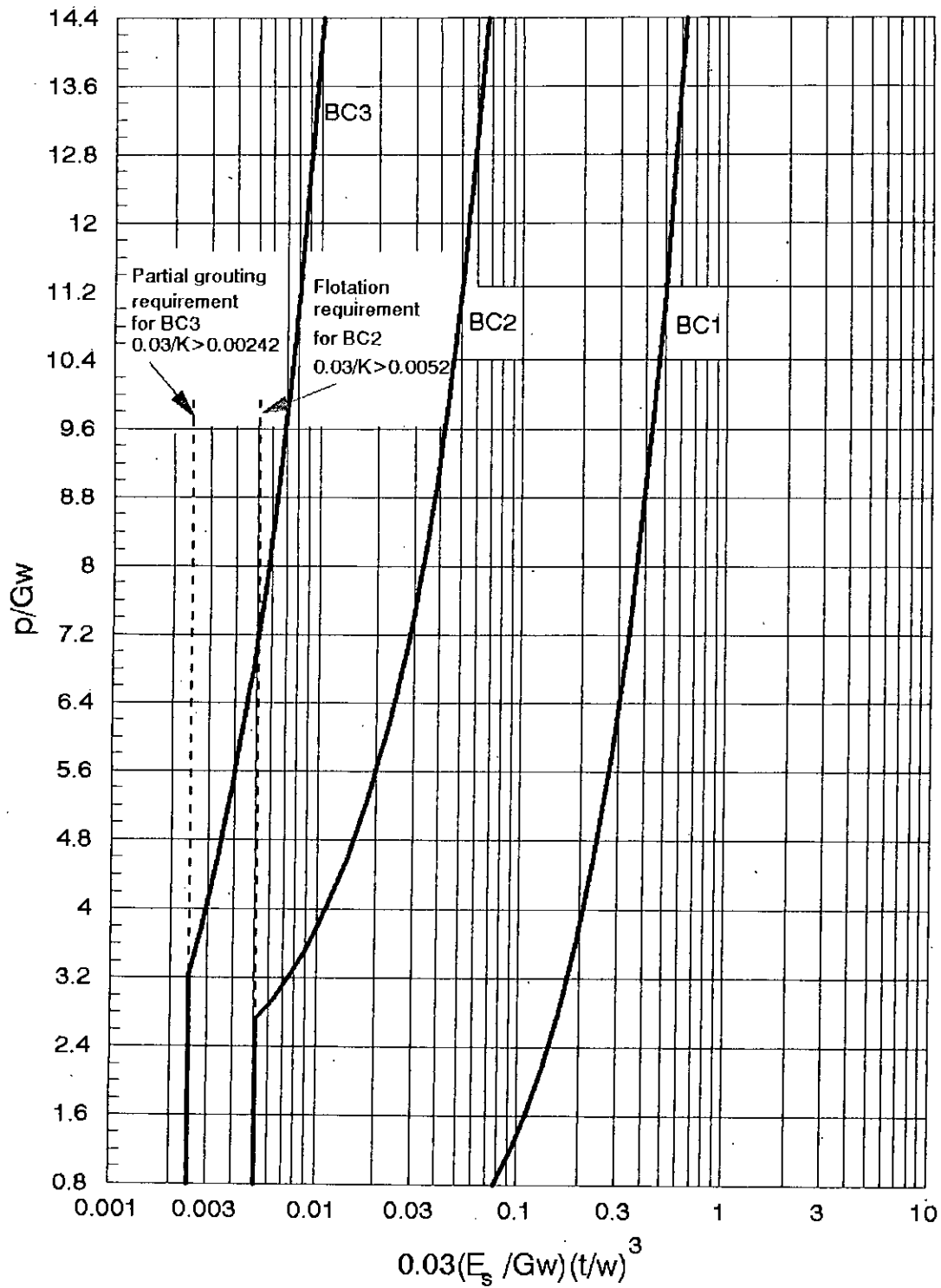


Fig.: 5.9: Horseshoe shaped lining: Allowable grouting pressure based on deflection-limit criteria for various boundary conditions

From the above mentioned equations, enhancement factors are calculated for boundary conditions 2 and 3, and plotted in Fig. 5.10. From the figure it can be deduced that the highest possible enhancement factors that can be achieved for boundary conditions 2 and 3 are 7.75 and 9.075, respectively. As the value of R increases gradually from 0.4482 to 0.582, the value of enhancement factor sharply decreases from 7.75 to 2.99 for boundary case 2 and from 9.075 to 3.77 for boundary case 3; and there after the EF gradually decreases and at last virtually attains constant values in both the cases.

It is interesting to note that, the EFs do not increase with the increase of lining thickness or the allowable bending stress; this means that with the increase of thickness or the allowable bending stress, the enhancement in allowable grouting pressure that can be achieved in case of boundary 1 is much higher than that of boundary case 2 or 3. It is found from the figure that for a particular value of R, the enhancement to be achieved in boundary case 3 is 1.1 to 1.3 times the enhancement to be gained in case of boundary condition 2.

### 5.7.2 Reduction factors

The definition of reduction factors (RF) is defined in Chapter 3. As for the enhancement factor, reduction factors are determined for each of the boundary case 2 or 3 based on the stress and deflection limit criteria. Here, stress limitations, once again, prove to be more critical. The ensuing equations that have been used to calculate the RF shown in Fig. 5.11 is as follows:

$$RF_2 = \left( \left| \frac{0.132412 + 0.00711 p/Gw}{0.38556 + 0.0783 p/Gw} \right| \right)^{1/2} \quad (5.13a)$$

$$\text{for } 0.8 < \frac{p}{Gw} < 2.5,$$

$$= \left( \left| \frac{0.132412 + 0.00711 p/Gw}{0.09082 + 0.1961 p/Gw} \right| \right)^{1/2} \quad (5.13b)$$

$$\text{for } 2.5 < \frac{p}{Gw} < 3.357,$$

$$= \left( \left| \frac{0.18846 - 0.1027 p/Gw}{0.09082 + 0.1961 p/Gw} \right| \right)^{1/2} \quad (5.13c)$$

$$\text{for } \frac{p}{Gw} > 3.357,$$

and,

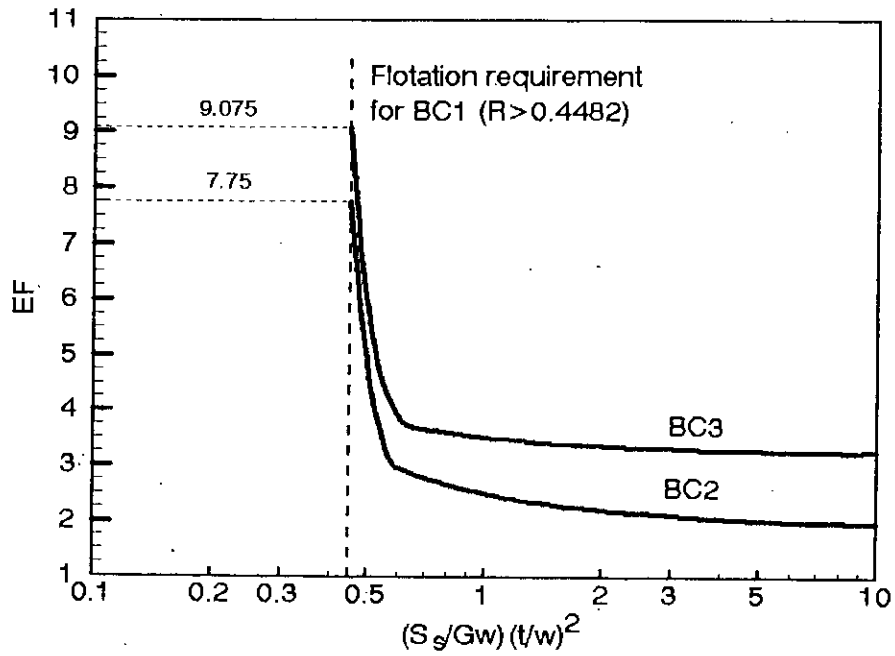


Fig. 5.10: Horseshoe shaped lining: Enhancement factors for allowable grouting pressure based on stress-limit criteria

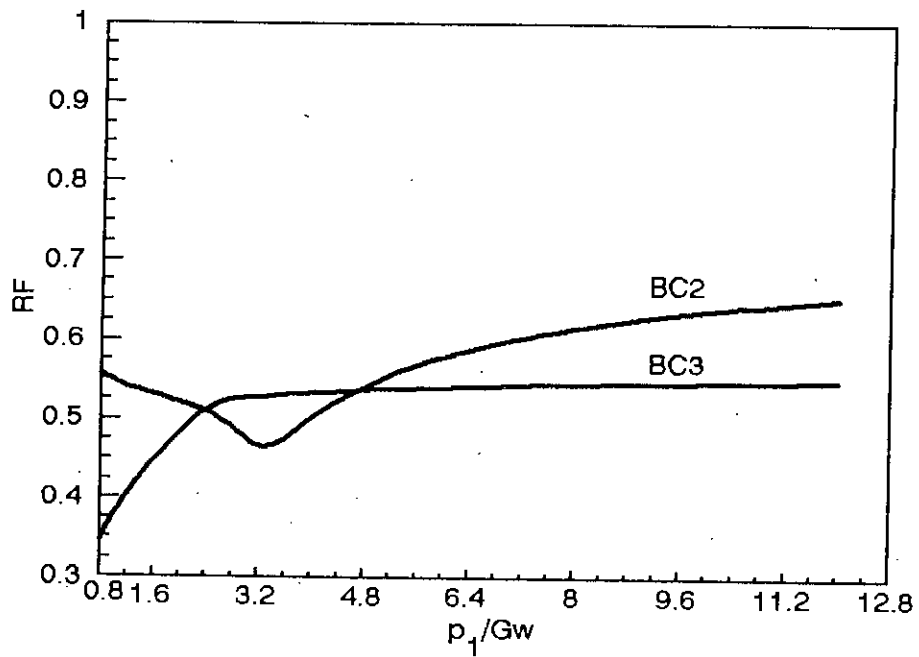


Fig. 5.11: Horseshoe shaped lining: Reduction factors for minimum permissible lining thickness based on stress-limit criteria

$$RF_3 = \left( \left| \frac{0.00459 + 0.0611 p/Gw}{0.38556 + 0.00783 p/Gw} \right| \right)^{1/2} \quad (5.14a)$$

$$\text{for } 0.8 < \frac{p}{Gw} < 2.5,$$

$$= \left( \left| \frac{0.00459 + 0.0611 p/Gw}{0.09082 + 0.1961 p/Gw} \right| \right)^{1/2} \quad (5.14b)$$

$$\text{for } \frac{p}{Gw} > 2.5$$

Figure 5.11 shows that except for small range of  $p_1/Gw$ , boundary condition 3 always provides reduction factors less than that of boundary condition 2. With the increase of  $p_1/Gw$ , the reduction factors virtually reaches constant values for both the boundary cases.

## CHAPTER 6

### STRUCTURAL BEHAVIOUR OF SEMIELLIPTICAL SHAPED LININGS

#### 6.1 INTRODUCTION

This chapter presents the analysis and design procedure of semielliptical shaped linings. The existing semielliptical shaped sewer is shown in Fig. 6.1. If this type of sewer is to be renovated, then the lining is to be such that, when inserted within the sewer, it leaves roughly a uniform gap between the sewer and the lining. When this gap is filled with grout, the lining is subjected to grout pressure. Extensive analysis is carried out under various installation loads and restraint set-ups in this chapter. On the basis of the analysis, discussions of the findings and subsequent design curves are proposed. Finally, an illustrative example has been solved using the proposed curves in Appendix 4.

#### 6.2 TWO-DIMENSIONAL FINITE ELEMENT (FE) MODEL

A linear two-dimensional FE program is used in order to simulate the structural behaviour of semielliptical shaped linings under different restraint set-ups and various probable loads which may arise during the installation of the lining.

##### 6.2.1 Two-Dimensional FE Mesh

The shape of the lining used in the present study is shown in Fig. 6.2a. It consists of two half ellipses. The major axis of one is exactly the half of the other. The minor axes of both ellipses are half of their respective major axes. Hence, from the figure, it can be said that the height ( $h$ ) of the lining is 1.25 times the width ( $w$ ) of the lining. It is to be noted here that in order to avoid sharp bend at the joining point of the ellipse and the circle of the existing sewer, the above-mentioned lining shape is selected. In doing so, the annulus gap between the sewer and the lining remains no longer uniform. In order to maximise the uniformity of the gap, the lower elliptical shape of the lining is selected. While the smoothing approach adopted here has been shown in Fig. 6.2a, the lining geometry with respect to semielliptical sewer is shown in Fig. 6.2b.

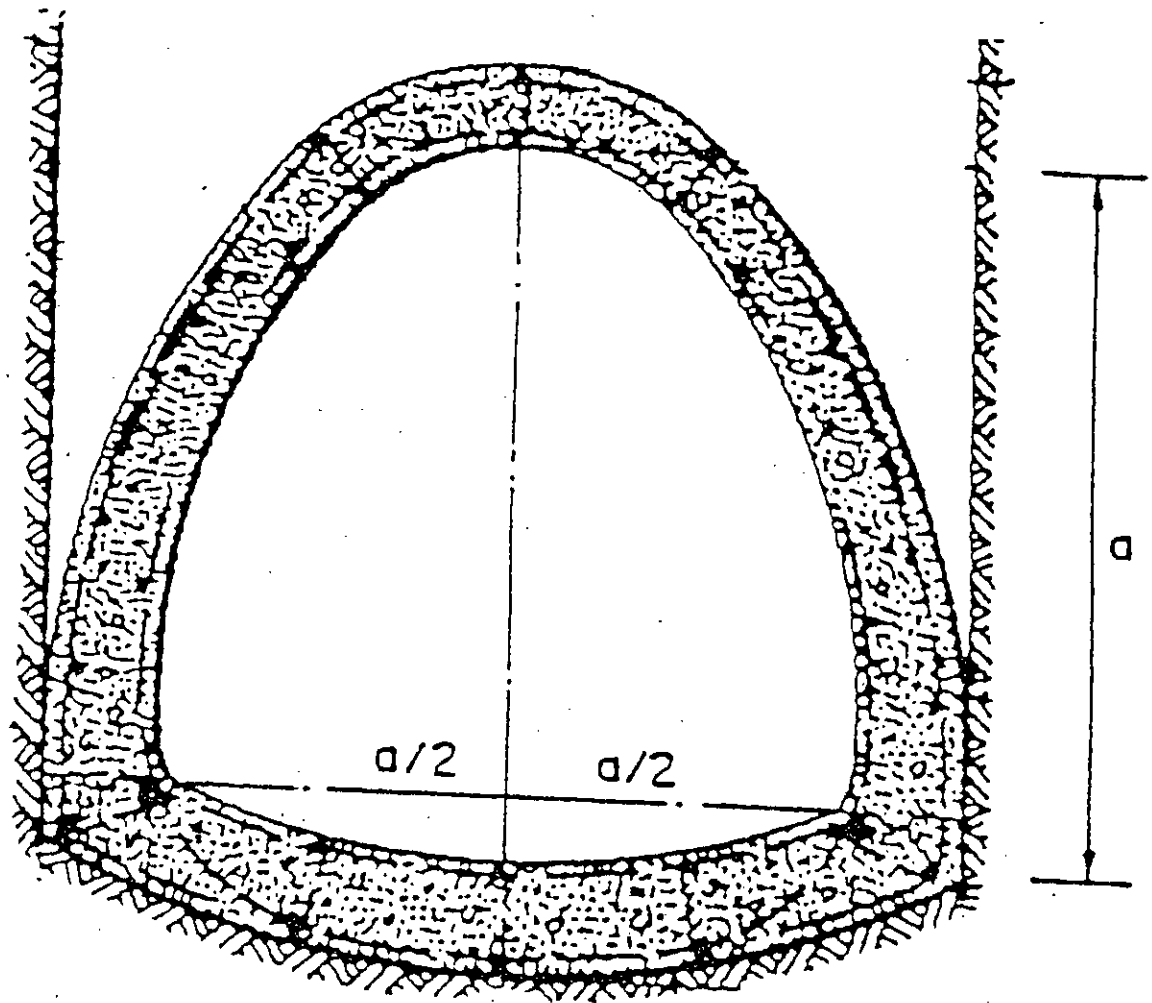
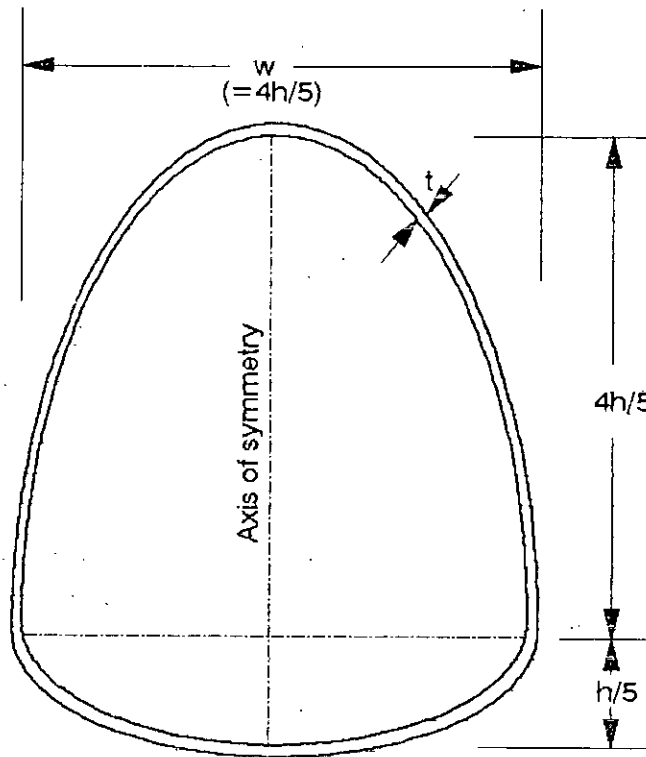
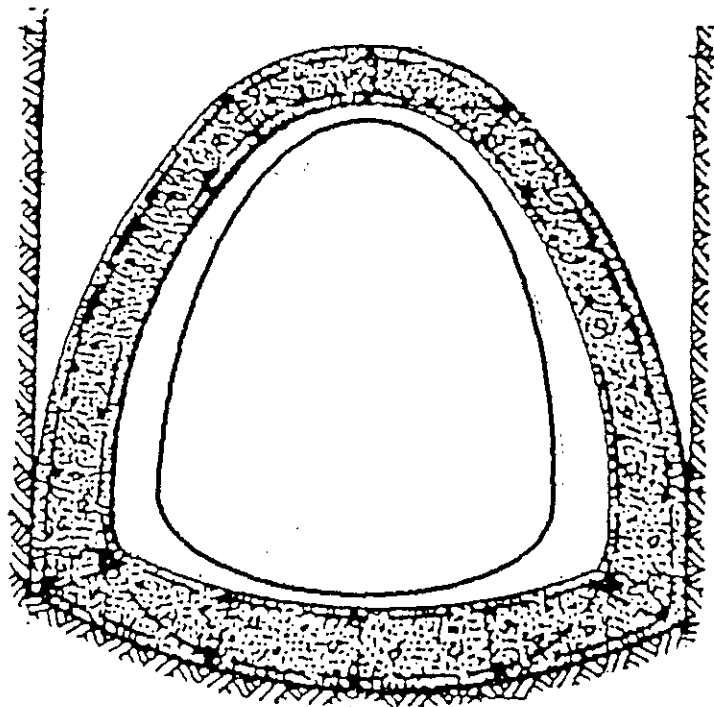


Fig. 6.1: Existing semielliptical sewer, Tulsa, U. S. A.





(a)



(b)

Fig. 6.2: Semielliptical shaped lining: (a) shape of the lining adopted in the analysis and (b) the lining in conjunction with the sewer

Due to the symmetry of the lining with respect to both geometry and loading, only half of the lining is analysed. This is shown in Fig. 6.3. Figure 6.3 shows that the two-dimensional finite element mesh consists of 25 beam elements with three degrees of freedom (horizontal displacement, vertical displacement and rotation) at each node.

### 6.2.2 Restraint Set-Ups

Three support systems are considered in the analysis. These are shown in Fig. 6.4. The first support system considered in the analysis (shown in Fig. 6.4a) consists of a single restraint at the crown of the lining. The second (Fig. 6.4b) comprises restraints at the crown and invert of the lining, while the third form of support system (Fig. 6.4c) consists of restraints at both the crown and invert, in addition to a point at two-third height (from top) of the lining (i.e. at node 14).

### 6.2.3. Simulation of the Restraints

These restraints are simulated in the analysis by fixing the horizontal and vertical components of displacements at the corresponding nodal points. For boundary case 1, all the three displacement components (vertical and horizontal displacements and rotation) at node 26 and horizontal and rotational components of displacements at node 1 are made equal to zero, while in second boundary case all the three displacements at both the nodes 1 and 26 are set to zero. In the third boundary condition, in addition to restraints of the horizontal, vertical and rotational components of displacements at nodes 1 and 26, the horizontal and vertical displacements at node 14 are fixed to zero.

## 6.3 LOADING CONFIGURATIONS

In the present study of semielliptical linings, three loading configurations are included. These are shown in Fig. 6.5. The first of these (Fig. 6.5a) corresponds to pressure from grout surrounding the lining up to one-third height of the lining. The second loading configuration (Fig. 6.5b) involves a head of grout up to the crown. Finally, the third loading configuration corresponds to the uniform pressure which may be applied on the lining as a consequence of excess head of grout shown in Fig. 6.5c.

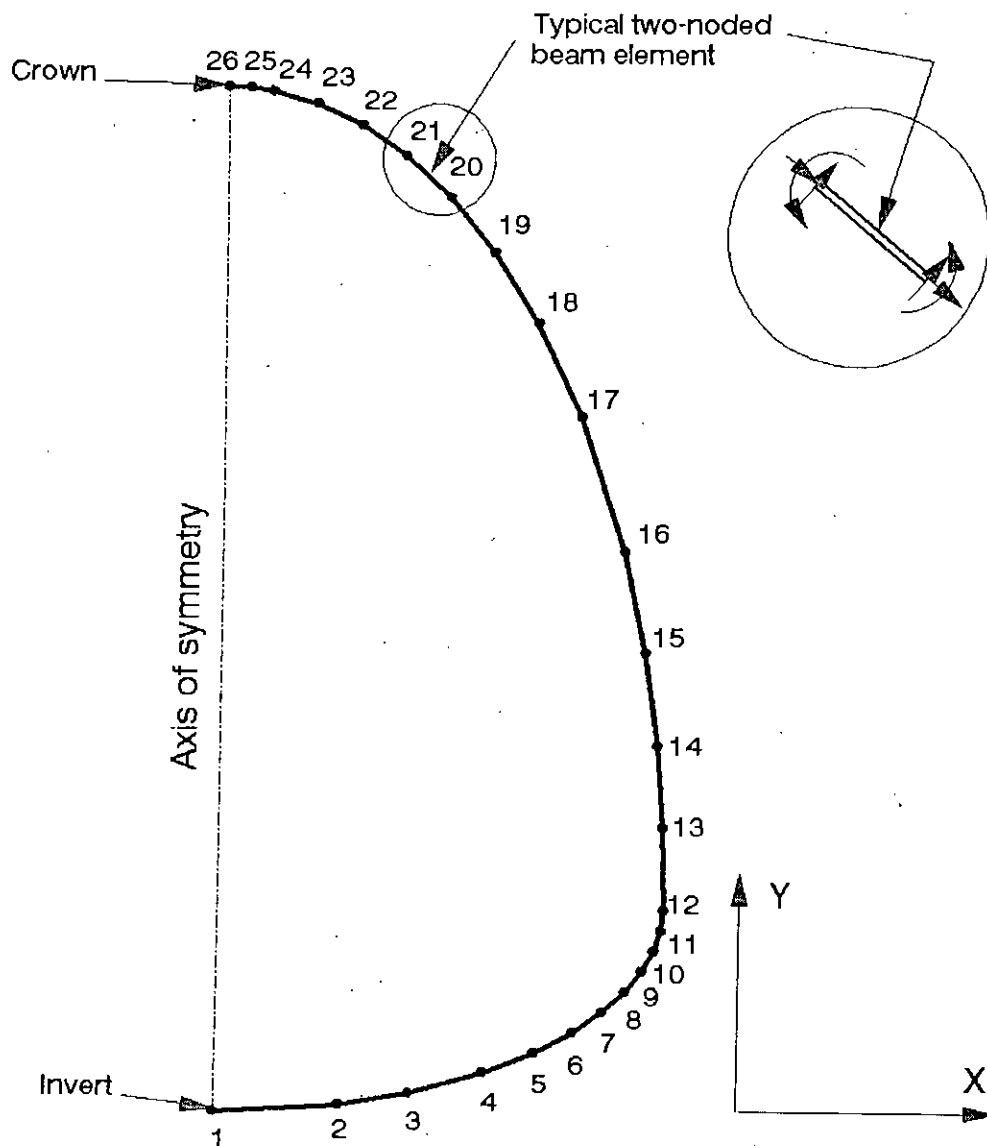
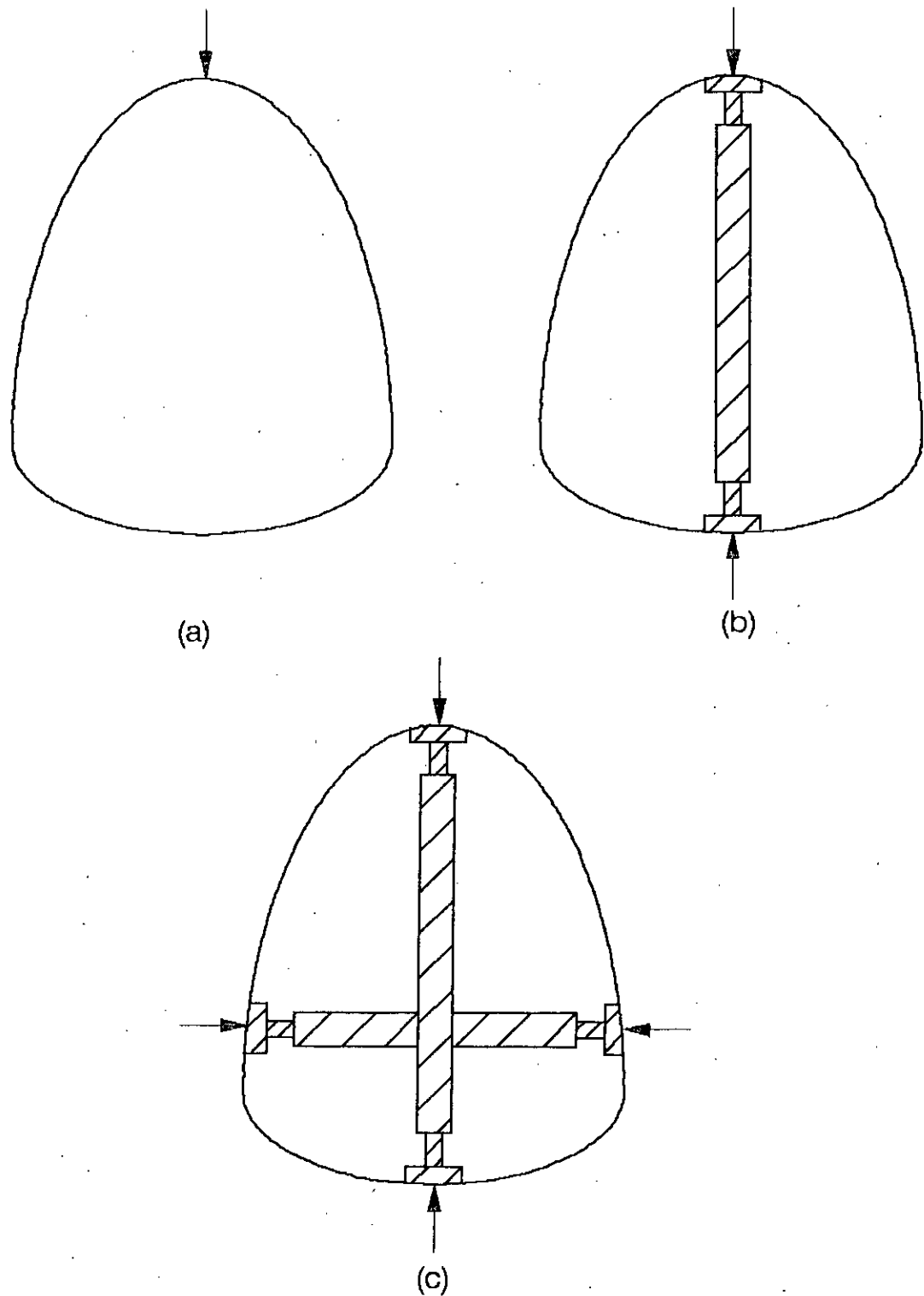
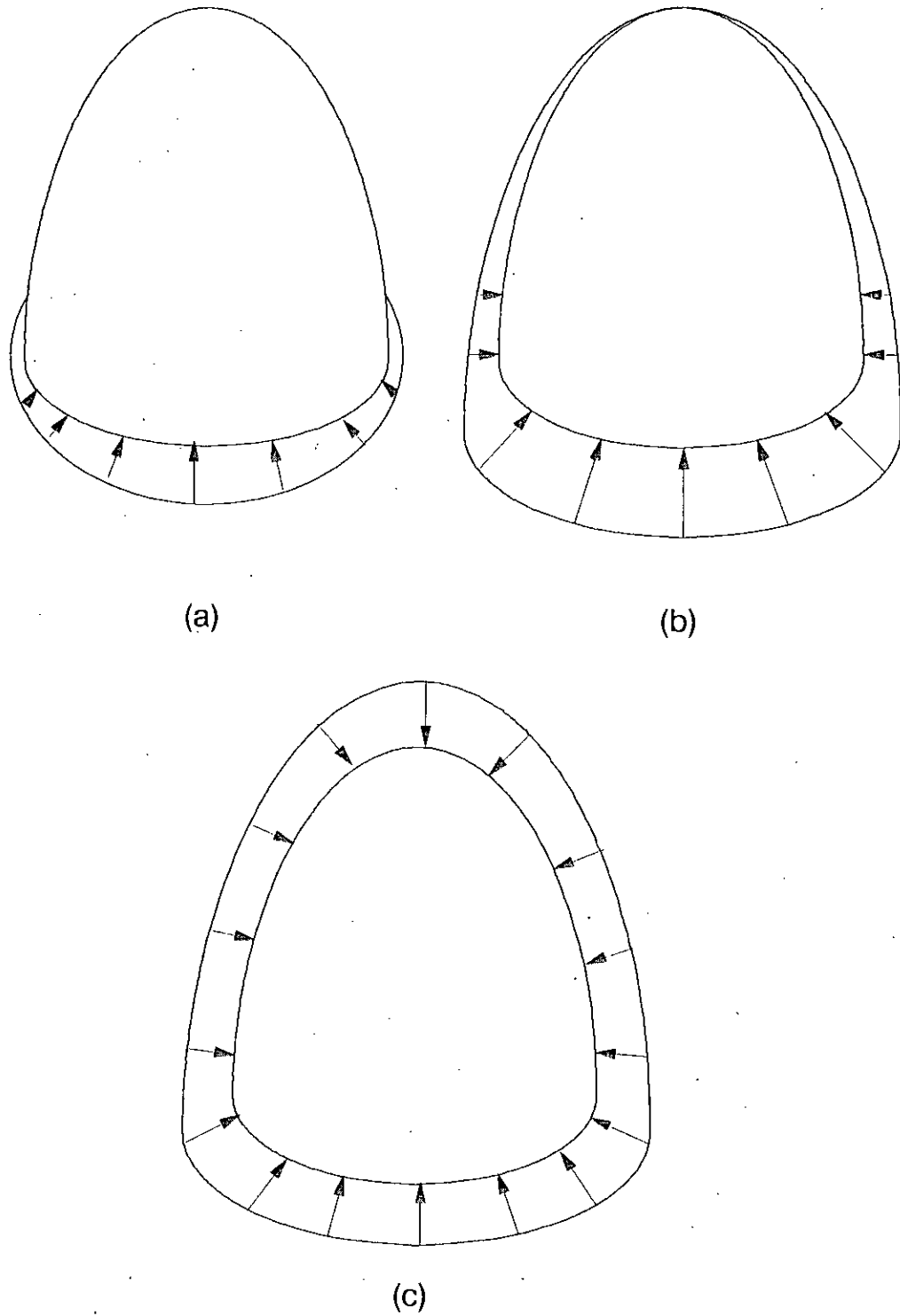


Fig. 6.3: Semielliptical shaped lining: Finite element mesh adopted in the analysis



*Fig.: 6.4: Semielliptical shaped lining: The support systems studied  
(a) boundary condition 1, (b) boundary condition 2 and  
(c) boundary condition 3*



*Fig. 6.5: Semielliptical shaped lining: The loading configurations studied: (a) staged grouting, (b) grout up to crown only and (c) uniform pressure*

## 6.4 PARAMETERS INCLUDED IN THE ANALYSIS

The parameters included in the subsequent analyses are divided into geometrical, material, and load parameters, which are as follows:

(a) Geometrical parameters:

$w$  = width of lining

$h$  = height of lining

$t$  = thickness of lining

(b) Material parameters:

$S_s$  = allowable short-term bending stress of lining material

$E_s$  = short-term modulus of elasticity of material

(c) Load parameters:

$G$  = unit weight of grout mix

$H$  = excess head of grout measured from crown of lining corresponding to uniform pressure load.

## 6.5 DETERMINATION OF THE NONDIMENSIONAL CONSTANTS

The non-dimensional equations used in the present study are given in Chapter 2. For each load and boundary case, parametric analysis is carried out varying one parameter at a time, keeping the others constant. The results of the analysis (bending stresses and deflections) are made dimensionless and plotted as per equations given in Article 2.10. These plots are shown in Fig. A4.1, A4.2, A4.3, A4.4, A4.5 and A4.6 in Appendix 4. From these curves, the various constants ( $A$ ,  $C$ ,  $E$ ,  $B_x$ ,  $B_y$ ,  $D_x$ ,  $D_y$ ,  $F_x$  and  $F_y$ ) are determined and these are shown in Table 6.1 and 6.2.

**Table 6.1:** Dimensionless constants for the maximum bending stress in the lining.  
 (Note: positive values of A, C and E imply tensile stresses at the inner surface of the lining)

|                  | Coefficient | Boundary case 1 | Boundary case 2 | Boundary case 3 |
|------------------|-------------|-----------------|-----------------|-----------------|
| Staged grouting  | A           | 0.362 Node 26   | -0.1153 Node 1  | 0.0496 Node 1   |
| Flotation        | C           | 0.428 Node 26   | 0.1970 Node 26  | -0.0970 Node 1  |
|                  |             | -0.208 Node 9   | -0.1020 Node 9  | 0.0520 Node 26  |
| Uniform pressure | E           | -0.400 Node 26  | -0.3030 Node 9  | 0.1100 Node 26  |
|                  |             | -0.200 Node 9   | -0.1590 Node 26 | -0.0694 Node 1  |

**Table 6.2:** Dimensionless constants for the maximum deflection in the lining  
 (Note: inward deflections are taken as positive)

|                  | Coefficient    | Boundary Case 1 | Boundary Case 2  | Boundary Case 3  |
|------------------|----------------|-----------------|------------------|------------------|
| Staged Grouting  | B <sub>x</sub> | 0.00 Node 1     | -0.00538 Node 17 | 0.0001 Node 4    |
|                  | B <sub>y</sub> | 0.0681 Node 1   | -0.00548 Node 17 | 0.00085 Node 4   |
| Flotation        | D <sub>x</sub> | 0.000 Node 1    | 0.00785 Node 16  | 0.00019 Node 3   |
|                  |                | -0.024 Node 16  |                  | 0.00128 Node 17  |
|                  | D <sub>y</sub> | 0.0607 Node 1   | 0.00052 Node 16  | 0.0016 Node 3    |
|                  |                | -0.022 Node 16  |                  | 0.000313 Node 17 |
| Uniform pressure | F <sub>x</sub> | 0.0631 Node 16  | 0.03 Node 16     | 0.0021 Node 17   |
|                  |                | 0.00 Node 1     |                  | 0.00013 Node 3   |
|                  | F <sub>y</sub> | 0.045 Node 16   | 0.0233 Node 16   | 0.000545 Node 17 |
|                  |                | -0.0634 Node 1  |                  | 0.0011 Node 3    |

## 6.6 FULL GROUTING DESIGN CURVES

### 6.6.1 Stress-Limit Criteria

#### Boundary Case 1: *Restrained at crown only*

Of all the values of A, C and E for boundary case 1 in Table 6.2, the value of C (in case of flotation load) is the highest (0.428) at node 26 of the lining. This means that the stress developed at node 26 i.e. at the crown of the lining during flotation load is the maximum of all the load cases taken into consideration in performing this analysis. The value of E for uniform load also has its maximum value (0.4) at node 26. But they are of opposite sense. Hence when the full grouting load (flotation plus uniform pressure) is simulated, the stress developed at the crown gets a value less than that developed due to flotation load alone. That is why the combined bending stress at all other nodes of the model are computed. It is found that in this case, the maximum bending stress is developed at node 9, not at node 26. So, the value of C and E are computed at the node 9. From the above discussion, it can be inferred that

i) the value of R must have at least 0.428 to withstand the flotation load i.e. grout up to the crown.

ii) for full grouting load, the value of R at node 26 will be (from equation 2.11)

$$\begin{aligned} R &= \left| 0.428 + (-0.4) \left( \frac{P}{G_w} - 1.25 \right) \right| \\ &= \left| 0.928 - 0.4 \frac{P}{G_w} \right| \end{aligned} \quad (6.1)$$

iii) for full grouting load, the value of R at node 9 follows the equation (from equation 2.11)

$$\begin{aligned} R &= \left| -0.208 + (-0.20) \left( \frac{P}{G_w} - 1.25 \right) \right| \\ &= \left| 0.042 - 0.2 \frac{P}{G_w} \right| \end{aligned} \quad (6.2)$$

These equations are plotted in Fig. 6.6. The plot of the equation at node 9 cuts that of at node 26 at a point (0.844, 4.43) beyond flotation limit. It is clear from Fig. 6.6



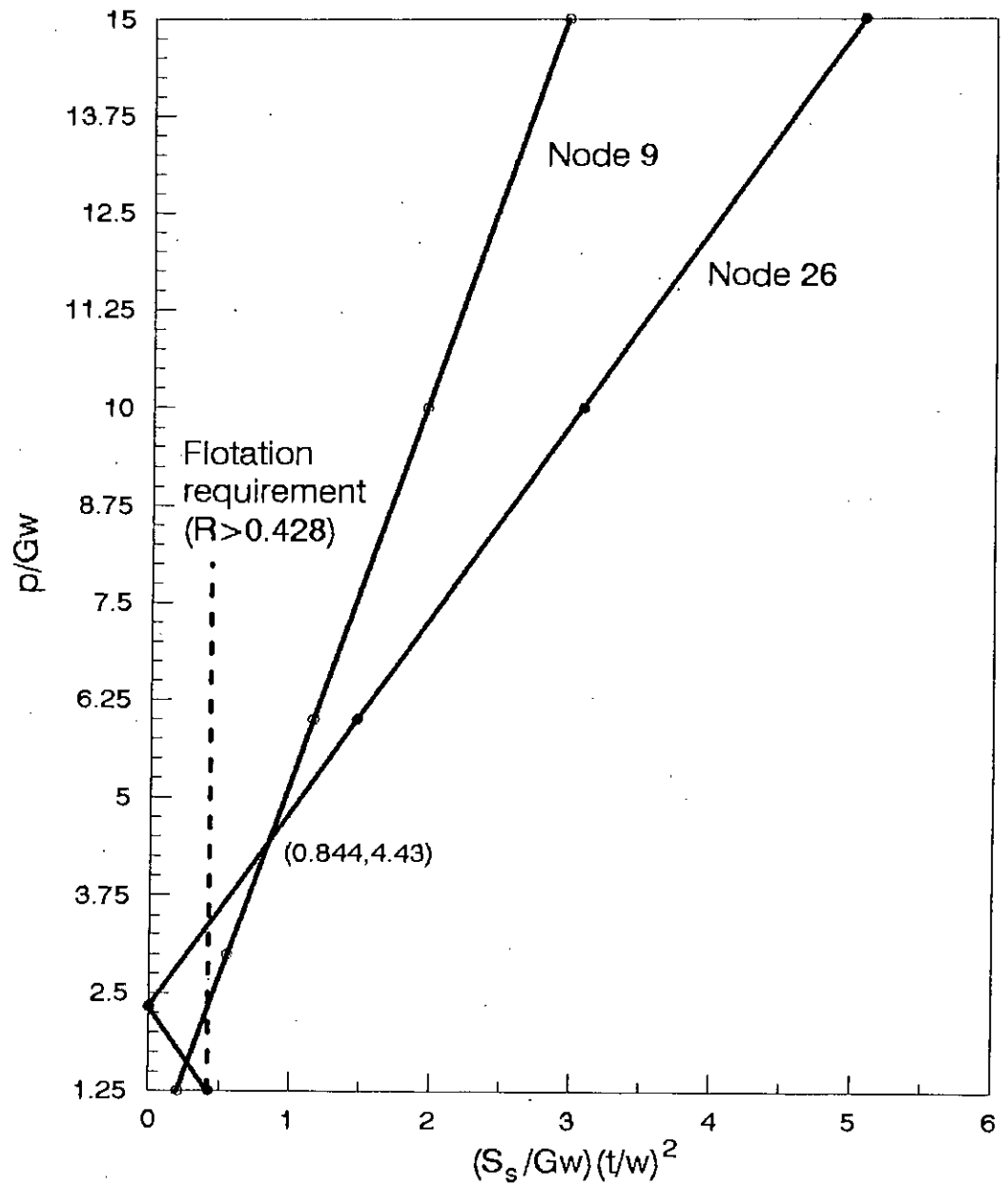


Fig. 6.6: Semielliptical shaped lining: Maximum bending stresses at nodes 9 and 26 of the lining for flotation ( $p/Gw=1.25$ ) and additional external pressure (Boundary Case 1)

that the allowable grouting pressure resulting from equation 6.2 (at node 9) becomes dominant within the values of R ranging from 0.428 to 0.844. Once the value of R exceeds 0.844, the bending stress at node 26 becomes critical.

Staged grouting is not critical in comparison with the full grouting load, the relevant permissible pressures can readily be obtained, if required, by means of equation 2.1.

### **Boundary Case 2: Restrained at crown and invert of the lining**

In this boundary case, it is seen that the maximum bending stresses for staged grouting, flotation and uniform pressures are located at nodes 1, 26, and 9 of the lining, respectively, and the respective values of A, C and E are shown in Table 6.2.

The maximum bending stress developed at node 1 due to staged grouting is less than that resulting from flotation load in which maximum stress occurs at node 26. Again, the node at which the maximum stress develops due to uniform pressure (node 9) differs from that of resulting from flotation load (node 26). Hence equation 2.11 must be satisfied at both the above nodes in case of full grouting load. It is to be noted here that, the combined bending stresses at all other nodes are calculated separately and found to be less critical than those at nodes 9 and 26. These leads to the following two design equations which are shown graphically in Fig. 6.7.

At node 26,

$$\begin{aligned}
 R &= \left| 0.197 + (-0.159) \left( \frac{P}{G_w} - 1.25 \right) \right| \\
 &= \left| 0.396 - 0.159 \frac{P}{G_w} \right| \qquad (6.3)
 \end{aligned}$$

and at node 9,

$$\begin{aligned}
 R &= \left| -0.102 + (-0.303) \left( \frac{P}{G_w} - 1.25 \right) \right| \\
 &= \left| 0.277 - 0.303 \frac{P}{G_w} \right| \qquad (6.4)
 \end{aligned}$$

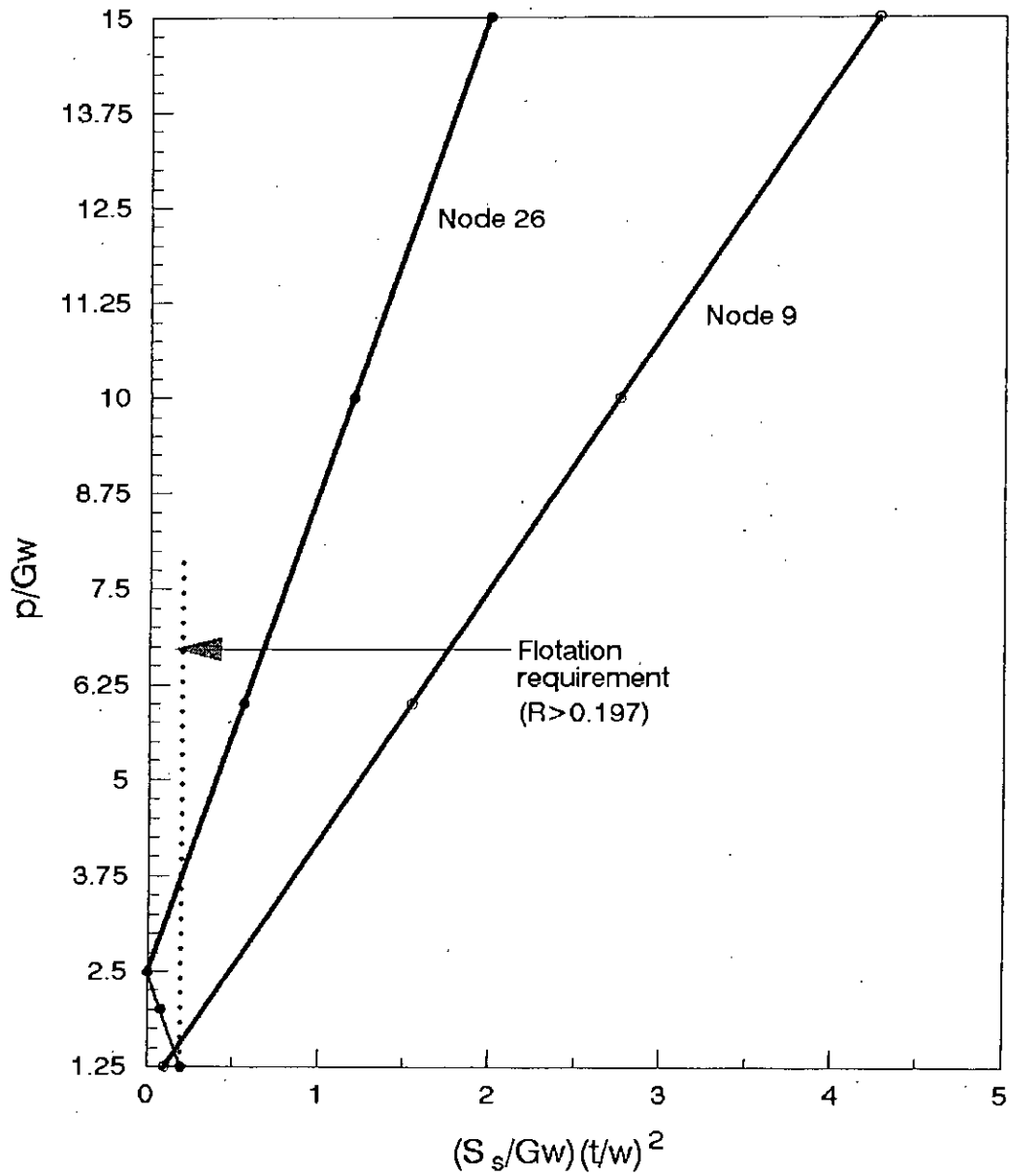


Fig. 6.7: Semielliptical shaped lining: Maximum bending stresses at node 26 and 9 of the lining for flotation ( $p/Gw=1.25$ ) and additional external pressure (Boundary Case 2)

Unlike the boundary condition 1, in this boundary case, the plot of equation at node 9 does not cut that of node 26 beyond the flotation requirement. It is seen from the figure that, in fact, it is the stress at node 9 which is always critical after the flotation requirement ( $R > 0.197$ ). As in boundary condition 1, the staged grouting is not critical in this load case as can be seen from Table 6.1.

### **Boundary Case 3: *Restrained at crown, invert and springing***

For similar reasoning as described in case of boundary condition 1 and 2, in this case equation 2.11 must be satisfied at nodes 1 and 26. The maximum stress developed due to flotation load is of opposite sense with respect to uniform pressure case. Hence, it was required to compute the bending stresses at all other nodes and the results proved to be less critical than those of at nodes 1 and 26. Hence the two design equations can be written as follows (using equation 2.11)

$$\begin{aligned} \text{At node 1, } R &= \left| -0.097 + (-0.0694) \left( \frac{P}{Gw} - 1.25 \right) \right| \\ &= \left| -0.01025 - 0.0694 \frac{P}{Gw} \right| \end{aligned} \quad (6.5)$$

and at node 26,

$$\begin{aligned} R &= \left| 0.0572 + (0.11) \left( \frac{P}{Gw} - 1.25 \right) \right| \\ &= \left| -0.0803 + 0.11 \frac{P}{Gw} \right| \end{aligned} \quad (6.6)$$

These two equations are plotted in Fig. 6.8. It is clear from the figure that the bending stress at node 1 is critical for the values of  $R$  within 0.097 to 0.165. Once its value exceeds 0.197, the bending stress at node 26 becomes critical and determines the allowable grouting pressure based on stress-limit criteria.

### **Summary of Stress-Limit Criteria:**

All the findings obtained for the three boundary cases described earlier, are summarised in Fig. 6.9. Once a boundary case is selected and the geometrical and material parameters are chosen, a value of allowable grouting pressure can be obtained from the figure based on stress-limit criteria.

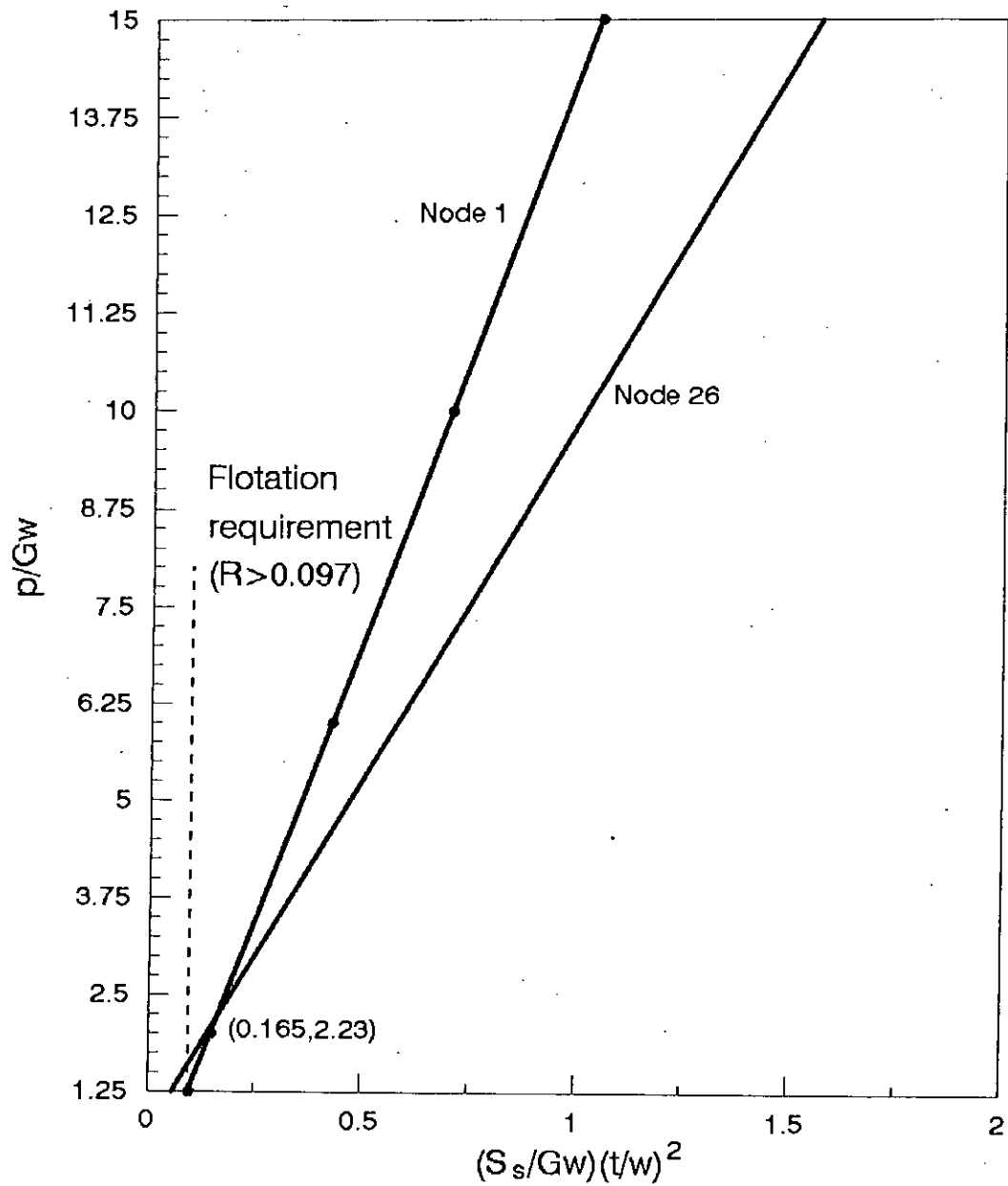


Fig. 6.8: Semielliptical shaped lining: Maximum bending stresses at the crown and the invert of the lining for full flotation ( $p/Gw=1.25$ ) and additional external pressure (Boundary Case 3)

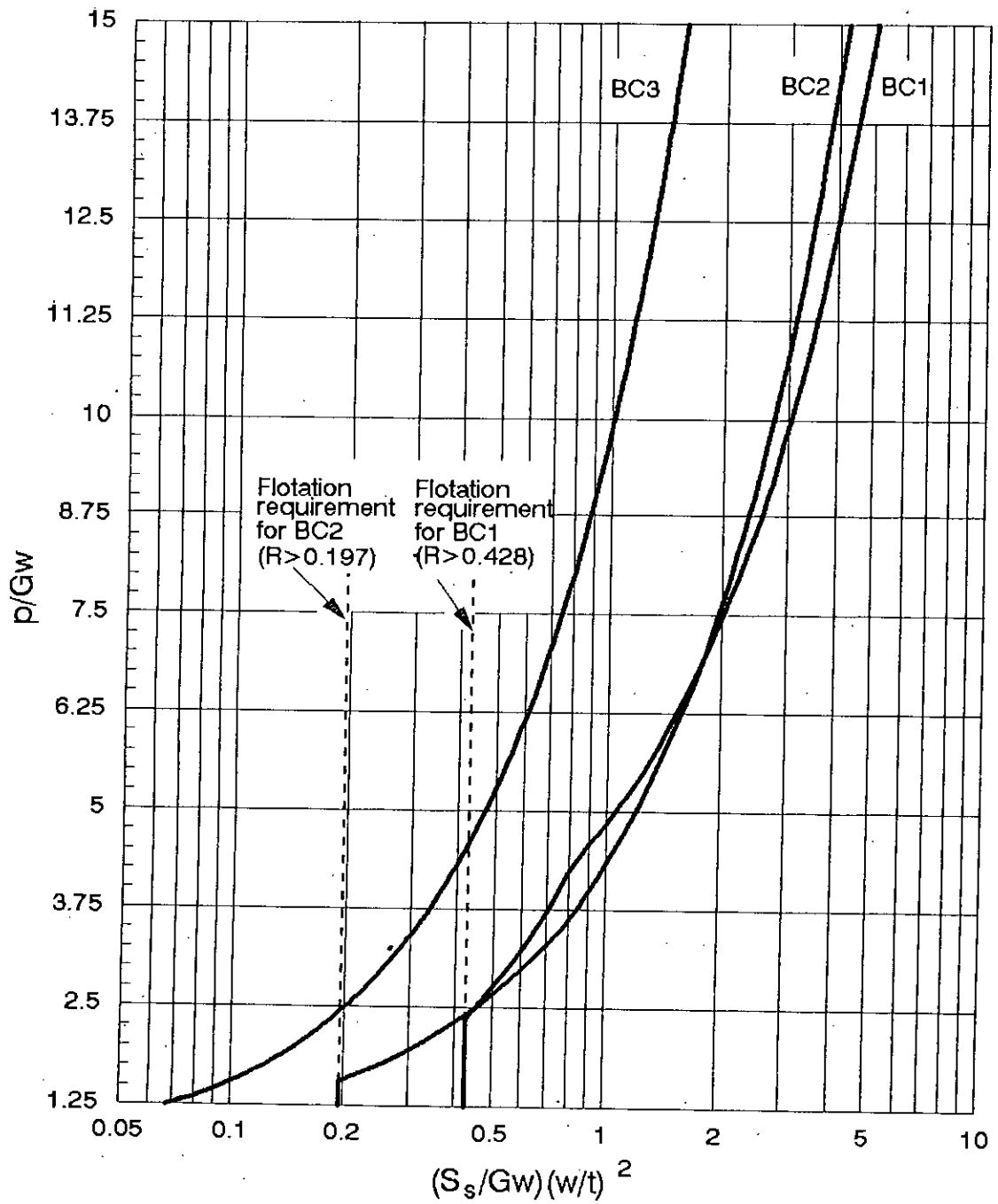


Fig. 6.9: Semielliptical shaped lining: Allowable grouting pressure, based on stress-limit criteria, for various boundary conditions

## 6.6.2 Deflection-Limit Criteria

### Boundary Case 1: *Restrained at crown only:*

Among the values of the constants  $B_x$ ,  $B_y$ ,  $D_x$ ,  $D_y$ ,  $F_x$  and  $F_y$  tabulated in the third column of Table 6.2 for different loadings (staged grouting, flotation and uniform pressure respectively) under boundary case 1, the constant  $\sqrt{B_x^2 + B_y^2}$  has got the highest value. This means that the maximum deflection resulting from staged grouting is greater than any other loadings if they were applied on the lining individually. This leads to the requirement that a minimum value of  $K$  equal to 0.0681 is needed in order for the lining to withstand the maximum allowable deflection (3% of  $w$ ) as recommended by WRC.

In case of flotation, the maximum displacement occurred at node 1, whereas that for uniform pressure case occurred at node 16. This suggests that the equation 2.13 must be satisfied at both the nodes 1 and 16. This leads to the following two design equations at the two nodes:

At node 1,

$$\frac{0.03}{K} = \left| 0.14 - 0.0634 \frac{p}{Gw} \right| \quad (6.7)$$

and at node 16,

$$\frac{0.03}{K} = \left| 0.0775 \frac{p}{Gw} - 0.129 \right| \quad (6.8)$$

These two equations are plotted in Fig. 6.10. It is seen from the figure that the displacement at node 16 is always critical and determines the allowable grouting pressure.

### Boundary Case 2: *Restrained at crown and invert of the lining*

The maximum deflection in the lining resulting from the combined effect of flotation and uniform pressure is located at node 16 of the lining. This implies that equation 2.13 must be satisfied at node 16 for values of  $\frac{p}{G}$  greater than  $h$ ; as a result the following design equation can be written:

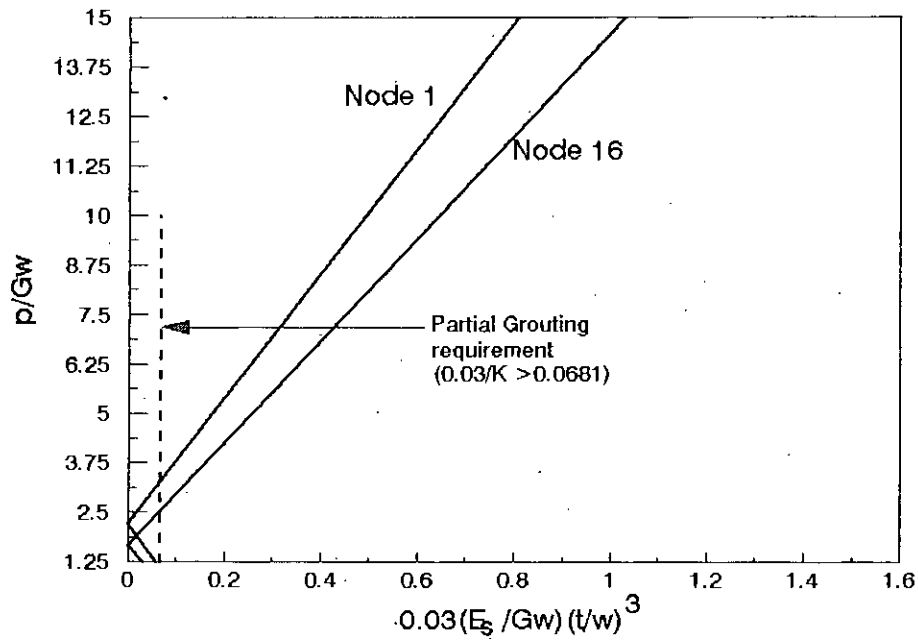


Fig. 6.10: Semielliptical shaped lining: Maximum deflections at nodes 1 and 16 of the lining for full flotation ( $p/Gw=1.25$ ) and additional external pressure (Boundary Case 1)

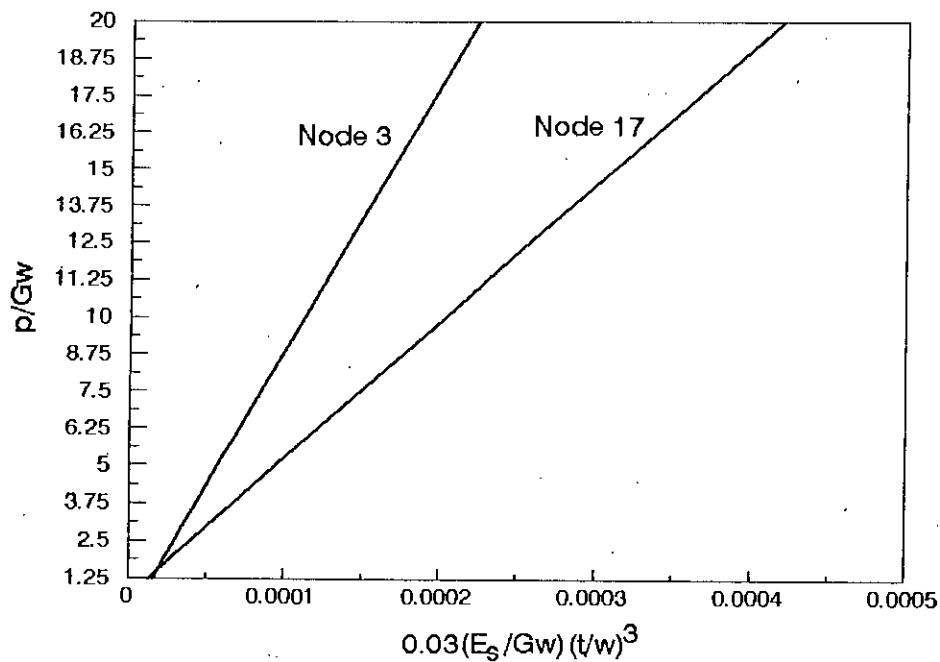


Fig. 6.11: Semielliptical shaped lining: Maximum deflections at nodes 3 and 17 of the lining for full flotation ( $p/Gw=1.25$ ) and additional external pressure (Boundary Case 3)



$$\frac{0.03}{K} = \left| 0.038 \frac{P}{G_w} - 0.041 \right| \quad (6.9)$$

For the case of partial grouting, the maximum deflection occurred at node 17 which is less than that of flotation or full grouting (flotation plus uniform pressure). Hence it is less critical, but if information regarding this type of grouting is required because of installation technique adopted, this can be found from Table 6.2 and using equation 2.2.

**Boundary Case 3: Restrained at crown, invert and springing of the lining:**

In this case the relevant constants for different loading cases are shown in the fifth column of Table 6.3. It is seen that the maximum deflection due to staged grouting occurs at node 4 which is less than that of flotation load in which case the maximum deflection occurs at node 3 of the lining.

For full load (flotation plus uniform pressure), equation 2.13 should be satisfied at both the nodes 3 and 17 for the reason described earlier in case of boundary condition 1. Hence the following two design expressions can be found (using equation 2.13):

At node 3,

$$\frac{0.03}{K} = \left| 0.00111 \frac{P}{G_w} + 0.00022 \right| \quad (6.10)$$

and at node 17,

$$\frac{0.03}{K} = \left| 0.00217 \frac{P}{G_w} - 0.001394 \right| \quad (6.11)$$

The above mentioned two equations are plotted in Fig. 6.11. The two curves of Fig. 6.11 intersects at a point of (0.0019, 1.51). It is found from the figure that deflection at node 17 is always critical except for the value of  $\frac{P}{G_w}$  ranging from 1.25 to 1.51 within which the deflection at node 3 becomes greater than that of node 17.

## Summary of Deflection-Limit Criteria

Figure 6.12 summarises the results of the above three boundary conditions; hence can be used to determine the allowable grouting pressure on any particular lining, based on the deflection-limit criteria. It can be seen in the figure that unlike the cut-off of the curve for boundary condition 1 at an abscissa value of 0.0681, curves for boundary condition 2 and 3 gradually reaches the horizontal axis.

## 6.7 DISCUSSION OF THE PRESENT STUDY

### 6.7.1 Enhancement Factor

As in the previous few lining shapes (egg shaped, inverted egg shaped and horseshoe shaped), the present study of semielliptical lining has revealed that both the maximum stress and deflection in a lining resulting from the grouting pressure load can be reduced when additional restraints are introduced during installation. This implies that an enhancement in the value of the grouting pressure can be achieved in this case also.

Two values of EF are determined for each of the boundary cases 2 and 3, based on stress- and deflection-limit criteria outlined earlier and the lower value is adopted in the design. The EFs are computed from the following equation

$$EF_i = \frac{P_i}{p_i} \quad (6.12)$$

where  $i$  corresponds to boundary cases 2 or 3.

and for stress-limit criteria,

$$p_1 = 5.0 (R + 0.042) Gw \quad (6.13a)$$

for  $0.428 < R < 0.844$ ,

$$= 25.0 (R + 0.928) Gw \quad (6.13b)$$

for  $R > 0.844$ ,

$$p_2 = 3.3 (R + 0.277) Gw \quad (6.14)$$

and,

$$p_3 = 9.09 (R + 0.0803) Gw \quad (6.15)$$

Hence, the expression for enhancement factor can be written as follows:

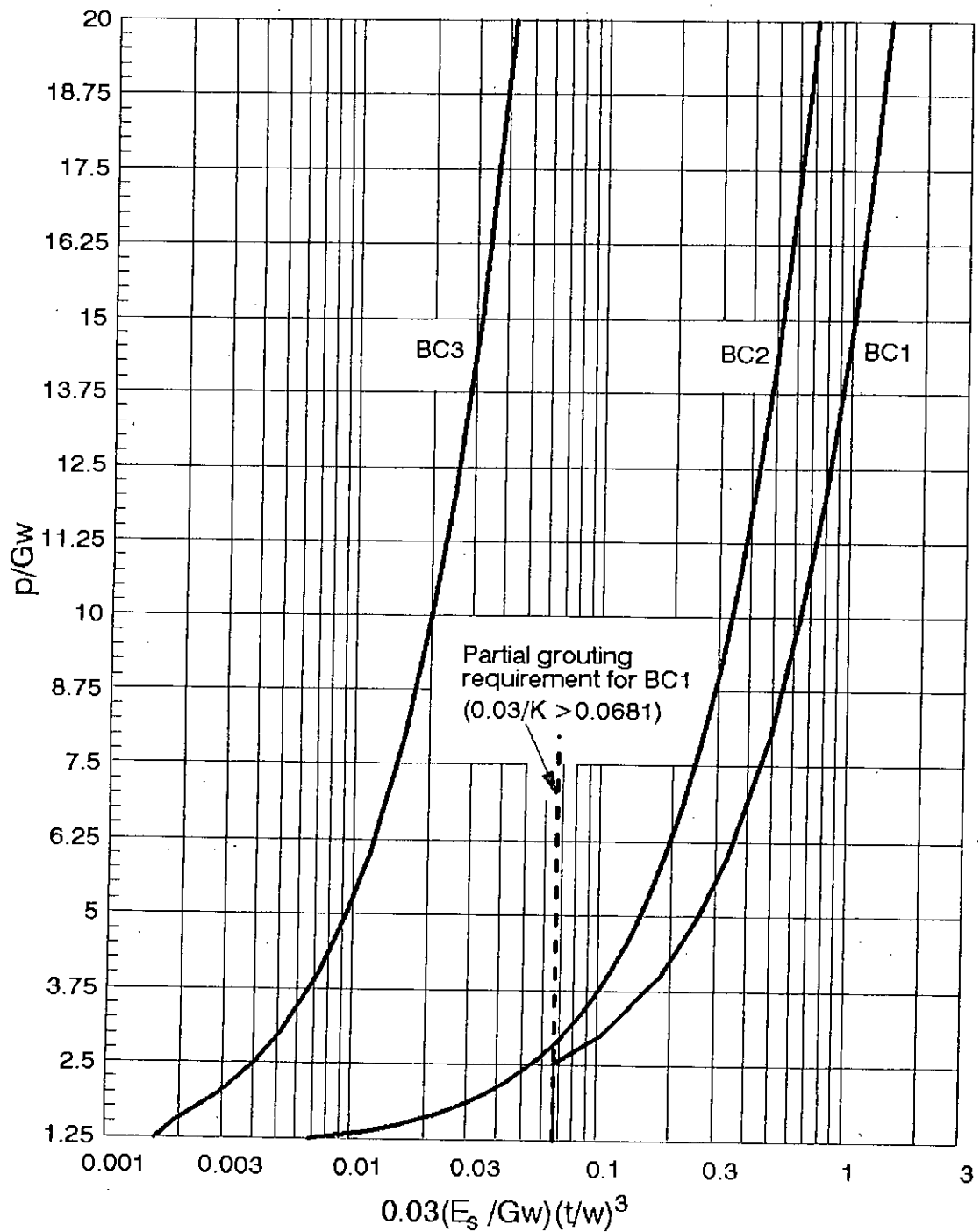


Fig. 6.12: Semielliptical shaped lining: Allowable grouting pressure for based on deflection-limit criteria for various boundary conditions

$$(EF)_2 = 0.66 \frac{R + 0.277}{R + 0.042} \quad (6.16a)$$

for  $0.428 < R < 0.844$ ,

$$= 1.32 \frac{R + 0.277}{R + 0.928} \quad (6.16b)$$

for  $R > 0.844$

$$(EF)_3 = 1.818 \frac{R + 0.0803}{R + 0.042} \quad (6.17a)$$

for  $0.428 < R < 0.844$ ,

$$= 3.636 \frac{R + 0.0803}{R + 0.928} \quad (6.17b)$$

for  $R > 0.844$

The enhancement factors for boundary cases 2 and 3, based on stress-limit criteria, are graphically shown in Fig. 6.13.

For deflection-limit criteria, the values of  $p_1$ ,  $p_2$ , and  $p_3$  can be deduced from the equations 6.8, 6.9 and 6.11 respectively. These are as follows:

$$p_1 = \left( \frac{0.03}{K} + 0.129 \right) 12.9Gw \quad (6.18)$$

$$p_2 = \left( \frac{0.03}{K} + 0.041 \right) 26.32Gw \quad (6.19)$$

$$p_3 = \left( \frac{0.03}{K} + 0.001394 \right) 460.83Gw \quad (6.20)$$

and hence, enhancement factors for boundary conditions 2 and 3, based on deflection-limit criteria, can be derived as follows,

$$(EF)_2 = 2.04 \frac{\frac{0.03}{K} + 0.041}{\frac{0.03}{K} + 0.129} \quad (6.21)$$

$$(EF)_3 = 35.66 \frac{\frac{0.03}{K} + 0.001394}{\frac{0.03}{K} + 0.129} \quad (6.22)$$

Equations 6.16 and 6.17, and 6.21 and 6.22 are pictorially shown in Figs. 6.13 and 6.14, respectively. From these two figures, it is found that for a particular lining geometry and material properties, enhancement factor achieved from stress-limit

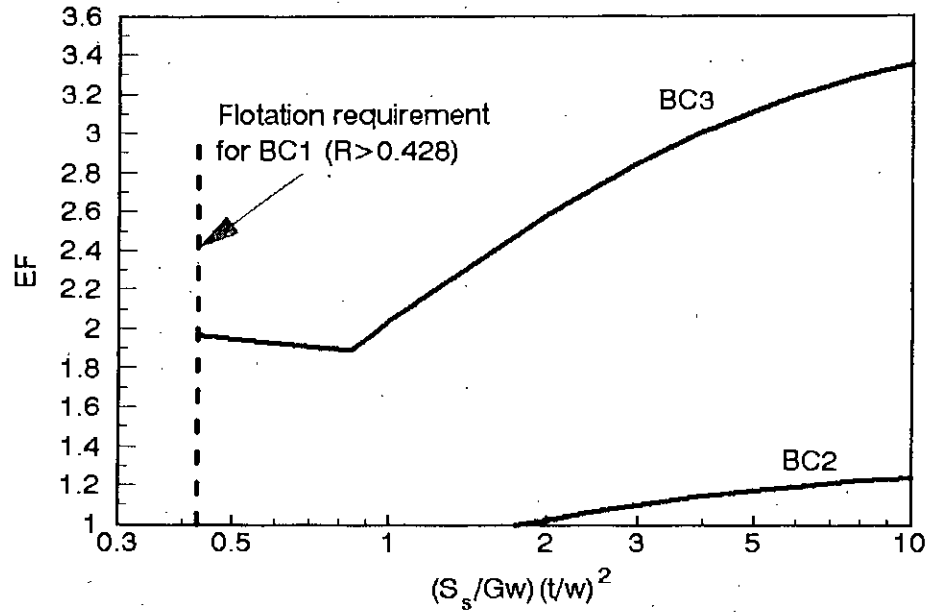


Fig. 6.13: Semielliptical shaped lining: Enhancement factors for allowable grouting pressure, based on stress-limit criteria

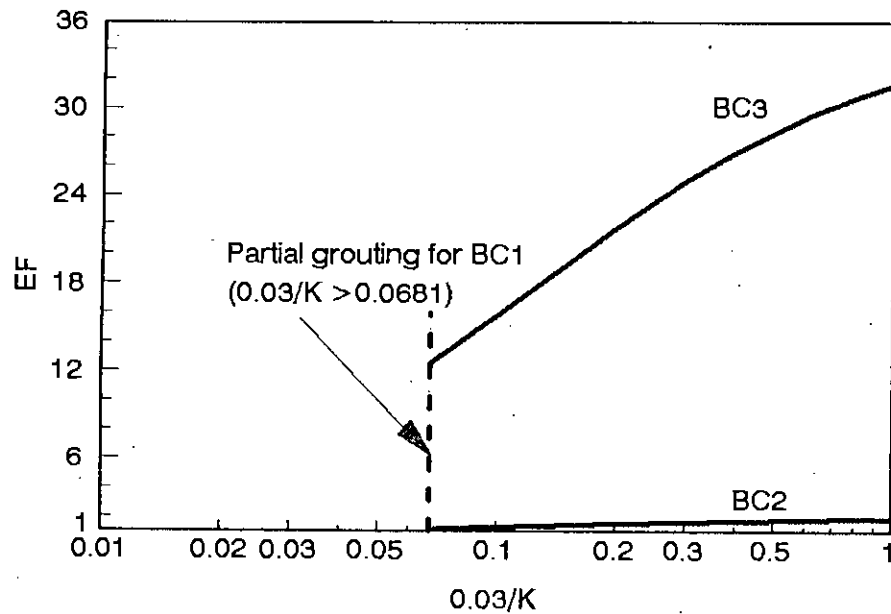


Fig. 6.14: Semielliptical shaped lining: Enhancement factors for allowable grouting pressure, based on deflection-limit criteria

criteria is much lower than that of achieved from deflection-limit criteria. Hence, stress-limitations govern the computation of enhancement factors in the present case.

It is seen from Fig. 6.13 that in case of boundary case 2, at least a value of R equal to 1.757 is needed in order to have an enhancement factor equal to or less than 1. This means that no beneficial effect can be achieved by adopting boundary case 2, if the value of R remains less than 1.757.

Adoption of boundary case 3 always provides an enhancement factor greater than 1. Lining, subjected to boundary condition 3, provides 2 to 3 times enhancement in bearing the grouting pressure than that of boundary condition 2.

### 6.7.2 Reduction Factors

In the present study, a reduction in the allowable lining thickness can be achieved, as before, if boundary case 2 or 3 is used instead of boundary case 1. Like the previous section, two values of RF are determined for each of the boundary cases 2 and 3, based on the stress- and deflection-limit criteria. Here, again, stress-limitations prove to be more critical, and the equations used to calculate the values of reduction factors shown in Fig. 6.15 are as follows:

$$(RF)_i = \frac{t_i}{t_1} \quad (6.23)$$

where  $t_i$  and  $t_1$  can be calculated from equations 6.1, 6.2, 6.4 and 6.6. The final equations that stem from these are given below:

$$(RF)_2 = \left( \left| \frac{0.277 - 0.303 \frac{p}{Gw}}{0.042 - 0.2 \frac{p}{Gw}} \right| \right)^{\frac{1}{2}} \quad (6.24a)$$

for  $2.35 < p/Gw < 4.43$ ,

$$= \left( \left| \frac{0.277 - 0.303 \frac{p}{Gw}}{0.928 - 0.4 \frac{p}{Gw}} \right| \right)^{\frac{1}{2}} \quad (6.24b)$$

for  $p/Gw > 4.43$

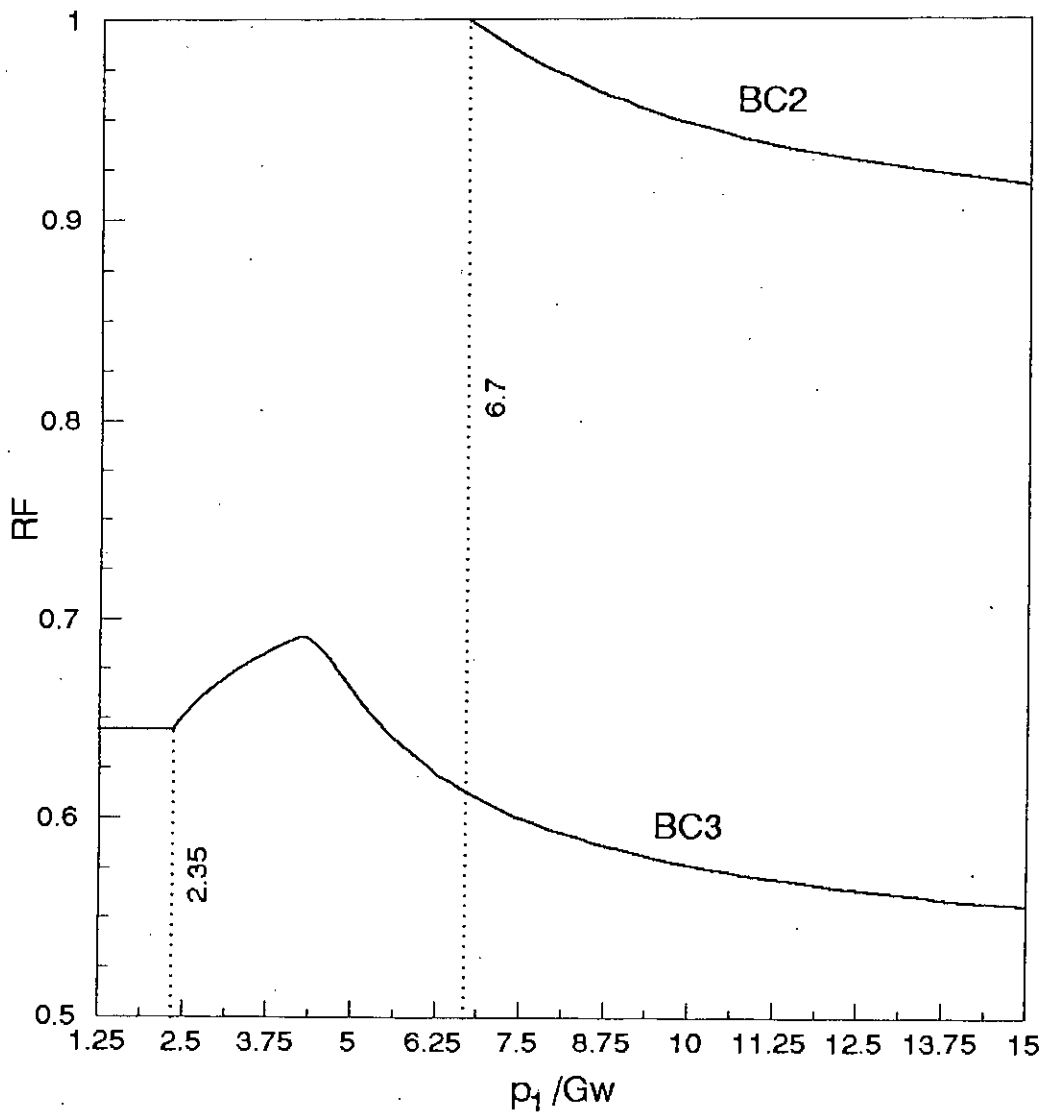


Fig. 6.15: Semielliptical shaped lining: Reduction factors for minimum permissible lining thickness, based on stress-limit criteria

$$(RF)_3 = \left( \left| \frac{-0.0803 + 0.11 p/Gw}{0.042 - 0.2 p/Gw} \right| \right)^{1/2} \quad (6.25a)$$

$$= \left( \left| \frac{-0.0803 + 0.11 p/Gw}{0.928 - 0.4 p/Gw} \right| \right)^{1/2} \quad (6.25b)$$

for  $p/Gw > 4.43$

Equations 6.24 and 6.25 are graphically shown in Fig. 6.15. It can be seen from the figure that considerably larger reduction factors are achieved by using boundary case 3 when compared with boundary case 2. It is to be noted that for higher values of  $p_1/Gw$ , the RF tends to a constant value. Finally, fig. 6.13 shows that, for boundary case 2, value of  $p_1/Gw$  equal to 6.7 is needed in order to achieve reduction factors less than one. This, again, means that no beneficial effect can result from the use of boundary case 2, if the value of  $p_1$ , which is defined earlier, is less than  $6.7Gw$ .



## CHAPTER 7

# STRUCTURAL BEHAVIOUR OF CIRCULAR SHAPED LININGS

### 7.1 INTRODUCTION

The analysis of circular shaped sewer linings, subjected to different types of grouting loads during installation, is to be carried out in this chapter. The circular shaped lining, loaded with radial uniform pressure and under various restraint conditions, produces very little or no bending moment in the structure. Hence, stress-limitations as described in earlier chapters will not act as a dominant design criterion here. The applied uniform load is resisted almost exclusively by axial forces, whose magnitude were not too much in case of moderately sized non-circular cross-sections, discussed in detail in the previous chapters. In fact, unlike egg-shaped, inverted egg shaped linings, horseshoe shaped, semielliptical shaped linings where bending was found to be predominant, buckling is likely to be the critical design criteria for circular linings. The present study initially investigates the validity of the non-dimensional equations described in Chapter 2. Finally, an attempt has been made to consider the buckling effect of circular linings under uniform compressive force. Of course, the lining material thickness must be enough to guard against the failure of the lining due to axial compressive stress. It is to be noticed here that as the lining material is thin, the buckling failure governs predominantly.

### 7.2 TWO-DIMENSIONAL FINITE ELEMENT MODEL

In order to simulate the structural behaviour of circular shaped linings under various possible loads and different restraints set-ups during grouting operations, a two-dimensional liner finite element program is used.

#### 7.2.1 Two-Dimensional Finite Element Mesh

The shape of the lining used in the present study is a circular one of radius  $R$  as is shown in Fig. 7.1. The thickness of the lining ( $t$ ) is assumed to be constant around

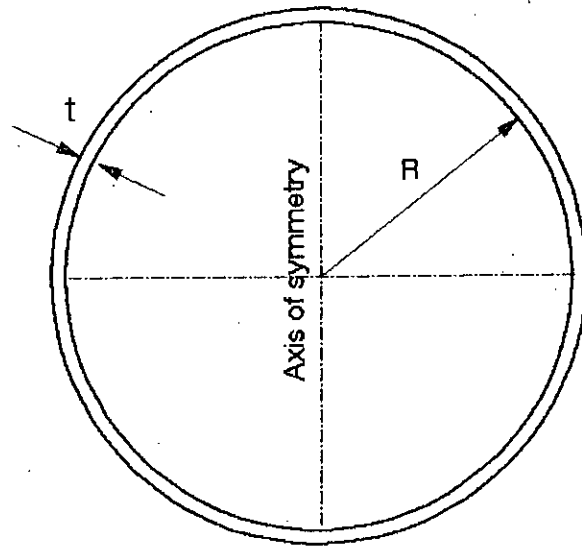


Fig. 7.1: Circular shaped lining: Geometry of the lining

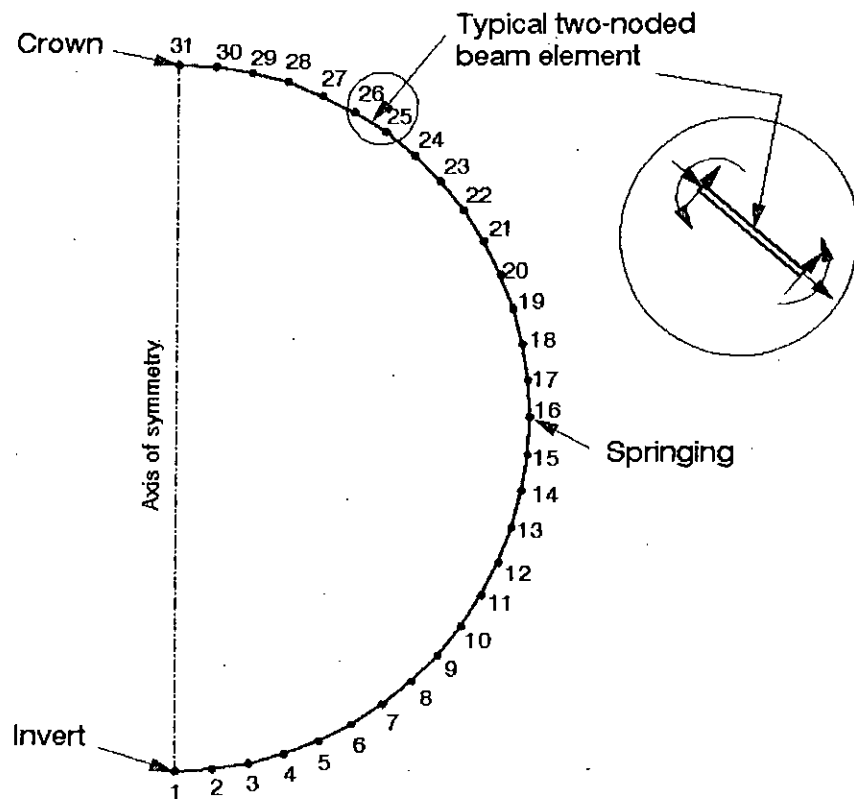


Fig.: 7.2: Circular shaped lining: Two-dimensional finite element mesh adopted in the analysis

the cross-section. In this case, the height (h) and width (w) of the lining is equal in magnitude. Hence, the ratio of h to w (h/w) is equal to 1. Due to symmetry of the cross-section with respect to geometry as well as loadings, only half of the cross-section is taken in the analysis as is shown in Fig. 7.2. This part of the structure consists of thirty 2-noded beam elements with three degrees of freedom (horizontal, vertical and rotation) at each node.

### 7.2.2 Restraint Set-Ups

Three support systems are considered in the analysis. These are shown in Fig. 7.3. Fig. 7.3a corresponds to first support system in which a single restraint is applied at the crown of the lining. The second support system consists of restraints at both the crown, and invert of the lining while the third comprises the restraints at invert, crown and springings of the analysis. These restraints are simulated numerically in the analysis, as usual, by fixing the horizontal and vertical components of displacement at the corresponding nodal points.

## 7.3 LOADING CONFIGURATIONS

In the present study of circular shaped lining, three loading configurations are included in the analysis as shown in Fig. 7.4. The first phase of loading consists of grout pressure up to the springing. The second loading configuration involves a head of grout up to the crown while the loading corresponds to the case of uniform pressure.

## 7.4. ANALYSIS OF LINING STRUCTURE

### 7.4.1 Use of Non-Dimensional Equations

For various lining geometry and material properties, the parametric study is carried out for all the three loading configurations described in the previous section. It has been found that the non-dimensional equations given in Art. 2.10 remains no longer valid for the present circular shaped lining structure when it is subjected to uniform grout pressure i.e. the third form of loading configuration. However, the deflections and bending stresses, developed due to load coming from staged grouting and flotation pressure, can be *approximated* by those relevant equations given in Chapter 2. Hence, the relevant bending stress and deflection constants are determined and tabulated in Table 7.1 and 7.2. The curves from which the values

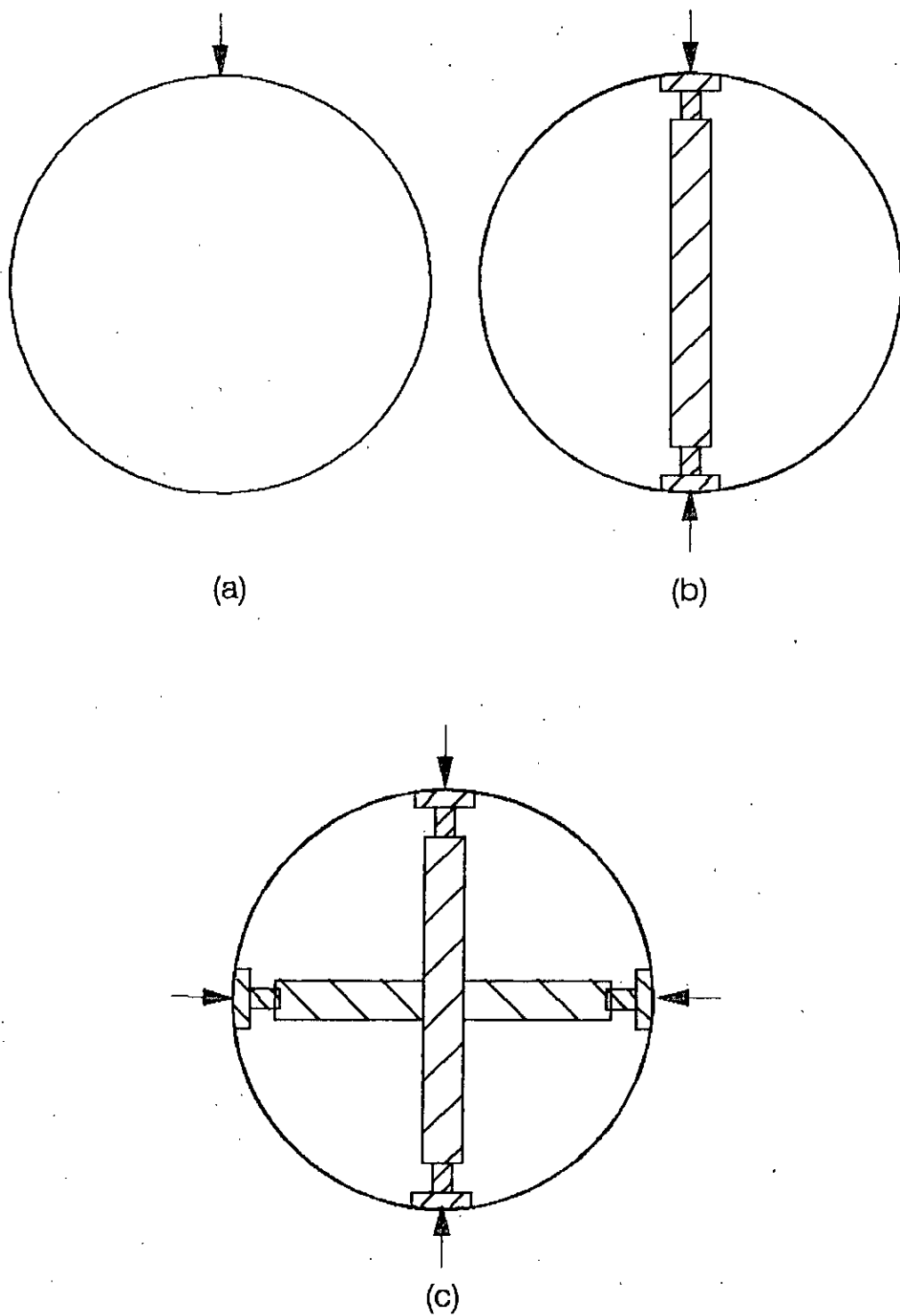
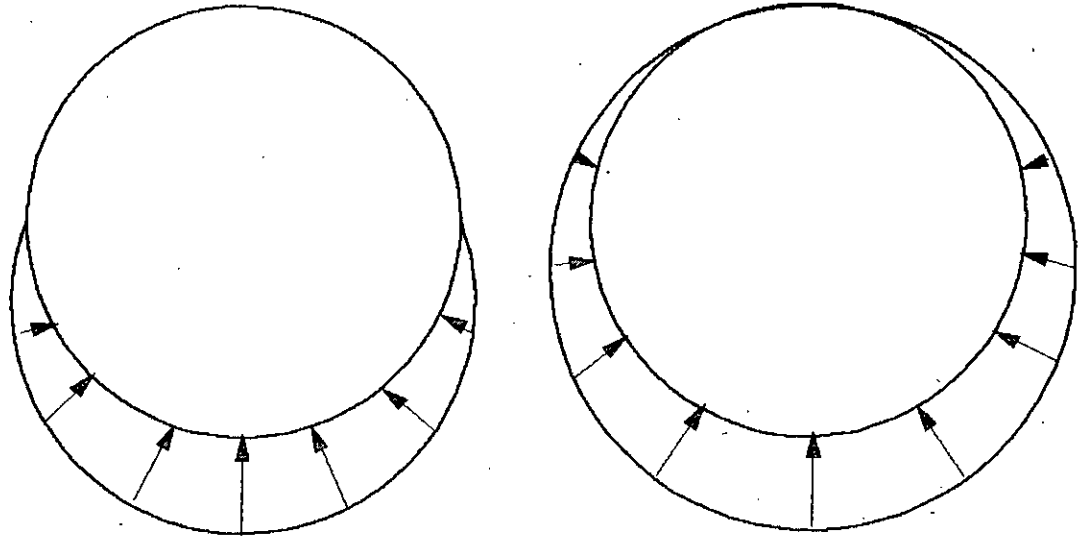
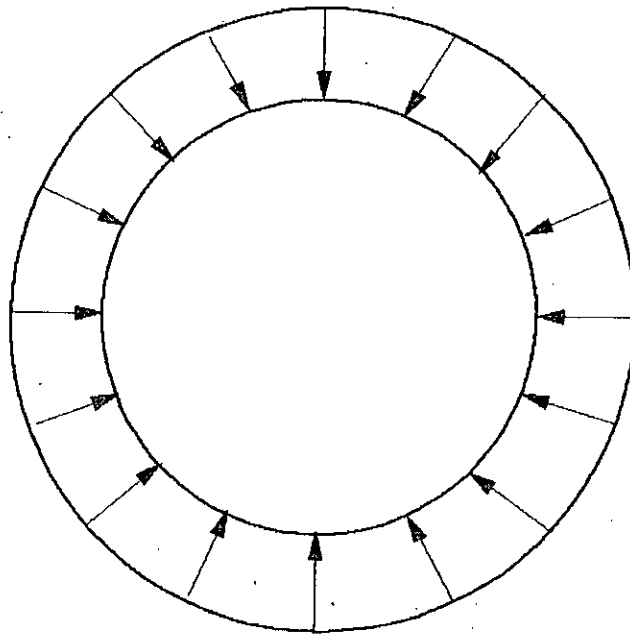


**Fig.: 7.3: Circular shaped lining: The support systems studied: (a) boundary condition 1, (b) boundary condition 2 and (c) boundary condition 3**



(a)

(b)



(c)

*Fig.: 7.4: Circular shaped lining: The loading configurations studied: (a) staged grouting, (b) grout up to crown only and (c) uniform pressure*

of these constants are determined are given in Fig. A5.1, A5.2, A5.3 and A5.4 in Appendix 5. In this connection, it is worth noting that co-efficient of regression in the present case was about 0.99; in case of various non-circular linings of the previous chapters such co-efficient was 1.0. Thus, it is clear that, whereas the non-dimensional equations of Chapter 2 are valid for non-circular linings subjected to all (uniform or non uniform) types of loadings, they are only approximately valid for (uniform shaped) circular linings under non-uniform loading, where bending stress is present. But for circular linings subjected to uniform load, the above mentioned equations become invalid as axial force and deformations dominates the design.

**Table 7.1:** Dimensionless constants for the maximum bending stress in the lining  
(positive values of A, C and E imply tensile stresses at the inner surface of the lining)

|                 | Coefficient | Boundary Case 1 | Boundary Case 2 | Boundary Case 3 |
|-----------------|-------------|-----------------|-----------------|-----------------|
| Staged grouting | A           | 0.333 Node 31   | 0.117 Node 1    | 0.0181 Node 1   |
| Flotation       | C           | 0.562 Node 31   | 0.187 Node 1    | 0.0214 Node 1   |

**Table 7.2:** Dimensionless constants for the maximum deflection in the lining  
(inward deflections are taken as positive)

|                 | Coefficient | Boundary Case 1 | Boundary Case 2 | Boundary Case 3 |
|-----------------|-------------|-----------------|-----------------|-----------------|
| Staged grouting | $B_x$       | 0.00 Node 1     | 0.00216 Node 10 | 0.000066 Node 6 |
|                 | $B_y$       | -0.058 Node 1   | 0.00484 Node 10 | 0.00025 Node 6  |
| Flotation       | $D_x$       | 0.00 Node 1     | 0.0045 Node 11  | 0.0001 Node 6   |
|                 | $D_y$       | -0.083 Node 1   | 0.0091 Node 11  | 0.000034 Node 6 |

It can be noticed that as the loading increases from springing to crown, the axial force also increases, but at a faster rate. On the other hand, bending stresses

increase with the increase in loading (up to crown) at a much slower rate. This means that as the grout load increases, the axial force becomes more and more a dominating criteria - which must be considered in the design of circular linings.

#### **7.4.2 Effect of Restraining on Axial Force**

When the uniform pressure is applied on the circular lining structure, the bending moment becomes nil if no restraint is applied on its boundary. However, if the lining is subjected to the restraints as described earlier in this chapter and loaded with uniform external pressure a very negligible amount of bending stresses are developed in the lining which can be safely neglected in design. The axial force developed in no-support condition will, of course, be equal to  $qR$ , where  $R$  is the radius of the circle and  $q$  is the uniform external pressure applied on the cross-section (Timoshenko and Gere, 1961). In this context, the effect of boundary restraints (which can not be avoided because of installation technique) on the axial force is observed for a particular data set described later, and is tabulated in Table 7.3.

From Table 7.3, it can be concluded that the effects of restraints (any one of the three support systems described earlier) on axial force is quite negligible. Thus, upper bound of the axial force that may develop in a circular lining of radius  $R$ , subjected to uniform external pressure and under various boundary restraints, may be calculated by using the relation  $F = qR$ , where  $F$  is the axial force.

#### **7.4.3 Simulation of Full-Grouting Loads**

The load exerted on the lining during full grouting is not uniform all around the cross-section. The full grouting load is exactly a pure hydrostatic pressure case i.e. the lining is subjected to a pressure similar to a thin ring is submerged in a liquid as is shown in Fig. 7.5.

**Table 7.3:** Comparison of axial forces developed due to uniform external pressure applied on the circular lining\* under various boundary Set-Ups:

| AXIAL FORCE (kN) |              |                      |                      |                      |
|------------------|--------------|----------------------|----------------------|----------------------|
| Element No       | No Restraint | Boundary Condition 1 | Boundary Condition 2 | Boundary Condition 3 |
| 1                | 8.25000      | 8.23871              | 8.23852              | 8.19870              |
| 2                | 8.25000      | 8.23875              | 8.23816              | 8.19512              |
| 3                | 8.25000      | 8.23884              | 8.23788              | 8.19209              |
| 4                | 8.25000      | 8.23891              | 8.23758              | 8.18954              |
| 5                | 8.25000      | 8.23891              | 8.23724              | 8.18748              |
| 6                | 8.25000      | 8.23899              | 8.23698              | 8.18605              |
| 7                | 8.25000      | 8.23905              | 8.23674              | 8.18517              |
| 8                | 8.25000      | 8.23912              | 8.23650              | 8.18489              |
| 9                | 8.25000      | 8.23914              | 8.23627              | 8.18519              |
| 10               | 8.25000      | 8.23917              | 8.23606              | 8.18604              |
| 11               | 8.25000      | 8.23919              | 8.23589              | 8.18749              |
| 12               | 8.25000      | 8.23924              | 8.23578              | 8.18954              |
| 13               | 8.25000      | 8.23925              | 8.23568              | 8.19209              |
| 14               | 8.25000      | 8.23923              | 8.23557              | 8.19513              |
| 15               | 8.25000      | 8.23928              | 8.23557              | 8.19869              |
| 16               | 8.25000      | 8.23926              | 8.23557              | 8.19867              |
| 17               | 8.25000      | 8.23924              | 8.23558              | 8.19510              |
| 18               | 8.25000      | 8.23929              | 8.23568              | 8.19207              |
| 19               | 8.25000      | 8.23927              | 8.23579              | 8.18953              |
| 20               | 8.25000      | 8.23920              | 8.23589              | 8.18747              |
| 21               | 8.25000      | 8.23918              | 8.23606              | 8.18603              |
| 22               | 8.25000      | 8.23916              | 8.23627              | 8.18516              |
| 23               | 8.25000      | 8.23914              | 8.23652              | 8.18489              |
| 24               | 8.25000      | 8.23907              | 8.23673              | 8.18516              |
| 25               | 8.25000      | 8.23899              | 8.23698              | 8.18602              |
| 26               | 8.25000      | 8.23894              | 8.23724              | 8.18748              |
| 27               | 8.25000      | 8.23891              | 8.23758              | 8.18953              |
| 28               | 8.25000      | 8.23884              | 8.23789              | 8.19208              |
| 29               | 8.25000      | 8.23874              | 8.23817              | 8.19511              |
| 30               | 8.25000      | 8.23870              | 8.23852              | 8.19868              |

\*The analysis is carried out on the basis of some arbitrary data.

These are given below:

Unit weight of the grout mix = 16.5 kN/cum

Diameter of the cross-section = 1.0 m

Uniform external pressure = 16.5 kN/sq.m which is equivalent to 1.0 m head of grout.

Thickness of the lining material = 13 mm



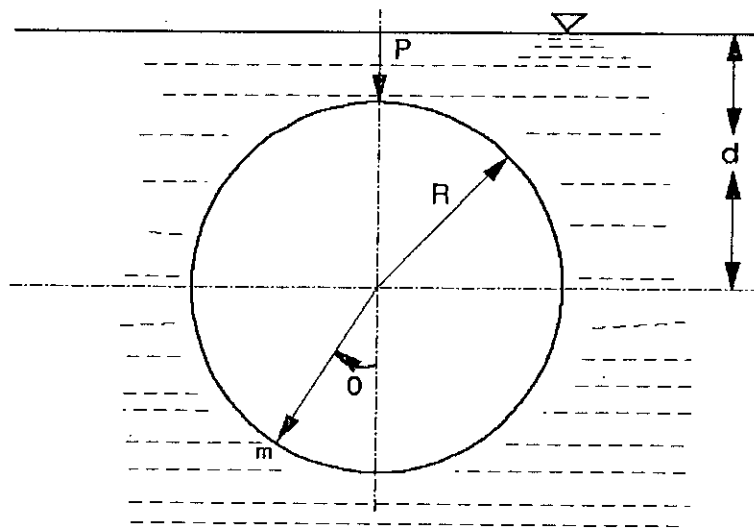


Fig.: 7.5: Circular shaped lining: A thin ring submerged in a liquid

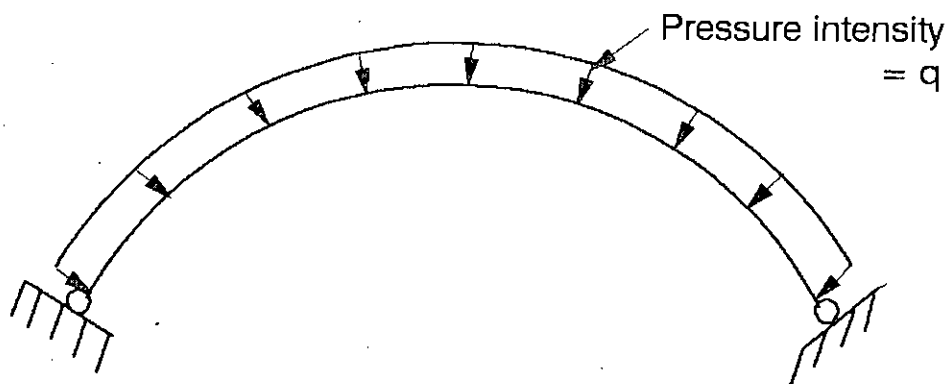


Fig.: 7.6: Circular shaped lining: uniformly loaded hinged arch

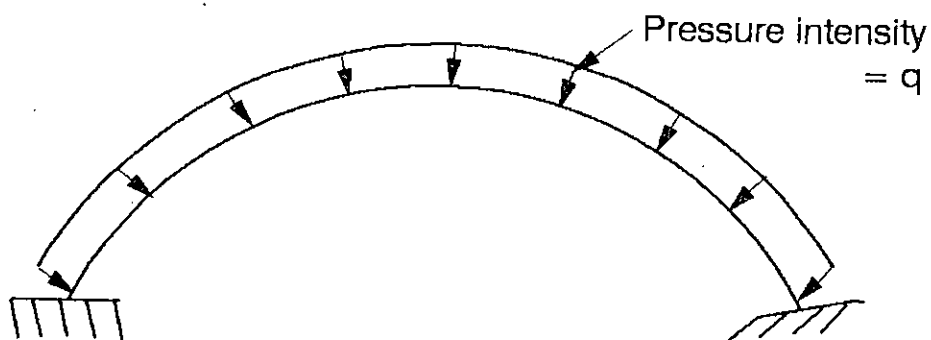


Fig. 7.7: Circular shaped lining: Uniformly loaded fixed arch

Assuming that the width of the ring in the direction perpendicular to the plane of the figure is unity and denoting by  $\gamma$  the weight of the liquid per unit volume, it can easily be found that intensity of hydrostatic pressure at any point  $m$  is  $\gamma(d+R\cos\theta)$ . Taking this hydrostatic pressure, Timoshenko and Gere (1961) analysed a thin ring with a single restraint at the crown of the ring which prevents the ring from going upward due to buoyancy force of liquid (of course, this vertical restraint is needed to maintain the ring in vertical equilibrium), and finally came out with the critical value of the axial compressive force - the maximum force a thin ring can sustain before undergoing buckling. The expression is given below:

$$F_{cr} = \frac{Et^3}{4(1-\nu^2)R^2} \quad (7.1)$$

where,

$E$  is the modulus of elasticity,  
 $\nu$  is the Poissons ratio,  
 $t$  is the thickness of the lining,  
 $R$  is the radius of the ring and  
 $F_{cr}$  is the critical axial force.

If an elemental ring of unit width is subjected to a uniform pressure of  $q$ , the axial force developed will be  $qR$ , and hence, the critical value of the pressure can be obtained from equation 7.1 as

$$q_{cr} = \frac{E}{4(1-\nu^2)} \left( \frac{t}{R} \right)^3 \quad (7.2)$$

where,  $q_{cr}$  is the critical pressure.

Alternatively, a direct stress-limit criteria which is equal to the critical buckling stress of a hinged arch of similar radius and unrestrained length (Timoshenko and Gere, 1961) may be adopted as a reasonable approximation. In this case (see Fig. 7.6), the following expression is valid:

$$q_{cr} = \frac{E}{12(1-\nu^2)} \left( \frac{t}{R} \right)^3 K \quad (7.3)$$

where  $K$  equals to 3 for boundary condition 2 and 15 for boundary condition 3. It is worth mentioning here that equation 7.3 is derived for uniformly loaded two hinged arch. In the present case, if the head of grout is large, a reasonably uniform state of compression can be assumed around the circumference and all arch portions are expected to initiate buckling simultaneously. The contents of Table 7.3 show that the value of the maximum membrane stress in the lining is not reduced considerably when additional restraints are introduced in a circular lining. However, the effective length of the arch between the restraints is reduced, thus leading to stiffer structure with higher critical buckling pressure. This phenomena has been adequately portrayed in equation 7.3. An alternative to the use of hinged arch is a fixed arch consideration (see Fig. 7.7), which is 2.16 to 2.67 times stiffer than its hinged counterpart. The actual behaviour of the lining that initiates buckling lies in-between hinged and fixed arches. Thus adoption of hinged arch assumption gives a lower bound (i.e. conservative) solution of the real case. In the actual design of lining, in determining the hydrostatic pressure, the pressure may be calculated at the invert of the lining; thus making the final solution more conservative. An example of the design of circular sewer lining is given in Appendix 5.

## CHAPTER 8

# CONCLUSIONS AND RECOMMENDATIONS FOR FUTURE RESEARCH

### 8.1 CONCLUSIONS

This research work has presented an analytical study of the two-dimensional behaviour of sewer linings of various existing shapes and under different restraint set-ups. The simplicity of the two-dimensional model enables a full parametric study to be carried out, and this has been summarised by means of a relatively small number of equations and their corresponding plots. Their usage in design is also illustrated. In the present study, permissible deflection in all types of sewer linings has been taken as 3% of the width of the sewer lining. However the proposed design curves are so flexible that it can be adopted without any modification for any other allowable deflection-limit criteria set by competent authority. Throughout the present analyses, it has been assumed that all restraints are fully effective, so that the restrained points of the lining are prevented from moving in any direction. Such ideal conditions will very nearly be realised if internal supports are provided. On the other hand, external packing may not always be effective, in which case it might be necessary to assume that boundary condition 1 or 2 applies. The following are the conclusions that can be drawn from the study described in the previous chapters:

- (1) By the introduction of additional temporary restraints to the linings of various shapes, considerably higher grouting pressures, leading to a more reliable grouting operation, can be attained. It is to be noted here that for all shapes of sewer linings other than circular, either the stress- or the deflection-limit criteria governs the design, whereas in the case of circular linings, axial force dictates the design and hence, buckling phenomena seems to be the deciding factor.
- (2) Although the design of moderately sized egg shaped, inverted egg shaped, semielliptical shaped and horseshoe shaped sewer linings are dependent on both stress- and deflection-limit criteria, it is the stress-limit criterion that dictates the determination of enhancement and reduction factors.

(3) For a particular lining geometry and material property, boundary condition 3 of egg-shaped sewer lining gives higher allowable grouting pressure than boundary condition 1 and 2 for both the stress and deflection limit criteria. However, for a small range of material stiffness, boundary condition 2 seems to be more critical than boundary condition 1 in case of stress limit criteria.

Here, enhancement and reduction factors are exclusively dependent on stress limit criteria. If boundary condition 3 is used in stead of boundary condition 2, the thickness of the liner can be reduced by 1.22 to 1.42 times the thickness required for boundary condition 2. On the other hand, enhancement in grouting pressure that can be achieved by using boundary condition 3 with respect to boundary condition 2 is nearly equal to a constant value of 1.7.

(4) In case of inverted egg shaped lining, for a smaller range of material stiffness, boundary condition 3 is more critical than that of boundary condition 1 and 2 (for stress limit criteria).

In this case, use of boundary condition 2 results in no beneficial effect unless the value of  $R$  (measure of stiffness) becomes greater than 0.424. Similar reasoning also applies to boundary condition 3 and in this case the value of  $R$  must be greater than 0.592 to have an enhancement in grouting pressure.

(5) In all the shapes of sewer linings studied, for all the three boundary conditions, an enhancement in the allowable grouting pressure has been achieved due to an increase in the thickness of the lining material and/or due to the use of a material which may sustain higher bending stresses. This gain in grouting pressure, for boundary condition 1, has been found to be more pronounced in case of horseshoe shaped linings in comparison to the other shapes studied. For the other non-circular linings, the rate of gain under similar circumstances were higher for boundary conditions 2 and 3.

(6) For semielliptical shaped lining, adoption of boundary case 3 always provides an enhancement in grouting pressure than the boundary condition 1. Lining subjected to boundary condition 3 provides 2 to 3 times enhancement in bearing the grouting pressure than that of boundary condition 2.

## 8.2: RECOMMENDATIONS

The following recommendations are made for future development of the present research work:

(1) Adequate information is now available to tackle the design of sewer linings having various shapes during their installation. The behaviour of these linings in the long term is less understood and there is a scope for further work in this line. In the latter context, two main areas of investigations can be identified. First, comprehensive structural testing of linings confined within a sewer-and-grout surround and subjected to hydrostatic pressure is required in order to ascertain the actual mode of failure and the safe head of water that a given lining may withstand during service conditions. Once such experimental results are available, it will be easy to idealise the behaviour of the linings in the long run. The second area of potential research is the time dependent behaviour of the linings involving creep effects; such investigations are especially important if economic and realistic design is to be achieved.

(2) The present study models sewer linings in a two-dimensional continuum. The two-dimensional assumption warrants the adoption of close packing throughout the whole length of the lining. A fully three dimensional model may be adopted in the future in an effort to understand the structural behaviour of sewer linings more realistically.

(3) The long time performance of sewer linings may be studied by employing suitable soil-structure analysis technique.

(4) Finally, it should be pointed out that current design guidelines are based on conservative assumptions relating to restraints conditions during installation. The additional restraints, discussed in the design of sewer linings of various shapes in this research work, have shown to provide considerable extra stiffness, which may allow significant reduction in the lining thickness. This leads to lining thicknesses which are presently assumed to be safe under long-term conditions, but physical tests are needed to appraise the validity of this assumption.

## REFERENCES

1. Arnaout, S. (1988), "The Structural Performance of Egg-Shaped Sewer Linings", Ph.D. Thesis, University of London.
2. Arnaout, S. and Pavlovic, M. N. (1988), "Studies on the structural behaviour of egg-shaped sewer linings under installation and operational conditions", *Structural Engg. Review*, Vol. 1, pp. 25-33.
3. Arnaout, S. and Pavlovic, M. N. (1989), "An investigation into the long-term behaviour of egg-shaped sewer linings", in *Foundations and Tunnels-89*, Proceedings of the Second International Conference on Foundations and Tunnels held in London, 19-21 September 1989, edited by M. C. Forde, 2 vols. Engineering Technics Press, Edinburgh, 1989, Vol. 2, pp. 207-213.
4. Arnaout, S., Pavlovic, M. N. and Dougill, J. W. (1988), "Structural behaviour of closely packed egg-shaped sewer linings during installation and under various restraint conditions", *Proc. ICE (Part 2)*, Vol. 85, pp. 49-65.
5. Arnaout, S., Pavlovic, M. N. and Dougill, J. W. (1990), "A new method for testing the tensile properties of curved specimens", *Materials & Struct., RILEM*, 23 (1990), 296-304.
6. Jackson, N. (1983), "Civil Engineering Materials", The Macmillan Press Ltd., London, 3rd. Edition.
7. Kays, W. B. (1986), "Construction of Linings for Reservoirs, Tanks, and Pollution Control Facilities", John Wiley & Sons, 2nd edition.

8. Pavlovic, M. N., Arnaout, S. And Hitchings, D. (1993), "Finite Element Modelling of Sewer Linings", in Developments in Structural Engineering Computing, Proceedings of the 5th International Conference on Civil and Structural Engineering Computing held in Edinburgh, 17-19 August 1993, edited by B. H. V. Topping, 6 Vols., Civil-Comp Press, Edinburgh, Vol. D, pp. 1-11.
9. Seraj, S. M. (1986), "Structure-Soil Interaction in Buried Rigid Culverts", M. Sc. thesis, BUET.
10. Seraj, S. M. (1993), "Disaster management in Metropolitan Dhaka", Proceedings at the IDNDR Disaster Conference, Nagoya, 1-4 November 1993.
11. Timoshenko, S. P. and Gere, J. M. (1961), "Theory of Elastic Stability", Mc Graw-Hill, London, 2nd edition.
12. Water Research Centre (1983), Sewerage Rehabilitation Manual., Swindon, U. K.



# APPENDIX 1

## A1.1 DERIVATION OF THE DESIGN EQUATIONS FOR FULL GROUTING LOAD (DEFLECTION-LIMIT CRITERIA)

For deflection-limit criteria, all the design equations (for full grouting load) given in Chapter 3, 4, 5 and 6, comes after a laborious calculation. As the calculations are similar, derivation of only one equation (equation 3.5) is given below for illustration.

$$N_x = D_x - 1.5F_x + F_x \frac{P}{Gw}$$

The values of the constants of the right hand side of above equation can be found from Table 3.3 and the value of  $N_x$  will be as follows:

$$\begin{aligned} N_x &= 0.035 - 1.5 \times 0.127 + 0.127 \frac{P}{Gw} \\ &= -0.1555 + 0.127 \frac{P}{Gw} \end{aligned}$$

Similarly, for  $N_y$

$$N_y = D_y - 1.5F_y + F_y \frac{P}{Gw}$$

Taking the values of  $D_y$  and  $F_y$  from Table 3.3,

$$\begin{aligned} N_y &= 0.052 - 1.5 \times (-0.0774) - 0.0774 \frac{P}{Gw} \\ &= 0.1681 - 0.0774 \frac{P}{Gw} \end{aligned}$$

Now, equation 2.13 gives,

$$\begin{aligned} \frac{0.03}{K} &= (N_x^2 + N_y^2)^{\frac{1}{2}} \\ &= \left[ \left( -0.1555 + 0.127 \frac{P}{Gw} \right)^2 + \left( 0.1681 - 0.0774 \frac{P}{Gw} \right)^2 \right]^{\frac{1}{2}} \end{aligned}$$

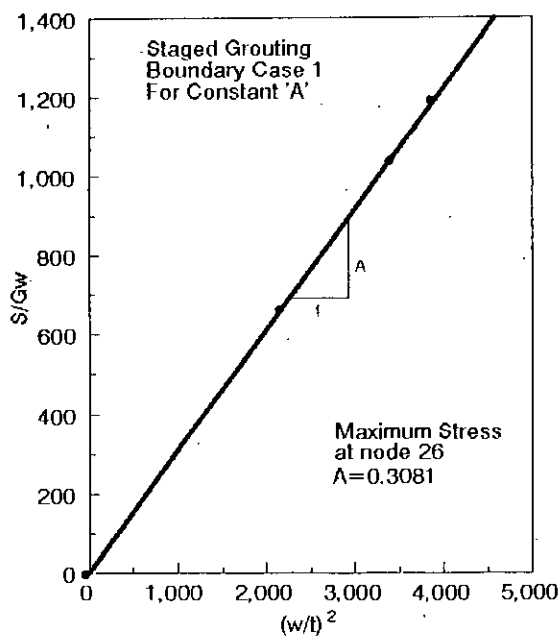
$$\begin{aligned}
&= \left[ 0.02212 \left( \frac{P}{Gw} \right)^2 - 0.0655 \frac{P}{Gw} + 0.0524 \right]^{\frac{1}{2}} \\
&= \left[ \left\{ \left( 0.148 \frac{P}{Gw} \right)^2 - 2.0 \times 0.148 \frac{P}{Gw} \times 0.221 + 0.221^2 \right\} + 0.0625^2 \right]^{\frac{1}{2}} \\
&= \left[ \left( 0.148 \frac{P}{Gw} - 0.221 \right)^2 + 0.0625^2 \right]^{\frac{1}{2}}
\end{aligned}$$

This can be best approximated to the following linear equation:

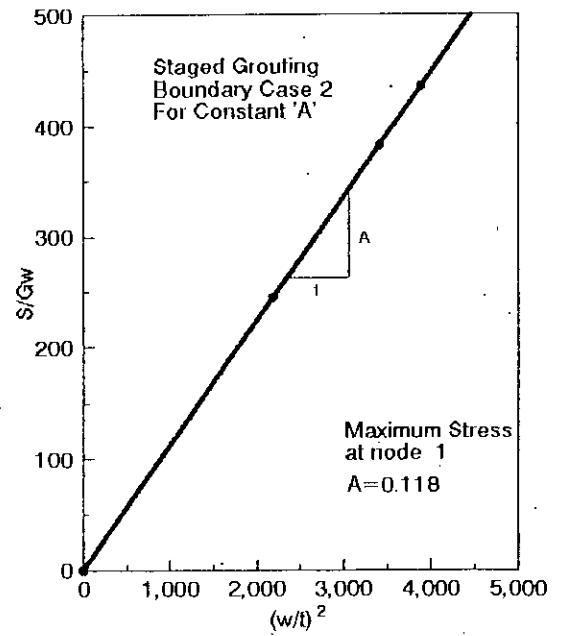
$$\frac{0.03}{K} = 0.148 \frac{P}{Gw} - 0.161$$

## **APPENDIX 2**

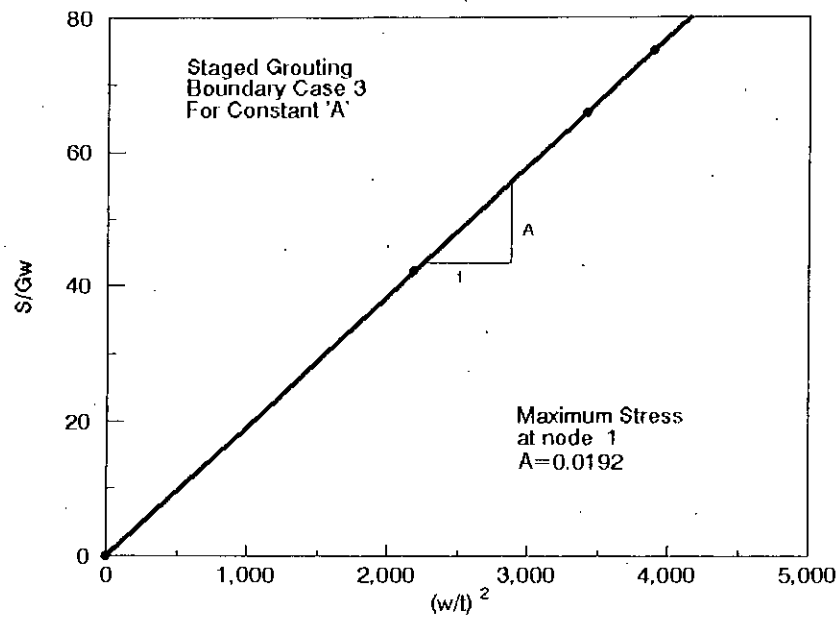
## A2.1: GRAPHS USED IN THE DETERMINATION OF DIMENSIONLESS CONSTANTS FOR INVERTED EGG SHAPED LINING



(a)

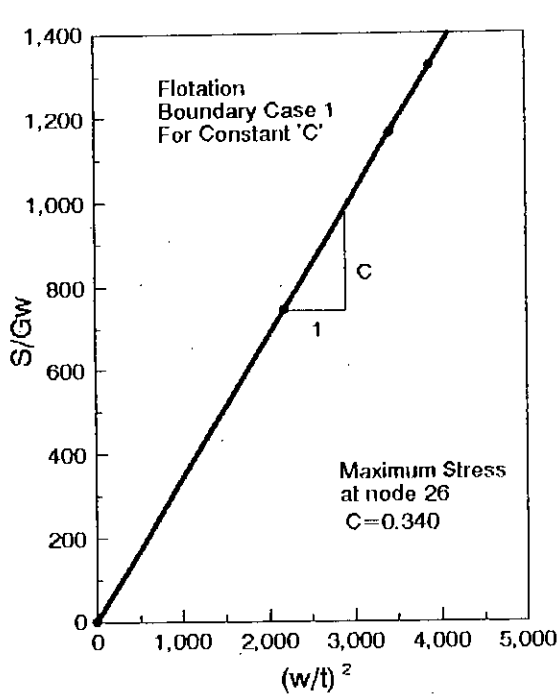


(b)

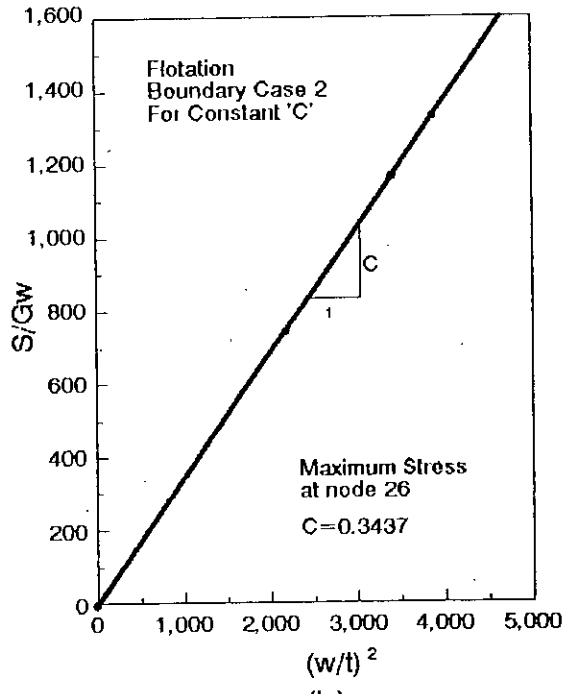


(c)

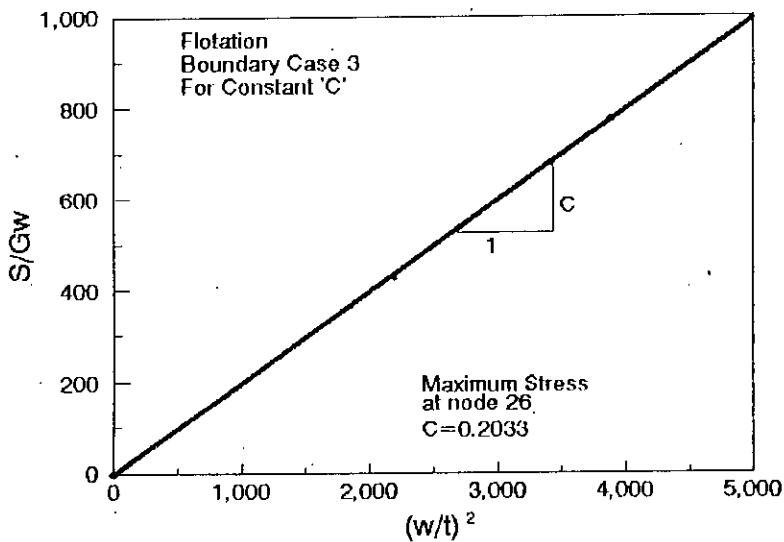
Fig. A2.1: Inverted egg shaped lining: Determination of the constant 'A' for staged grouting for (a) boundary case 1, (b) boundary case 2 and (c) boundary case 3



(a)



(b)



(c)

Fig A2.2: Inverted egg shaped lining: Determination of the constant 'C' for flotation for (a) boundary case 1, (b) boundary case 2 and (c) boundary case 3

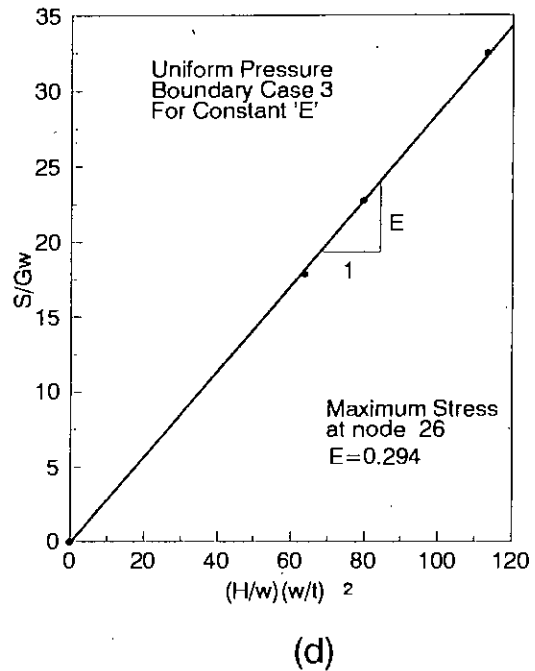
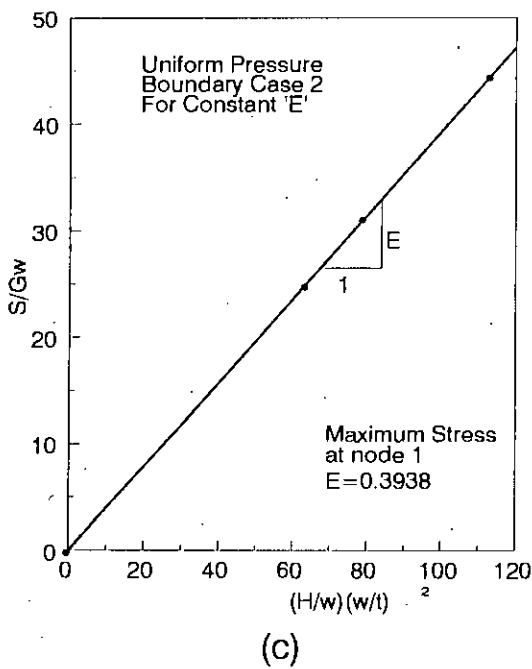
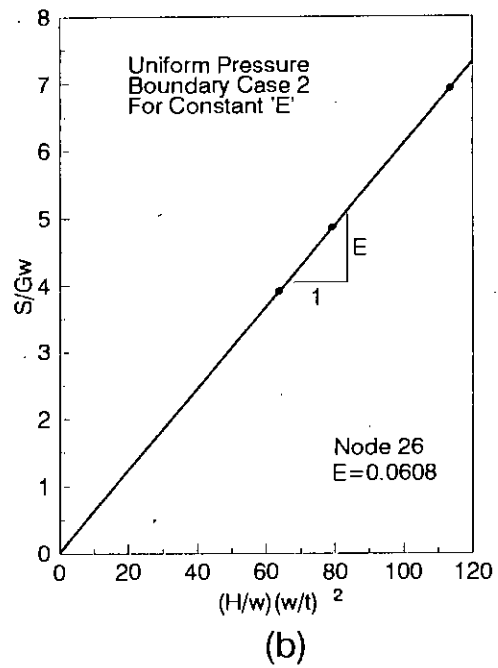
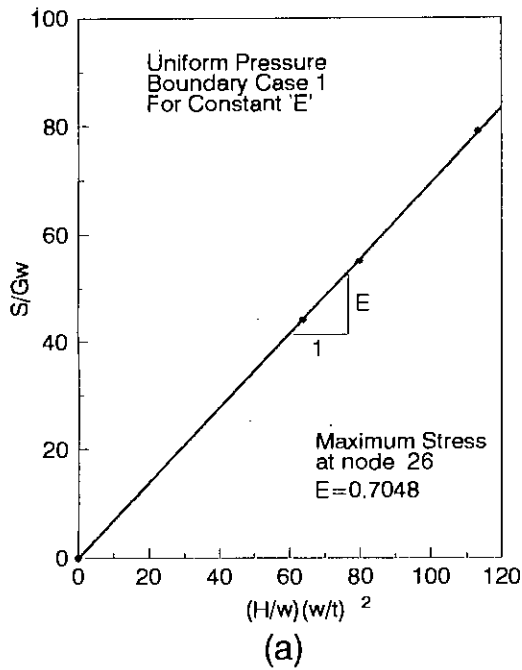
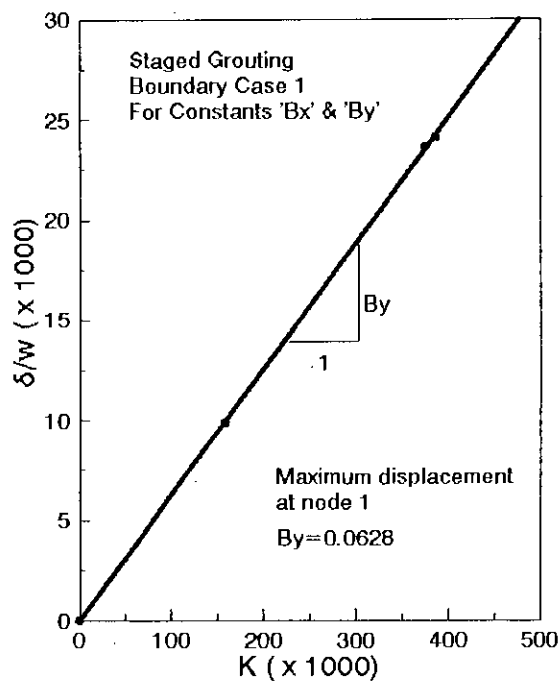
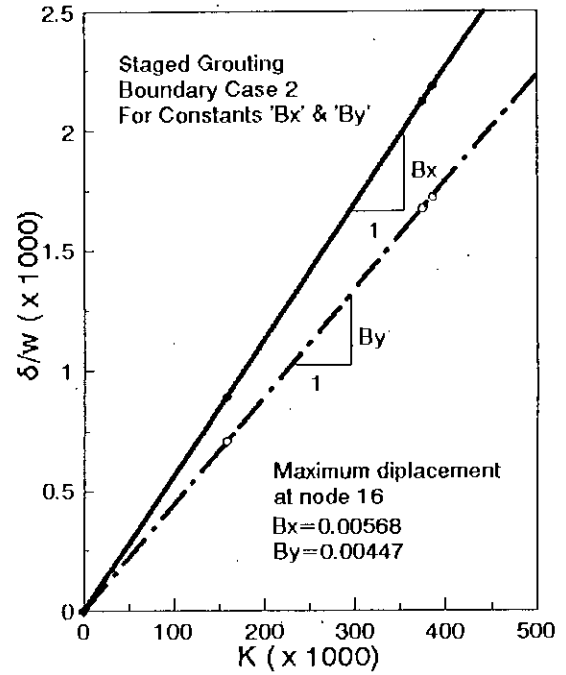


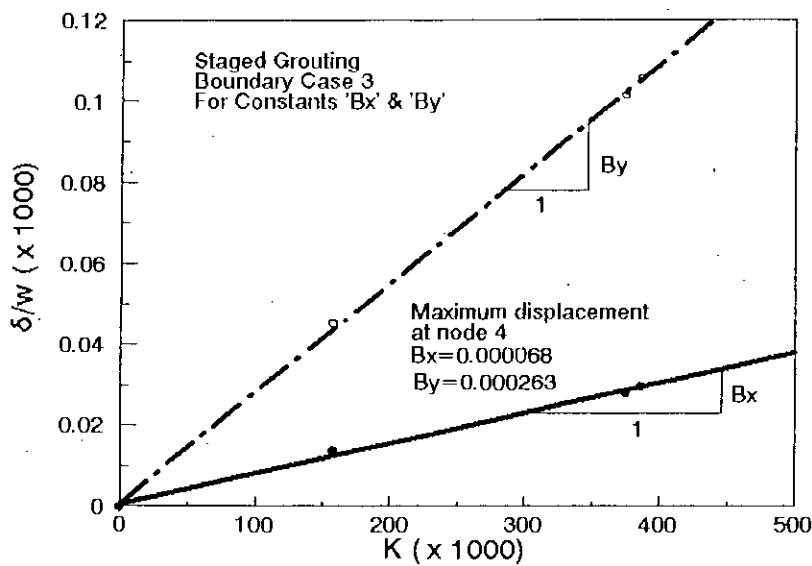
Fig. A2.3: Inverted egg shaped lining: Determination of the constant 'E' for uniform pressure for (a) boundary case 1, (b) boundary case 2 (at node 26), (c) boundary case 2 (at node 1) and (d) boundary case 3



(a)



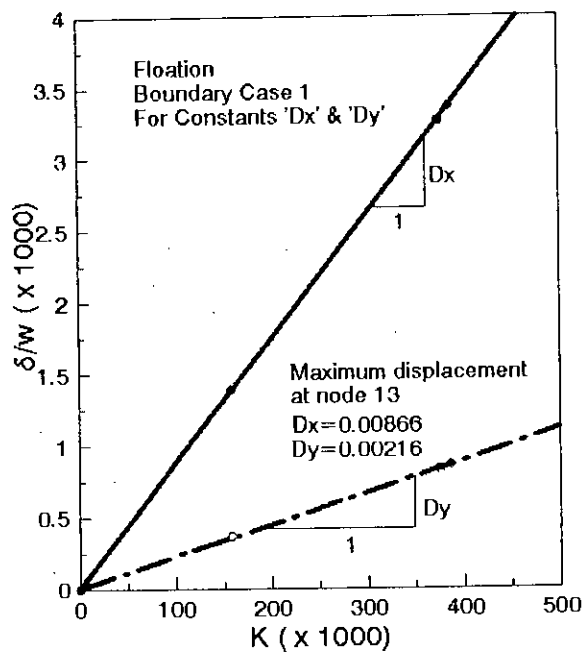
(b)



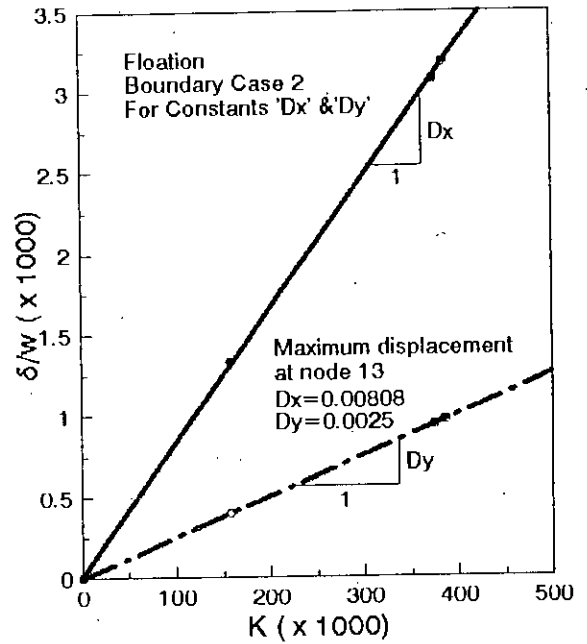
(c)

*Fig. A2.4: Inverted egg shaped lining: Determination of the constant 'Bx' and 'By' for sataged grouting for (a) boundary case 1, (b) boundary case 2 and (c) boundary case 3*

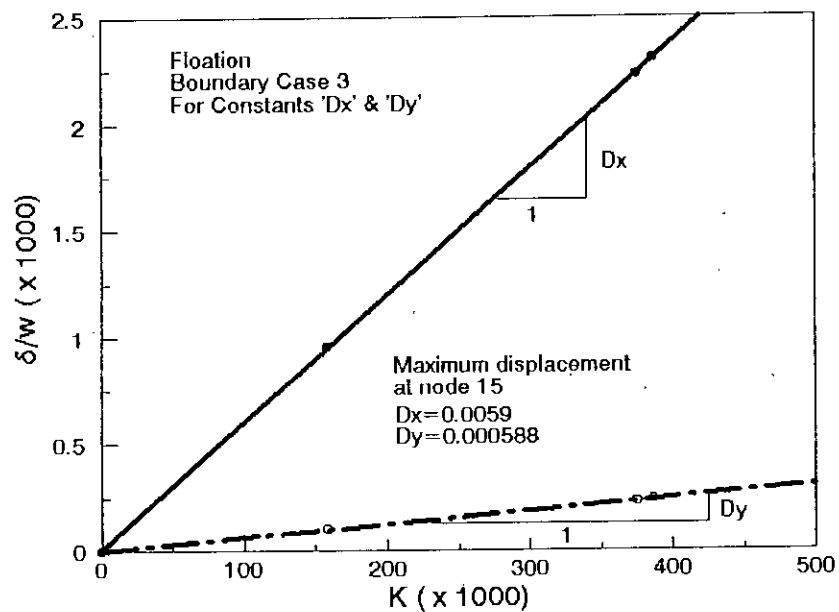




(a)

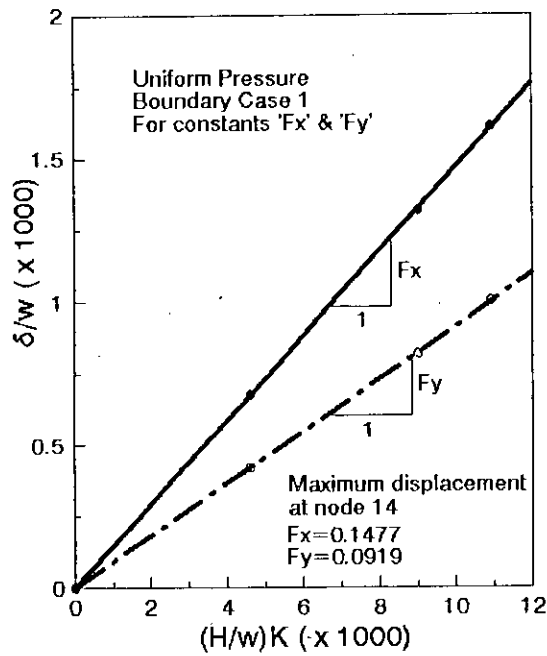


(b)

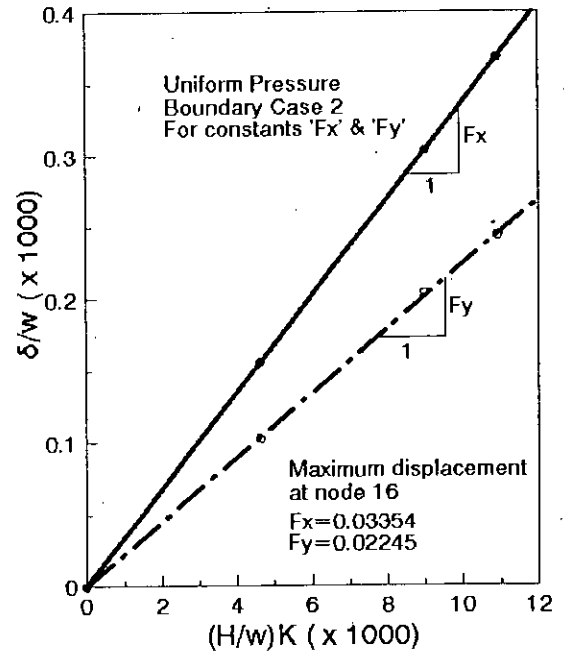


(c)

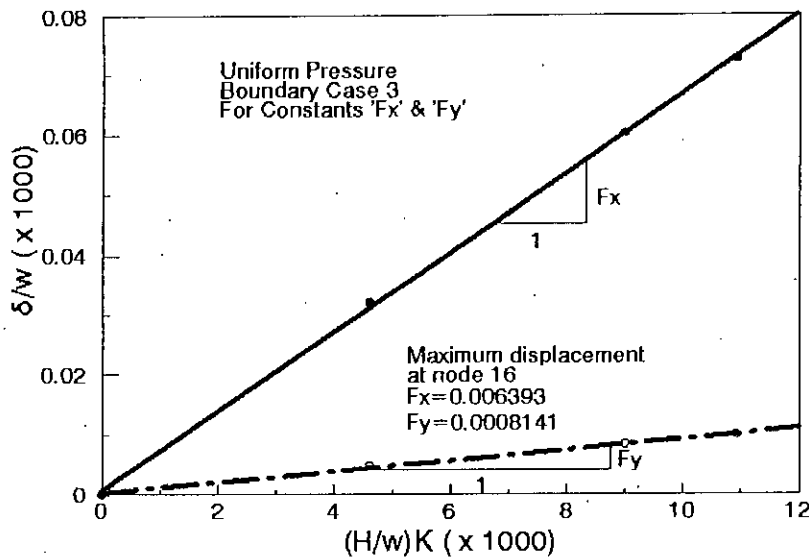
Fig. A2.5: Inverted egg shaped lining: Determination of the constants 'Dx' and 'Dy' for flotation for (a) boundary case 1, (b) boundary case 2 and (c) boundary case 3



(a)



(b)



(c)

Fig. A2.6: Inverted egg shaped lining: Determination of the constants 'Fx' and 'Fy' for uniform pressure for (a) boundary case 1, (b) boundary case 2 and (c) boundary case 3

## A2.2 STRUCTURAL DESIGN OF INVERTED EGG SHAPED LINING

A problem is solved here in order to show how the proposed curves (of Chapter 5) are to be used in designing an inverted egg-shaped lining. The geometrical and material parameters for this illustrative example is taken as exactly the same as those of the problem solved in chapter 3.

From the given data, the value of  $R$  and  $\frac{0.03}{K}$  were calculated in chapter 3; these are

$$R=2.443 \text{ and} \\ \frac{0.03}{K}=0.461$$

Using Fig. 4.7, for  $R=2.443$ ,  $\frac{P}{G_w}=5.45$  and

Using Fig. 4.11, for  $\frac{0.03}{K}=0.461$ ,  $\frac{P}{G_w}=4.086$  (governs)

Hence allowable grouting pressure on the lining during installation will be

$$p = 4.086 \times 16.5 \times 0.53 \\ = 35.7 \text{ kN/m}^2 \text{ which is equal to 2.16 m head of grout from the invert of the} \\ \text{lining.}$$

**APPENDIX 3**

### A3.1: GRAPHS USED IN THE DETERMINATION OF DIMENSIONLESS CONSTANTS FOR HORSESHOE SHAPED LINING

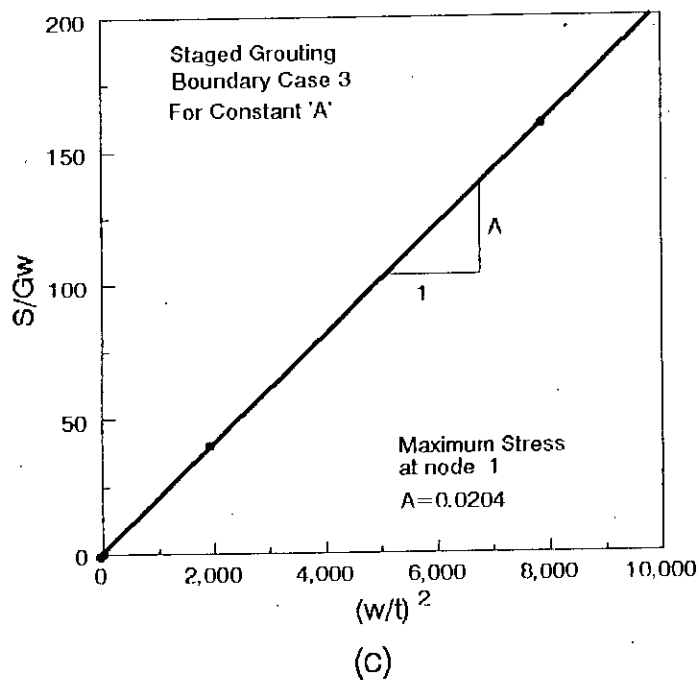
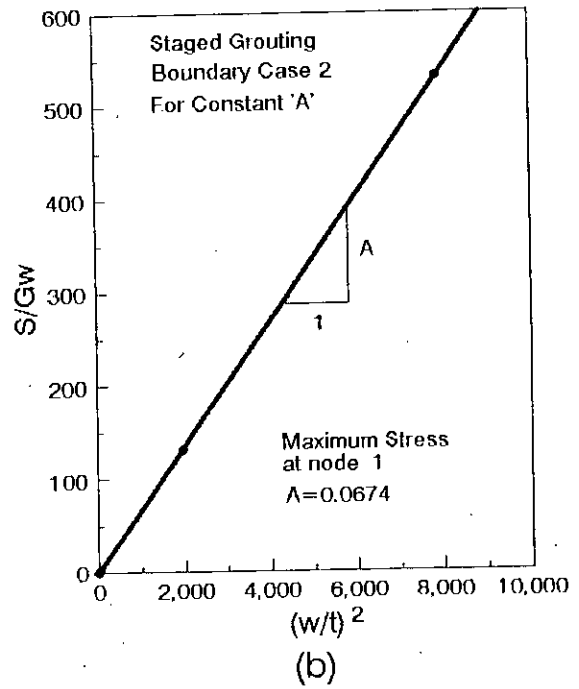
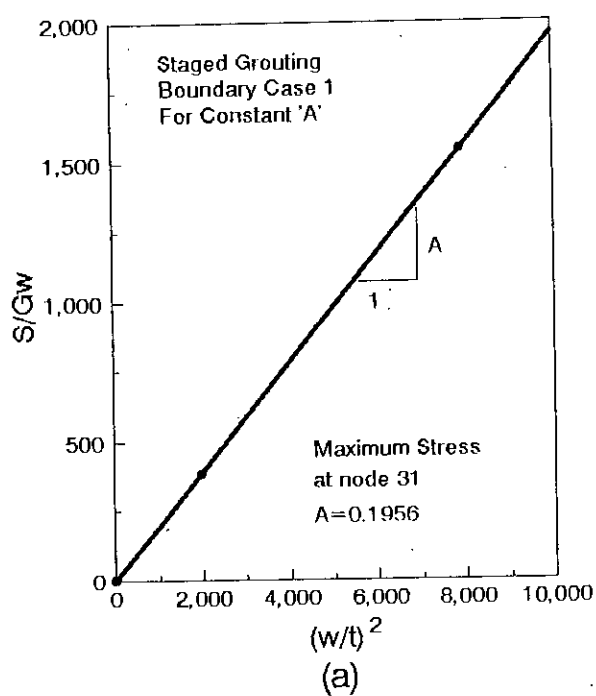
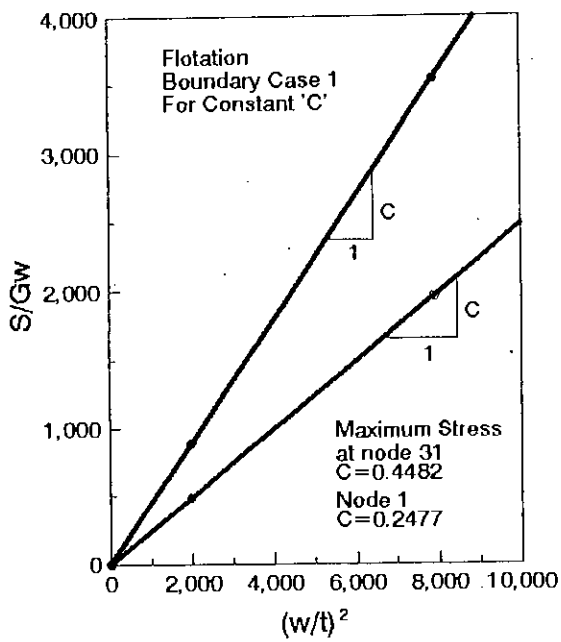
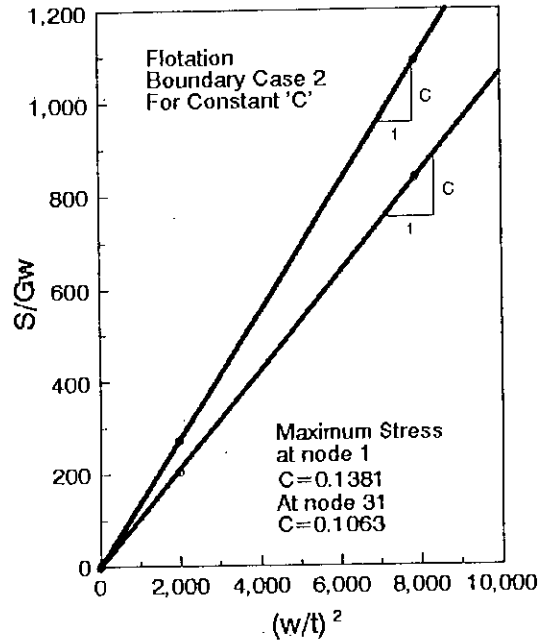


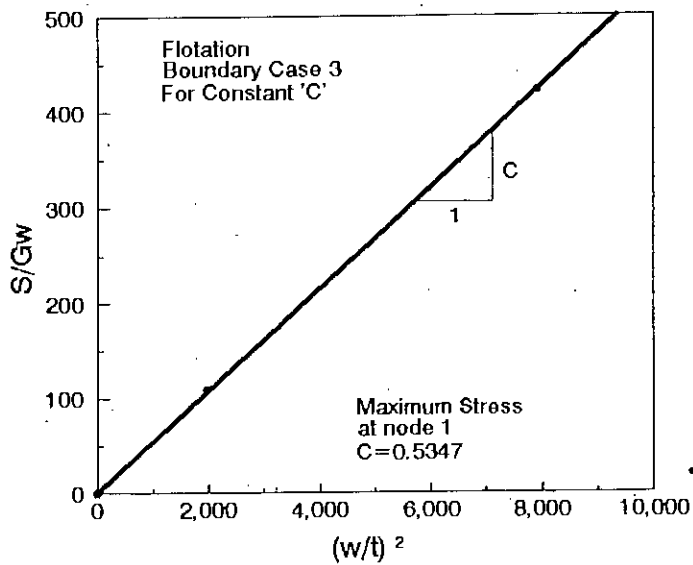
Fig. A3.1: Horse-shoe shaped lining: Determination of the constant 'A' for staged grouting for (a) boundary case 1, (b) boundary case 2 and (c) boundary case 3



(a)

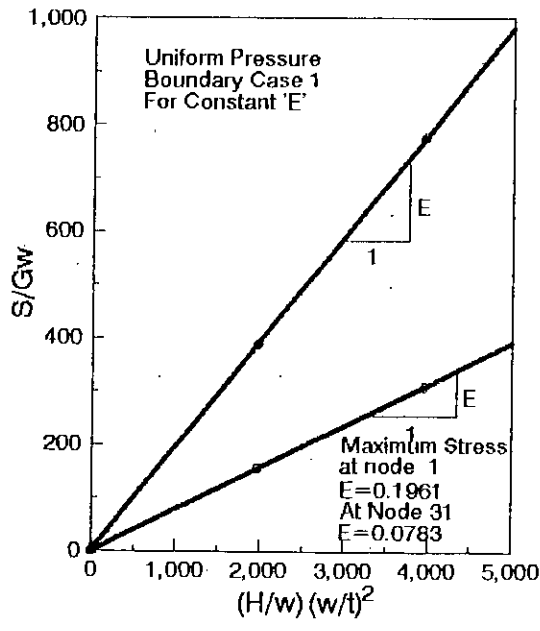


(b)

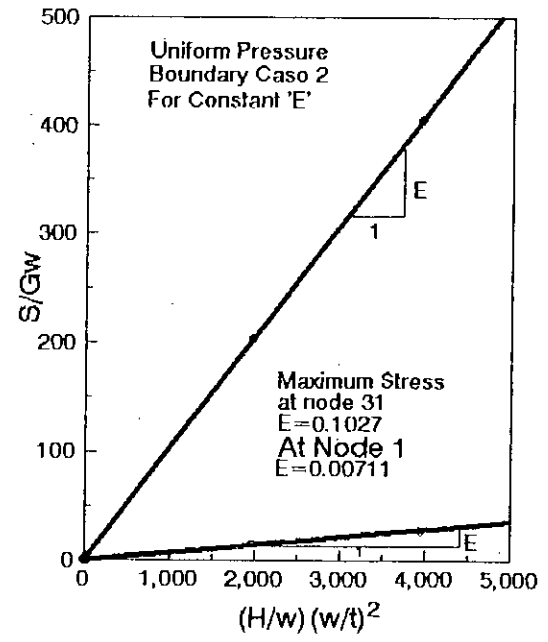


(c)

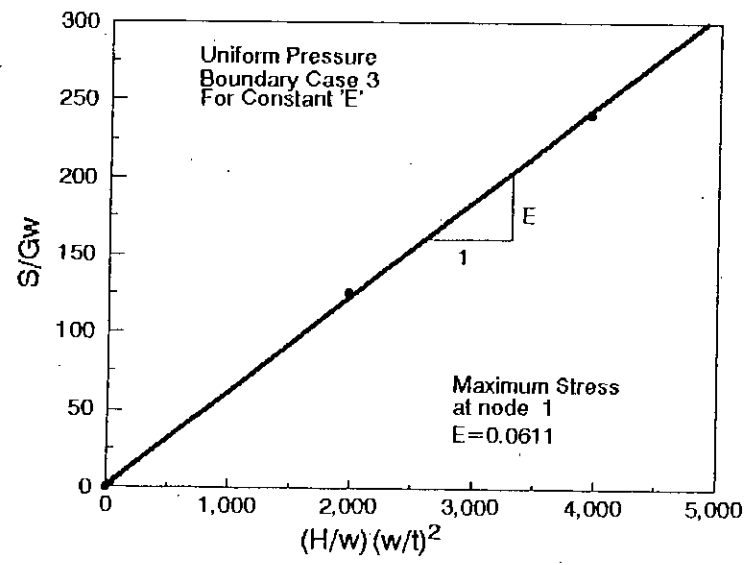
Fig. A3.2: Horse-shoe shaped lining: Determination of the constant 'C' for flotation for (a) boundary case 1, (b) boundary case 2 and (c) boundary case 3



(a)

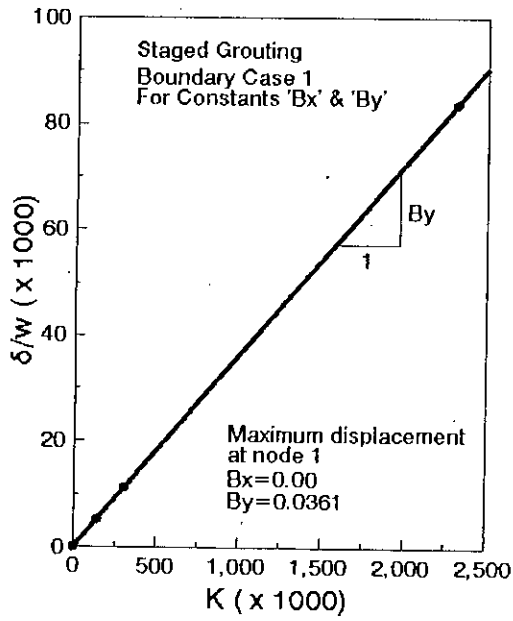


(b)

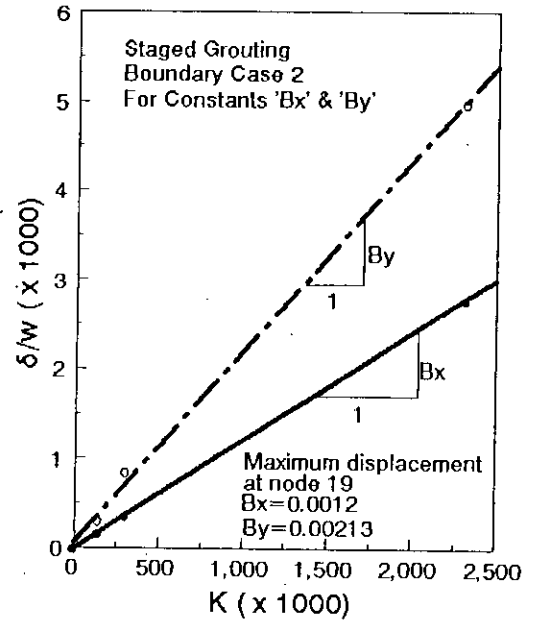


(c)

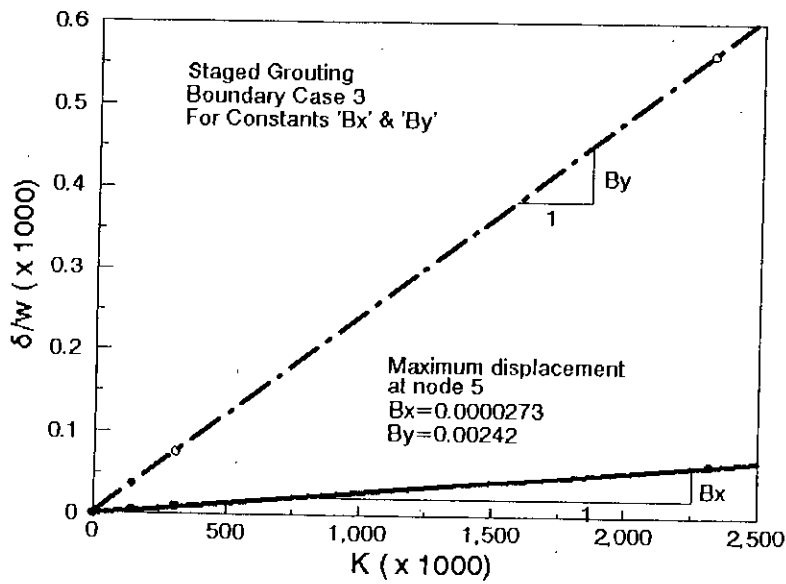
Fig. A3.3: Horse-shoe shaped lining: Determination of the constant 'E' for uniform pressure for (a) boundary case 1, (b) boundary case 2 and (c) boundary case 3



(a)



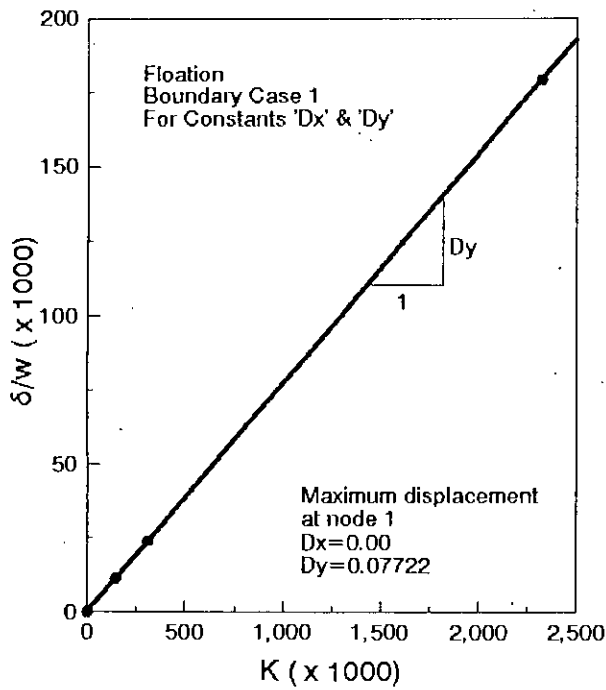
(b)



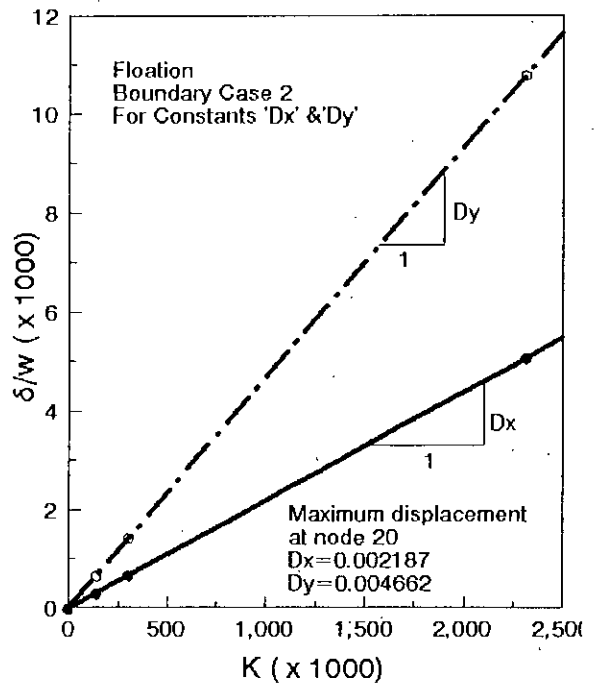
(c)

Fig. A3.4: Horse-shoe shaped lining: Determination of the constant 'Bx' and 'By' for staged grouting for (a) boundary case 1 (b) boundary case 2 and (c) boundary case 3

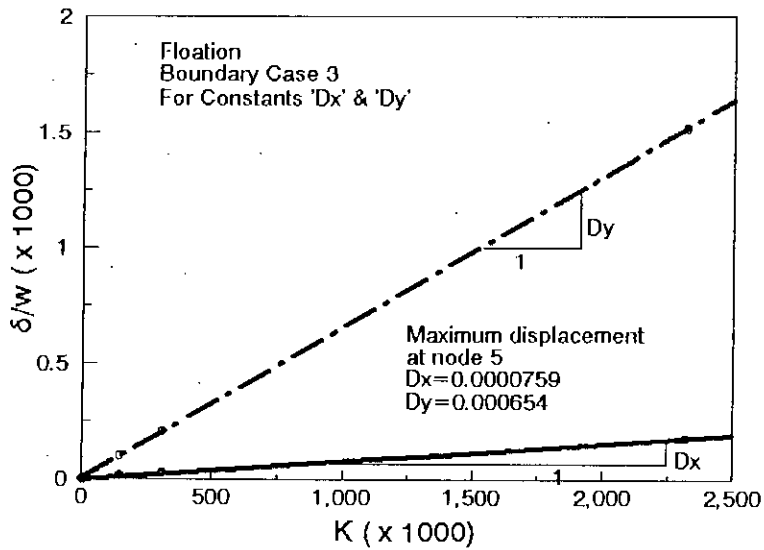




(a)

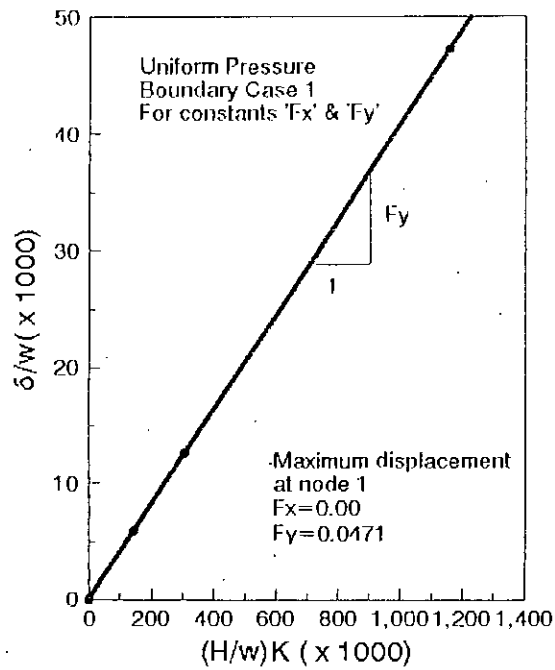


(b)

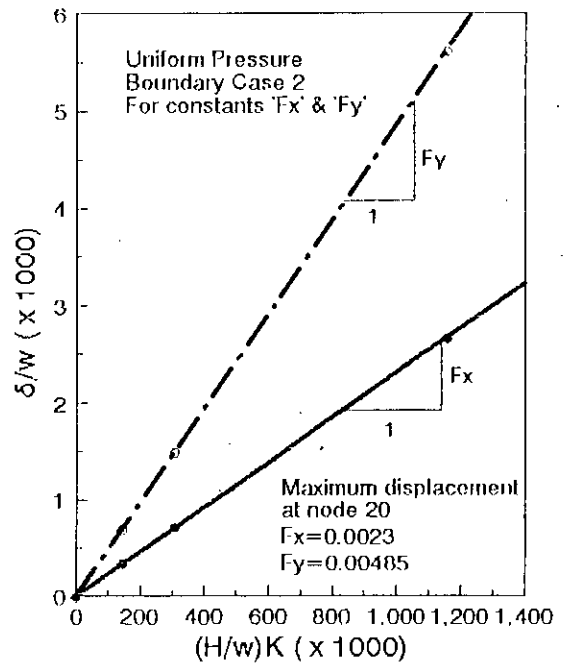


(c)

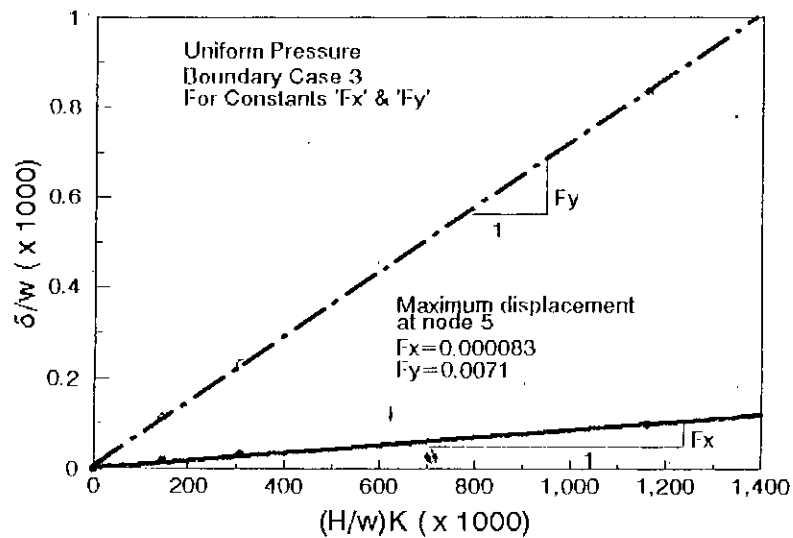
Fig. A3.5: Horse-shoe shaped lining: Determination of the constants 'Dx' and 'Dy' for flotation for (a) boundary case 1, (b) boundary case 2 and (c) boundary case 3



(a)



(b)



(c)

Fig. A3.6: Horse-shoe shaped lining: Determination of the constant 'Fx' and 'Fy' for uniform pressure for (a) boundary case 1, (b) boundary case 2, (c) boundary case 3

### A3.2 STRUCTURAL DESIGN OF HORSESHOE SHAPED LINING

The following design example demonstrates the use of the structural design method outlined in Chapter 5. It is to be noticed here that, in addition to the present short-term installation design checks, long-term design checks, which is not performed in this research work, must also be carried out. Also, the use of a particular lining material is merely illustrative.

An existing brick-sewer is horse-shoe shaped. Its different parameters are as follows:

(a) Geometrical parameters:-

Overall height of the sewer = 1270 mm

Overall width of the sewer = 1570 mm

The minimum annulus grouting thickness to be provided = 23 mm, and the lining thickness = 12 mm

(b) Material properties:-

The value of the short-term Young's modulus ( $E_s$ ) of the GRP lining material be equal to  $20 \times 10^6$  kN/m<sup>2</sup>.

The value of allowable short-term bending stress ( $S_s$ ) of the GRP lining equals to  $60.0 \times 10^3$  kN/m<sup>2</sup>

The specific weight ( $G$ ) of the grout mix equals to 16.0 kN/m<sup>3</sup>

Using boundary case 2 as the temporary support system, the allowable grouting pressure is to be determined.

#### Solution:

From the values of geometrical parameters, the internal dimensions of the lining (h and w) can be calculated as below:

$$\begin{aligned} h &= 1270 - (23 \times 2 + 12 \times 2) \\ &= 1200 \text{ mm} \end{aligned}$$

$$\begin{aligned} w &= 1570 - (23 \times 2 + 12 \times 2) \\ &= 1500 \text{ mm} \end{aligned}$$

Using the values of material properties, the non-dimensional strength of the lining  $R$  and permissible deflection  $0.03/K$  are calculated. These are as follows:

$$\begin{aligned}
 R &= \left( \frac{S_s}{Gw} \right) \left( \frac{t}{w} \right)^2 \\
 &= \frac{60 \times 10^3}{16.0 \times 1.5} \left( \frac{0.012}{1.5} \right)^2 \\
 &= 0.16
 \end{aligned}$$

$$\begin{aligned}
 \frac{0.03}{K} &= 0.03 \left( \frac{E_s}{Gw} \right) \left( \frac{t}{w} \right)^3 \\
 &= 0.03 \left( \frac{20 \times 10^6}{16.0 \times 1.5} \right) \left( \frac{0.012}{1.5} \right)^3 \\
 &= 0.0128
 \end{aligned}$$

Using the value of  $R$  equal to 0.16 and Fig. 5.8 (for stress-limit criteria),

$$p/Gw = 3.4 \text{ and}$$

using the value of  $0.03/K$  equal to 0.0128 and Fig 5.9 (for deflection-limit criteria),

$$p/Gw = 4.14 \text{ can be obtained.}$$

Hence, the minimum of these two values i.e.  $p/Gw = 3.4$  is to be taken in design.

$p/Gw = 3.4$ , or  $p = 3.4 \times 16.0 \times 1.5 = 81.6 \text{ kN/m}^2$  which is equal to 5.1 m head of grout from the invert or 3.9 m head of grout from the crown of the lining.

**APPENDIX 4**

### A4.1: GRAPHS USED IN THE DETERMINATION OF DIMENSIONLESS CONSTANTS FOR SEMI-ELLIPTICAL SHAPED LINING

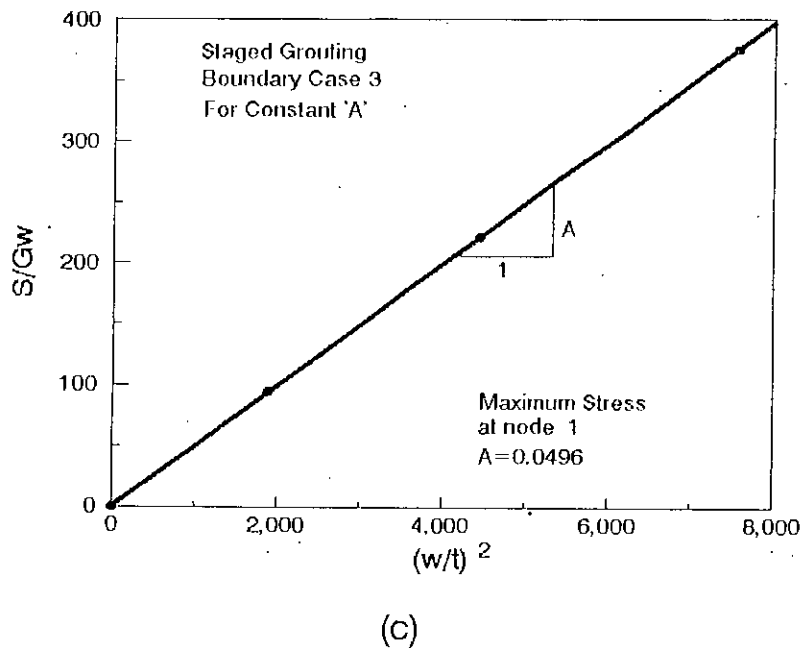
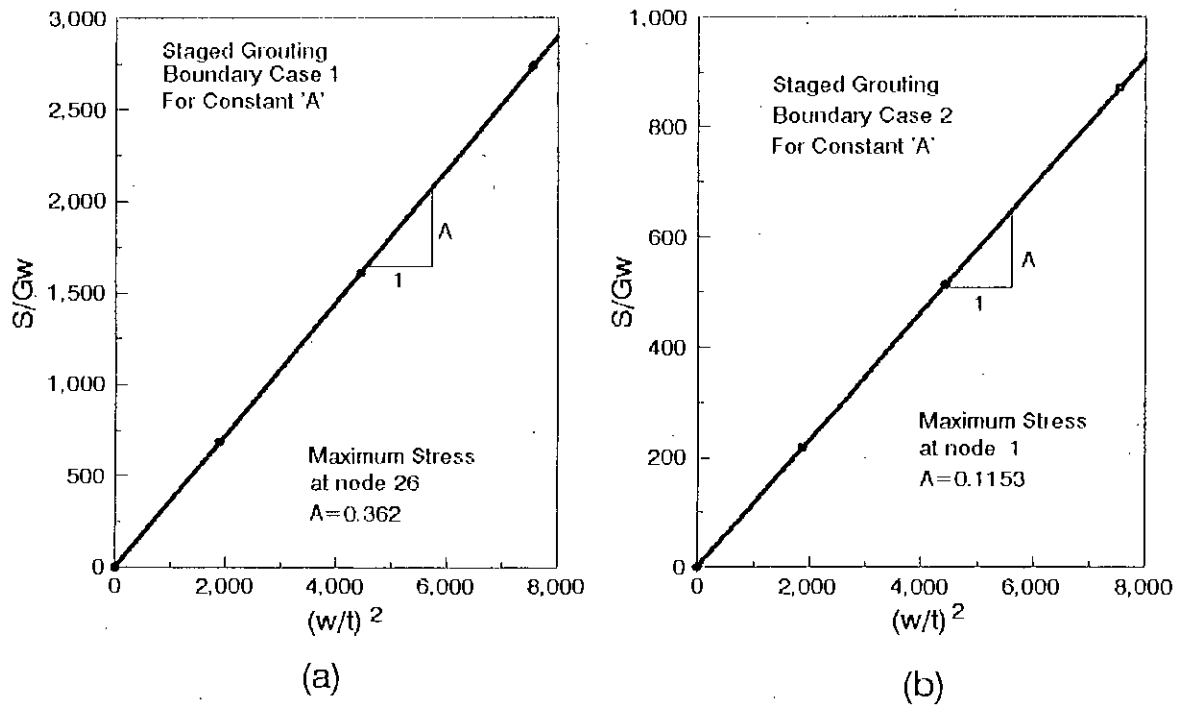
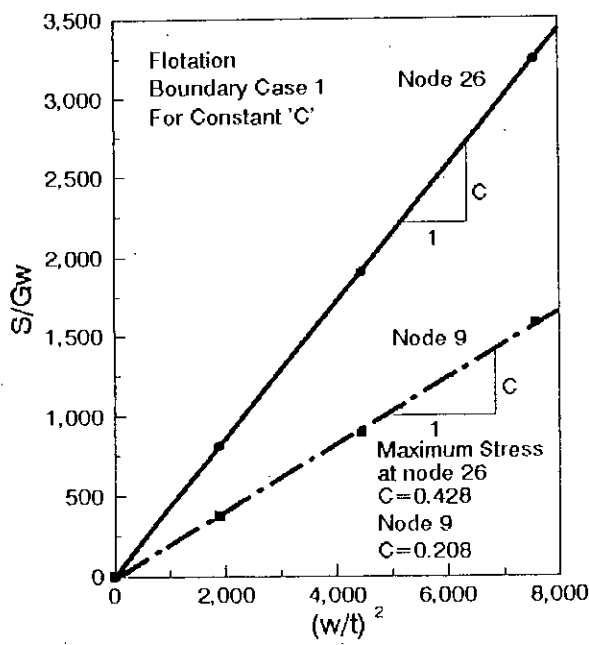
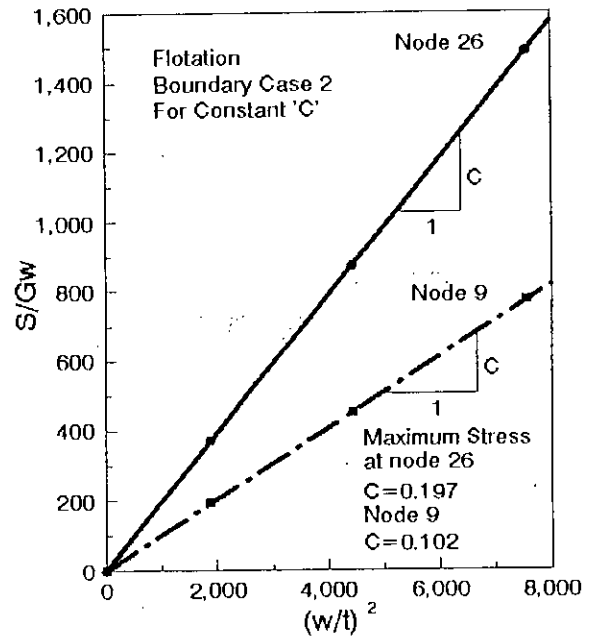


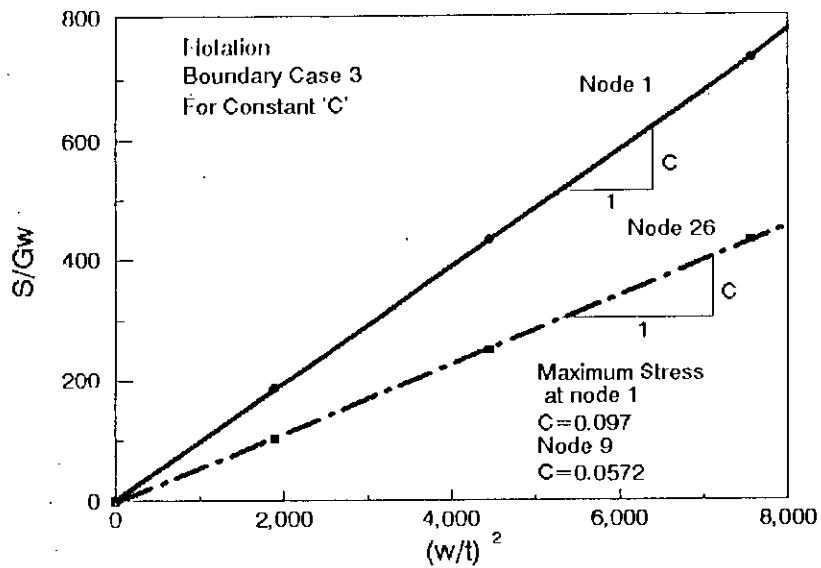
Fig. A4.1: Semi-elliptical shaped lining: Determination of the constant 'A' for staged grouting for (a) boundary case 1, (b) boundary case 2 and (c) boundary case 3



(a)

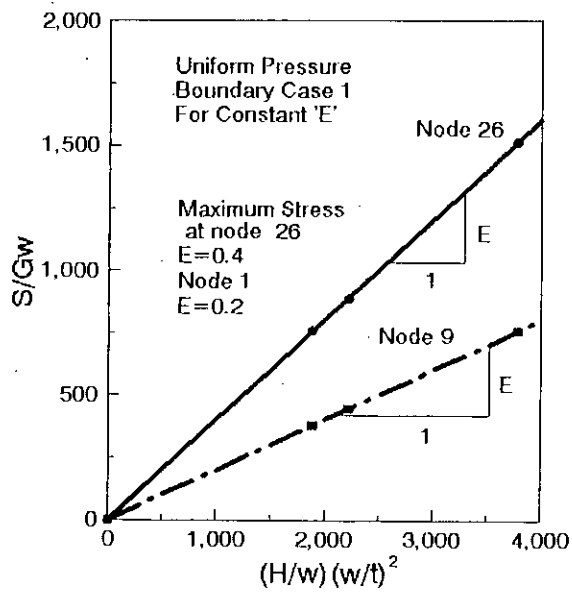


(b)

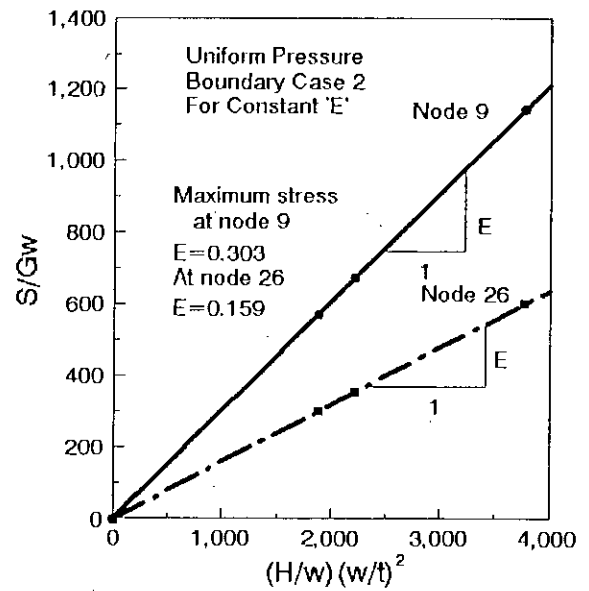


(c)

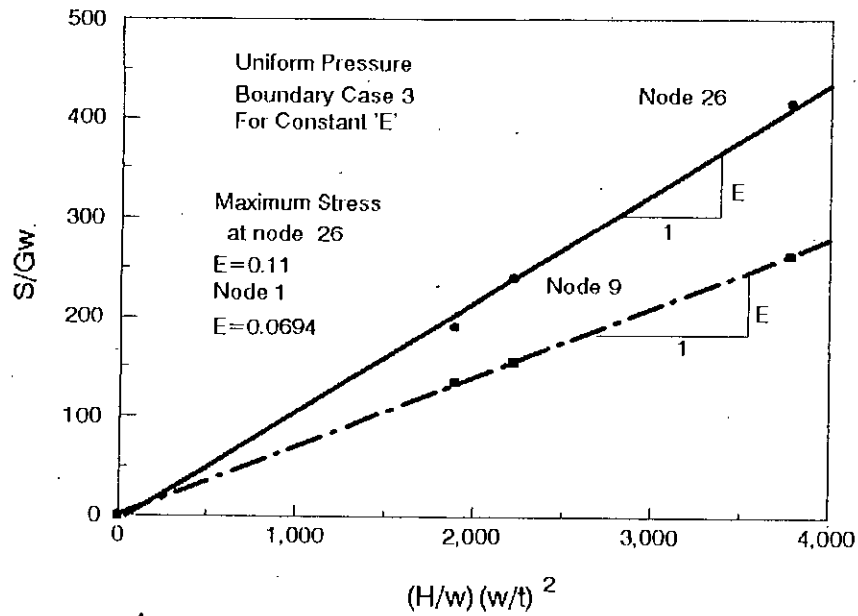
Fig. A4.2: Semi-elliptical shaped lining: Determination of the constant 'C' for flotation for (a) boundary case 1, (b) boundary case 2 and (c) boundary case 3



(a)



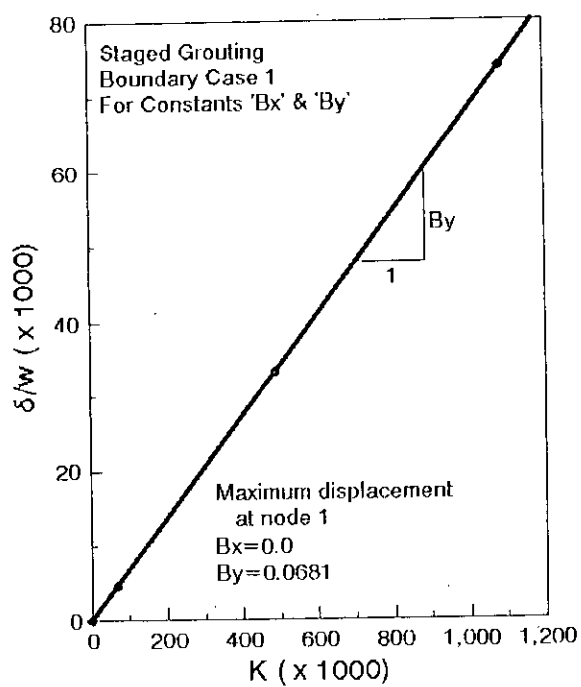
(b)



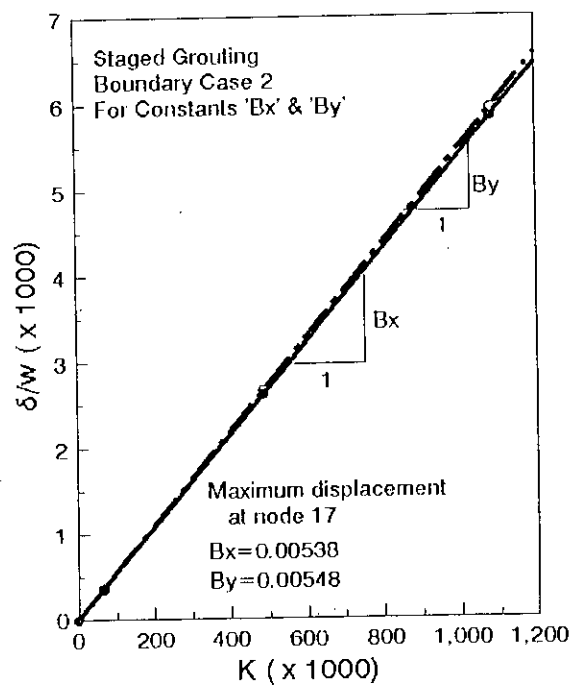
(c)

Fig. A4.3: Semi-elliptical shaped lining: Determination of the constant 'E' for uniform pressure for (a) boundary condition 1, (b) boundary condition 2 and (c) boundary condition 3.

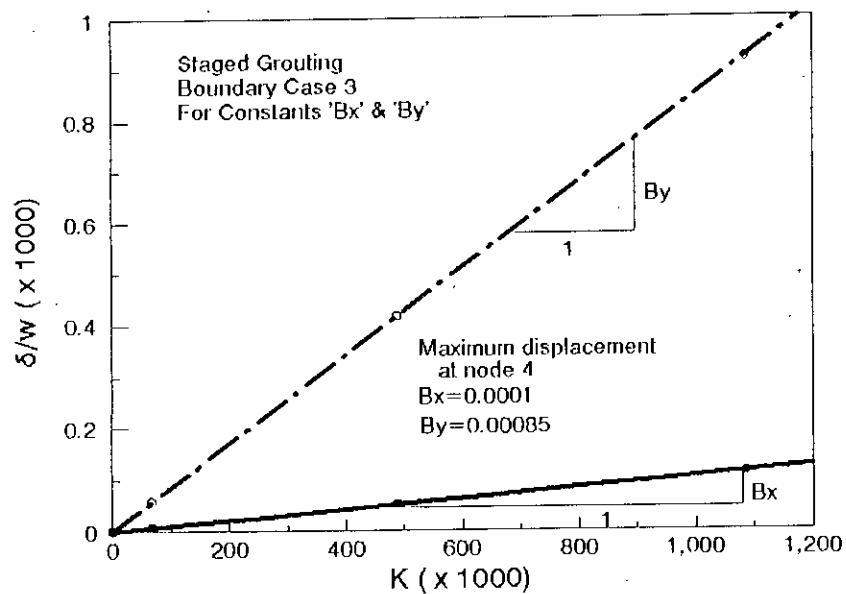




(a)

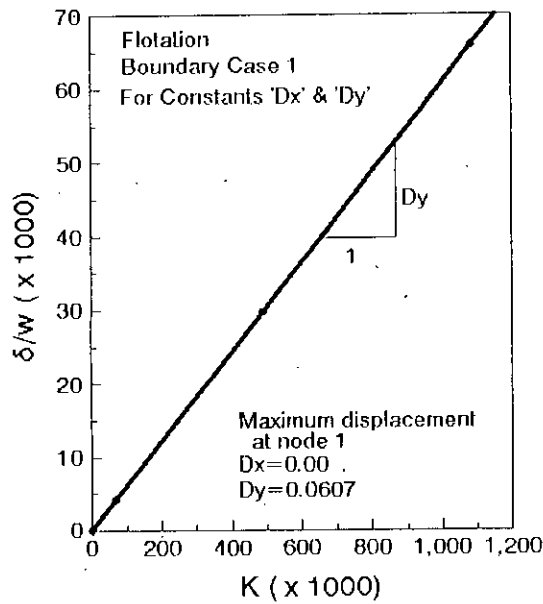


(b)

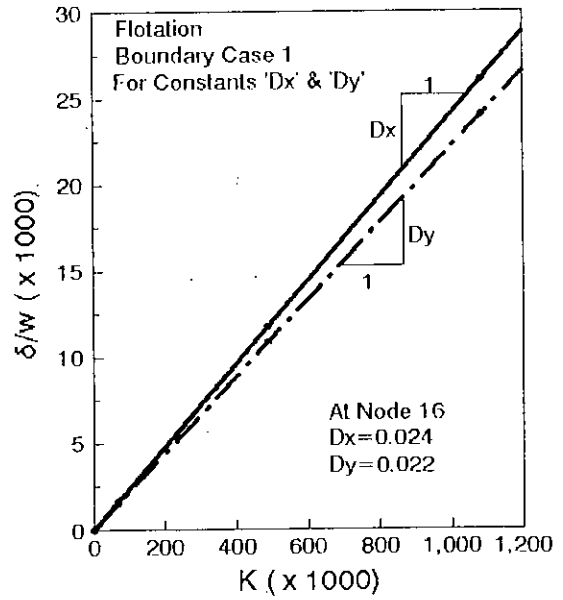


(c)

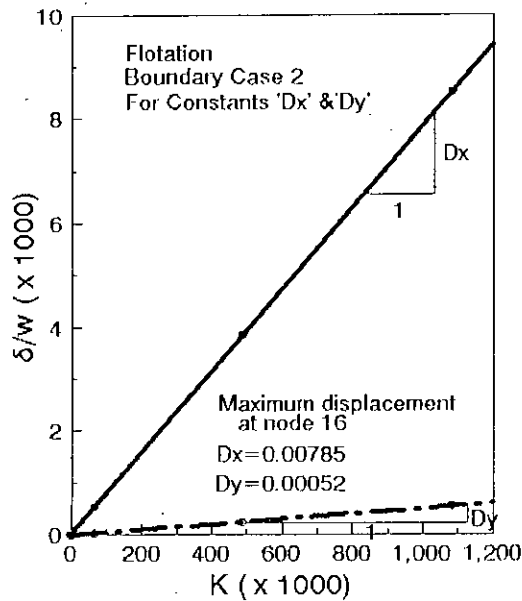
**Fig. A4.4: Semielliptical shaped lining: Determination of the constants 'Bx' and 'By' for staged grouting for (a) boundary case 1, (b) boundary case 2 and (c) boundary case 3**



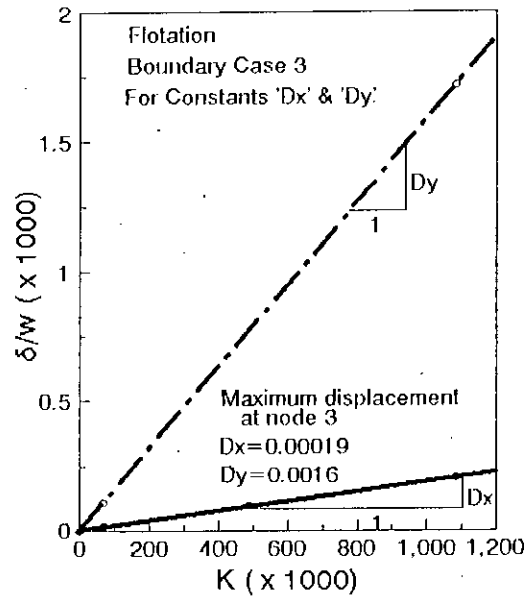
(a)



(b)

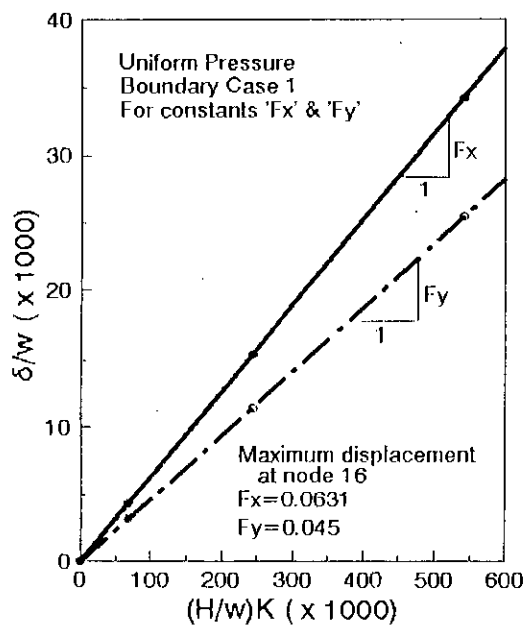


(c)

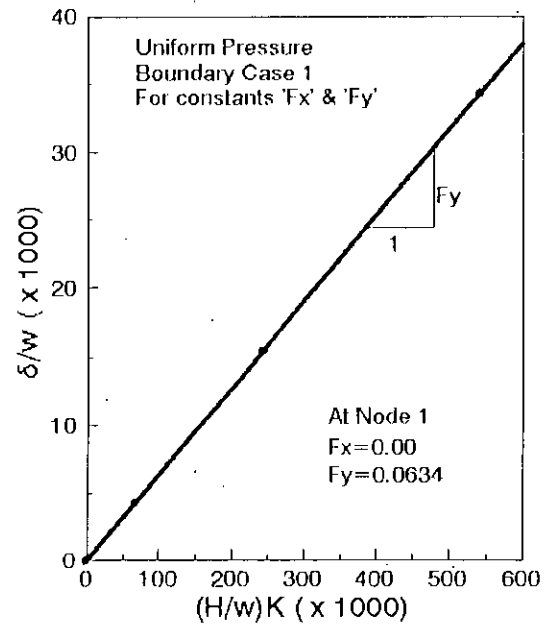


(d)

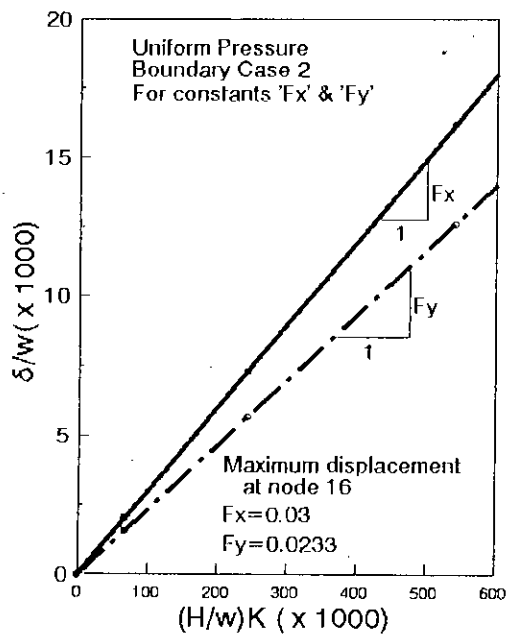
Fig. A4.5: Semielliptical shaped lining: Determination of the constants 'Dx' and 'Dy' for flotation for (a) boundary case 1 (node 1), (b) boundary case 1 (node 16), (c) boundary case 2 and (d) boundary case 3



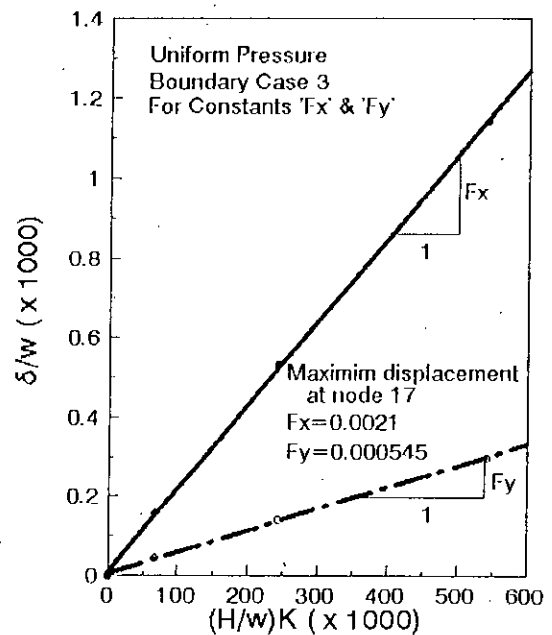
(a)



(b)



(c)



(d)

Fig. A4.6: Semielliptical shaped lining: Determination of the constants 'Fx' and 'Fy' for uniform pressure for (a) Boundary case 1 (node 16), (b) boundary case 1 (node 1), (c) boundary case 2 and (d) boundary case 3

## A4.2 STRUCTURAL DESIGN OF SEMIELLIPTICAL LINING

The following example illustrates the use of the structural design method of semielliptical shaped sewer lining outlined in Chapter 6. It is important to note here that, in addition to the present short-term installation design checks, long-term design checks (which is not performed in this research work) must also be carried out. Also, the use of a particular lining material is merely illustrative.

An existing brick-sewer is semielliptical shaped as shown in Fig. 6.1. The proposed renovation technique consists of lining the sewer with GRP pipe lining units. The different parameters of the sewer geometry and properties of the GRP lining material, are as follows:

(a) Geometrical parameters:-

Overall height of the sewer = 1250 mm,

Overall width of the sewer = 1000 mm,

The minimum annulus grouting thickness to be provided = 30 mm, and  
the lining thickness = 15 mm.

(b) Material properties:-

The value of the short-term Young's modulus ( $E_s$ ) of the GRP lining material be equal to  $20 \times 10^6$  kN/m<sup>2</sup>,

The value of allowable short-term bending stress ( $S_s$ ) of the GRP lining material be equal to  $55.0 \times 10^3$  kN/m<sup>2</sup>,

The unit weight of the grout mix (G) equals to 16.5 kN/m<sup>3</sup>

### Solution:

Using the values of the geometrical parameters, the internal dimensions of the lining are found out to be equal to 1160 mm (h) and 910 mm (w).

Similarly using the values of the material parameters, the non-dimensional strength of the lining R and the permissible deflection  $0.03/K$  can be calculated as follows:

$$\begin{aligned}
 R &= \left( \frac{S_s}{Gw} \right) \left( \frac{t}{w} \right)^2 \\
 &= \frac{55 \times 10^3}{16.5 \times 0.91} \left( \frac{0.015}{0.91} \right)^2 \\
 &= 0.995
 \end{aligned}$$

and,

$$\begin{aligned}
 \frac{0.03}{K} &= 0.03 \left( \frac{E_s}{Gw} \right) \left( \frac{t}{w} \right)^3 \\
 &= 0.03 \left( \frac{20 \times 10^6}{16.5 \times 0.91} \right) \left( \frac{0.015}{0.91} \right)^3 \\
 &= 0.18
 \end{aligned}$$

Using Fig. 6.9 (for stress-limit criteria) and adopting boundary case 2 as the temporary support system to be used during grouting, the following is obtained

$$\begin{aligned}
 \frac{p}{Gw} &= 4.2 \\
 \text{or, } p &= 63.063 \text{ kN / sq.m}
 \end{aligned}$$

which is equivalent to 3.82 m head of grout from the invert of the lining.

Using Fig. 6.12 (for deflection-limit criteria), the following is obtained for boundary condition 2

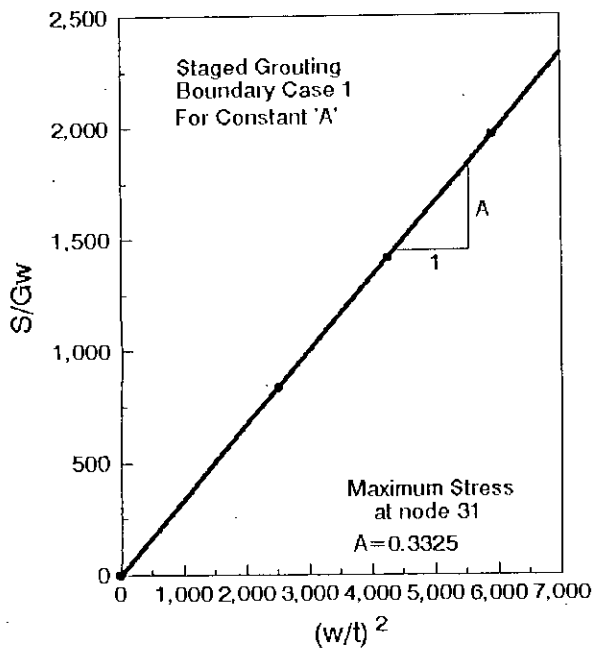
$$\begin{aligned}
 \frac{p}{Gw} &= 5.79 \\
 \text{or, } p &= 86.94 \text{ kN / sq.m}
 \end{aligned}$$

which is equivalent to a head of grout equal to 5.27 m from the invert of the lining.

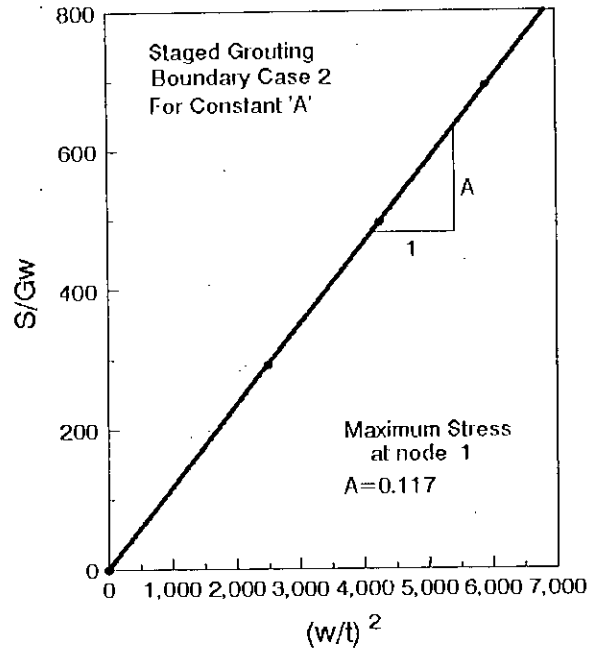
Here, stress-limitation govern the design and the safe head of grout that can be imposed on the lining (from the invert) equal to 3.82 m.

**APPENDIX 5**

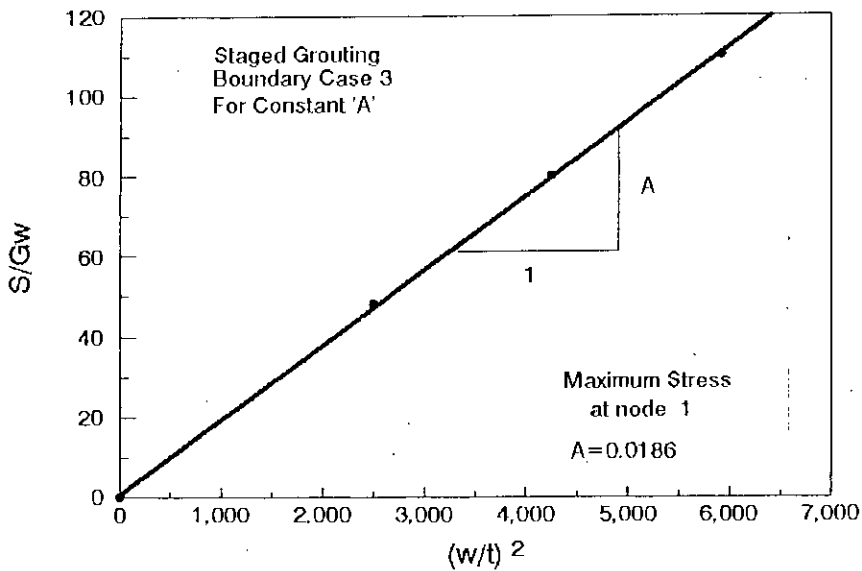
## A5.1: GRAPHS USED IN THE DETERMINATION OF DIMENSIONLESS CONSTANTS FOR CIRCULAR SHAPED LINING



(a)

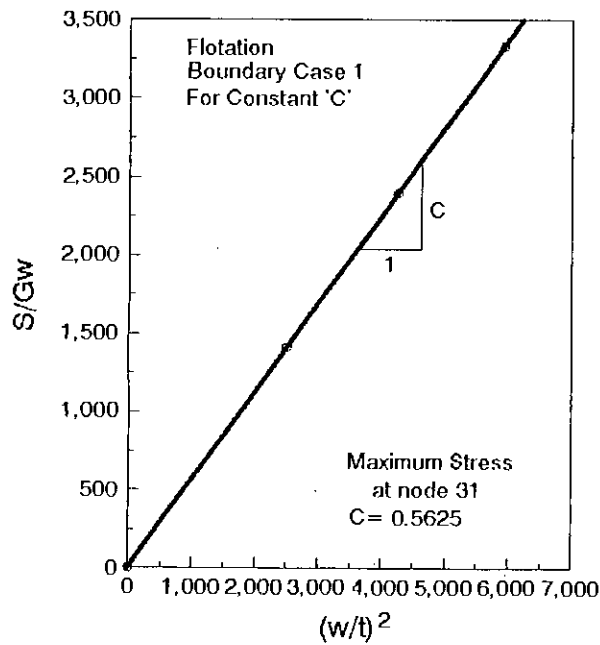


(b)

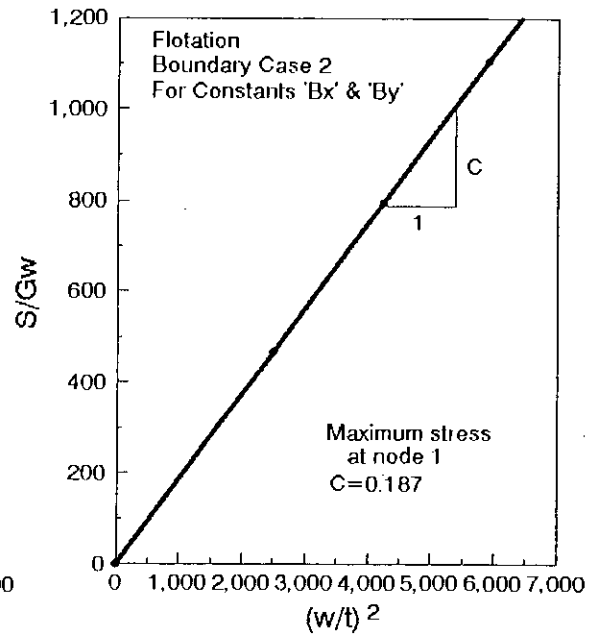


(c)

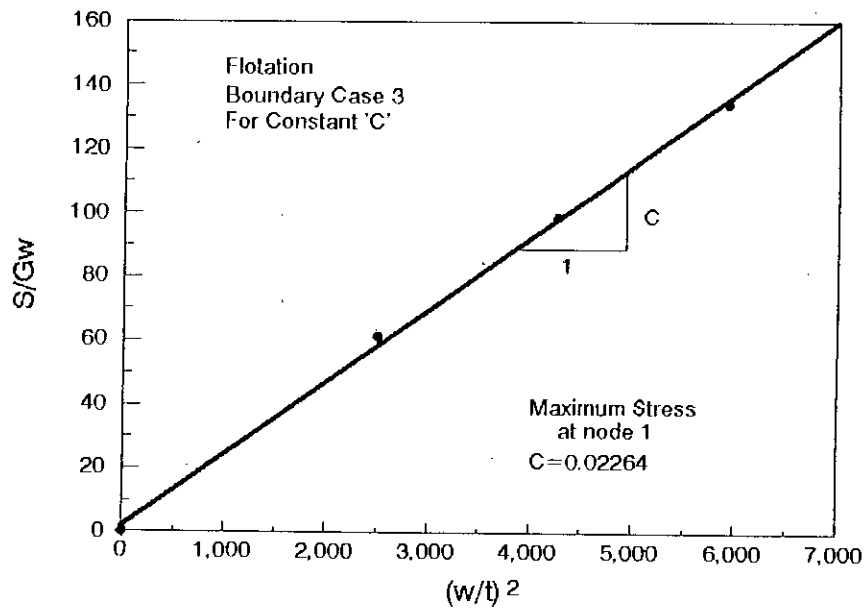
Fig. A5.1: Circular shaped lining: Determination of the constant 'A' for staged grouting for (a) boundary case 1, (b) boundary case 2, and (c) boundary case 3



(a)



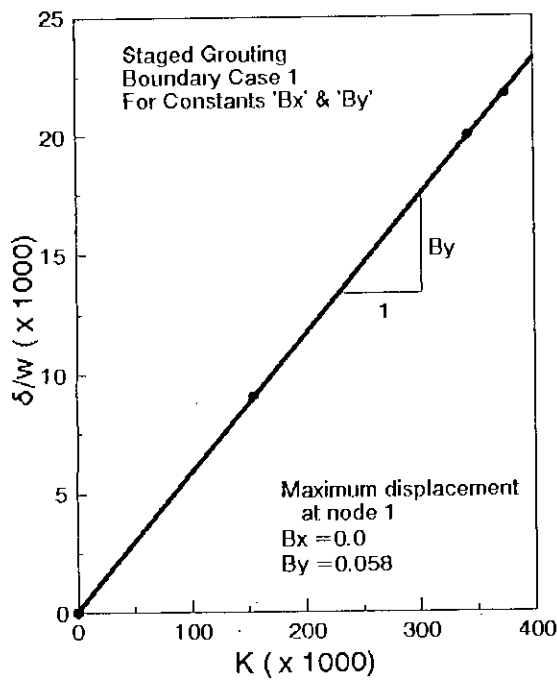
(b)



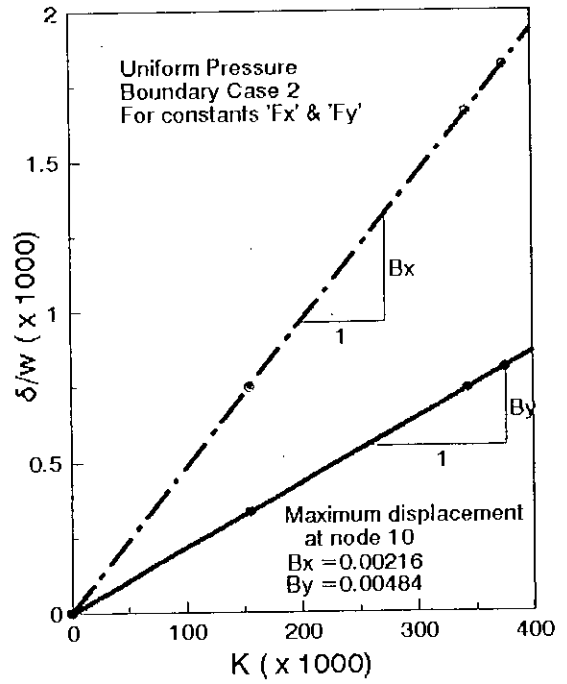
(c)

Fig. A5.2: Circular shaped lining: Determination of the constant 'C' for flotation for (a) boundary case 1, (b) boundary case 2 and (c) boundary case 3

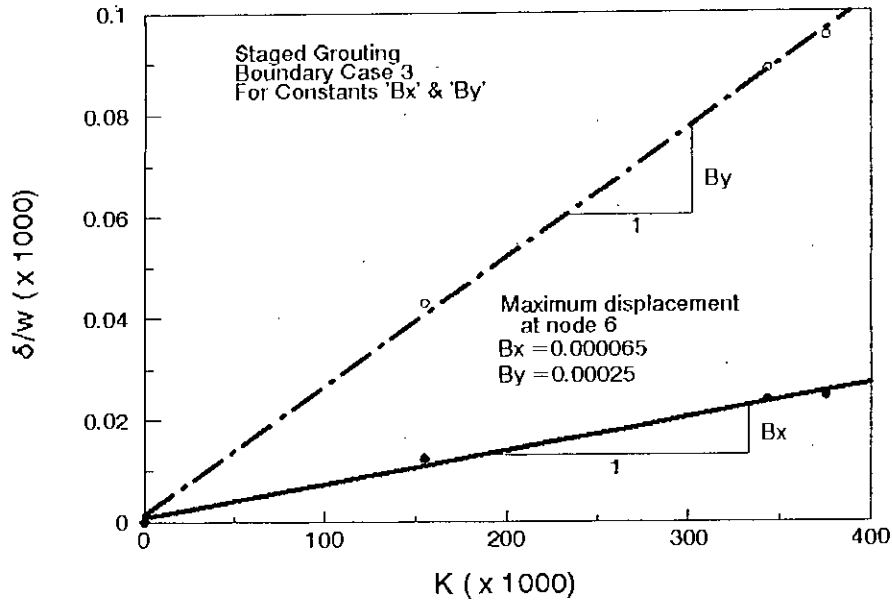




(a)

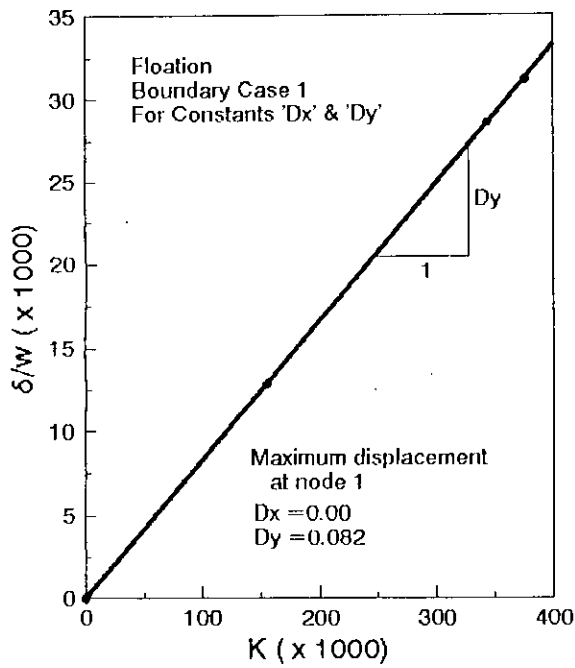


(b)

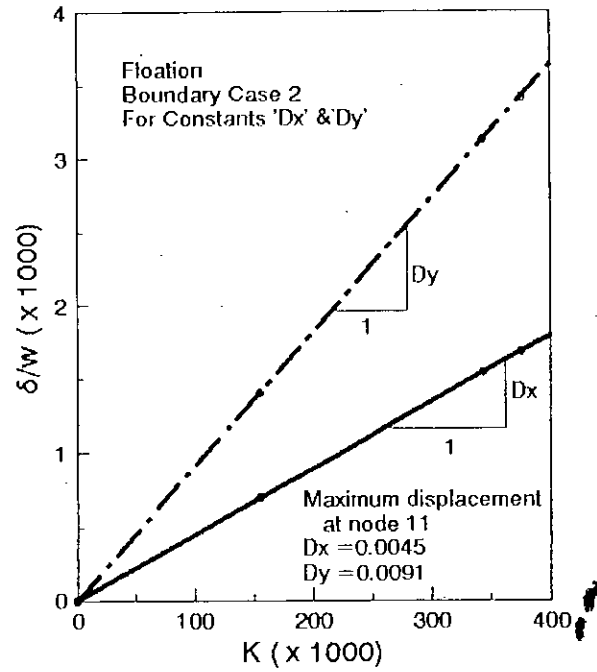


(c)

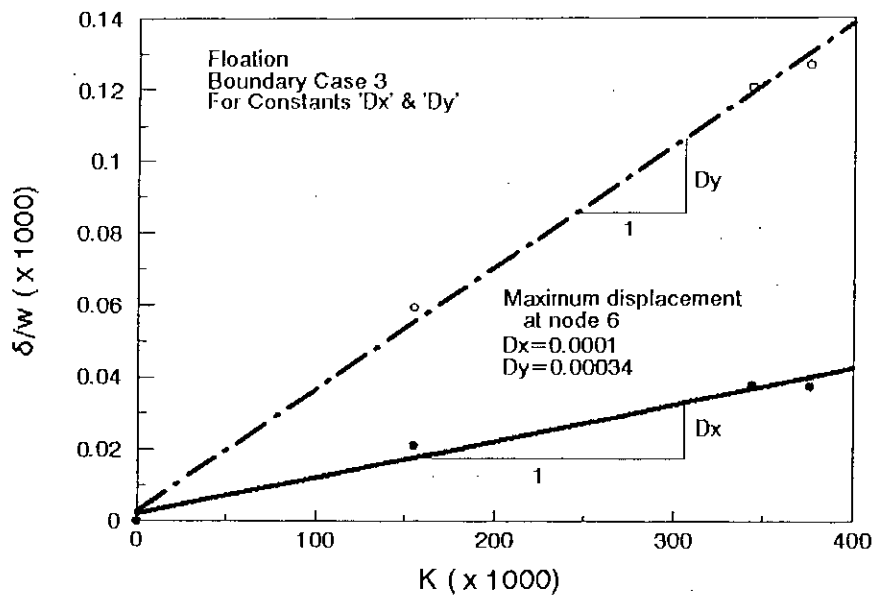
Fig. A5.3: Circular shaped lining: Determination of the constants 'Bx' and 'By' for staged grouting for (a) boundary case 1, (b) boundary case 2 and (c) boundary case 3



(a)



(b)



(c)

Fig. A5.4: Circular shaped lining: Determination of the constants 'Dx' and 'Dy' for flotation for (a) boundary case 1, (b) boundary case 2 and (c) boundary case 3

## A5.2 STRUCTURAL DESIGN OF CIRCULAR LININGS

An existing sewer is of circular shape of diameter 1.0 m. The sewer now needs to be renovated by lining technique. As before, the lining material is taken as the glass reinforced plastic (because the properties of this material are determined experimentally (Ref. 5) and the material is now being successfully used as a liner in foreign countries).

(a) Geometrical parameters:-

The minimum annulus grouting thickness to be provided =20 mm, and the lining thickness =10 mm.

(b) Material properties:-

The value of the short-term Young's modulus ( $E_s$ ) of the GRP lining material be equal to  $20 \times 10^6$  kN/m<sup>2</sup>,

The value of allowable short-term bending stress ( $S_s$ ) of the GRP lining material be equal to  $55.0 \times 10^3$  kN/m<sup>2</sup>,

The unit weight of the grout mix (G) equals to 16.5 kN/m<sup>3</sup>

### SOLUTION:

From the data given above, the radius of the lining can be determined can be as follows:

Radius of the lining (R) =  $0.5 - 0.01 = 0.49$  m.

If boundary case 2 (Fig. 7.3b) is taken as the temporary support system during installation of the lining, the value of K in equation 7.3 would be 3. Now, using equation 7.3:

$$\begin{aligned} q_{cr} &= \frac{E}{12(1-\nu^2)} \left( \frac{t}{R} \right)^3 K \\ &= \frac{20 \times 10^6}{12(1-0.23^2)} \left( \frac{0.01}{0.49} \right)^3 \times 3 \\ &= 44.87 \text{ kN / m}^2. \end{aligned}$$

$q_{cr}$  is a uniform pressure, but the full grouting pressure, as mentioned in Chapter 7, is hydrostatic. Hence, if the pressure at the invert of the lining is taken as  $q_{cr}$ , the design, of course, will be conservative. Therefore, the safe head of grout that can be imposed on the lining during installation will be 2.72 m. from the invert of the lining.

